ALTERNATIVE BINDER MATERIALS FOR RIGID PAVEMENTS – AN INVESTIGATION INTO THE STRUCTURAL AND SUSTAINABILITY EFFECTS OF PARTIAL CEMENT REPLACEMENT WITH PULP AND PAPER MILL WASTE ASH IN CONCRETE PAVEMENTS

by

Deveshan Pillay
214510044

Submitted in fulfillment of the requirements for the degree of
Master of Science in Engineering; College of Agriculture, Engineering and Science;
University of KwaZulu-Natal
26 January 2021

Name of supervisor(s): Professor MMH Mostafa and Dr OB Olalusi

ABSTRACT

The drastic surge in urbanisation and the constantly changing human lifestyle are the main contributory factors to the increased demand for concrete construction-related activities. Concrete is widely utilised for various structural applications, including rigid pavement construction, due to its superior mechanical and durability performance. However, the cement production process releases harmful greenhouse gases, leads to the depletion of calcareous materials and consumes significant quantities of energy. Therefore, there is an increased need for sustainable pavement designs that maintain a high level of service. In the case of rigid pavement applications, this can be achieved by incorporating alternate binder systems, such as paper mill ash (PMA). This research study aims to investigate the engineering performance of concrete manufactured with PMA. This was achieved by assessing the workability, mechanical and durability properties of concrete specimens containing 0%, 5%, 10%, 15% and 20% of PMA as supplementary cementitious material (w/b = 0.64). Frictional resistance investigations, an equivalent carbon dioxide (CO_{2e}) assessment, material cost analysis and construction cost analysis were also adopted to evaluate the viability of PMA based concrete for sustainable rigid pavement construction. Reduced workability performance was noted in the concrete mixes containing PMA, which is ideal for fresh concrete used for paving purposes. Favourable mechanical strength results were documented, with the 10% PMA replacement level achieving the optimum 28-day compressive, flexural and tensile splitting strength results. Numerous disparities were noted in the durability index test readings, which requires clarification with further investigations. Although the skid resistance and texture depth test results were inconclusive, it was still determined that PMA will have a minimal effect on the frictional resistance of concrete pavements. Advantageous sustainability and economic performance were noted from the CO_{2e} analysis and both cost assessments, whereby the CO_{2e} value and costs incurred decreased for high PMA contents. Based on the favourable fresh state, mechanical strength, durability and economic results attained in this research study, coupled with the negligible CO_{2e} emission value, it can be concluded that PMA is a feasible alternate binder system for enhancing the serviceability and sustainability states of rigid pavements.

Keywords: supplementary cementitious materials; rigid pavements; sustainability; paper mill ash

DECLARATION 1 – PLAGIARISM

I, ……..Deveshan Loganathan Pillay……., declare that:

1. The research reported in this thesis, except where otherwise indicated, is my original research.
2. This thesis has not been submitted for any degree or examination at any other university.
3. This thesis does not contain other persons' data, pictures, graphs or other information, unless specifically acknowledged as being sourced from other persons.
4. This thesis does not contain other persons' writing, unless specifically acknowledged as being sourced from other researchers. Where other written sources have been quoted, then:

a. Their words have been re-written, but the general information attributed to them has been referenced

b. Where their exact words have been used, then their writing has been placed in italics and inside quotation marks and referenced.

5. This thesis does not contain text, graphics or tables copied and pasted from the Internet, unless specifically acknowledged, and the source being detailed in the thesis and in the References sections.

…… ..……16/01/2021…….
DEVESHAN PILLAY (STUDENT) DATE

As the Candidate's supervisor I agree to the submission of this thesis:

[redacted]…… ..……19/01/2021……..
PROF MOSTAFA (SUPERVISOR) DATE

….[redacted]…… ..……19/01/2021……..
DR OLALUSI (CO-SUPERVISOR) DATE

DECLARATION 2 – PUBLICATIONS

DETAILS OF CONTRIBUTION TO PUBLICATIONS that form part and/or include research presented in this thesis:

Publication 1

Pillay, D.L., Olalusi, O.B. and Mostafa, M.M. (2020). A review of the engineering properties of concrete with paper mill waste ash—towards sustainable rigid pavement construction. *Silicon*, pp.1-17.

Contributions of each author

Pillay, D.L. – Main contributing author, performed the necessary research required and conducted the literature review.

Olalusi, O.B. – provided technical advice.

Mostafa, M.M. – provided technical advice.

…… ……16/01/2021……
DEVESHAN PILLAY (STUDENT) DATE

[redacted]…… ……19/01/2021……
PROF MOSTAFA (CO-AUTHOR) DATE

[redacted] ……19/01/2021……
DR OLALUSI (CO-AUTHOR) DATE

ACKNOWLEDGEMENTS

I would like to express my sincere thanks and appreciation to the following persons and/or organisations:

- My family, Derek, Jeniffer and Jerishka Pillay, for their everlasting support and encouragement throughout my studies.
- My supervisors, Prof Mostafa and Dr Olalusi, for their mentorship, technical advice and encouragement throughout this dissertation.
- My civil engineering friends and colleagues for their companionship and inspiration.
- The UKZN Civil Engineering lab staff, technicians and vacation work students, for their assistance with the casting, demoulding and testing of the concrete samples.
- Mondi Merebank, for providing the paper mill ash that was used for the experimental investigation in this study.
- Contest – Concrete Technology Services, for their assistance with conducting the durability index tests.
- LA Consulting Engineers (Pty) Ltd and Raubex KZN, for the technical advice provided for the construction cost analysis.
- Umlaas Road Cartage and Just Build, for providing the material rates used in the cost analysis.

TABLE OF CONTENTS

LIST OF FIGURES

LIST OF TABLES

LIST OF ABBREVIATIONS

C&CI	Cement & Concrete Institute
CEPI	Confederation of European Paper Industries
CO_{2e}	Equivalent Carbon Dioxide
CRC	Continuously Reinforced Concrete
C-S-H	Calcium Silicate Hydrate
DCP	Dynamic Cone Penetrometer
DOT	South African National Department of Transport
GGBS	Ground Granulated Blastfurnace Slag
HCP	Hardened Cement Paste
ITZ	Interfacial Transition Zone
MFB	Multi Fuel Boiler
MIP	Mercury Intrusion Porosimetry
NPC	Natal Portland Cement
OPC	Ordinary Portland Cement
PC	Portland Cement
SAPEM	South African Pavement Engineering Manual
SEM	Scanning Electron Microscope
SFRC	Steel Fibre Reinforced Concrete
TG	Thermogravimetry
UTCRC	Ultra-thin Continuously Reinforced Concrete
UTRC	Ultra-thin Reinforced Concrete
w/b	Water-binder Ratio
XRF	X-ray Diffraction

CHAPTER 1: INTRODUCTION

1.1) Background to the study

Concrete is the most used material in the construction sector, owing to its superior mechanical properties (versatility, superior strength and durability properties). Approximately, more than 1 m^3 of concrete is evaluated to be produced universally per individual every year (Tamanna et al., 2020). The cement manufacturing industry accounts for about 5 to 7% of the total carbon dioxide (CO_2) emissions worldwide (Tamanna et al., 2020; Schneider, 2019; Doudart de la Grée et al., 2018). In 2020, the global annual cement production is expected to be 5.9 billion tons with more than 4.8 billion tons of CO_2 production (Singh and Middendorf, 2020). Other harmful greenhouse gases such as sulphur trioxide (SO_3) and nitrogen oxides (NO_X) are also emitted during the cement manufacturing process and can have a detrimental effect on the environment. In addition to releasing harmful compounds into the atmosphere, the production of Portland cement (PC) consumes significant quantities of raw materials and energy.

Concrete pavements, more commonly known as rigid pavements, are used predominantly in roadways and for other transportation applications such as parking lots, bridge decks, ports, airport aprons, toll stations and military facilities (Plati, 2019; Poongodi et al., 2020). Di Mascio et al. (2019) revealed that rigid pavements are 35% cheaper than flexible pavements over the service life of 20 years and are more suitable for areas with weak subgrade soil and poor drainage conditions (Pandey and Kumar, 2020). According to Jiao (2013), fuel consumption decreases by 3.2% for passenger vehicles and 4.5% for heavy vehicles while operating on rigid pavements. Also, there is a lower emission of CO_2. Based on these benefits, most of the national highways and expressways are being constructed as rigid pavements (Pandey and Kumar, 2020). The total proclaimed roads in South Africa amounts to approximately 535,000 km in length, with 366,872 km classified as non-urban roads and 168,000 km categorised as urban roads (SANRAL, 2020). It has been well documented that the pavement structure of numerous roadways within South Africa's ever-expanding road network are experiencing rapid mechanical and physical deterioration. This results in the reduction of the functional and structural levels of service provided by the roadway (SANRAL, 2013). Anderson et al. (2002) attribute this to poor design and construction practices, increased traffic volumes, inadequate materials selection and higher service life than the design life.

Plati (2019) reported that high bearing capacity, resistance to static and dynamic vehicular loading and long-term durability are the most important mechanical characteristics of rigid pavements. It is also established that rigid pavements achieve an improved service life and reduced maintenance costs when the available design guidelines and correct construction practices are followed

(Pandey and Kumar, 2020; SAPEM, 2013a). Large quantities of PC and aggregates are utilised during the construction of rigid pavements. However, the production of cement increases carbon footprint; and the source of natural aggregates depletes (Murthi et al., 2020; Thangapandi et al., 2020). The construction of rigid pavements comes at the expense of the environment (Pandey and Kumar, 2020). Therefore, a pavement design that incorporates sustainable materials and achieves a consistent level of quality is one of the primary goals for improving the sustainability of rigid pavements. Besides, there is an increased demand for alternate binder systems to address the growing concerns regarding the CO_2 emissions from the cement manufacturing (Schneider, 2019; Doudart de la Grée et al., 2018; Singh and Middendorf, 2020; Pandey and Kumar, 2020; Kumar et al., 2020). The amount of cement being manufactured for concrete production purposes can be reduced by incorporating supplementary cementitious binder materials, such as paper mill ash (PMA).

In 2014, global paper production exceeded 400 million tonnes per year, which was also the year that atmospheric CO_2 levels surpassed 400 ppm (Environmental Paper Network, 2018). Environmental Paper Network (2018) reported that Africa consumes 2% of the total paper produced on a global scale, which is equivalent to approximately 8 million tonnes per year. As of 2018, South Africa had consumed 2.344 million tonnes of paper, which increased by 4% in comparison with 2017s consumption levels (PAMSA, 2018). South Africa is the 15th largest producer of pulp in the world and is ranked 24th when it comes to global paper production (FP&M SETA, 2014). However, PMA is still a relatively new binder material to South Africa's concrete industry.

The use of PMA, as a partial cement replacement material in concrete production significantly affects the performance of concrete. To use such concrete in rigid pavement construction, it is vital to understand its engineering properties thoroughly. Therefore, this research study will investigate the effectiveness of PMA as an alternative binder material in concrete and assess its feasibility for rigid pavement applications. The research to be undertaken will also provide further information that can be utilized to expand the sustainability and serviceability state of rigid pavements.

1.2) Motivation

South Africa experiences countless economic and social factors, such as unemployment and poverty, which inhibits development within the country. In South Africa, the road network is viewed as one of the key contributors to economic and social development (DOT, 2017). After comparing the economic factors associated with the numerous types of infrastructure, it was found that South African roadways deliver the highest return on investment (DOT, 2017). However, challenges such as increased road use, construction delays, inadequate maintenance procedures

and low investment prevents the road transportation industry from accomplishing the national objectives for social and economic growth. As a country, South Africa can attain a prosperous and well-functioning economy by adopting road design, construction and maintenance processes that are effective and efficient.

The construction of rigid pavements in South Africa only began in earnest during 1968, with it only being used in special circumstances prior to 1968 (Mitchell et al., 1988). The high traffic volumes that were being experienced on South African roadways at the time were making it increasingly difficult and expensive to repair and maintain the pre-existing national routes. This led to the construction of rigid pavements, as these pavements required minimal maintenance which resulted in reduced service life costs (Di Mascio et al., 2019). According to Plati (2019), high bearing capacity, resistance to static and dynamic traffic loads and long-term durability are some of the other beneficial characteristics associated with rigid pavements.

However, it is worth noting that numerous South African roadways are displaying signs of mechanical and physical deterioration. Furthermore, the construction of rigid pavements results in adverse environmental impacts, as large quantities of PC, natural aggregate material and energy are consumed. With growing concerns surrounding the CO_2 emissions from the cement manufacturing industry, there is an increased need for pavement designs that utilize sustainable construction materials and satisfies the service life design requirements for South African roadways. For rigid pavements, this is achieved by implementing alternate binder systems that reduces the amount of cement that is produced for concrete construction purposes.

In this research study, paper mill ash (PMA) was the supplementary cementitious material that was selected. The incorporation of PMA as a partial cement replacement in concrete serves as a more sustainable alternative to disposing of the waste material via land spreading or landfilling operations. A systematic review of past research studies revealed that PMA exhibited pozzolanic properties when the incineration temperature ranged from 700 °C to 750 °C (Frías et al., 2008a; Garcia et al., 2008; Pera and Amrouz, 1998; Vegas et al., 2006). The extensive review of previous literature also revealed that the workability performance of PMA based concrete declined as the PMA replacement level increased. Reduced workability is a favourable characteristic for concrete used in paving operations. Numerous past studies have recommended incorporating superplasticisers and water-reducing admixtures to improve the workability performance of PMA concrete. However, the effect a higher w/b ratio has on the workability properties of concrete containing PMA has not been investigated. This point will be addressed in this research study. The mechanical properties, namely compressive, flexural and tensile splitting strength, improved until the optimum PMA content (5 to 10%) was achieved. The experimental investigations conducted by Gailius and Laurikietytė (2003) and Bai et al. (2003) both determined that GGBS

is a complimentary blending agent with PMA, which was the main consideration when selecting the primary binding agent for this research study.

Tensile or flexural strength is considered to be the defining design variable for rigid pavements. Therefore, the favourable flexural and tensile splitting strength performance that was documented across the numerous research studies proves the feasibility of concrete containing PMA for use in rigid pavement applications. The long-term strength development of PMA based concrete, in combination with the negligible CO_{2e} emission value of PMA further highlights the beneficial effect PMA can have in enhancing the serviceability and sustainability performance of rigid pavements.

However, it is also worth mentioning that the engineering performance of concrete containing PMA has not been evaluated in accordance with the standards outlined in the South African Pavement Engineering Manual (SAPEM). Frictional resistance, cracking resistance, shrinkage, creep and construction costs have been identified as important pavement properties that were not assessed for PMA based concrete. Furthermore, minimal research has been undertaken to analyse the durability and microstructure performance of concrete incorporating PMA as an alternate binder material. It was also noted that the durability performance of concrete containing PMA had not been evaluated in relation with the South African durability index tests. Therefore, the findings documented in this research study will be useful for researchers and stakeholders in the construction industry to acquire more understanding of PMA concrete.

1.3) Research question

This research study seeks to provide answers to the following questions:

- What effect does partial replacement of Portland cement with paper mill ash have on the fresh and hardened state properties of concrete?
- How viable is it to use paper mill ash as an alternate binder material for rigid pavements?

1.4) Aims

This research study aims to investigate the engineering properties of concrete containing paper mill ash as supplementary cementitious material, with a view to examining its suitability for rigid pavement applications.

1.5) Objectives

The specific objectives of this research study are to:

- Conduct a review of literature studies pertaining to the mechanical, durability and sustainability properties of concrete and to present a detailed assessment of the use of concrete in rigid pavement applications.
- Examine the effect of the partial replacement of Portland cement, with paper mill ash, on the fresh state properties of concrete.
- Investigate the effect of the partial replacement of Portland cement, with paper mill ash, on the mechanical and durability properties of concrete.
- Determine the optimum paper mill ash incremental level for achieving the best fresh and hardened state properties in conventional concrete.
- Evaluate the feasibility of paper mill ash as an alternative binder material for rigid pavements by:
    i) Comparing the engineering properties of paper mill ash-based concrete to the relevant design standards for rigid pavements in South Africa
    ii) Assessing the equivalent carbon dioxide (CO_{2e}) levels and material cost for each mix used in the experimental investigation
    iii) Conducting a construction cost analysis for a typical rigid pavement scenario.
- Perform a comprehensive analysis of the results obtained and provision of recommendations for future research.

1.6) Scope and limitations of the research study

The scope of this research study consists of the following engineering parameters, which will be used to assess the feasibility of PMA as an alternate binder material for rigid pavement applications:

- Fresh state performance, i.e. workability, of concrete containing varying amounts of PMA.
- Mechanical strength properties, namely the 7- and 28-day compressive, flexural and tensile splitting strength, of concrete incorporating paper mill ash as a supplementary cementitious material.
- Oxygen permeability, water sorptivity and chloride conductivity performance of PMA based concrete in relation with the South African Durability Index standards.
- Frictional resistance characteristics of concrete slabs containing various increments of PMA.
- Sustainability (CO_{2e}) properties of all PMA based concrete mixes that were utilized in this research study.
- Economic analysis, namely the material and construction costs, of concrete incorporating PMA as a partial cement replacement.

The following limitations were experienced during this research study:

- 7, 28- and 56-day strength tests were originally planned for all concrete mixes. However, due to lockdown restrictions resulting from the Coronavirus (Covid-19) pandemic in South Africa, it was not possible to conduct the 28 and 56 day strength tests for the 0%, 5% and 10% PMA concrete mixes (the 15% and 20% PMA samples were yet to be cast at this stage). After consultation with the research supervisors and laboratory staff, it was agreed that 180 and 200-day strength tests would be performed for the specimens that were already cast pre-lockdown in order to create an accurate data set that was used to predict the 28-day strength of these samples. Likewise, only 7- and 28-day samples were cast for the 15% and 20% PMA mixes. This plan of action (i.e. testing the existing specimens and reducing the number of samples for the remaining mixes) was deemed to be the most feasible as there were a limited number of laboratory technician's available post-lockdown to assist with the mixing phase.
- Due to the coronavirus lockdown, the 0%, 5% and 10% PMA samples were removed from the bath after the 7-day strength tests and air cured for the remaining period of time. This process, which was repeated for the 15% and 20% PMA concrete mixes, could have led to variations in the strength results that were achieved.
- The UKZN Civil Engineering laboratory did not have any blending equipment, which meant that the PMA could not be blended with the cement during the mixing phase (this process was performed in most past year studies). This could have resulted in an uneven distribution amongst the constituent materials, which impacts on the results that were obtained.
- A concrete microstructural analysis and a chemical analysis of the PMA sample could not be performed as the scanning electron microscope (SEM) at UKZN Westville campus was broken.
- Only two slabs were cast for each concrete mix, therefore it was not possible to assess the skid resistance and surface texture properties of concrete slabs containing other forms of texturing (tining and burlap drag).
- Due to the limited time constraints that were available, the cracking resistance, shrinkage, elastic modulus and creep properties of the PMA concrete could not be assessed.
- The construction cost analysis only considered the cost to produce the concrete layer in the real-world scenario documented in Section 3.3 and not the total cost of the works to be undertaken. The project life costs were not accounted for in the cost analysis as this would constitute an entirely new research study.

1.7) Structure of the dissertation

This research thesis/dissertation consists of five chapters that outline the effect of paper mill ash on the engineering performance of concrete when incorporated as an alternative binder material.

The relevant information has been presented in an easily understandable and sequential manner with the following chapters:

Chapter 1 summarises the motivation and background information pertaining to the research study. This chapter also outlines the main research question, and the key aims and objectives that will be satisfied in the subsequent chapters of this document.

Chapter 2 details the review of pertinent literature which aims to provide background knowledge and understanding of the important concepts associated with rigid pavements. This includes a detailed analysis of the pavement properties, design requirements, variations, joint design, construction processes, repair and rehabilitation mechanisms for rigid pavements. This chapter also focused on the fresh state, mechanical strength, durability and microstructure properties of concrete used to construct rigid pavements. The literature review then analysed the engineering performance of paper mill ash-based concrete for potential use as an alternate material for sustainable rigid pavement construction.

Chapter 3 describes the various research approaches that were adopted to achieve the aims and objectives for this study. This chapter also outlined the experimental testing procedures that were followed during the experimental investigations that focused on evaluating the engineering performance (namely workability, mechanical strength and durability) of paper mill ash as a supplementary cementitious material for concrete manufacturing purposes. Frictional resistance tests, a CO_{2e} assessment, material cost analysis and a construction cost analysis based on a typical rigid pavement scenario were also used to evaluate the viability of concrete containing paper mill ash for sustainable concrete pavement construction.

Chapter 4 presents the results that were attained from the numerous experimental investigations that were undertaken in this research study. The experimental results were also comprehensively analysed in this chapter, in order to determine the feasibility of paper mill ash as an alternate binder material for sustainable rigid pavement construction. This in-depth assessment sets the background for the concluding remarks and recommendations for future research studies that will be noted in Chapter 5.

Chapter 5 discusses the conclusions that were provided in Chapter 4 and evaluates the degree of success in achieving the research aims and objectives that were summarised in Chapter 1 before providing the final concluding remarks. This chapter also outlines the potential research gaps that could be addressed in future investigations.

CHAPTER 2: LITERATURE REVIEW

2.1) Introduction

This chapter consists of a review of the relevant literature pertaining to the key areas of interest that are associated with the research topic. Chapter 2 initially discusses the local road network in South Africa and the various uses of concrete in the transportation engineering sector. This leads to a detailed analysis of the properties, design requirements, variations, joint design, construction procedures, repair and rehabilitation strategies for rigid pavements. This chapter then outlines the main fresh state, mechanical, durability and microstructure properties of concrete used for rigid pavement applications. The literature review also introduces the idea of incorporating alternate binder materials for concrete pavements. This point is further elaborated with a critical assessment of the engineering properties of paper mill ash as a partial cement replacement material for sustainable concrete pavement construction. The assessment included a systematic review of the experimental results documented across various literature works, from which it was concluded that paper mill ash is a feasible alternate binder material for rigid pavement applications.

2.2) South African Road Network

As a country, South Africa encounters countless developmental impediments and numerous social and economic demands such as inequality, unemployment, and poverty. The South African road network is one of the main contributors towards economic growth in the country. When comparing the various types of infrastructure's economic factors, it is often found that roads deliver the highest return on investment (DOT, 2017). Even though the road transportation industry is a significant constituent in South Africa's economy, there are still several challenges that constrain its role in accomplishing the country's objectives for social and economic development. Challenges such as delayed road implementation, increased road use, poor maintenance, and low investment lead to increased transportation costs and transport bottlenecks (DOT, 2017).

A successful, well-functioning economy can be achieved by implementing an efficient design, construction, maintenance, and rehabilitation procedures for roads in South Africa. Roads play a major part in attaining the societal requirements for mobility and connection in South Africa's continuously expanding human settlements, while the construction and maintenance processes associated with roads provide opportunities to address the country's high unemployment rate. With growing concerns surrounding the global effects of air pollution and climate change, there is an increased emphasis for the needs of roads to switch focus away from servicing mainly private vehicles and road based freight, and should be geared more towards creating integrated mobility systems based on public transport, walking, cycling and rail/sea freight (DOT, 2017).

In response to the aforementioned, South Africa needs to make sure that the national roads policies utilize infrastructure budgets efficiently to advance social, environmental, and economic development in the country. It is also the prerogative to develop a "greener" road network in South Africa that supports an approach inclined towards improving the roads management sector (DOT, 2017).

The South African road network is categorized under the prerogative of the three spheres of government (National, Provincial and Municipal). The main responsibility of the South African National Department of Transport (DOT) is to facilitate the development of an integrated and efficient transportation system. This is achieved by implementing suitable policies, models and regulations that are sustainable and can be easily implemented by the various Road Authorities (DOT, 2017).

South African Road Authorities are required to deliver an effective, efficient, integrated, and reliable transport system that supplements the country's sustainable social and economic development targets. According to DOT (2017), it is the duty of all Road Authorities to:

- Ensure successful planning, designing, construction and maintenance of the road network
- Monitor the public investment associated with the road infrastructure
- Ensure that the transportation system has continuous functionality
- Endorse the safety of all individuals that utilize the road network

South Africa's National Development Plan (NDP 2030) states that road infrastructure is a key contributor to the country's economy (DOT, 2017). However, key factors such as insufficient funding for the implementation and maintenance of road infrastructure are often viewed as being common inhibitors (DOT, 2017). Hence, roads are a key asset in South Africa and will begin to deteriorate without any major investment.

Therefore, South African road networks must be designed, constructed, and maintained to complement the objectives outlined in the National Development Plan. Furthermore, the national roadways should be controlled as assets, with overall responsibility being allocated to the relevant Road Authorities. South Africa's roads must first and foremost be safe and accessible for all users but should also provide a high level of service at an affordable cost, while being well maintained on a regular basis (DOT, 2017).

2.3) Concrete applications in transportation engineering

This section of the literature review contains an outline of the various concrete applications in transportation and roads engineering, with an emphasis on concrete pavements, and the requirements for the design and assessment of the aforementioned applications.

2.3.1) Concrete used for road structures

Due to concrete's versatility and superior durability properties, it is able to serve a wide variety of purposes in road structures and furniture for pavements. Concrete may be utilized in its fresh state for on-site applications, or alternatively it can be used for precast applications either on or off-site.

- **In situ concrete –** concrete can be used to cast in situ applications such as bridges, culverts, manholes, kerbs, side drains, median and other barriers as well as foundation bases for lighting masts and road signs (SAPEM, 2013d). In situ concrete is generally selected to construct the decks, support columns and abutments for bridges. Various construction techniques such as in situ, launched and balanced cantilever can be adopted when constructing bridge decks.
- **Precast concrete –** concrete in its precast form can be used in numerous construction applications, including stormwater pipes, kerbing, manhole covers, culverts, bridge beams, bridge decks, median and other temporary or permanent barriers (SAPEM, 2013d). These items can be procured from a supplier or cast in a designated precast yard on site.

2.3.2) Concrete used for pavements

Road pavements are classified according to the type of materials used for constructing the upper pavement layers, specifically the surfacing for the road. Flexible pavements have an asphalt or seal surfacing which enables them to bend on the support, whereas rigid pavements have a concrete surfacing layer that behaves in a rigid manner and does not bend (SAPEM, 2013a). The type of material selected for the pavement surfacing determines the performance of the pavement in a particular climate with a specific level of traffic, and the distress mechanisms that may develop in the pavement structure over time (SAPEM, 2013a).

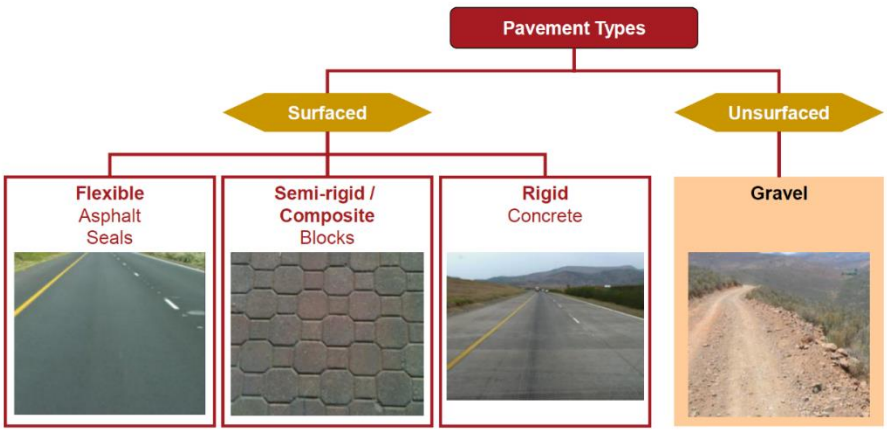

Figure 2-1: Pavement types classified according to surfacing material (SAPEM, 2013a)

2.4) Rigid pavements

2.4.1) Rigid pavements in South Africa

Preceding 1968 rigid pavements were utilized only in special circumstances in South Africa. Hand methods and rudimentary plant were the primary procedures adopted to construct concrete pavements, however these methods failed to produce the longitudinal profile required to accommodate modern traffic (Mitchell et al., 1988). The transverse joints were created manually, and bitumen was used as the sealing agent. The bitumen tended to extrude from the pavement, which resulted in an uneven paved surface with a poor ride quality for moving motor vehicles (Mitchell et al., 1988).

Consequently, the construction of rigid pavements ceased during the 1950's and 1960's (Brink, 2006). The results observed during the AASHTO road test, in conjunction with the various studies relating to rigid pavement performance that were conducted at the time, encouraged interest in using rigid pavements to counteract the rapidly increasing traffic loads experienced on South African roads (Mitchell et al., 1988).

The high traffic volumes made it dangerous and expensive to repair and rehabilitate the pre-existing national routes, therefore the need for a pavement surface that required minimal maintenance arose. As a result of this, construction of rigid pavements began in 1968 in South Africa (Mitchell et al., 1988). This process involved incorporating continuously reinforced and jointed unreinforced concrete pavements for construction and rehabilitation purposes on selected routes (Brink, 2006). According to Brink (2006), the following routes were integrated with rigid pavements:

Table 2-1: Selected South African routes that were constructed with a rigid pavement (Source: Brink, 2006)

Route	Route Description	Year of Construction
N2 (Cape Town – Somerset West)	National Route	1968
N4 (Witbank – Middelburg)	National Route	1971
R22 (Witbank – Springs)	Provincial Route	1973
N3 (Estcourt – Frere)	National Route	1978
N1 (Vaal River – Johannesburg)	National Route	1979
N1 (Johannesburg – Pretoria)	National Route	1987/8

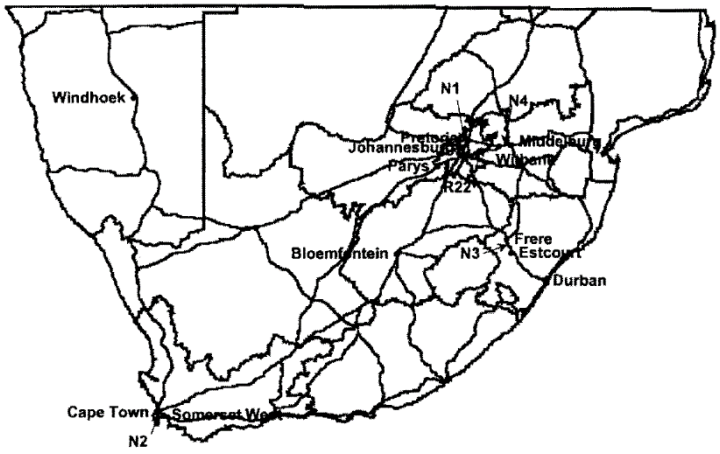

Figure 2-2: South African roads that have a concrete pavement (Source: Brink, 2006)

2.4.2) Properties of rigid pavements

As discussed in Section 2.3.2, pavement composition is the main variation between rigid and flexible pavements. Rigid pavements or concrete pavements typically consist of a concrete layer, with a thickness ranging from 150 mm to 350 mm, that functions as the surfacing and base layers of the pavement structure (SAPEM, 2013d). Flexible pavements on the other hand have an asphalt wearing course layer and a distinguishable base layer.

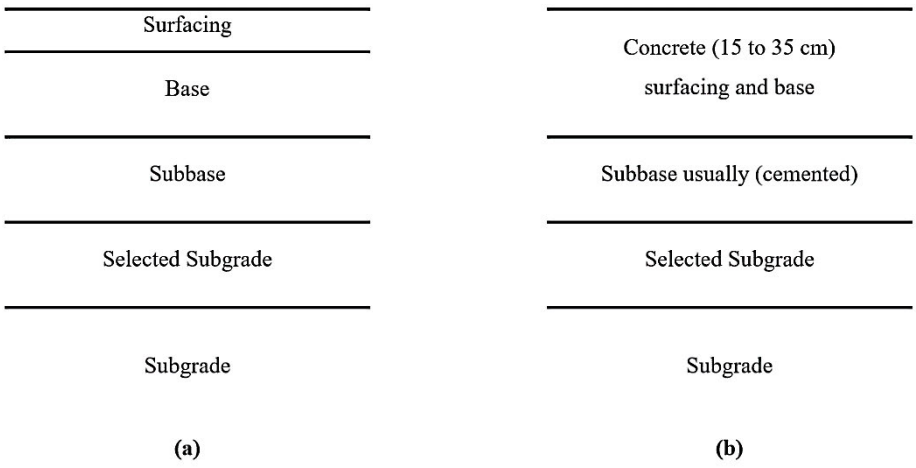

Figure 2-3: Typical pavement layerworks for (a) flexible pavements and (b) rigid pavements (Source: SAPEM, 2013a)

Much like the pavement design principles applied to conventional flexible pavements, similar design ideologies are also applied to rigid pavements. The stresses that are imposed by vehicle tyres at the tyre-pavement interface are dissipated over an area that increases with increasing depth within the pavement structure (SAPEM, 2013e). This leads to a reduction in the shear stress and stress concentration as the pavement structure depth increases. Therefore, the material

constituents used to construct the upper layers of the pavement structure require a high flexural and shear strength to resist the stress conditions that will be experienced.

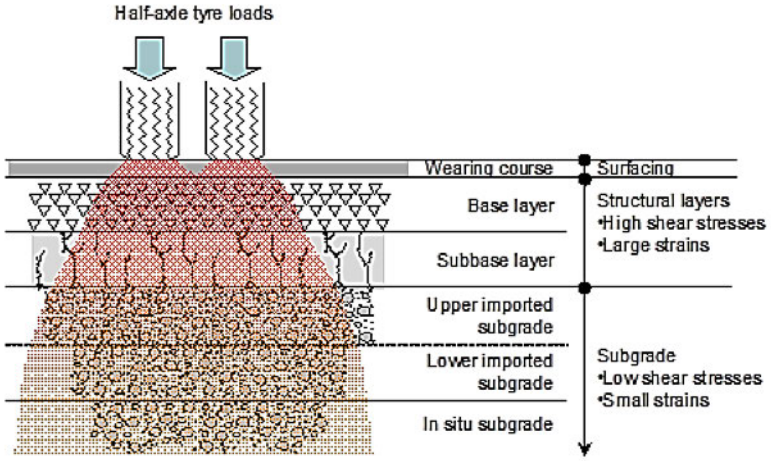

Figure 2-4: Typical stress distribution in a flexible pavement (Source: SAPEM, 2013e)

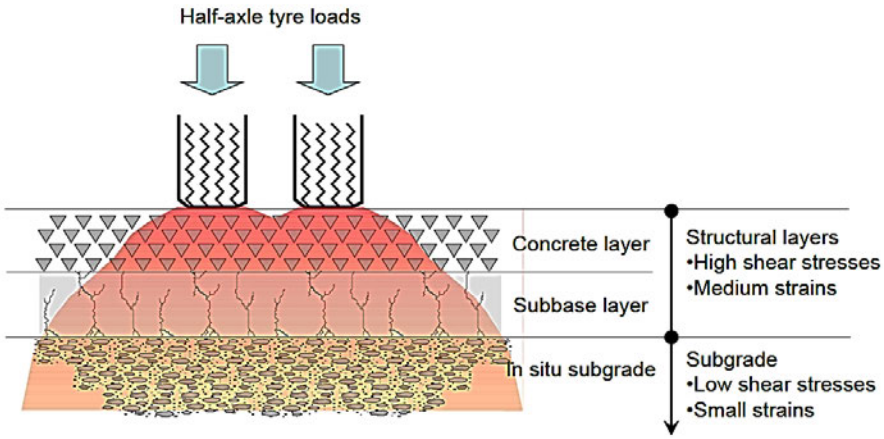

Figure 2-5: Typical stress distribution in a rigid pavement (Source: SAPEM, 2013e)

The shear strength, modulus of elasticity and material stiffness of concrete is higher than that of the asphalt or crushed stone base layers in flexible pavements, and the imposed stresses are dissipated more rapidly through the rigid layer (SAPEM, 2013e). Therefore, the thin concrete layer present in rigid pavements will offer similar protection to the subgrade as the much thicker layers of asphalt, crushed stone and gravel materials found in flexible pavements.

2.4.3) Requirements for rigid pavements

As with any pavement structure, the main function of a rigid pavement is to withstand the imposed traffic loadings and to satisfy the required performance criteria of the roadway over its design life. According to SAPEM (2013d), rigid pavements need to:

- Enable the imposed stresses experienced in the subgrade to be kept within a set of parameters that the subgrade can withstand, without developing a substantial elastic strain that may cause deterioration and deformation within the pavement structure.
- Withstand the imposed stresses caused by drying shrinkage and varying moisture and temperature conditions present in the concrete base.
- Be designed and constructed such that effects of subgrade moisture and temperature variation are minimal – failure to achieve this may lead to the propagation of cracks in the pavement structure due to changes in the subgrade strength and volume.

2.4.4) Types of rigid pavements

Various types of concrete pavements have been trialled both in South Africa and globally. The following are the most common types of rigid pavements to be constructed in South Africa, with the major difference being their crack control criteria.

2.4.4.1) Jointed Unreinforced/Plain Concrete Pavement

This type of rigid pavement usually contains no reinforcement, however in cases such as bridge approach slabs, small irregular areas with curved or angled edges or mismatched joints, reinforcement is incorporated into the pavement design (SAPEM, 2013d). Tie bars, which are used to keep the longitudinal joints closed, and dowel bars, which are used to distribute loads along transverse contraction joints, are commonly used in this type of pavement but are not considered to be reinforcement.

According to SAPEM (2013d), the majority of the existing concrete roads in South Africa have been designed and constructed with this type of rigid pavement. Dowels are only used in some jointed unreinforced concrete pavements and not all, while transverse contraction joints are constructed at regular intervals. Mohod and Kadam (2016) indicate that joint spacing varies between 5 to 10 m in jointed unreinforced pavements, whereas the joint spacing increases to between 10 and 30 m with the addition of reinforcement. Past research studies indicate that the addition of dowel bars makes jointed unreinforced concrete pavements a more cost-effective pavement alternative. This can be attributed to the improved pavement performance that was observed and a decrease in the frequency of faulting and failure occurrences (SAPEM, 2013d).

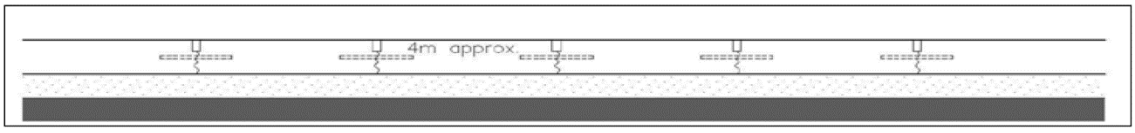

Figure 2-6: Jointed unreinforced/plain concrete pavement (Source: SAPEM, 2013d)

2.4.4.2) Continuously Reinforced Concrete (CRC) Pavement

Continuously reinforced concrete (CRC) pavements are being increasingly used in South Africa to construct overlays and inlays for existing asphalt and concrete pavements that are subject to deterioration (SAPEM, 2013d). The thickness for this type of rigid pavement ranges from 200 to 250 mm, which is usually less than the thickness of a typical jointed concrete pavement. The key design feature of CRC pavements, as indicated in Figure 2-7, is the presence of longitudinal reinforcement that is continuous for the length of the roadway.

The incorporation of longitudinal reinforcement into the design eliminates the need for transverse control joints and simultaneously reduces the disruption costs associated with the maintenance of these joints (SAPEM, 2013d). In the case of limited access roads that experience high traffic volumes, the latter is a key factor to consider when selecting the type of rigid pavement to be designed and constructed as the main reason for closing a lane to traffic will be eliminated with a CRC pavement.

Figure 2-7: Longitudinal reinforcement in a Continuously Reinforced Concrete (CRC) pavement (Source: SAPEM, 2013d)

The humid environmental conditions found in most parts of South Africa often leads to the loss of water in the cementitious elements of the concrete pavement structure, which results in drying shrinkage and the development of microcracks that are approximately 0.3 mm wide. The reinforcement present in CRC pavements, coupled with subbase friction, prevents the randomly spaced microcracks from widening and spreading. In order to satisfy a preferred microcrack spacing (1 m to 3 m), the required longitudinal steel reinforcement must lie within 0.5% and 0.7% of the concrete cross-sectional area (SAPEM, 2013d).

Although a larger quantity of steel is used, crack control is still the main function of the reinforcement in CRC pavements. Despite the fact that a CRC pavement has a higher amount of

reinforcement in comparison with a jointed reinforced pavement, the absence of dowels and joints results in an overall reduction of the associated construction costs.

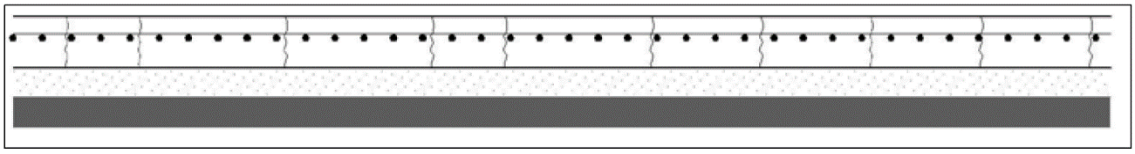

Figure 2-8: Continuously Reinforced Concrete (CRC) pavement (Source: SAPEM, 2013d)

2.4.4.3) Prestressed Concrete Pavement

According to SAPEM (2013d), prestressed concrete pavements were initially developed in the 1920s, however, major developments only occurred in the late 1940s with the following advantages being noted:

- Very few joints are required, and in some cases, it has been documented that no joints are needed
- Lack of cracking in the pavement structure when exposed to normal loads
- Minimal deformation under thermally induced warping stresses
- Reduced pavement thickness
- Flexible pavement structure

Even though a prestressed concrete pavement is significantly thinner than a jointed pavement, it is often found that the construction costs are considerably higher. It is important that the supporting layers for a prestressed concrete pavement are designed and constructed to a sufficient strength, which will enable the pavement structure to withstand excessive deflections resulting from the reduced thickness (SAPEM, 2013d).

2.4.4.4) Steel Fibre Reinforced Concrete (SFRC) Pavement

In this type of rigid pavement, a minimal amount of short steel fibres is dispersed all over the concrete, as illustrated in Figure 2-9. The steel fibres improve the fatigue resistance and flexural strength of the concrete, which results in a reduced pavement thickness. According to SAPEM (2013d), SFRC pavements have been trialled in the Gauteng province of South Africa and their performance is being observed continuously. SFRC pavements are a feasible option for scenarios that require unusual shapes (e.g. roundabouts), where it is difficult to incorporate an even distribution of joints. The financial feasibility of SFRC pavements can be improved by balancing the low construction costs associated with the reduction in pavement thickness against the inflated cost of including steel fibres in the concrete mix.

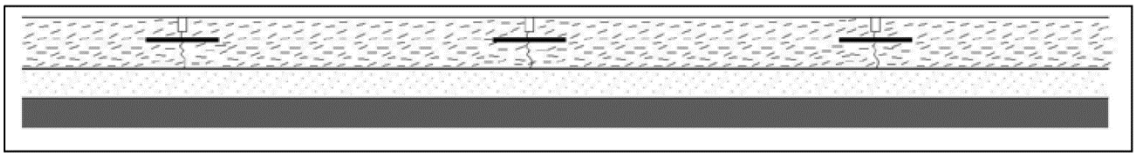

Figure 2-9: Steel Fibre Reinforced Concrete (SFRC) pavement (Source: SAPEM, 2013d)

2.4.4.5) Ultra-Thin Concrete Pavement

In the South African context, there are two forms of ultra-thin concrete pavements presently being used for rehabilitation purposes:

- Ultra-thin continuously reinforced concrete (UTCRC) pavements – used predominantly for heavy duty roadways that experience high traffic volumes.
- Ultra-thin reinforced concrete (UTRC) pavements – used on light duty roadways, such as township streets, that experience low traffic volumes.

2.4.4.5 (a) Ultra-Thin Continuously Reinforced Concrete (UTCRC) Pavement

An ultra-thin continuously reinforced concrete (UTCRC) pavement has a composite structure and is made up of high strength concrete that is fibre reinforced (Ebels et al., 2007). UTCRC pavements initially originated in Europe, where it has been used for industrial flooring purposes and rehabilitation of the pavement surface layer on bridge decks (Braam et al., 2004).

However, due to South Africa's deteriorating road network, major investment into the structural repair and rehabilitation of roadways is required from the various road authorities. The South African National Roads Agency Ltd (SANRAL) has since incorporated and developed the UTCRC pavement as a cost effective and innovative pavement repair plan that complies with South Africa's pavement requirements. In South Africa, UTCRC pavements serve as an alternate rehabilitation measure by offering a thin layer of flexible, high strength concrete that is constructed as a durable cover above a deteriorating pavement (Ebels et al., 2007).

The potential applications for UTCRC pavements are not only restricted to rehabilitative purposes on major roadways that are exposed to heavy traffic loads. According to Ebels et al. (2007), UTCRC pavements can also be applied as a durable, low maintenance surface layer in the following scenarios:

- Intersections that experience heavy stop/start traffic movement
- Truck inspection stations and weighbridges
- Solid waste stations and waste disposal sites
- Distribution centres and warehouses
- Container terminals

- Airport pavements

UTCRC pavements incorporate strain hardening cement-based composites (SHCC) and are constructed using high strength concrete that contains steel fibres and continuous steel mesh reinforcement in the middle of the pavement layer (Ebels et al., 2007). SAPEM (2013d) gives the following as the key features of UTCRC pavements:

- Thickness of the concrete layer ranges from 50 mm to 65 mm
- High strength cement is used to produce the concrete
- Strengths exceed 100 MPa
- The required longitudinal steel reinforcement must be approximately 3% of the gross cross-sectional area
- Can be fibre reinforced using steel or plastic fibres

Since 2005, numerous research studies and trial sections have been conducted to assess the feasibility of UTCRC pavements in South Africa. Kannemeyer et al. (2008) used a Heavy Vehicle Simulator (HVS) to conduct extensive research, which determined that UTCRC pavements are able to accommodate up to 90 000 000 Equivalent Standard Axles (E80's).

In 2010, the first trial section of a UTCRC pavement was successfully constructed on the National Route 1 (N1) near Cape Town in the Western Cape. This 4.3 km long section had a total surface area of 17 500 m^2 and served as a truck crawling lane connecting the Huguenot Tunnel to the Huguenot Toll Plaza (Ebels et al., 2007). The successful construction and implementation of the innovative UTCRC pavement section on the N1 demonstrated that UTCRC pavements are a viable option for heavy duty roadways in South Africa.

The main advantage of a UTCRC pavement is that it serves as a long-lasting pavement layer that requires minimal maintenance, which can be attributed to the inclusion of concrete and reinforcement in the design. Due to the reduced pavement thickness, only a thin layer of the existing layerworks will be milled off when constructing a UTCRC pavement (SAPEM, 2013d). This proves to be advantageous when UTCRC pavements are constructed in areas with limited vertical clearance (e.g. below bridges and overpasses).

Table 2-2: Description of various South African projects incorporating UTCRC pavements (Source: SAPEM, 2013d)

Project	Year	Pavement Thickness	Description
Heidelberg Traffic Control Central Center (N3)	2007	50 mm	Used for HVS testing
N1 (Cape Town)	2010	50 mm	Extreme temperatures (>40°C) resulted in buckling – resolved by adding edge restraints
N2 Tongaat Toll Plaza	2011	50 mm	Constructed without joints, due to the width of the pavement – resulted in longitudinal buckling
N12 (Benoni & Boksburg)	2012	50 mm	Pavement was overlaid with an asphalt ultra-thin friction course to improve noise and skid resistance

UTCRC pavements have been applied in numerous projects in South Africa, the details of which have been summarized in Table 2-2. The main challenge experienced in the above-mentioned projects was the amount of monitoring and quality control required during the construction phase, particularly when constructing the joints. In order to mitigate these problems, SAPEM (2013d) recommends using a pavement thickness ranging from 60 to 65 mm.

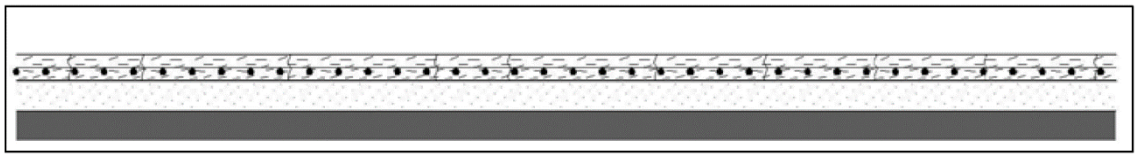

Figure 2-10: Ultra-Thin Continuously Reinforced Concrete (UTCRC) pavement (Source: SAPEM, 2013d)

2.4.4.5 (b) Ultra-Thin Reinforced Concrete (UTRC) Pavement

According to SAPEM (2013d), Ultra-Thin Reinforced Concrete (UTRC) pavements are commonly used for light duty pavements, and has the following features:

- Pavement thickness is approximately 60 mm
- Longitudinal steel reinforcement constitutes 0.3% of the pavement structure – no fibre reinforcement is used

UTRC pavements have been analyzed in detail at the Roodekrans testing facility using heavy vehicle loading, where it was determined that UTRC pavements are able to carry a load of up to 1 000 000 E80's (Steyn et al., 2005; du Plessis et al., 2011).

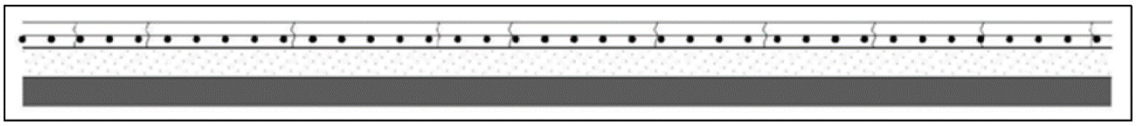

Figure 2-11: Ultra-Thin Reinforced Concrete (UTRC) pavement (Source: SAPEM, 2013d)

2.4.4.6) Composite pavement

According to Goel and Das (2004), there are two types of composite pavements, namely flexible composite pavement and rigid composite pavement. Flexible composite pavements consist of a top layer of concrete laid directly above a flexible (i.e. bituminous) base. Conversely, rigid composite pavements are made up of a bituminous top layer laid directly over a concrete base (Goel and Das, 2004). The main purpose of composite pavements is to combine the favourable flexibility, strength and durability properties associated with rigid and flexible pavements (Goel and Das, 2004).

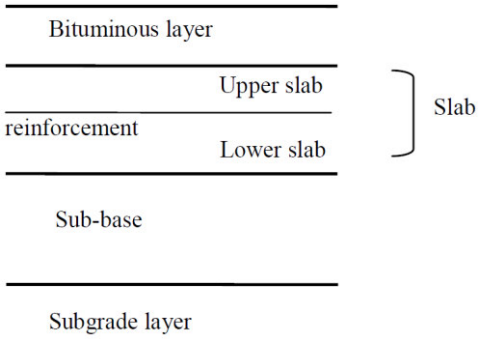

Figure 2-12: Layerworks for rigid composite pavement (Source: Goel and Das, 2004)

2.4.4.7) Ultra-thin whitetopping

Overlaying is a widely recognized rehabilitation technique for deteriorating pavements. However, according to Goel and Das (2004), ultra-thin whitetopping is still a relatively new design concept that is gradually gaining acceptance from industry professionals. It involves overlaying the existing asphalt pavement with a thin layer of concrete. This type of pavement is more feasible that conventional overlays when considering the durability performance, construction time and costs associated (Goel and Das, 2004). Ultra-thin whitetopping is better suited to areas with low volumes of traffic, i.e. bus stops, toll plazas, intersections, airport runways and taxiways.

With this paving technique, a thin layer of high strength concrete (usually fibre reinforced) is laid over a bituminous pavement that has been milled (Goel and Das, 2004). The bond between the two pavement layers enables it to share load similarly to a monolithic section. The bond also shifts the neutral axis of the concrete from the center of the concrete layer to the bottom, which reduces the stresses in the lower portion of the concrete layer. The shift to the neutral axis will also lead to the critical load moving from the edges to the corners of the pavement which increases the

corner stresses (Goel and Das, 2004). However, this effect can be counteracted by using short joint spacing to reduce the area of the concrete slab that can warp or curl (Goel and Das, 2004)

2.4.5) Types of joints for rigid pavements

According to Perrie (2003), rigid pavements are furnished with joints to:

- Reduce stresses experienced, limit cracking as a result of restrained contraction and control the effects of restrained warping and vehicular loading
- Simplify construction and level control
- Accommodate movements resulting from expansion and contraction

Joints are required to provide tolerable transfer of imposed loads to improve the structural and serviceability performance of concrete pavements. When joints are closely spaced in low volume concrete roads, then rebar is not required (Perrie, 2003). However, Perrie (2003) goes on to explain that the addition of mesh reinforcement or reinforcing steel bars may be effective in scenarios such as: bridge approaches, pavement sections with substandard subgrade layerworks, irregularly shaped slabs and slabs that have a length to width ratio that is higher than 1:25.

The following are the most commonly used joint types in rigid pavements:

- Longitudinal joints
- Transverse joints
- Isolation joints

2.4.5.1) Longitudinal joints

Longitudinal joints constitute both construction and contraction joints and are incorporated to limit longitudinal cracking. The permissible longitudinal joint spacing limits for the respective road categories has been summarized in Table 2-3.

Table 2-3: Permissible longitudinal joint spacing for various road categories (Source: Perrie, 2003)

Road Category	Joint Spacing
Two-lane and multi-lane roadways	3 to 4 m
Arterial streets	< 4 m*

*Joints should be sufficiently spaced to provide delineation for traffic and parked vehicles

Longitudinal joints are dependent on tie bars to transfer imposed loads, maintain structural and serviceability capacity and provide lane delineation. In cases where the pavement is laterally restrained by backfill behind the kerbing, there is no need for tie bars (Perrie, 2003). However, in scenarios where the pavement is not laterally restrained, tie bars are required to be positioned 600 or 750 mm apart at mid-depth of the concrete pavement.

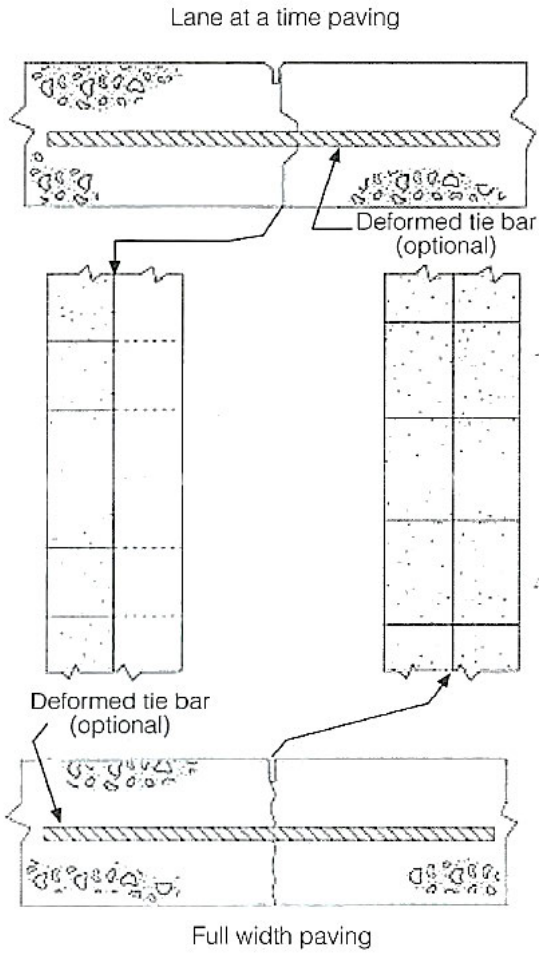

Figure 2-13: Longitudinal joints incorporating tie bars (Source: Perrie, 2003)

2.4.5.2) Transverse joints

Transverse joints serve the primary purpose of controlling the propagation of cracks across the pavement width. According to Perrie (2003), these joints also reduce the tensile stresses caused by the contraction of the pavement slab and limits the amount of curling stresses resulting from the temperature and moisture gradients present. Much like longitudinal joints, transverse joints also constitute both construction and contraction joints.

Perrie (2003) states that transverse construction joints are typically keyed and left untied. In rigid pavements these joints are commonly used when concrete is poured at different periods of the project. This includes the following interruptions to paving operations:

- Interruptions occurring at the end of the day's paving operations
- Unplanned interruptions greater than 30 minutes resulting from inclement weather or breakdown of equipment
- Interruptions resulting from casting alternate panels in between pre-determined longitudinal and transverse construction joints

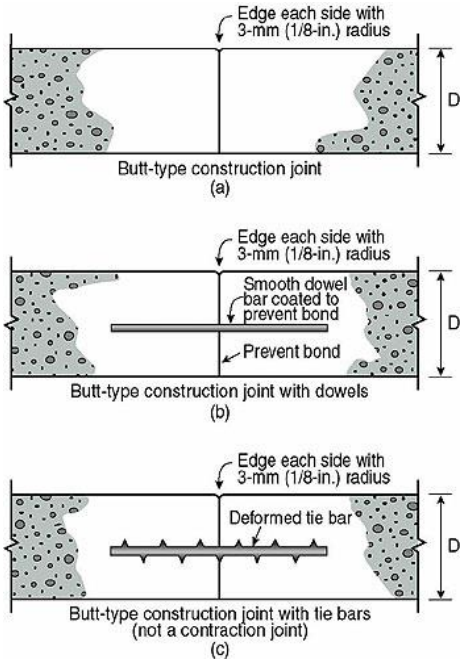

Figure 2-14: Section view of typical construction joints (Source: Day, 2020)

Transverse contraction joints are constructed by either saw-cutting the panel after the concrete has set or by inserting a strip of plastic/preformed material as the fresh concrete is being poured. The construction method to be selected is dependent on numerous extrinsic factors, such as the weather conditions experienced during construction, the aggregate characteristics, the operational costs associated, and the experimental results obtained. The joint depth for transverse contraction joints should be approximately a quarter of the concrete pavement slab thickness or a third of the pavement thickness for rigid pavements resting on cement-stabilized subbase material (Perrie, 2003).

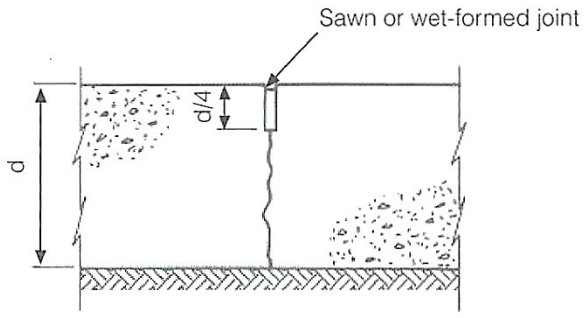

Figure 2-15: Section view of a typical transverse contraction joint (Source: Perrie, 2003)

However, based on the design requirements for the pavement thickness, load-transfer devices, such as round mild steel dowels, are added to the transverse contraction joint to provide supplementary load transfer via aggregate interlock (Perrie, 2003). Careful installation procedures need to be followed, as the dowels complicate the construction process.

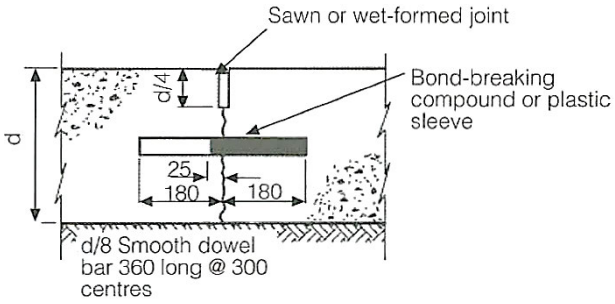

Figure 2-16: Section view of a typical transverse contraction joint with dowel bars inserted (Source: Perrie, 2003)

2.4.5.3) Isolation joints

Isolation joints segregate the rigid pavement from another structure, paved area or in-pavement structures such as stormwater drainage inlets, manholes, footings and lighting structures (Perrie, 2003). Other examples of isolation joints include full-depth and full-width joints at ramps, T-junctions, unsymmetrical intersections, bridge approaches or along the interface between old and newly paved areas.

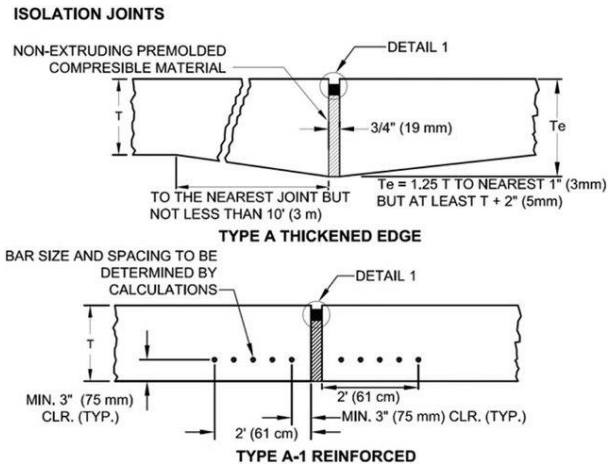

Figure 2-17: Section view of a typical isolation joint (Source: Cunliffe et al., 2016)

2.4.5.4) Joints between concrete and asphalt pavements

In South Africa, concrete inlays can be constructed on the slow lane of major roadways, with asphalt being used to construct the remaining lanes and shoulders. Special construction procedures should be followed when constructing the joint between concrete and asphalt pavements in order to enable the asphalt to form a strong bond with the concrete. According to SAPEM (2013f), an edge form with a chamfered edge that creates a 45° angle is used to construct the concrete layer. The concrete layer is usually constructed marginally higher than the existing pavement surface before the asphalt layer is paved into the chamfered edge of the concrete inlay (SAPEM, 2013f). The joint between concrete and asphalt pavements are only required for the

longitudinal joint, while a straight vertical joint that can be sealed is only required along the transverse direction between the concrete and asphalt layers (SAPEM, 2013f).

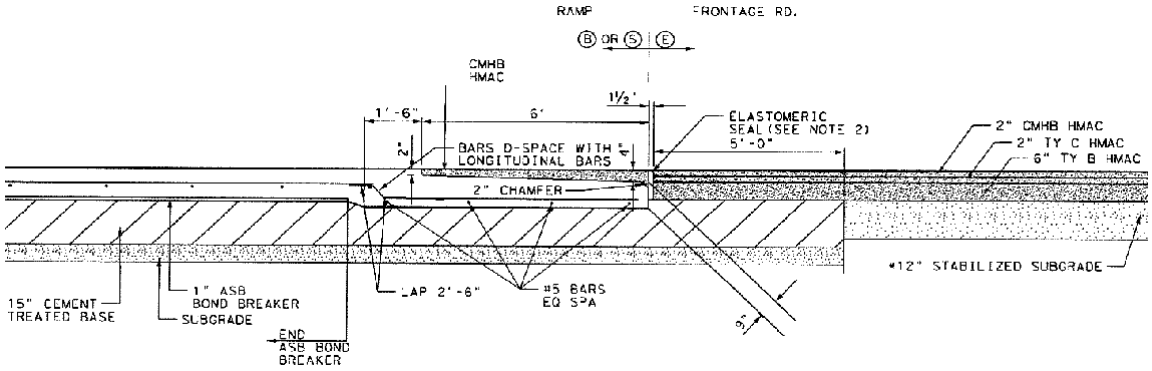

Figure 2-18: Section view of a typical joint between concrete and asphalt pavements (Source: Zollinger and Tayabji, 2007)

2.4.6) Layout of joints

Perrie (2003) gives the following guidelines for designing the layout of joints in rigid pavements:

- Avoid creating irregularly shaped panels
- Maximum longitudinal joint spacing = 3.8 m
- Maximum transverse joint spacing = 25 times the pavement thickness or 4.5 m
- Keep the panel shape as close as possible to a square
- Joints should intersect one another to mitigate the development of reflection cracking into neighboring lanes, i.e. joints should not be stepped
- Joint angle should be greater than 60°
- Secondary structures, for example manholes, should be segregated from the pavement
- Pavement thickness of paved areas adjacent to secondary structures should be increased by 20%
- Pavement slabs that are non-rectangular or adjacent to manholes must be reinforced in two equally perpendicular directions with 0.5% mesh reinforcement that is 50 mm below the top of the slab
- Reinforcement must not pass through the joint and should stop 75 mm on either side of the joint

2.4.7) Joint sealing

The primary purpose of joint sealant in rigid pavements is to mitigate infiltration of surface runoff and incompressibles into the pavement joint (Perrie, 2003). The incompressibles produce point-bearing pressures within the pavement structure which results in surface distress such as spalling.

According to Perrie (2003), transverse contraction joints that are narrow (i.e. 2 to 3,5 mm wide) can remain unsealed if:

- Traffic loading is light
- Traffic loading is heavy, and the pavement is located in a dry climate
- Traffic loading is heavy, the pavement is located in a wet climate and dowels are added to the joint

Perrie (2003) also stipulates that an annual precipitation of 800 mm is the indicator distinguishing dry and wet climatic conditions. Joints can be sealed using preformed elastomeric compression joint seals or a single component silicone with a low modulus of elasticity.

2.5) Construction processes for rigid pavements

Studies have shown that zones of early failure in rigid pavements can be attributed to poor construction processes and substandard workmanship. Therefore, it is crucial that control measures are implemented consistently, and continuous monitoring occurs regularly during the construction phase (SAPEM, 2013f). Equipment used for concrete paving operations can range from rudimentary equipment, which requires a great deal of manual work, to much more advanced mechanized paving trains. There are various types and models of paving machines that can be used for constructing concrete pavements, with slip form and fixed form machines being the most widely used.

2.5.1) Fixed form paving

During the fixed form paving construction phase, the concrete is spread, compacted, and finished between side forms that are fixed. These forms are made from timber or steel that are temporarily secured to the subbase and should also incorporate rails to support and direct the paving machine (SAPEM, 2013f). Fixed form paving usually requires additional equipment, such as a spreader, compactor/vibrator, and a beam finisher; to supplement the paving machine. Extra machinery is needed to form the joints, place the rebar and dowels, and to add surface texturing to the finished pavement surface. According to SAPEM (2013c), the fresh concrete should have a slump ranging from 20 to 70 mm when fixed form paving equipment is used. Likewise, when manually operated fixed form paving equipment is utilized, the recommended concrete slump should lie between 50 and 100 mm (SAPEM, 2013c).

Figure 2-19: Fixed form paving methods used to construct a rigid pavement (Source: SAPEM, 2013f)

2.5.2) Slip form paving

During the slip form paving process, concrete is compacted and finished within the length of a single slip form paving machine frame and between travelling side forms (SAPEM, 2013f). Depending on the type of slip form paving machine used, concrete can either be supplied directly to the machine, or spread and initially finished by another machine operating ahead of the main paving machine. Concrete used in the slip form paving process requires careful control and monitoring of the workability and compaction properties, which can be attributed to the short length of the travelling side forms (SAPEM, 2013f).

The sole purpose of the travelling side forms is to provide edge support, therefore automated level and steering control is required. The slip form paving machine uses internal vibration or an amalgamation of internal and surface vibration to compact the fresh concrete across the entire paving width. SAPEM (2013f) states that the rate of advancement of the paver should not be greater than the rate at which the concrete is compacted. An uninterrupted supply of concrete with a low slump (10 to 50 mm) is required to achieve an efficient and favorable rate of slipform paving.

Figure 2-20: Slipform paving methods used to construct a rigid pavement (Source: Constro Facilitator, 2020)

2.5.3) Subbase construction

The subbase layer in a rigid pavement has a significant impact on the long-term pavement performance properties, by offering uniform support and providing an erosion resistant layer below the concrete (SAPEM, 2013f). During the pavement construction process, the subbase is constructed prior to the final pavement layer and is generally used as a temporary haul route for plant and other vehicles on site. According to SAPEM (2013f), the following requirements must be considered when constructing the subbase:

- Layer thickness
- Material selection (bound or unbound) dependent on the traffic volumes
- Subgrade conditions
- Type of rigid pavement to be constructed
- Economics

The subbase plays a vital role in enabling the pavement to achieve the stipulated design requirements. Therefore, subbases are usually constructed to a high quality, using bituminous or cementitious stabilized layers. In order to reduce the risk of heating the concrete layer which can result in premature cracking, it is crucial that the subbase surface is kept cool and damp before the fresh concrete is poured (SAPEM, 2013f).

2.5.4) Formwork

Side forms are usually made from steel sections approximately 3 m long and are able to support the paving equipment, while shorter side form lengths are used in scenarios with undulating topography or for curves with tight radii (SAPEM, 2013f). Side forms can also be made from

wood, however this is only used in minor projects or cases where steel side forms are unfavorable, such as curves with small radii.

All formwork should be fastened securely to ensure that there is no visible settlement resulting from the vibration created by the compacting machinery. According to SAPEM (2013f), formwork should also be regularly inspected for straightness and should not differ by more than:

- 3 mm from the top of the true plane surface for every 3 m
- 6 mm for every 3 m along the face of the form

Formwork should be kept in place for a minimum of 8 hours from the time the concrete is poured or up until the joints are ready to be saw cut. The forms need to remain in place if the temperature is less than 10 °C, in order to prevent damage to the pavement edges. Forms should be removed cautiously to avoid damage to the top edge of the pavement and any tie bars projecting from the longitudinal joints (SAPEM, 2013f).

2.5.5) Guide wires

For slip form paving applications, two guide wires known as string lines are strung on either side of the concrete pavement at a constant height above, and a constant horizontal distance away from the proposed pavement edge (SAPEM, 2013f). The string lines are supported by connectors secured to steel stakes placed 8 m apart on most road sections, and closer on horizontal and vertical curves.

2.5.6) Manufacturing and placing of concrete

From a rigid pavement engineering perspective, the fresh state consistency and the level of compaction applied to paving concrete impacts on the surface finish and riding quality of the finished pavement (SAPEM, 2013f). Concrete roads have a significantly larger surface area in relation with its volume, and the pavement surface is exposed to fluctuating temperature and wind conditions directly after the concrete has been placed (SAPEM, 2013f). Therefore, the concrete mix should be designed to the stiffest consistency that is compatible with the paving machinery. This will reduce the effects resulting from the respective temperature and wind conditions, while also enabling early finishing and curing of the concrete (SAPEM, 2013f).

Paving concrete needs to be poured continuously in order to achieve a consistent surface finish, therefore an uninterrupted supply of concrete is required when undertaking paving operations. According to SAPEM (2013f), the following facets must be considered to achieve continuity during the concrete mixing and paving process:

- The batch plant needs to have sufficient capacity to produce a continuous supply of concrete to the paving machine.

- The concrete demand (per hour) is dependent on the rate of advancement of the paving machine and the relevant volume calculations.
- The aggregate moisture content must remain consistent and be checked regularly – wet aggregate must be left to dry for a minimum of 12 hours.
- The required materials for concrete mixing operations should be batched according to their masses. In the case of volume batching, container masses and the related volumes must be checked on a daily basis.
- Cement pockets to be utilized on a first in first out basis.
- The number and haulage volumes of the construction vehicles should be sufficient to meet the desired batch plant capacity, haulage distances and various other site issues (rebar, tie bars, dowel bars and shutters). Plant with provision for side tipping may be required to circumvent driving over the rebar and dowel bar cages.
- When using concrete truck mixers/agitators, the time elapsed from mixing up until discharge should not be more than 60 minutes.
- When non-agitating machinery is used to transport concrete, the time until discharge occurs should not exceed 45 minutes after mixing. This can reduce to 30 minutes when high environmental temperatures are experienced.
- No water can be added to the concrete while it is being transported.

When constructing rigid pavements, concrete is placed continuously between proposed construction joints, which eliminates the need for intermediate header boards. If the time between placing two consecutive concrete mixes is greater than thirty minutes, then the paving operations must be stopped, and a construction joint must be made in the concrete that has already been placed.

When constructing concrete roads with steep grades, the paving operations should be conducted in the direction going up the slope and the slots for the keyed joints are located on the downhill side to ensure that the concrete flows into the cavity (SAPEM, 2013f). The water content of concrete used for paving purposes is reduced to achieve a stiffer mix thus enabling it to resist flowing downhill when it is compacted. To prevent bulging on the downhill portion of a sloped roadway, an increased rate of compaction and finishing is required. With steep grades and cross falls, there also comes an increased need for reliable skid resistance, especially during inclimate weather.

According to SAPEM (2013f), the air temperature should be carefully monitored during the first 48 hours after the concrete is placed, to ensure that the pavement concrete temperature stays above 5 °C as hot, dry weather leads to the development of cracks on the pavement surface and impairs

the concrete quality. This can be counteracted by placing the concrete during the coolest time of the day and also ensuring that the aggregates and mixing water are kept cool.

2.5.7) Compaction of the concrete

Concrete is compacted to ensure that the maximum material density is achieved, and to also obtain complete contact among the concrete and reinforcing steel, tie bars, dowels, and side forms. An effective and efficient rate of compaction should be applied across the entire pavement volume, with special attention being given to the pavement edges and joints. Over compaction must be avoided as it results in segregation, leakage, and surface laitance. However, if the concrete mix is well designed, segregation resulting from over compaction is minimal (SAPEM, 2013f).

Vibrating beams and trusses, which are typically used during fixed form paving, offers compaction in addition to level control. This is achieved by placing the vibrating beam/truss on the spread concrete, and as the concrete is being compacted, the base of beam/truss rests on the side forms (SAPEM, 2013f). Poker vibrators are used at the corners and edges of the pavement, and usually operate in conjunction with vibrating beams or hand tampers. In scenarios where the pavement thickness is greater than 150 mm, poker vibrators are used to compact the entire surface area and depth of the concrete pavement.

Figure 2-21: Vibrating beam used for compaction and level control (Source: SAPEM, 2013f)

2.5.8) Finishing and application of texturing to the concrete pavement surface

According to SAPEM (2013f), finishing of the concrete pavement surface includes initial finishing (screeding of the concrete to achieve the required cross-section profile) and final finishing (floating of the pavement surface). Controlled and precise finishing techniques are required to achieve an acceptable concrete pavement surface. The initial finishing process or screeding enables the concrete pavement surface to achieve its final tolerance levels, while the final finishing process commences once the surface has lost its sheen.

The final finishing process or floating typically occurs after screeding and involves smoothing of any surface irregularities and preparing the concrete pavement surface for texturing (SAPEM, 2013f). Floating also helps to close up insignificant cracks that may develop as the pavement surface dries up. However, it is worth noting that floating should not be used as an alternate measure for compaction after the concrete has been placed, it should only be used to the absolute minimum required to achieve the desired results (SAPEM, 2013f).

In scenarios incorporating air-entrained mixes the concrete may be finished after a short delay, as there will be a minimal amount of bleed water and no discernible sheen on the surface. If the finishing process starts too early, it will produce a weak pavement surface and laitance. Furthermore, if the finishing process begins too late, then a significantly higher finishing effort will be required which could lead to crumbling of the concrete pavement surface (SAPEM, 2013f).

Engineers can assist with applying these finishing techniques, by designing the concrete mix to incorporate a sufficient amount of fines (sand and cement), which enables mortar to rise to the pavement surface during compaction. Although a concrete mix with a high fines content can simplify the finishing process, it can also lead to surface bleeding, and the manufacturing costs are significantly higher than that of a well-proportioned concrete mix (SAPEM, 2013f). Designing paving concrete mixes with a high-water content often results in delays to the finishing process, and also produces a weakened pavement surface with insufficient abrasion and wear resistance.

When constructing rigid pavements, it is crucial to ensure that the pavement surface is checked on a regular basis and any irregularities present should be rectified while the concrete is in a plastic state (SAPEM, 2013f). It is relatively more difficult and costly to correct surface irregularities once the concrete has hardened. Freshly mixed concrete should be used to fill up any depressions instead of mortar or slush. The concrete must then be struck off, compacted, screeded and refinished (SAPEM, 2013f). At areas with high cross-section profiles, the excess concrete should be trimmed off and the pavement surface must be refinished.

(a)

(b)

(c)

Figure 2-22: Final finishing procedures (a) tube float, (b) truss float and (c) trailing float (Source: SAPEM, 2013f)

Surface texturing is applied to the pavement surface after the concrete has been placed, compacted, finished and the wet-formed joints have been completed (SAPEM, 2013f). This operation takes place before curing has commenced, while the concrete surface is in a state where it cannot be torn, and thereby loosening the coarse aggregate particles.

During mechanized paving operations, the surface texturing may be applied by using a machine spanning across the concrete slab, with level and directional control being offered by the side forms, guide wires or by any suitable manually operated machinery (SAPEM, 2013f). Hand drawn brooms are typically used for surface texturing purposes during manual paving operations or scenarios where a single lane is paved at a time.

When using a burlap drag to add texturing to the pavement surface, the first pass should begin before the surface loses its watery sheen. The number of passes is dependent on the required texture depth, and there should be no delays between each pass (SAPEM, 2013f). The burlap must be kept damp and clean when in use and should not contain any encrusted mortar. Surface texturing can also be provided by grooving the pavement with a metal tining device. The depth of the grooves must be regularly monitored and should be kept between 2 to 4 mm (SAPEM, 2013f).

(a) (b)

Figure 2-23: Surface texturing procedures (a) tining and (b) burlap drag (Source: SAPEM, 2013f)

2.5.9) Curing

Concrete must be protected against deterioration and damage resulting from various environmental factors for the first few days after the concrete has been placed and compacted (SAPEM, 2013f). The main damage experienced is cracking due to drying shrinkage, which is subsequently influenced by the air temperature, concrete temperature, wind velocity and relative humidity. Numerous techniques can be employed to reduce the temperature and rate of evaporation, which minimizes the propagation of plastic shrinkage induced cracks. Furthermore, the concrete should be left to cure completely by ensuring that there is proper hydration in conjunction with a curing compound or a covering that is either wet or impermeable (SAPEM, 2013f).

2.6) Repair and rehabilitation strategies for rigid pavements

Numerous roadways within South Africa's continuously growing road network are experiencing high rates of mechanical and physical deterioration to their pavement structure. This leads to a reduction of the functional and structural levels of service provided by the roadway (SAPEM, 2013a). Anderson et al. (2002) associate this with inadequate design and construction practices, increased traffic volumes, poor materials selection, and a service life greater than the design life. This places extra financial stress on the various stakeholders, such as road owners, road administrators, planners, designers and contractors, that have been tasked with rectifying these problems with repair, rehabilitation and reconstruction strategies.

According to Anderson et al. (2002), the following factors directly influence the repair and rehabilitation strategy that will be implemented:

- **Funds available** – additional project funds may be required to implement strategies that are suitable and cost-effective.

- **Safety** – safe traffic and construction management practices are required to protect both labourers and motorists during the repair and rehabilitation process.
- **Traffic congestion** – along with safety, traffic and construction management practices also need to reduce the amount and duration of congestion created and account for the degree of driver dissatisfaction.
- **Road agency policies** – when selecting an appropriate repair and rehabilitation strategy it is important to consider the various road agency policies, as potential modifications may need to be submitted for approval.
- **Public opinion** – information campaigns can be introduced to ensure active public involvement, which helps prevent delays resulting from public opposition.

A detailed understanding of the causes and mechanisms of failure is required to develop repair and rehabilitation strategies that will enable rigid pavements to achieve their optimum service life. This section will outline the various types of distress commonly found in rigid pavements and the repair/rehabilitation process needed to address it.

2.6.1) Full depth repair

Figure 2-24: Example of a punchout in CRC pavements (Source: Stacks, 2019)

Figure 2-25: Example of deep spalling in CRC pavements (Source: Stacks, 2019)

According to Stacks (2019), the following types of concrete pavement distress require a full depth repair:

Table 2-4: Types of pavement distress that require full-depth repair (Source: Stacks, 2019)

Type of pavement distress	Cause
Transverse cracks extending through the depth of the pavement slab	• Variations in temperature and moisture levels • Stresses due to wheel loads • Design issues (insufficient slab length or thickness) • Construction issues (non-uniform base support)
Deep plastic shrinkage cracks occurring through the depth of the pavement slab	• Evaporation rate from the concrete surface is greater than the rate at which bleed water forms
Shattered slabs	• Design issues (insufficient slab thickness) • Construction issues (non-uniform base support)
Breaks to the corner of the pavement slab	• Design issues (insufficient slab thickness) • Construction issues (non-uniform base support)
Punchouts in CRC pavements	• Design issues (insufficient slab thickness) • Construction issues (non-uniform base support)
Deep spalling in CRC pavements	• Pressure resulting from corrosion of steel reinforcement • Inadequate cover depth • Poorly constructed joints • Using coarse aggregates with a high thermal expansion coefficient
Pumping	• Stresses due to heavy traffic loads • Plastic deformation of the base material • Warping of the pavement slab due to varying temperature gradients • Accumulation of free water in void spaces below deflected pavement slabs
Blow-ups	• Localised expansion and contraction of joints or cracks due to changing environmental and temperature conditions

Figure 2-26: Example of a blow-up in concrete pavements (Source: Stacks, 2019)

Stacks (2019) outlines the following procedures that need to be conducted when implementing full depth repair strategies:

- **Identify the limits of the repair area** – the repair limits should encompass all zones that have developed voids below the concrete pavement and can be identified by using visual assessments to analyse the extent of the pavement distress. However, in cases with punchouts and spalling, falling weight deflectometer and coring/non-destructive tests are respectively the most effective methods of evaluation (Stacks, 2019).
- **Saw-cut the edge of the repair limits** – the perimeter of the repair area should be saw-cut through the depth of the concrete slab with a diamond blade saw. A larger repair area may be needed in CRC pavements, as there is no load transfer between the existing pavement and the concrete block that has been saw-cut (Stacks, 2019). When exposed to traffic loading, this leads to larger deflections in the concrete block and along the perimeter of the repair area.
- **Remove the saw-cut concrete slab** – the concrete slab can be removed by either lifting it out with a crane/front-end loader or by breaking up the slab and removing the smaller pieces.
- **Remove the base (only if it is damaged)** – in cases where the base is damaged, all loose material should be removed and recompacted (as directed by the Engineer).
- **Drill holes for tie/dowel bars** – in order to attain the optimum bond between the tie bars and concrete, the holes should be drilled to an adequate length with no moisture and dust present in them. After the drilled holes have been cleaned, they are filled with low viscosity epoxy. When removing an entire concrete slab, dowel bars should be provided along all transverse joints, which can be done by either drilling and epoxying or by executing a dowel bar retrofit (Stacks, 2019).

Figure 2-27: Drilling holes for tie and dowel bars (Source: Stacks, 2019)

- **Provision of steel reinforcement in CRC pavements** – it is crucial that longitudinal continuity is maintained for the tie bars in CRC pavements. To prevent failure due to pull-out, the embedment length of the steel reinforcement should be at least 33 times the rebar diameter (Stacks, 2019).
- **Placing and finishing of concrete** – after the reinforcement has been placed, the concrete is placed, vibrated, and finished by hand. The surface texturing on the new concrete pavement section should match the texturing on the surrounding concrete. The concrete must be properly cured to reduce the development of map cracks resulting from fluctuating temperature gradients and high rates of evaporation (Stacks, 2019).

Figure 2-28: Development of map cracks due to improper curing procedures (Source: Stacks, 2019)

- **Restore existing joints** – all existing joints found within the repair area should be restored as per the relevant standards.

2.6.2) Bonded concrete overlay

Most of the older concrete pavements in South Africa's road network have not been designed and constructed to accommodate the increased traffic demand that presently exists. Therefore, this

insufficient pavement thickness leads to pavement distresses such as mid-slab cracking, joint faulting and punchouts (Stacks, 2019). Bonded concrete overlays serve as a cost-effective repair and rehabilitation strategy in cases where the concrete pavement does not display any substantial signs of distress and remains structurally stable.

A bonded concrete overlay is constructed by applying a new layer of concrete to the surface of the existing concrete pavement, which increases the thickness of the pavement slab and therefore reduces the stresses resulting from traffic loading (Stacks, 2019). In order to construct an effective bonded concrete overlay, it is important to provide a strong bond between the old and new layers of concrete. If the bond between the old and new concrete layers is good, then the new composite slab will behave in a monolithic manner, much like a thicker concrete slab (Stacks, 2019). Alternatively, if the bond between the two layers is weak, then each layer will perform as individual slabs, which leads to increased stress due to traffic loads in the new concrete layer and compromises the performance of the entire pavement structure.

According to Stacks (2019), the following procedures should be applied when incorporating bonded concrete overlays to existing concrete pavements:

- **Repair distresses in the existing concrete pavement** – before constructing the overlay, the existing pavement should be assessed to identify and repair any distresses that could affect the performance of the concrete overlay in a few years' time. According to Stacks (2019), this includes distresses such as punchouts, delaminations, deteriorated patches and deep spalling. All existing asphalt-concrete patches must be changed to full concrete patches, in order to make the existing pavement more structurally stable.
- **Prepare the existing pavement surface for the concrete overlay** – a good bond between both layers can be achieved by adding surface texture to the existing concrete layer. This enables both layers to perform as a single structure by allowing the new concrete overlay to form a favourable bond with the existing concrete surface that has been roughened. The most commonly used methods for preparing the surface of the existing concrete layer includes shot blasting, cold milling, and sandblasting.
- **Provision of steel reinforcement** – steel reinforcement is required when constructing a bonded concrete overlay for CRC pavements. Stacks (2019) indicates that if the thickness of the overlay does not provide sufficient concrete cover, then the steel reinforcement may be placed directly onto the surface of the existing concrete layer. This can reduce the construction time and costs associated, while also reducing any concrete volume changes present at the interface. However, placing the rebar directly on the existing surface will reduce the interface area between the existing concrete and the overlay (Stacks, 2019).

- **Placing, finishing, and curing of concrete** – much like regular rigid pavements, bonded concrete overlays can be constructing using fixed form or slip form paving techniques. The materials used for the concrete overlay mix design must be carefully selected to ensure material compatibility. This can be achieved by utilizing aggregates that produce thermal coefficients and moduli that are less than or equal to those of the materials used in the existing concrete pavement, which results in lower stresses at the bond interface (Stacks, 2019). Before placing the fresh concrete for the overlay, the position of the joints on the existing concrete pavement should be identified to ensure that the joints for the concrete overlay can be saw cut directly above the existing joints. Paving operations should cease during adverse environmental conditions, such as high air and concrete temperature, low relative humidity and high wind velocity, as these conditions promote increased rates of water evaporation in fresh concrete (Stacks, 2019). Excessive rates of water evaporation can cause changes to the fresh concrete volume, which results in debonding issues at the interface between the existing concrete pavement and the new overlay.
- **Saw cut and seal new overlay joints** – the likelihood of early age shrinkage and contraction is significantly greater in thinner concrete overlays therefore construction of all joints should commence as soon as possible. Overlay joints must be saw cut directly above the joints on the existing concrete pavement, in order to prevent the propagation of reflective cracking from the existing joints onto the new overlay (Stacks, 2019).

2.6.3) Unbonded concrete overlay

Unbonded and bonded concrete overlay repair strategies are similar in the sense that both are constructed by applying a new layer of concrete to the surface of the existing concrete pavement. However, the key difference between them is that an interlayer is incorporated in unbonded concrete overlays to break the bond between the existing concrete pavement and the new concrete layer (Stacks, 2019).

Unbonded concrete overlays have been successfully applied on numerous roadways in America and were typically found to cost more than bonded concrete overlays due to their increased thickness. The key advantage that an unbonded concrete overlay has over its bonded counterpart is that it can be used on existing roadways experiencing significant forms of deterioration, whereas bonded concrete overlays can only be applied in cases where the existing pavement is still in fairly good condition.

When constructing unbonded concrete overlays, the existing concrete layer usually requires very little preparation work except in cases where there are shattered slabs or punchouts in the existing concrete pavement (Stacks, 2019). The thickness and material quality of the interlayer has a major influence on the performance properties of unbonded concrete overlays. According to Stacks

(2019), bituminous mixtures are the best material to use for interlayers, which can be attributed to its lower modulus that assists with reducing the stresses due to warping and curling in the new concrete slab.

Stacks (2019) provides the following steps for constructing unbonded concrete overlays:

- **Repair distresses in the existing concrete pavement** – prior to constructing the overlay, the existing concrete pavement should be examined to identify and repair any distresses which may impact on the performance properties of the overlay. According to Stacks (2019), punchouts must be repaired with a full depth repair and shattered slabs should be removed and replaced, while deep or shallow spalling does not require any prior repairs.
- **Place the interlayer** – the interlayer should be placed as per the relevant standards.
- **Construct the unbonded concrete overlay** – after all the distresses in the existing pavement have been repaired and the interlayer has been placed, the unbonded concrete overlay is constructed using the same approach used when constructing a new concrete pavement.

2.6.4) Stitching

Stitching is a repair technique that is used at longitudinal cracks to sustain aggregate interlock and provide extra reinforcement to reduce the relative movement of concrete slabs located at the cracks (Stacks, 2019). Stitching is also performed at longitudinal joints to prevent separation of the slabs and may also be used to alleviate any problems resulting from the omission of tie bar reinforcement during the construction phase.

Stacks (2019) states that stitching should never be applied at transverse cracks as this may create a build-up of stress from volume changes due to temperature variations and often results in the development of additional cracks and spalling. Longitudinal cracks are typically formed by late or shallow saw cutting of the longitudinal contraction joints (Stacks, 2019). Early repairs to longitudinal cracks prevent further deterioration and possible separation of the concrete, while also saving money in the long term.

The deterioration rate of longitudinal cracks differs from that of transverse cracks therefore the concrete slab will not need to be removed and replaced. In cases where longitudinal cracks do not widen, crack sealing serves as a sufficient repair strategy, whereas stitching is the most feasible option when longitudinal cracks continue to widen. In CRC pavements, stitching is only used in areas where lanes are separated by longitudinal contraction joints. Punchouts are often formed in CRC pavements when longitudinal cracks extend through the entire depth of the slab, with full depth repair being the most appropriate strategy.

According to Stacks (2019), the following are the three main types of stitching methods:

- **Cross stitching** – used to repair tight cracks and separations. Holes for cross stitching are drilled at an angle to ensure that they intersect the longitudinal crack or joint at the mid-depth of the concrete slab (Stacks, 2019). After all dust has been removed, the holes are filled with epoxy and the tie bar reinforcement is inserted.
- **Slot stitching** – is the most economical repair strategy for preventing lane separations, improving the performance of wide longitudinal cracks, and restoring load transfer (Stacks, 2019). The slots are typically cut with a walk behind saw or a slot cutting machine and are cleaned thoroughly to remove any dust that may be present. Deformed bars are inserted into each slot before a high strength repair mortar is placed, finished, and cured. When slot stitching is applied, adjacent concrete slabs are held together by the shear stresses experienced in the deformed bars (Stacks, 2019).
- **U-bar stitching** – a major part of the restraining force is provided by the anchoring action due to the U-bars. Slots for U-bar stitching are usually cut with a slot cutting machine and the excess concrete is broken with a pneumatic hammer. Stacks (2019) states that high quality repair materials should be used during U-bar stitching and it is important to ensure that there is sufficient consolidation around the ends of the U-bars.

Figure 2-29: Example of slots and U-bars (Source: Stacks, 2019)

2.6.5) Dowel bar retrofit

Stacks (2019) defines load transfer as the capability of a crack or joint to transfer vehicular loads from one slab to another. The performance properties of concrete pavements can be enhanced by ensuring that adequate load transfer is provided at the joints. A large part of the load transfer mechanism is attributed to the dowel bars that cross the transverse joints. Aggregate interlock also contributes towards load transfer; however, its effectiveness reduces with time as the concrete will begin to experience drying shrinkage which causes it to contract. During the winter months, the effect aggregate interlock has on load transfer diminishes, as the joint openings widen due to the low air temperature.

Dowel bars are needed in rigid pavements to ensure that an adequate amount of load transfer is provided throughout the service life of the pavement. Figure 2-30 shows that some concrete pavement sections have been constructed without dowels, which coupled with insufficient base/subgrade support leads to faulting and the development of cracks at the joints (Stacks, 2019).

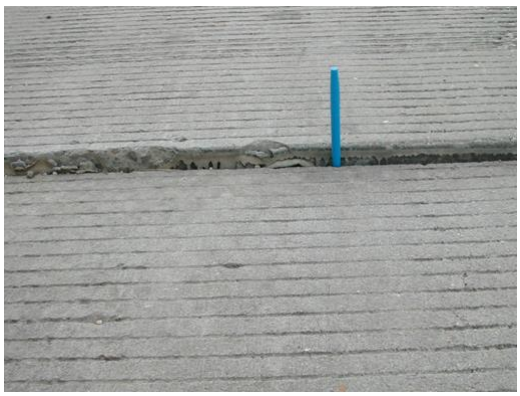

Figure 2-30: Example of faulting at the transverse joint of a concrete pavement (Source: Stacks, 2019)

In concrete pavement sections without dowel bars, the lack of load transfer will result in bigger dynamic wheel loads which increases the risk of faulting (Stacks, 2019). A dowel bar retrofit is the most effective method for restoring load transfer at the pavement joints, however this repair strategy cannot be applied in CRC pavements. Many countries have utilized dowel bar retrofits to successfully rehabilitate and restore old concrete pavements that have not been constructed with dowel bars (Stacks, 2019).

Stacks (2019) stipulates the following procedures for conducting a dowel bar retrofit:

- **Assess the need for a dowel bar retrofit** – Dowel bar retrofits are typically applied when the load transfer efficiency of the pavement is below 60 % and when there are excessive amounts of faulting and differential deflection in the pavement slab (Stacks, 2019). In cases where the concrete pavement is still in good condition, but no dowels were used, a dowel bar retrofit can be used to improve the structural properties of the pavement. However, if an insufficient base support leads to faulting in the pavement, then a base repair should be done in conjunction with a dowel bar retrofit.
- **Saw cut the dowel bar slots** – the slots for the dowel bar retrofit are cut using a diamond saw slot cutter, which provides three dowel bar slots along each wheel path. Each dowel bar slot needs to be wide enough to enable the largest aggregates in the repair material to encase each bar with sufficient consolidation (Stacks, 2019).

Figure 2-31: Diamond saw slot cutter used to cut the dowel bar slots (Source: Stacks, 2019)

- **Prepare the dowel bar slots** – handheld jackhammers are used to remove the pieces of concrete that have been cut with the diamond saw slot cutter. Each slot is sandblasted, and the bottom is flattened with a small brush hammerhead to ensure that the dowel bars are level and properly aligned (Stacks, 2019). The slots are then cleaned with water to provide a satisfactory bond between the slot and the repair material which assists with load transfer.

Figure 2-32: Example of dowel bar slots after being flattened and cleaned (Source: Stacks, 2019)

- **Place the dowels** – the dowels are lubricated with a bond breaker before being placed in the slots. As depicted in Figure 2-33, the dowel bar assembly consists of a joint reformer, end caps and chairs (Stacks, 2019). The joint reformer and end caps are used to enable the concrete pavement slab to move without bearing on the dowel, while chairs are used to support the dowel bars at the bottom of the slots and allow each bar to be encased by the repair mortar.

Figure 2-33: Dowel bar assembly consisting of a joint reformer, end caps and a chair (Source: Stacks, 2019)

- **Placing the repair mortar in the dowel bar slots** – high early strength repair mortar is used to fill the slots after the dowel bars have been placed. Stacks (2019) states that the repair mortar must have similar thermal properties to the surrounding concrete, be fast setting, have minimal shrinkage, develop a sufficient amount of early strength to enable traffic use and provide a strong bond with the existing concrete. After the repair mortar has been vibrated, the surface is finished, and texturing is applied to match the surrounding concrete pavement.

2.6.6) Joint repair

Joints are incorporated into rigid pavements to accommodate any volume changes in the concrete resulting from moisture and air temperature variations. Longitudinal joints, transverse construction joints and expansion joints (at bridge approaches) are the only types of joints used in CRC pavements (Stacks, 2019). Rigid pavement joints serve the main purpose of relieving stresses in the concrete, which prevents the propagation of uncontrolled cracks. Concrete pavements experience substantial amounts of movement at the joints, therefore joint sealants are incorporated to protect them against infiltration of water and other foreign materials (Stacks, 2019).

The joints are the weakest portion of the pavement, as they create a gap in the concrete which prevents the entire wheel load from being transferred from one slab to another and produces higher wheel load stresses (Stacks, 2019). When incompressible materials enter the pavement joints during environmental conditions with elevated air temperatures, the concrete slab will expand and squeeze the foreign materials. This expansion leads to increased localized stresses in the concrete, which can cause spalling in the joints (Stacks, 2019). Figure 2-34 illustrates that if a poor joint seal is provided, then water can infiltrate the joint resulting in the corrosion of the dowel bars.

Figure 2-34: Example of infiltration of water into the pavement joint which causes corrosion of the dowel bar (Source: Stacks, 2019)

Dowels are used in transverse joints to enhance the load transfer efficiency of the pavement, i.e. a concrete pavement with a higher load transfer efficiency will experience lower wheel load stresses and therefore have improved pavement performance characteristics (Stacks, 2019). However, this can only be achieved by ensuring that the dowel bars are aligned parallel to the direction of movement. As depicted in Figure 2-35, misaligned dowel bars will produce high stress concentrations which leads to the propagation of cracks in the concrete.

Figure 2-35: Example of cracking caused by misaligned dowel bars (Source: Stacks, 2019)

According to Stacks (2019), pavement distresses such as spalling, cracking or breaking of the slab edges on either side of a transverse joint will require a joint repair. The type of joint repair strategy selected is dependent on the extent of the distress, with full depth repair or half depth repair being the most commonly used techniques. In CRC pavements, full depth joint repairs are required when the transverse construction joints fail. This type of distress is often attributed to poor compaction of the concrete under the longitudinal reinforcement, which results in delamination and joint failure (Stacks, 2019).

Figure 2-36: Example of construction joint failure in concrete pavements (Source: Stacks, 2019)

2.6.7) Diamond grinding

Diamond grinding uses closely spaced diamond blades to remove a thin layer of the hardened concrete pavement surface. It was initially an expensive operation, however the introduction of innovative equipment, such as improved synthetic diamonds for the saw blades, has since made diamond grinding a more cost-effective repair strategy for rigid pavements (Stacks, 2019). Diamond grinding has mainly been used to correct functional pavement distresses, such as roughness, skid resistance and noise, that are often caused by various surface defects. This is achieved by removing uneven sections of concrete on newly placed pavements.

According to Stacks (2019), pavement roughness increases the dynamic loads and the resultant wheel load stresses that are experienced, which may eventually reduce the service life of the concrete pavement. Diamond grinding can be used to rectify this problem by increasing the macro-texture on the concrete surface which results in improved skid resistance and drainage properties. A flat concrete surface is obtained by moving the blade assembly along the pavement surface at a fixed level, which creates saw cut grooves in the concrete (Stacks, 2019). The uncut portions of concrete found between each saw cut are then removed, which produces a level concrete surface with longitudinal texturing.

Figure 2-37: Example of the concrete surface after diamond grinding operations (Source: Stacks, 2019)

Diamond grinding is a suitable repair strategy for restoring rigid pavements with an average level of faulting below 4 mm. It can also be used to address the problem of aggregates with polished surfaces in concrete pavements, which typically occurs as the pavement is exposed to recurring traffic loads over time. According to Stacks (2019), the following are the main advantages of applying diamond grinding as a repair and rehabilitation strategy in rigid pavements:

- Enhances the smoothness of the pavement surface
- Significantly cheaper than a concrete overlay
- Improves the skid resistance and safety aspects of old concrete pavements
- Reduction of the noise produced by the tyre-pavement interaction
- Has no effect on the material durability or fatigue life of the pavement
- Can be conducted during off-peak hours with minor disruptions to traffic and short lane closures
- Eradicates the need for tapers at side streets and entrances/exits to highways
- Has no effect on overhead clearances below bridges or the hydraulic performance of gutters and kerbs on municipal roads

The main disadvantage of diamond grinding is that it reduces the concrete slab thickness, which increases the wheel load stresses experienced, however this effect is compensated by a notable reduction in the dynamic loads. According to Stacks (2019), diamond grinding to a higher depth will expose the coarse aggregates in the concrete, which may cause polishing over time and result in reduced skid resistance.

2.6.8) Thin hot-mix asphalt overlays

Thin hot-mix asphalt overlays can be added to older CRC pavements (that are still in good structural condition) to extend their service life by a number of years. This repair strategy can be applied to pavements that are displaying early signs of deterioration, are getting rough, are experiencing a high rate of punchouts, or have experienced a reduction in skid resistance (Stacks, 2019).

The main reason why thin hot-mix asphalt overlays have been used successfully to rehabilitate pavements experiencing punchouts is attributed to the fact that the new smooth surface reduces the dynamic loads resulting from heavy vehicles riding over the rough surface (Stacks, 2019). The thin hot-mix asphalt overlay will also prevent water from infiltrating into the base layerworks. However, it should not be used to repair areas where a punchout is beginning to form, this will instead require a full depth repair before performing an overlay (Stacks, 2019).

Thin hot-mix asphalt overlays can also be applied to concrete pavements that are structurally deficient, however this operation has a minimal level of success as it is expensive and only extends the service life of the pavement by a short period of time. A thicker hot-mix asphalt overlay is required to rehabilitate concrete pavements with transverse contraction joint failures and faulting. If a thin overlay is used in this scenario, then the loss of load transfer at the transverse joint will lead to independent movement of the concrete slabs, which leads to the formation of a crack in the overlay that will reflect through to the pavement surface (Stacks, 2019).

2.7) Fresh state properties of concrete used to construct rigid pavements

Concrete exists in its fresh state from the time the mixing process occurs up until setting takes place (Owens, 2013). The fresh state lifecycle of concrete usually lasts for a few hours, during which time the fresh concrete is handled, transported, poured and vibrated. The consistency and workability of fresh concrete decreases after the mixing procedure, which is indicative of a direct correlation between the fresh and hardened state properties of concrete. In addition, the fresh state consistency and level of compaction applied to the concrete mix plays an integral role in the development of strength and durability in hardened concrete.

From a rigid pavement engineering perspective, the fresh state properties of concrete influences the surface finish and riding quality of the finished pavement (SAPEM, 2013d). The main fresh state properties of concrete used for rigid pavement applications has been summarized in Table 2-5.

Table 2-5: Fresh state properties of concrete used to construct rigid pavements (Source: SAPEM, 2013d)

Property	Description
Workability	Concrete must retain sufficient workability to ensure that it retains an even rate of compaction when vibrated. However, compacted concrete requires sufficient rigidity to prevent flow on sections with steep gradients and camber. Concrete workability is directly influenced by the stone size, stone content, fines content of the sand and the cement content (Owens, 2013). The slump test is the most widely used method for quantifying the workability properties of fresh concrete. Concrete workability can also be determined by observing the degree of spreading of the fresh concrete that is moulded on the base plate.
Consistency	Much like workability, consistency indicates the stiffness of the concrete mix and is measured using the slump test. Establishing the optimum fresh concrete consistency is crucial, as this directly influences the final surface finish achieved and the functional level of service for the pavement.
Flowability	The flow properties of fresh concrete under vibration is evaluated by making a mound of concrete in a conventional pan mixer. The mound of concrete is vibrated with a poker vibrator, while a rectangular steel float is placed sideways against the mound. Flowability is then assessed by observing the amount of concrete that flows around the edges of the trowel.
Place-ability	When constructing rigid pavements, fresh concrete needs to be able to be worked and placed using the paving equipment available. This includes the following methods: slipform paving, side form paving or hand placing.
Cohesiveness	Cohesiveness refers to the propensity of fresh concrete to withstand separation. It is evaluated by tapping the base plate immediately after conducting the slump test. If the concrete mix is cohesive, then the concrete mound will settle gradually without falling apart instantaneously.
Bleeding	Bleeding refers to the segregation of water from the hydrated cement paste and is detected by observing if water is visible on the surface of recently placed concrete. While bleeding reduces the overall w/b ratio of the concrete mix, it does have the following disadvantages: • Water trapped below dowels, tie bars or aggregate particles produce zones of weakness once the concrete hardens. • Water trapped underneath rebar spanning horizontally will weaken the bond that exists between the concrete and steel. • If obstructions, such as horizontal reinforcement, prevent the solid particles from settling, then cracks will propagate before the concrete hardens. • Severe cases of bleeding have a negative effect on the abrasion resistance of the pavement surface and results in a poor level of service. The tendency for bleeding to transpire is evaluated by observing the severity of bleeding when concrete is compacted until it lies slightly below the top surface of a cube mould. Concrete with a low degree of bleeding is susceptible to the development of plastic shrinkage cracks when it is placed in a hot, windy, and dry environmental setting.
Texture ability	When fresh concrete is vibrated, sufficient cement paste must be worked to the pavement surface to achieve the required texture and riding quality. The amount of cement paste required at the surface is dependent on the surface texturing method applied, i.e. tining requires a thicker layer of cement paste than a brushed finish. Using steel tine or broom bristles on the vibrated and floated concrete surface is an accurate method for

	indicating if sufficient cement paste is available. However, the thickness of the cement paste layer should not be disproportionate as this could result in the development of surface wear, plastic shrinkage cracks and drying shrinkage cracks
Dowel and tie bar insert ability	Dowel and tie bars should be inserted into rigid pavements with minimal effort and without disrupting the coarse aggregate distribution in the concrete mix. This assists with achieving a good pavement surface finish and riding quality. A simple method for assessing this property is by inserting a short piece of rebar or a portion of coarse aggregate into a concrete cube mould while it is being compacted on a vibrating table. The portion of rebar or coarse aggregate should be able to be pushed into the fresh concrete with ease and a mortar plug must not remain above it.

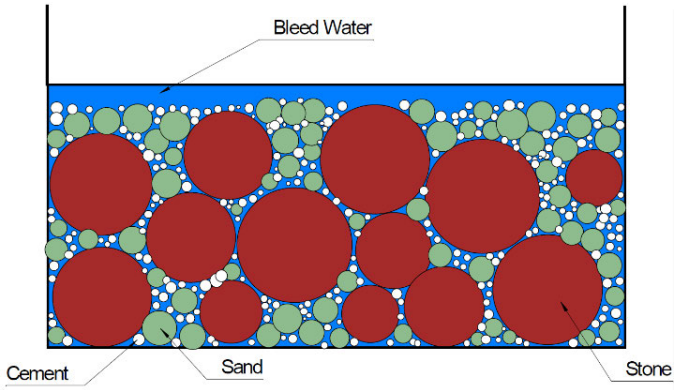

Figure 2-38: Bleeding and settlement in a typical fresh concrete mix (Source: SAPEM, 2013d)

As discussed in Table 2-5, the slump test is commonly used to determine the consistency and workability properties of fresh concrete. There are three types of slump that can be achieved and have been depicted in Figure 2-39 below. Shear slumps usually occur in concrete mixes with a low cement content and in cases where the concrete has been unevenly tamped (Owens, 2013).

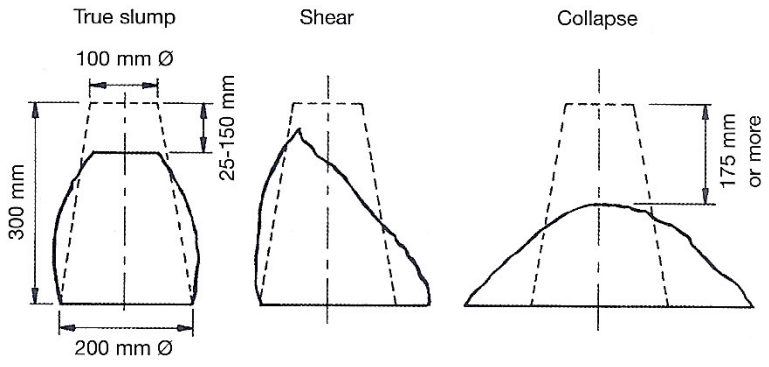

Figure 2-39: Various types of slump that can be obtained (Source: Owens, 2013)

The slump test is an acceptable test method for slumps ranging from 5 mm to 175 mm (Owens, 2013; SAPEM, 2013b). The slump results obtained vary in accordance with the concrete mix design and should lie within the specified tolerances. According to Owens (2013), the achieved

slump should be ±1/3 of the designed or target slump. Alternatively, SAPEM (2013c) provides various allowable tolerances that are directly linked to the designed/target slump, which have been tabulated below.

Table 2-6: Slump tolerances for conventional concrete (Source: SAPEM, 2013c)

Designed/Target Slump (mm)	Tolerance (mm)
<50	-15 to +25
50 to 100	±25
>100	±40

2.8) Mechanical properties of concrete used to construct rigid pavements

The mechanical properties of concrete are determined by manufacturing, handling, curing and testing concrete samples in a laboratory setting, with strength (compressive, flexural and tensile), creep, shrinkage and modulus of elasticity being the main mechanical characteristics in concrete (Ayub et al., 2014). Along with strength and shrinkage, SAPEM (2013d) also provides saw ability as one of the main factors considered for concrete used in rigid pavements.

The strength of concrete in its hardened state is a crucial variable used for both structural and pavement design purposes and often serves as a guide for predicting the performance and quality of concrete (Owens, 2013). Concrete used in structural and pavement engineering applications are constantly subjected to multiaxial variable loads. However, concrete strength is quantified in accordance with test results obtained from exposing laboratory samples to a uniform loading rate and uniaxial stresses. Therefore, the measured strength determined from laboratory investigations is merely an indication of the true concrete strength (Owens, 2013).

2.8.1) Concrete strength

Compressive strength is the most widely used variable for structural design and engineering purposes (Owens, 2013). In concrete, compressive strength is determined by dividing the maximum uniaxial load the concrete can withstand with the cross-sectional area of the laboratory sample. As indicated in Figure 2-40, the most commonly used testing methods for quantifying compressive strength in concrete are the cube and core test. In South Africa, cube tests are typically carried out as per SANS 5860, 5861-2, 5861-3 and 5863, whereas core tests are conducted in accordance with SANS 5865.

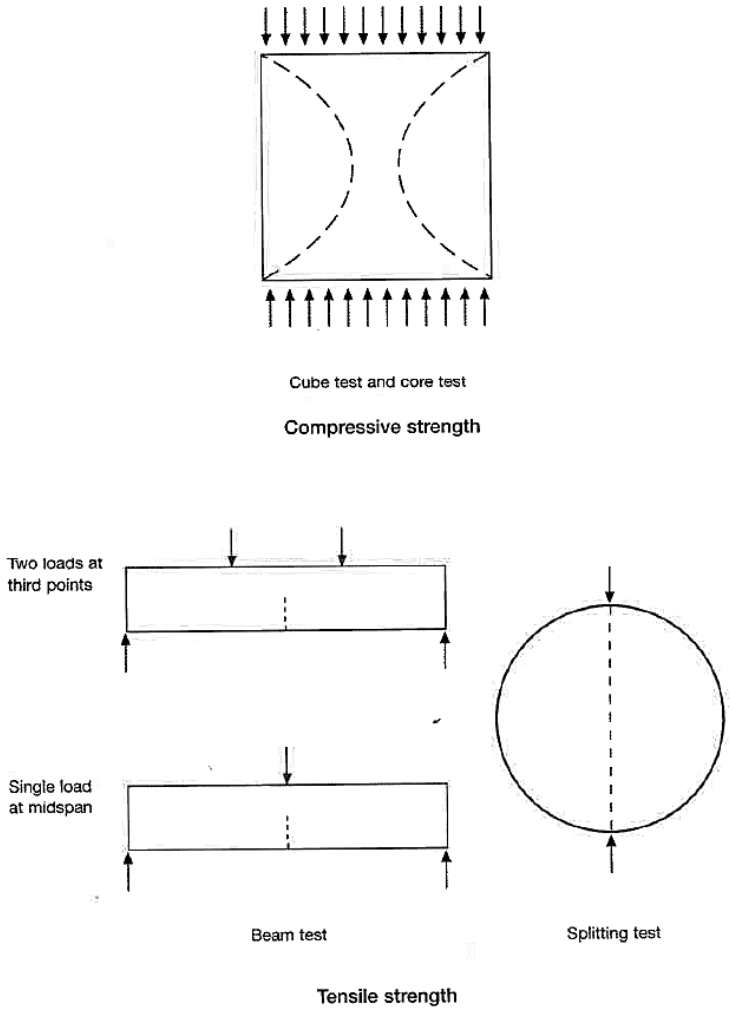

Figure 2-40: Laboratory tests used to determine the compressive and tensile strength of concrete (Source: Owens, 2013)

Tensile or flexural strength is the defining variable used for the design of rigid pavements. The tensile strength of concrete can be indirectly quantified using the flexural strength test or the tensile splitting test. According to Owens (2013), the flexural strength test involves subjecting concrete beam specimens to either a single load located at midspan or two loads placed at third points. The tensile splitting test comprises of exposing cylindrical or cube samples to compressive forces applied along two opposed lines (Owens, 2013). In the South African context, the flexural strength and tensile splitting tests are conducted as per SANS 5864 and 6253 respectively.

In concrete, the compressive strength is significantly higher than the tensile strength, however Owens (2013) explains that no definitive relationship exists between compressive and tensile strength. This can be attributed to the fact that variables such as w/b ratio, curing conditions, concrete age, aggregate properties and mix proportions have varying degrees of influence on the compressive and tensile strength.

Concrete used to construct rigid pavements requires sufficient strength to produce a solid and durable surface resistant to skidding. Concrete pavements also require adequate strength to withstand the resultant tensile stresses that develop due to shrinkage, warping and loading (SAPEM, 2013d). This is achieved in minor roads by stipulating a desired flexural strength/modulus of rupture, which is typically a third point load below 4 MPa after 28 days (SAPEM, 2013d).

Furthermore, a characteristic 28-day compressive strength above 30 MPa usually meets the above-mentioned requirement for flexural strength, except in cases where alluvial pebbles are the selected coarse aggregate (SAPEM, 2013d). Some coarse aggregates coupled with a cautious mix design may also achieve a flexural strength higher than 4.5 MPa.

Although favourable flexural strength results are crucial in rigid pavements, there is little benefit achieved by increasing the concrete compressive strength above 30 MPa to produce a resultant increase in the flexural strength. SAPEM (2013d) attributes this to the trend whereby an increase of the compressive strength in concrete does not necessarily produce a proportionate increase of the flexural strength. Concrete with extremely high compressive strengths may also be disadvantageous, when considering the construction costs associated and the potential construction problems that may arise.

2.8.1.1) Factors influencing concrete strength

According to Owens (2013), the main factors influencing the characteristic concrete strength includes the following:

- Nature of the concrete
- Intrinsic factors (i.e. the aggregate used, aggregate-paste interface and the hydrated cement paste)
- Testing methods applied or extrinsic factors

The nature of the concrete produced can affect the concrete strength in numerous ways:

- **Heterogeneity** – the concrete constituents occur in various phases and have dissimilar properties, making concrete a heterogeneous material. Therefore, when a load is applied to concrete, the internal stresses and strains experienced are non-uniform, which has an adverse effect on the strength and microstructure properties (Owens, 2013).
- **Porosity and flaws** – concrete strength decreases with an increase in porosity, which Owens (2013) associates with the relationship that exists between w/b ratio and compressive strength. Micro-cracks found in the aggregate-hardened cement paste (HCP) interface results in reduced concrete strength and durability properties (Owens, 2013).

According to Owens (2013), the intrinsic factors discussed below are the most influential on concrete strength:

- **Aggregate** – the aggregate selected is usually the strongest contributor towards the strength of concrete. Owens (2013) also states that the influence of aggregate on strength increases as the concrete strength increases.
- **Aggregate-paste interface** – the strength properties of the aggregate-paste interface is normally the weakest parameter in the strength chain and is influenced by the w/b ratio, concrete age, rate of bleeding present in the fresh concrete, cementitious material added to the mix and roughness of the aggregate surface (Owens, 2013).
- **Hardened cement paste (HCP)** – the strength of concrete is directly influenced by HCP strength, with the porosity and microstructure properties having the strongest impact on the strength of HCP (Owens, 2013).

From a roads and pavement engineering perspective, the extrinsic factor with the largest influence on the strength properties of rigid pavements is the direction and rate of loading in relation to the direction of casting. Bleed water trapped below the aggregate particles, produce zones of weakness once the concrete hardens, which causes concrete to exhibit traits similar to a horizontally layered material with horizontal planes of weakness (Owens, 2013). Concrete exhibits improved strength when the direction of loading is perpendicular to the horizontal planes of weakness, which Owens (2013) attributes to the fact that the main failure mode is tensile in nature for concrete exposed to compressive loading.

Numerous other extrinsic factors have also been identified by Owens (2013) as having an impact on the strength properties of conventional concrete:

- Shape and size of the concrete specimen
- Moisture content of the concrete sections
- Eccentricity of the applied loading
- Temperature
- Defective testing machines
- Relation of maximum particle size distribution to the specimen size

2.8.2) Drying shrinkage

Drying shrinkage is defined as the loss of moisture in concrete which occurs once the curing process ceases (Owens, 2013). Shrinkage produces an increase in tensile stress that results in cracking, internal warping and external deflection of concrete prior to experiencing loading (Koratich, 2020). All concrete experiences drying shrinkage or a loss of capillary water as concrete age progresses.

According to Owens (2013), drying shrinkage is dependent on the properties of each concrete component, proportions of the concrete constituents, mixing process followed, amount of moisture present during curing and relative humidity. SAPEM (2013b) questions the validity of shrinkage tests for rigid pavements, as they are undertaken with specimens dried in a desiccation oven and is not an accurate simulation of shrinkage in concrete pavements.

2.8.3) Saw ability

The saw ability characteristics of rigid pavements is influenced by the early age strength gain in the concrete and the class of aggregate used. SAPEM (2013d) states that the risk of random cracking reduces if the construction joints are saw-cut during the early stages of the pavement life. In scenarios where it is essential to evaluate the effect of incorporating numerous types of binders, admixtures and/or aggregates, the following assessment methods can be applied:

- Several concrete cube specimens are cast for testing purposes at 8, 10, 14, 16, 18, 20 and 24 hours, while some additional cubes are set aside specifically for sawing (SAPEM, 2013d).
- At the above-mentioned times, the compressive strength is determined by conducting the cube test. Concurrently, a diamond saw is used to saw cut a separate cube specimen to a depth of 25 to 40 mm, and the degree of plucking and ravelling is assessed (SAPEM, 2013d).
- This process is repeated until a saw cut with a suitable degree of plucking and ravelling is achieved.
- This assessment method can also be conducted using concrete cube samples that have been cured in different temperature settings.

Table 2-7: Influence the type of aggregate has on the saw ability properties (Source: SAPEM, 2013d)

Type of Aggregate	Compressive Strength (MPa)*
Granite, Quartzite	3 – 5
Dolerite, Andesite	4 – 6
Felsite	> 8

* Compressive strength when a suitable cut is obtained

2.9) Durability properties of concrete used to construct rigid pavements

Owens (2013) defines durability as the ability of a concrete element to withstand extreme environmental conditions over its design life, without disproportionate loss of serviceability or need for drastic repair and rehabilitation strategies. The durability of concrete used for both structural and pavement design purposes is directly related to the concrete performance properties, which infers that it may be durable in a certain setting but not in another (Owens, 2013).

The concrete construction industry has experienced numerous changes during the course of the last century. This has led to an increased need for concrete structures to be built in the fastest time possible. This can be achieved by utilizing high-early-strength concrete, simplified construction methods, economical construction materials and thin, slender concrete sections with a high steel reinforcement content (Owens, 2013). Owens (2013) lists the following as being extrinsic issues that influence the durability properties of concrete structures:

- Carbon dioxide emissions associated with the production processes of cementitious materials
- Over-reliance on the lowest tender system when selecting suitable contractors
- Lack of knowledgeable and skilled construction workers

Presently, companies are prioritising sustainability and focusing on limiting the environmental footprint of their structures. This is accomplished by implementing the Triple Bottom Line concept, which involves balancing the relevant environmental, economic and social factors as shown in Figure 2-41 (Owens, 2013). Concrete durability plays a major part in decreasing the life-cycle costs associated with a construction project, and simultaneously promoting the incorporation of sustainable construction practices.

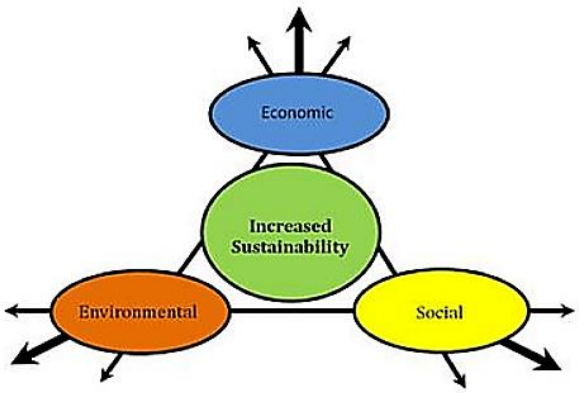

Figure 2-41: Various factors that constitute the Triple Bottom Line concept (Source: Owens, 2013)

2.9.1) Properties influencing the durability of concrete

Concrete durability is directly related to the porosity, permeation and microstructure properties of the specimen (Saleh, 2008). The durability performance of concrete can be enhanced with the addition of a supplementary cementitious material that has the holistic effect of strengthening the internal pore structure and improving the permeation properties (Saleh, 2008). According to Owens (2013), the transport (permeation, absorption, diffusion and migration), mechanical, physical and chemical properties are the most influential on the durability performance of both concrete structures and pavements. Each of the above-mentioned properties should be linked to the prevalent environmental conditions during the concrete production and construction phase.

2.9.1.1) Transport properties

Owens (2013) defines the transport properties as being the ease with which ions are able to pass through the concrete microstructure. The main deterioration mechanisms (chloride, carbonation, chemical attack, and leaching) of concrete exposed to aggressive environmental conditions are directly related to the transport properties of the concrete specimen (Owens, 2013). There is often a combination of various transport mechanisms present in conventional concrete. According to Owens (2013), the following are the main types of transport mechanisms that are encountered:

- **Permeation** – a process where ions/fluids move through the saturated pore structure, with the assistance of a pressure gradient that is externally applied (Owens, 2013). The permeability properties of concrete are dependent on the age, degree of compaction, moisture setting and the microstructure of the concrete.

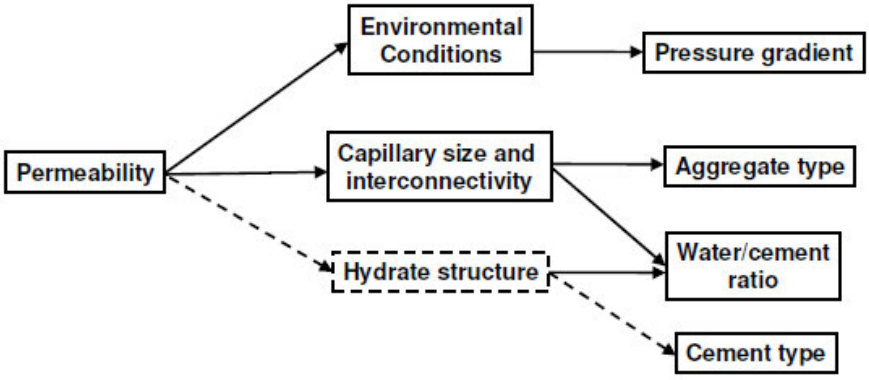

Figure 2-42: Factors influencing the permeability properties of concrete (Source: Saleh, 2008)

- **Capillary absorption** – a process during which ions/fluids are drawn into the porous, unsaturated structure by capillary action (Owens, 2013). Capillary absorption is typically encountered in structures, such as concrete pavements, that experience cyclic wetting and drying. There is direct correlation between absorption, the degree of saturation and the pore geometry.

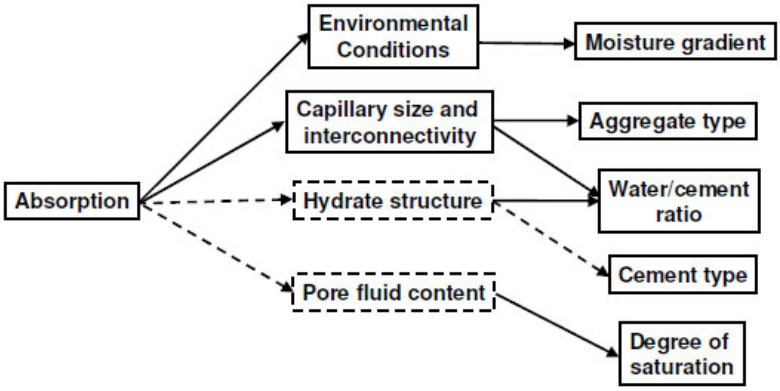

Figure 2-43: Factors influencing the absorption properties of concrete (Source: Saleh, 2008)

- **Diffusion** – a process whereby liquids, ions or gases move through the porous structure which can be attributed to a concentration gradient (Owens, 2013). Diffusion is a key transport mechanism in concrete roads situated in a coastal/marine setting, whereby chloride ions enter the microstructure of the concrete pavement. Diffusion is dependent on the pore geometry, degree of reactivity and concentration gradients.

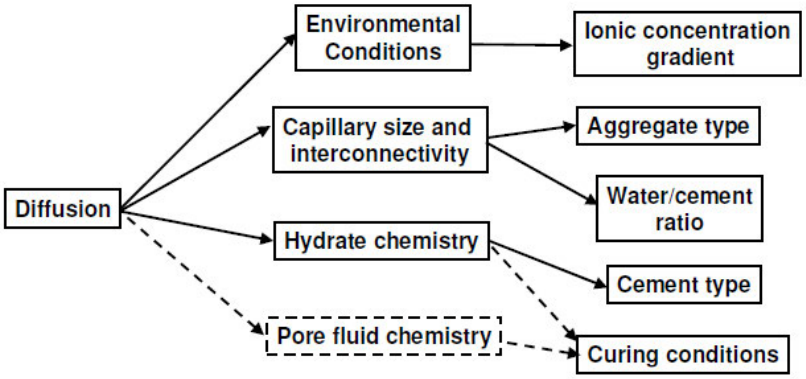

Figure 2-44: Factors influencing the diffusion properties of concrete (Source: Saleh, 2008)

- **Migration** – refers to the movement of ions in a solution exposed to an electrical current (Owens, 2013). Migration can also be called accelerated diffusion and is typically observed in laboratory investigations that simulate diffusion.

2.9.1.2) Physical and mechanical properties

The physical and mechanical properties of concrete (strength, stiffness, and density) are typically considered when designing rigid pavements which results in them being utilized as a way of stipulating and controlling the durability properties (Owens, 2013). There is a direct correlation between the strength of concrete and its durability, however, the specified concrete strength should not be used as the only provision of durability. Therefore, durable and economical concrete roads can be constructed by incorporating a more explicit and rational approach (Owens, 2013).

2.9.1.3) Chemical properties

The durability characteristics of concrete are emphasised by its capacity to perform successfully in aggressive environmental conditions. However, there are some forms of deterioration detected in concrete structures exposed to extremely harsh environments, which is typically attributed to the chemical properties of the concrete. According to Owens (2013), the durability performance of concrete is enhanced by incorporating blended cement (i.e. cement containing extenders) which have the overall effect of altering the chemical properties of the concrete. Adding a cement extender to the concrete mix will increase the amount of hydrates and improve the concrete's pore structure and microstructure, therefore resulting in a more durable concrete structure (Owens, 2013).

2.9.2) Mechanisms of deterioration

Deterioration typically occurs when the concrete elements of structures are exposed to adverse environmental conditions. According to Owens (2013), the critical mechanisms of deterioration are characterised as mechanical, chemical and corrosion of reinforcement. Furthermore, it is important to recognise the relevant mechanisms of deterioration, to ensure that a suitable solution can be applied to prevent or reduce the rate of concrete deterioration. The mechanical, chemical and reinforcement corrosion mechanisms of deterioration have been summarised in the respective tables below.

Table 2-8: Mechanical mechanisms of deterioration in concrete pavements (Source: Owens, 2013)

Mechanism	Summary
Abrasion	Wearing away of the concrete surface resulting from friction. The abrasion resistance of concrete is related to its aggregate and strength properties and can be enhanced by incorporating harder aggregates, reducing the water-binder ratio and applying suitable curing methods. Mechanical abrasion typically occurs in concrete pavements and often leads to increased roughness and a minor loss of the pavement surface.
Cavitation	In rigid pavements, sudden changes to the direction of fast flowing water will produce low pressure regions that may implode and create localised impact stresses on the pavement surface. Cavitation can be obviated by strengthening the aggregate paste bond characteristics and with the incorporation of silica fume as a supplementary cementitious material.
Erosion	Wearing of the concrete pavement surface due to erosion caused by the abrasive nature of rapidly flowing surface runoff.
Freezing	When freezing occurs, water present in the concrete pore structure will produce expansive forces that results in the propagation of cracks. Air-entraining admixtures serve as a suitable preventative measure for freeze-thawing.
Salt crystallisation	Salt (as a solution) enters the concrete microstructure due to cyclic wetting and drying, which leads to the formation of crystals. These

	crystals produce expansive forces that result in the formation of cracks. This mechanical mechanism of deterioration is common in rigid pavements situated in the splash zone of a coastal/marine environmental setting.

Table 2-9: Chemical mechanisms of deterioration in concrete pavements (Source: Owens, 2013)

Mechanism	Summary
Ion exchange /substitution	Replacement or substitution of ions between acids and sections of the hardened cement paste. Acid attack is a common example of this mechanism, where an acid reacts with the alkaline constituents which results in deterioration of the concrete matrix.
Ion removal	Removal of ions from the products formed during the hydration process of the cement. An example of this chemical deterioration is pure water attack, which is the process whereby pure water molecules leach the calcium silicate hydrate (C-S-H) and calcium hydroxide ($Ca(OH)_2$) from the cement paste after it has hardened.
Ion addition	Addition of ions from external sources to the hydration products. Sulphate attack is an example of this mechanism and refers to the process where sulphates react with $Ca(OH)_2$ and aluminates present in the cement paste matrix. This reaction is expansive in nature and results in the formation of cracks and deterioration of the concrete.

Corrosion of the steel rebar is the most common cause for the loss of durability in concrete that is reinforced, with pH decrease and chloride attack being the prevailing mechanisms of deterioration (Owens, 2013). The environmental exposure settings and the capability of the concrete cover to protect the steel reinforcement has a major effect on the rate at which the concrete structure begins to lose its ability to resist corrosion.

Concrete provides exceptional chemical and physical protection to the rebar. $Ca(OH)_2$ (which has a pH between 12 -13) is produced during the hydration of cement and is responsible for the high alkalinity of concrete (Owens, 2013). The alkaline properties of the pore solution create the ideal conditions for protecting the embedded steel reinforcement from corrosion (Berrocal et al., 2016). The passivating layer (which is a thin, stable and dense ferric-oxide film) is formed along the surface of the rebar and reduces the amount of ions moving between the embedded steel and the surrounding concrete (Berrocal et al., 2016).

This effect results in a decrease in the rate of corrosion, however, as time passes the corrosion protection offered by the concrete may decline such that the embedded steel begins to corrode.

Table 2-10: Mechanisms of corrosion in reinforced concrete (Source: Owens, 2013)

Mechanism	Summary
pH decrease	The resultant corrosion protection offered by the passivating layer is reduced when the pH level of the concrete drops below 9 (Saleh, 2008). Carbonation is the most common contributor towards pH reduction in concrete and refers to the process whereby calcium carbonate (pH of 8.5) is formed by the reaction between atmospheric carbon dioxide and calcium hydroxide present in the concrete.
Chloride attack	The passivating layer begins to deteriorate when the total chloride content of the concrete is greater than the chloride threshold level (critical chloride content that signals the commencement of the corrosion process). The time taken to achieve this level is increased with the incorporation of cement extenders (such as PMA) and the provision of additional concrete cover depth.

2.9.3) South African durability testing procedures

Problems linked to the durability performance of structures constructed with reinforced concrete can have a direct impact on the natural resources, human safety and economic growth (Kessy et al., 2015). Consequently, an innovative testing method has been applied in South Africa to improve the durability performance of concrete structures. This new testing method uses durability index tests to assess concrete transport properties. The durability index tests are performed in accordance with SANS 3001 and comprise of the Oxygen permeability, Water sorptivity and Chloride conductivity index tests (Owens, 2013).

The South African Durability Indexes are utilized alongside the minimum parameters that restrict the durability index values and concrete cover depth for numerous environmental exposure categories and several binder types (Owens, 2013). Regular checks are performed during the concrete mix design and construction phases to ensure that the durability index values lie within the specified limits. The durability index tests are typically performed on early-age (28 days) concrete specimens and are used to test the cover zone as indicated in the figure below (Owens, 2013).

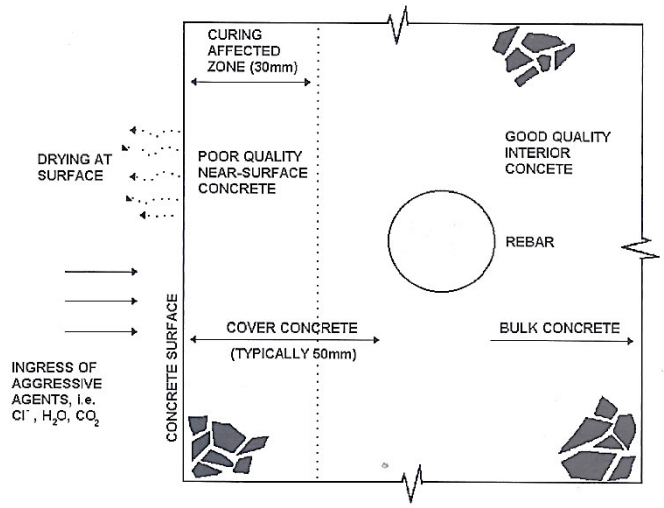

Figure 2-45: Drawing depicting the concrete cover zone (Source: Owens, 2013)

2.10) Microstructure properties of concrete used to construct rigid pavements

Despite containing numerous heterogeneous and complex constituents, concrete still remains the most commonly utilized material in the construction industry. However, this makes it problematic for researchers and engineers trying to create microstructural analysis models to predict the performance of concrete across various length parameters (Mehta and Monteiro, 2001). Therefore, there is an increased demand for an advanced theoretical understanding of the physical developments and structural characteristics that take place at various length scales (Garboczi and Bentz, 1996). The relationship that exists between each length scale is also a crucial variable for accurately predicting the concrete performance (Garboczi and Bentz, 1996).

Garboczi and Bentz (1996) provide the following length scales for assessing the microstructure properties of concrete:

- **Millimetres (mm)** – concrete is observed as aggregates along with a group of air voids enclosed by cement paste.
- **Micrometres (µm)** – the cement paste matrix of concrete is viewed as containing unhydrated clinker grains, capillary voids and hydration products.
- **Nanometres (nm)** – concrete pores contain calcium silicate hydrate (C-S-H) gel and numerous other nanometre sized constituents.

According to Diamond (2004), the durability characteristics of concrete microstructure is related to the w/b ratio, concrete mix design, chemical admixtures included in the mix, curing settings and mixing process followed. Concrete mixes incorporating Ordinary Portland Cement (OPC) are susceptible to deterioration resulting from a combination of the following (Courard et al., 2003):

- the porous disposition of the HCP and interfacial transition zone (ITZ)

- the high reactivity and soluble characteristics of calcium hydroxide produced during the hydration process

Mehta and Monteiro (2001) state that HCP, ITZ and aggregate material are the three key constituents of concrete microstructure. Chemical admixtures are commonly incorporated into the concrete mix to enhance the concrete microstructure properties, while also decreasing the calcium hydroxide concentration with pozzolanic reactions. This alteration to the microstructure aids in improving the durability and serviceability properties of concrete (Courard et al., 2003).

2.10.1) Aggregate material structure

The strength and bulk density properties of the aggregate material are the foremost contributors to the dimensional stability, unit weight and elastic modulus of concrete (Mehta and Monteiro, 2001). The physical characteristics, such as shape, size, volume, particle texture and pore distribution, of the aggregate material is superior to the chemical characteristics in concrete. According to Mehta and Monteiro (2001), the aggregate phase is significantly stronger than the ITZ and HCP, however, it does not have a direct impact on the strength of concrete. Nevertheless, the physical properties of the aggregate material have an indirect effect on concrete strength. Concrete comprising of large particle aggregates with a high proportion of flat and elongated particles tends to build up water films around the aggregate surface, which produces deterioration in the ITZ (Mehta and Monteiro, 2001). This process is called internal bleeding and has an unfavourable impact on the performance properties of concrete, particularly if the concrete is utilized in rigid pavement applications where high loads are experienced.

2.10.2) Hydrated cement paste structure

The clinker particle size of PC typically ranges from 1 to 50 μm (Mehta and Monteiro, 2001). Therefore, owing to the minimal clinker particle size, a scanning electron microscope needed to assess the microstructure properties of the HCP. Solids, voids and water are the three phases constituting the microstructure of HCP.

2.10.2.1) Solid phase of hydrated cement paste

According to Mehta and Monteiro (2001), the following elements make up the solid phase of the HCP:

- **Calcium silicate hydrate (C-S-H)** – has the largest influence on the performance properties of the HCP as it constitutes 50 to 60% of the total volume of solids. The C-S-H morphology can vary from poorly crystalline fibres to a reticular matrix network (Mehta and Monteiro, 2001).

- **Calcium hydroxide or Portlandite** – constitutes 20 to 25% of the total volume of solids present in the HCP. Calcium hydroxide tends to form large crystals with a hexagonal-prism structure that is influenced by the hydration temperature, presence of impurities and the amount of space that is available (Mehta and Monteiro, 2001).
- **Calcium sulfoaluminates** – has a minor influence on the structural properties of the HCP as it constitutes 15 to 20% of the total solids volume (Mehta and Monteiro, 2001).
- **Unhydrated clinker grains** – these grains are usually found in the HCP microstructure, even after hydration has taken place. This is due to the advancement of the hydration process, which shows that the smaller clinker grains are dissolved faster than the larger clinker grains (Mehta and Monteiro, 2001).

2.10.2.2) Voids found in the hydrated cement paste

Along with solids, various types of voids can be found in the HCP and has differing rates of influence on its properties:

- **Interlayer space in the C-S-H** – the C-S-H microstructure is made up of irregularly shaped layers, which are randomly positioned to form interlayer spaces. These resultant spaces accumulate water, which could possibly result in drying shrinkage and creep when the water is removed (Mehta and Monteiro, 2001).
- **Capillary voids** – denotes zones of the HCP matrix which are not occupied by solids. In HCP pastes with high w/b ratios, the size of the capillary voids present ranges from 3 to 5 μm, whereas in pastes with a low w/b ratio the voids are from 10 to 50 nm (Mehta and Monteiro, 2001). Capillary voids larger than 50 nm are referred to as macropores and have an adverse influence on the permeability and strength performance of concrete. In addition, voids smaller than 50 nm are identified as micropores and affects the creep and drying shrinkage properties (Mehta and Monteiro, 2001).
- **Air voids** – these voids are identified by their spherical shape and are typically found in air entrained concrete mixes. Air voids are significantly bigger than capillary voids, with entrained air voids ranging between 50 to 200 μm and entrapped air voids achieving up to 3 nm in size. Both types of air voids have an adverse influence on the permeability and strength properties of concrete (Mehta and Monteiro, 2001).

2.10.2.3) Water present in the hydrated cement paste

Numerous types of water can be found in the HCP and are categorized in accordance with the difficulty or ease with which it can be removed from the HCP (Mehta and Monteiro, 2001). The following types of water are present:

- **Capillary water** – made up of free water, which is present in voids larger than 50 nm, and/or water that is held by capillary tension which is found in small voids between 5 and 50 μm in size (Mehta and Monteiro, 2001). Removing the free water held by capillary tension in the smaller voids often leads to shrinkage of the HCP (Mehta and Monteiro, 2001).
- **Adsorbed water** – denotes the water located near the solid surface that could potentially be adsorbed by the solids found in the HCP (Mehta and Monteiro, 2001). This adsorption results in shrinkage once the HCP has dried.
- **Interlayer water** – consists of the water present in the C-S-H structure. The loss of this water leads to the development of shrinkage within the C-S-H matrix (Mehta and Monteiro, 2001).
- **Chemically combined water** – made up of water that constitutes a crucial structural element of the hydration products in cement (Mehta and Monteiro, 2001). In contrast, this water is not lost during drying, instead it is transformed once the hydrates are heated.

2.10.2.4) Mechanical-property relationships in the hydrated cement paste

In concrete, the key hardened state properties (strength, durability and dimensional stability) are directly related to the microstructural properties of the HCP (quantity, class and distribution of voids and solids) (Mehta and Monteiro, 2001).

- **Strength** – the intermolecular forces of attraction that exist between the C-S-H crystalline matrix, hexagonal calcium aluminate hydrates, calcium sulfoaluminate hydrates and the minimal surface area solids (anhydrous clinker grains, calcium hydroxide, coarse and fine aggregates) are the most significant contributors to HCP strength (Mehta and Monteiro, 2001). The strength properties of concrete are usually linked to the solids present in the HCP microstructure, whereas voids have a negative impact on strength performance.
- **Dimensional stability** – the water content of the HCP decreases when concrete is exposed to a humid environmental setting, which results in drying shrinkage and the propagation of cracks. Adsorbed water present in the HCP structure leads to a reduction in the disjoining pressure, which may also result in the development of drying shrinkage in concrete (Mehta and Monteiro, 2001).
- **Durability** – the concrete microstructure properties and the subsequent HCP permeability performance are key factors when assessing the durability of concrete. According to Mehta and Monteiro (2001), an impermeable HCP matrix usually leads to impermeable concrete. In concrete exposed to an aggressive environment, this results in corrosion of the rebar which ultimately leads to deterioration and failure of the concrete element. The HCP permeability is not affected by the small capillaries present or the porosity of the interlayer region of the C-S-H structure. Mehta and Monteiro (2001) go on to explain that the pore volume of the

small capillaries and C-S-H increases when the rate of hydration rises, which has the holistic effect of reducing the HCP permeability.

2.10.3) Interfacial Transition Zone (ITZ)

The ITZ is typically located between the aggregate particles and the HCP. It is made up of the same constituents as the HCP, however, it has a different elemental structure and properties, which includes an increased porosity and w/b ratio (Mehta and Monteiro, 2001).

2.10.3.1) Strength properties of the ITZ

The volume and size of the voids present have the largest influence on the strength properties of the ITZ (Mehta and Monteiro, 2001). With the progression of time, the ITZ strength improves until it is equivalent to or greater than the strength of the cement paste. Mehta and Monteiro (2001) associate this with the reactions occurring between the cement paste elements and the aggregate particles. These reactions reduce the calcium hydroxide levels in the ITZ, which inadvertently affects the concrete strength performance.

The presence of microcracks also has an adverse effect on the strength of concrete and is dependent on the w/b ratio, aggregate size, cement content, rate of compaction applied to the fresh concrete, curing conditions and environmental setting (Mehta and Monteiro, 2001). Cracks are primarily created in the ITZ when there are differential movements occurring between the aggregate material and the HCP (Mehta and Monteiro, 2001). These movements are a result of cooling or drying of concrete, which implies that microcracks can be found in concrete prior to loading. The rate at which microcracks are formed is augmented once the concrete is exposed to short term impact loads and sustained loads at high-stress levels (Mehta and Monteiro, 2001). This can have a detrimental effect on the performance of concrete used in rigid pavement applications.

2.10.3.2) Impact of the ITZ on concrete performance

The strength and durability properties of concrete is related to the performance of the ITZ. Owing to the relationship that exists between the w/b ratio and the HCP porosity, the w/b ratio also influences the strength and permeability characteristics of concrete (Mehta and Monteiro, 2001). The w/b ratio of the ITZ varies in accordance with the aggregate properties, i.e. large aggregates produce highly permeable concrete when a high w/b ratio is applied (Mehta and Monteiro, 2001).

Concrete exposed to a chloride-laden environment typically fails as a result of chloride attack and corrosion of the steel rebar. Therefore, the microcracks present in the ITZ of concrete pavements situated in a marine/coastal setting has the adverse effect of increasing the concrete permeability and consequently promotes the propagation of chloride attack.

2.10.4) Concrete microstructure testing procedures

Various techniques can be used to conduct a microstructural analysis of concrete, these techniques can be divided into two groups, specifically the direct or microscopical techniques and the indirect or bulk techniques. The direct or microscopical procedures are used to evaluate the arrangement of the constituent phases present in the microstructure of a concrete sample (Scrivener, 1998).

A scanning electron microscope (SEM) is the preferred apparatus for undertaking an optical microscopic study. The results obtained from the microscopic study are documented as images, which indicates that any comparison of the results attained are dependent on the researcher's understanding of the concrete microstructure properties (Scrivener, 1998).

Alternatively, indirect or bulk test procedures are used to characterise the chemical composition of the specimen and includes thermogravimetry (TG) and X-ray diffraction (XRF) studies (Scrivener, 1998). Techniques such as mercury intrusion porosimetry (MIP) and methanol absorption, which are used to analyse the pore size distribution, can also be characterised as indirect or bulk test procedures (Scrivener, 1998). The main advantage of indirect testing methods is that they produce quantitative test results, which enables various concrete specimens to be objectively compared.

2.11) Alternative binder materials for concrete pavements

As stated previously, there is a growing demand for alternate binder materials to address the increased concerns surrounding the CO_2 emissions resulting from the cement manufacturing process (Schneider, 2019; Doudart de la Grée et al., 2018; Singh and Middendorf, 2020; Pandey and Kumar, 2020; Kumar et al., 2020). This can be achieved by incorporating supplementary cementitious materials, such as paper mill ash, which reduces the amount of cement that is manufactured for concrete production purposes. Along with improving the sustainability of rigid pavements, alternative binder systems can also be used to enhance the fresh state, mechanical and durability performance of concrete. Ayub et al. (2013) has noted that using alternate binder systems will reduce the cement content thereby reducing the heat of hydration, while also improving the concrete durability properties. The research undertaken in this study includes the use of paper mill ash (PMA) as a supplementary cementitious material for rigid pavement applications.

2.11.1) Material properties of Paper Mill Ash

2.11.1.1) Manufacturing process and chemical composition

Paper mill sludge is a waste product generated during the deinking and re-pulping stages in the pulp and paper manufacturing process and is often viewed as being a substantial economic and

environmental problem to the pulp and paper industry (Dunster, 2007). Likon and Trebše (2012) reported that for every unit of paper manufactured, up to 23.4% of the waste generated is classified as paper mill sludge. Over 4.7 million tonnes of paper mill sludge are produced each year by the member countries of the Confederation of European Paper Industries (CEPI). However, based on current trends, this value is expected to rise by 48 to 86% across the next fifty years (Likon and Trebše, 2012; Mabee and Roy, 2003). Paper mill sludge comprises of cellulose fibres, mineral fillers, water, inorganic salts and organic compounds (Fava et al., 2011; Furlani et al., 2008). Paper mill sludge is commonly recycled and disposed of via land spreading (serves as an agricultural fertiliser) or landfill. Land spreading proves to be inefficient as an ample land space is required, while strong odours prevent it from being applied close to residential areas (Likon and Trebše, 2012). More than 69% of the paper mill sludge that is produced by the pulp and paper industry is disposed of via landfill, which places an additional strain on landfill operations and can have a hazardous effect on nearby groundwater (Bujulu et al., 2007; Elliott and Mahmood, 2006).

In order to minimise landfill volumes and recover energy, paper mill sludge can also be dewatered and incinerated in combined heat and power plants located within the paper mill. The resultant fly ash, which is classified as a waste, is known as paper mill ash (PMA) and has high contents of silicon dioxide (SiO_2), aluminium trioxide (Al_2O_3), calcium oxide (CaO), ferric trioxide (Fe_2O_3) and magnesium oxide (MgO) (Fava et al., 2011). Since these oxides are commonly found in PC, PMA can also serve as a potential supplementary cementitious binder material in concrete (Wong et al., 2015). This will help alleviate the costs associated with the disposal of paper mill sludge, maintain land capacity, safeguard the decreasing supply of raw materials and mitigate the adverse environmental impacts related to the cement manufacturing industry (bin Mohd Sani et al., 2011).

The chemical composition of PMA is mostly dependent on the incineration temperature (Ferrándiz-Mas et al., 2014). If the combustion temperature ranges from 700 °C to 750 °C, then the clay minerals (e.g. kaolinite) present in the paper mill sludge are converted into metakaolinite, and the resultant PMA exhibits pozzolanic properties (Frías et al., 2008a; Garcia et al., 2008; Pera and Amrouz, 1998; Vegas et al., 2006). Furthermore, if the calcination temperature lies between 850 °C and 1200 °C, then there are minimal amounts of metakaolinite in the PMA. At this stage, it will longer behave like a pozzolanic material (Ferrándiz-Mas et al., 2014; García Giménez et al., 2015; Mozaffari et al., 2006). This may be attributed to the fact that the higher combustion temperatures prevent the kaolinite mineral in the sludge from being converted into metakaolin, which is responsible for pozzolanic activity in cementitious materials (Mozaffari et al., 2006).

Table 2-11: Chemical composition of PMA samples used in past research studies

Research Study	Oxides (%)														
	CaO	**SiO_2**	**Al_2O_3**	**Fe_2O_3**	**MgO**	**K_2O**	**P_2O_5**	**SO_3**	**Na_2O**	**Li_2O**	**TiO_2**	**MnO**	**BaO**	**SrO**	**LOI**
Ahmad et al. (2013)	43.51	25.70	18.86	0.87	5.15	1.31	0.52	1.05	1.56	0.01	0.68	0.04	0.04	0.09	1.2
Gailius and Laurikietytė (2003)	8.69	59.47	10.45	10.45	3.13	–	–	–	–	–	–	–	–	–	–
Dunster (2007)	43.51	25.70	18.86	0.87	5.15	1.31	0.52	1.05	1.56	0.01	0.68	0.04	0.04	0.09	–
Likon and Trebše (2012)	8.69	59.47	10.45	10.45	3.13	–	–	–	–	–	–	–	–	–	–
Mabee and Roy (2003)	55.87	15.16	6.06	1.11	2.00	0.34	0.48	0.78	0.19	–	0.45	0.05	–	–	17.51
Furlani et al. (2008)	12.45	67.33	2.62	1.42	2.74	0.64	0.05	–	12.05	–	0.16	–	–	0.02	–
Bujulu et al. (2007)	19.82	18.01	10.14	0.55	2.58	0.21	0.10	0.33	0.25	–	0.26	–	–	–	47.62

ASTM (2008) states that the percentage of the three main oxide constituents, i.e. SiO_2, Al_2O_3 and Fe_2O_3 must summate to a minimum of 50%, for a material to be classified as being pozzolanic. Based on this, only the PMA samples utilised by Kumar and Rani (2016), Poojitha and Bhanu Pravallika (2017) and Sudha et al. (2018) may be deemed to be pozzolanic (Table 2-11).

2.11.1.2) Hydration process

In contrast with cementitious materials like PC, PMA absorbs water at a much faster and more extensive rate (Mozaffari et al., 2009). The hydration process in PC concrete commences upon the addition of water and progresses at a decreasing rate inward from the individual particle surfaces. Furthermore, PMA displays significant variations in chemical composition and particle size, as shown in Table 2-11, which prevents it from similarly undergoing hydration as PC. According to Mozaffari et al. (2009), this disparity in chemical composition and particle size distribution enables rapid reactions to occur in some phases. It also produces a chemical environment that is suitable for hydration and pozzolanic reactions in other phases, while some phases may also be deemed to be inert (Mozaffari et al., 2009). When water is added to PMA, two key processes occur, namely the dissolution of available free lime to produce slaked lime and the dissolution of silica and alumina resulting from a pH increase (Mozaffari et al., 2009).

Hydration of the free lime triggers the release of hydroxyl ions to create an alkaline solution. The hydration of the α'-C_2S and the bredigite and the dissociation of the glassy phases then occurs, which releases alumina and silica (Mozaffari et al., 2009). The hydration process culminates when the calcium ions bind with the Al_2O_3 and SiO_2 to produce additional calcium silicate hydrate (C-S-H) gel (Mozaffari et al., 2009). The hydration products commonly found in PMA cement pastes are: CH, C_4AH_{13}, $C_3A.0.5C\bar{C}.0.5CH.H_{11\,5}$, C_2ASH_8, $C_3A.3CS.H_{32}$ and C-S-H gel (Bai et al., 2003). However, when PMA is used as the sole binder material in concrete, it is not particularly

cementitious in nature. This can be attributed to the unsound hydration of CaO, resulting from the presence of a significant amount of non-hydraulic products, such as gehlenite, that are inaccessible by water (Mozaffari et al., 2009). Various research (Kinuthia et al., 2001; Veerappan et al., 2003; Chaipanich et al., 2005) have shown that the PMA hydration process can be improved by blending the PMA with ground granulated blastfurnace slag (GGBS), which will be discussed in great detail later in this chapter.

2.11.1.3) Morphology

The performance of PMA as a partial cement replacement in concrete is largely dependent on the morphology and particle size of the PMA sample (Vigil de la Villa et al., 2007). The morphological properties of PMA directly influence the fresh state, mechanical and durability properties of concrete containing PMA (Zhang et al., 2018). Morphology is an effective property for assessing the feasibility of PMA as supplementary cementitious material, with a Scanning Electron Microscope (SEM) investigation being the most used method for determining the morphology of PMA.

The SEM observations documented in various research studies indicate that PMA particles are porous, agglomerated and heterogeneous in nature (Ferrándiz-Mas et al., 2014; Mozaffari et al., 2009; Segui et al., 2011; Segui et al., 2012a; Segui et al., 2012b). The SEM analysis undertaken by (Pachamuthu and Thangaraju, 2017) also found that PMA particles are predominantly wide, flat and hexagonally shaped. Consequently, this agglomeration is a result of the incineration stage when manufacturing the PMA. The increased porosity of the PMA particles points towards a higher water demand and reduced workability properties when PMA is incorporated as a partial cement replacement in concrete (Monosi et al., 2012). The high-water demand is linked to the high microporous structure of PMA, which leads to an increased particle surface area and a hypothesised high free lime content (Goñi et al., 2012;; Wu et al., 2016; Frías et al., 2008b; Doudart de la Grée et al., 2018). The poor workability of PMA concrete can be compensated with the addition of a water-reducing admixture or increasing the water-binder (w/b) ratio (Segui et al., 2012a).

Mozaffari et al. (2009) also found that the surface of a single PMA particle displayed a degree of roughness (see Figure 2-46[a]). Figure 2-46(b) shows that some individual mineral constituents are bound together with other mineral grains, which may also be attributed to the incineration process followed to produce the PMA (Mozaffari et al., 2009).

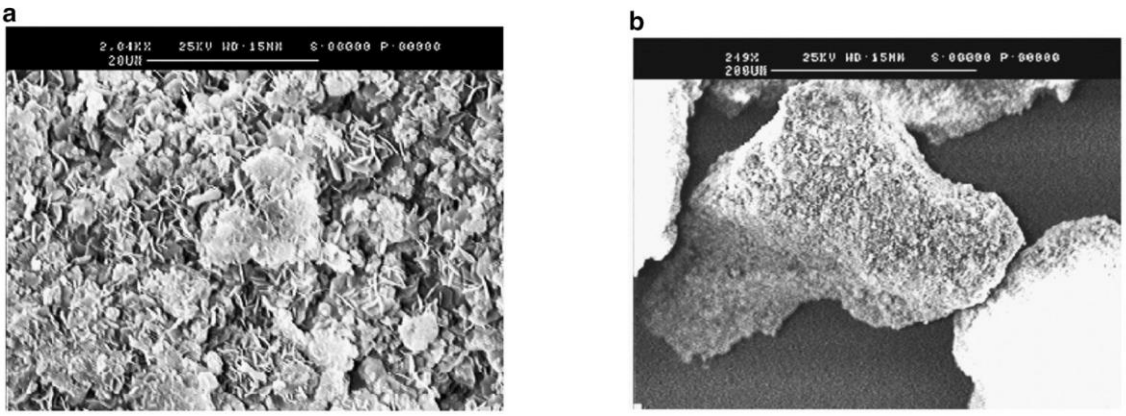

Figure 2-46: (a) SEM image depicting roughness of PMA particle surface, (b) SEM image depicting the individual mineral grains of PMA (Source: Mozaffari et al., 2009)

Aini et al. (2013) investigated the effect of PMA particle size on the morphological properties of PMA. This involved observing SEM images of unsieved PMA and PMA retained on the 63 μm sieve, 45 μm sieve and pan. From the SEM images, it was noted that the PMA particles become more densely packed as the particle size decreased. This suggests that the much finer PMA particles will have a more positive contribution towards the filler effect, by filling the voids present in the cement matrix of conventional concrete (Abdul Ghani et al., 2015). Aini et al. (2013) also found that the PMA particles have a porous structure and are irregularly shaped, which is in agreement with the findings from the other research studies discussed earlier.

2.11.1.4) Equivalent Carbon Dioxide

Owens (2013) uses the equivalent carbon dioxide (CO_{2e}) values for each concrete constituent to ultimately determine the carbon footprint of concrete. From a sustainability perspective, this study only focuses on the environmental impact of producing the most frequently used raw materials (i.e. cement, GGBS, FA, admixtures, aggregates and water). It is worth noting from Table 2-12 that the CO_{2e} of PMA is zero.

Table 2-12: Average CO_{2e} emission values for various concrete constituents

Material Type	Notation	Average Emission Values (kg CO_{2e}/ton)	Source
Portland Cement	CEM I	985	(Owens, 2013)
Portland-Limestone Cement	CEM II A-L	840	(Owens, 2013)
	CEM II B-L	720	(Owens, 2013)
Portland-Slag Cement	CEM II A-S	815	(Owens, 2013)
	CEM II B-S	730	(Owens, 2013)
Portland-Fly Ash Cement	CEM II A-V	790	(Owens, 2013)
	CEM II B-V	690	(Owens, 2013)
Blast furnace Cement	CEM III A	560	(Owens, 2013)
Pozzolanic Cement	CEM IV A	640	(Owens, 2013)
	CEM IV B	570	(Owens, 2013)
Composite Cement	CEM V A	590	(Owens, 2013)
	CEM V B	415	(Owens, 2013)
Admixtures	–	220	(Owens, 2013)
Aggregates	–	5	(Owens, 2013)
Water	–	1	(Owens, 2013)
Paper Mill Ash	PMA	0	(Fava et al., 2011; Gavrilescu, 2008; Babalola et al., 2020; Jarnerud, 2019)

2.11.2) Fresh state properties of concrete containing Paper Mill Ash

The main fresh state properties of concrete considered for rigid pavement construction includes workability, consistency, flowability, place-ability, cohesiveness, bleeding and texture ability. The addition of paper mill ash, as a partial cement replacement, has a significant effect on the fresh state properties of concrete. This section includes an evaluation of the experimental results obtained from previous studies on the fresh state properties of concrete containing paper mill ash.

2.11.2.1) Workability

Ahmad et al. (2013) investigated the fresh state properties of concrete containing varying amounts (i.e. 5, 10, 15 and 20%) of wastepaper sludge ash (or PMA) as supplementary cementitious material. This was achieved by conducting a slump test to determine the effect of PMA on the workability characteristics of concrete. As depicted in Figure 2-47, the authors revealed that the slump decreased as the PMA content increased. This indicates that PMA particles absorb more water than ordinary Portland cement (OPC), which leads to reduced workability in fresh concrete.

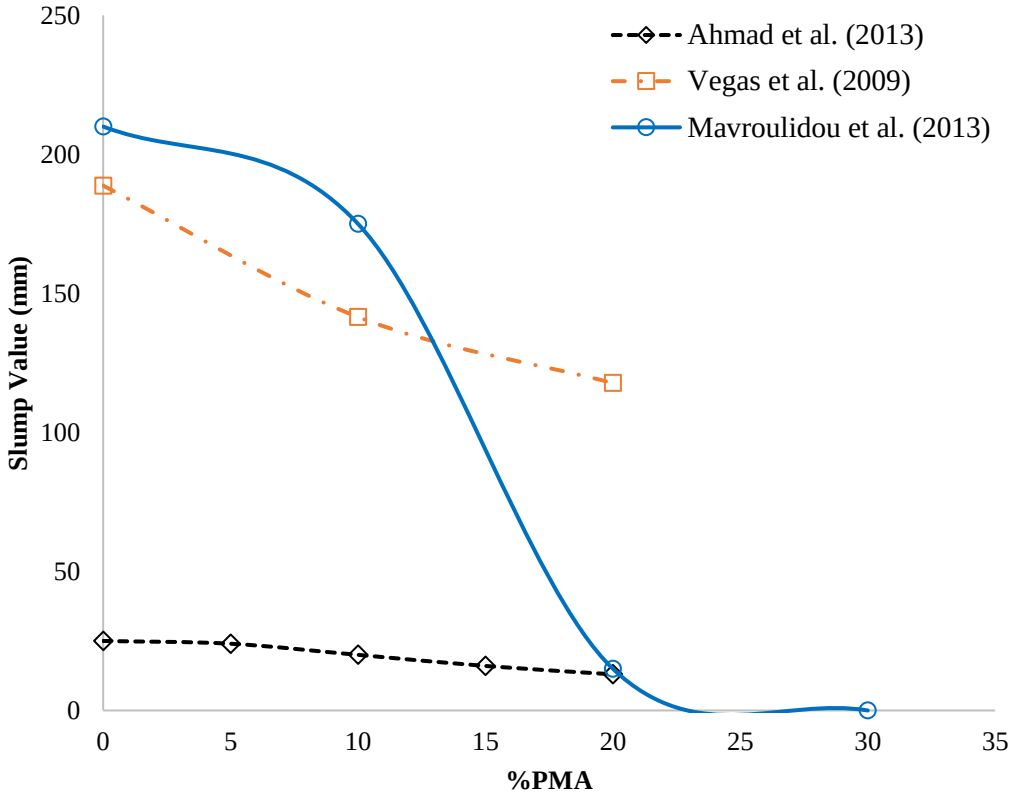

Figure 2-47: Effect of wastepaper sludge ash on concrete workability

Mavroulidou et al. (2013) further examined the workability of different concrete mixes containing various percentage of PMA as a partial replacement for OPC. The slump test results obtained in this experimental investigation shows that increasing the PMA content results in a reduction of the workability and consistency of the mix, with a 30% PMA content achieving a slump of zero (Figure 2-47). This can be attributed to the high-water demand required by PMA for the formation of hydration products (Mavroulidou et al., 2013).

The setting time and slump properties of cement mortar samples blended with 0, 10 and 20% of calcined paper sludge or PMA was investigated by Vegas et al. (2009). A w/b ratio of 0.5 was adopted for all the cement mortar mix designs. The results, as indicated in Table 2-13, show that PMA reduces the setting time of blended cement mortars. This can be associated with the presence of metakaolin and calcium carbonate ($CaCO_3$) in the PMA sample, which accelerates the hydration of C_3S and reduces the setting time (Vegas et al. 2009). The study also revealed that slump decreases as the PMA replacement level increases (Figure 2-47). The authors reported that PMA is much finer than OPC and requires more water for hydration, therefore increasing the PMA content results in the production of more interparticle attractions.

It was also noted that the PMA sample used in the experimental investigations conducted by Mavroulidou et al. (2013) had higher percentages of CaO, SiO_2, Al_2O_3 and Na_2O in comparison

with the sample used by Vegas et al. (2009). This may explain the significantly lower slump test result obtained for the 20% PMA replacement level in Mavroulidou et al. (2013), as the higher oxide concentration of PMA sample is expected to accelerate the hydration process, reduce the setting time and consequently decrease the workability performance of the fresh concrete.

Table 2-13: Setting time for cement mortar specimens (Source: Vegas et al. 2009)

% PMA	Initial Set (min)	Final Set (min)
0% PMA	145	255
10% PMA	120	170
20% PMA	60	130

Gailius and Laurikietytė (2003) studied the workability properties of fresh concrete containing different proportions of PMA and GGBS as a combined binder replacement for cement. The concrete mixes used in the research study were designed for two water-binder (w/b) ratios – 0.4 and 0.5, with the following PMA to GGBS proportions (replacement by percentage weight): 30:70, 40:60, 50:50, 60:40 and 70:30. Furthermore, Daracem SP1 (a superplasticiser) was added to the mixes that achieved a slump below 30 mm. The results obtained show that higher amounts of superplasticiser were required as the PMA content increased (Table 2-14). This can be attributed to the 35% of CaO present in the PMA sample used in the experimental investigations, which when hydrated forms $Ca(OH)_2$ and result in rapid initial hydration and setting (Gailius and Laurikietytė, 2003). The increased need for a superplasticiser to achieve desirable slump points to reduced workability in fresh concrete containing PMA.

Table 2-14: Concrete mix designs and slump test results (Source: Gailius and Laurikietytė, 2003)

Mix WSA: GGBS	Amount of SP1% by weight of binder		Slump (mm)	
	0.5	0.4	0.5	0.4
30:70	0	6.5	42	32
40:60	3.2	8.0	38	30
50:50	3.8	9.7	35	30
60:40	3.8	9.7	34	32
70:30	8.1	18.3	58	28

Gailius and Laurikietytė (2003) found that the addition of a superplasticiser or water-reducing admixture helps to improve the fresh state properties of concrete containing PMA; however, a higher amount of superplasticiser was required for the concrete mixes designed to a lower w/b ratio. Babafemi et al. (2018) attribute this to the impact of w/b ratio and the amount of cement paste on the concrete slump and the mobility of the constituents. It was observed that the w/b ratios used in the existing research studies ranged from 0.4 to 0.55; therefore, additional

experimental investigations are required to examine the impact of higher w/b ratio (>0.55) towards improving the fresh state properties of PMA concrete.

Even though a minimal amount of research has been conducted on the fresh state properties (namely workability and consistency) of concrete containing PMA, a common trend of results was observed in the available experimental studies. The slump test results obtained in all the research studies indicate that the incorporation of PMA into the concrete mix as a partial cement replacement results in a reduction of the workability.

2.11.3) Mechanical Properties of Concrete Containing Paper Mill Ash

The incorporation of paper mill ash, as supplementary cementitious material, has a significant effect on the mechanical properties of concrete (Ayub et al., 2014). This section includes an assessment of the experimental results attained from the literature relating to the mechanical properties of concrete containing paper mill ash.

2.11.3.1) Compressive, Tensile and Flexural Strengths

Gailius and Laurikietytė (2003) examined the compressive strength properties of concrete containing various amounts of PMA and GGBS as a combined binder replacement for OPC. The concrete samples contained the following ratios of PMA to GGBS – 30:70, 40:60, 50:50, 60:40 and 70:30, and were designed using two w/b ratios (0.4 and 0.5). The results indicate that the 50:50 mix ratio between PMA and GGBS achieved the highest compressive strength across all curing periods. The author hypothesised that this occurred because PMA and GGBS complemented one another when incorporated as supplementary binder materials in concrete. The study also found that the mixes containing a higher amount of PMA (i.e. 60:40 and 70:30) and a w/b = 0.4 attained lower compressive strength results than those specimens with a w/b = 0.5, which is due to the increased water requirement of mixes containing a higher ratio of PMA to GGBS (Gailius and Laurikietytė, 2003).

Likewise, Bai et al. (2003) explored the strength development and compressive strength properties of blended pastes containing the following ratios of wastepaper sludge ash (WSA or PMA) to GGBS – 20:80, 30:70, 40:60, 50:50, 60:40 and 70:30. Samples containing 100% PMA and 100% PC acted as a control to ensure an accurate comparison. As displayed in Figure 2-48, the compressive strength of the 100% PC specimens is significantly higher than the strength of the PMA-GGBS and 100% PMA blended pastes. It is also worth noting that the pastes containing PMA achieved a low development of initial strength up until the 28-day period.

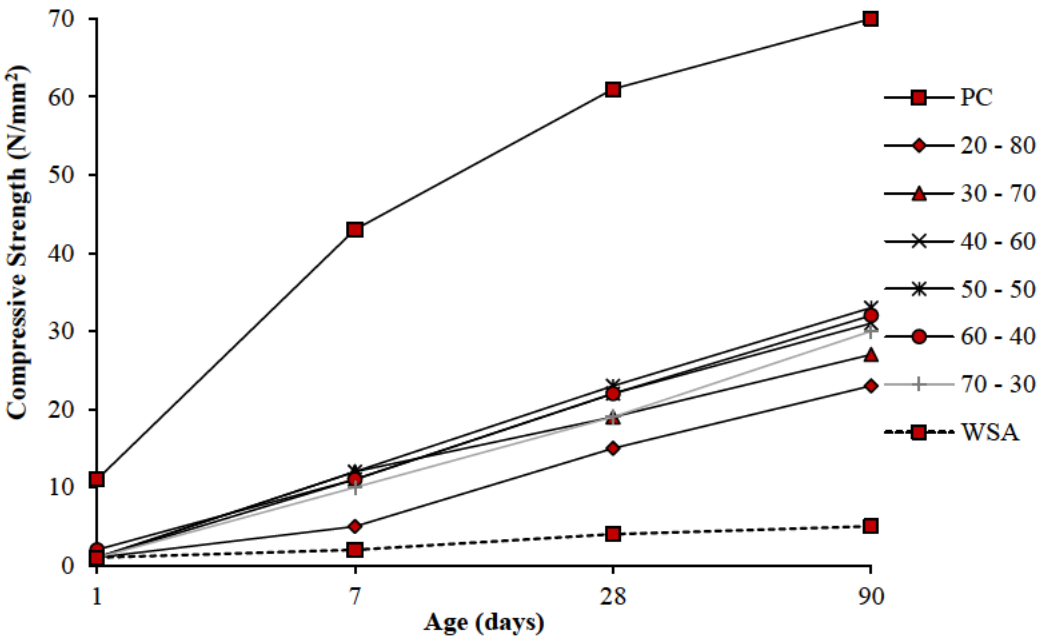

Figure 2-48: Strength development of blended pastes containing PC, PMA-GGBS and PMA (w/b = 0.5) (Source: Bai et al., 2003)

The relative strength results presented in Figure 2-49 are the calculated ratio of the compressive strength for each paste to the compressive strength of the 100% PC paste for the same age (Bai et al., 2003). From the results obtained, it is evident that blending the PMA with GGBS improves the compressive strength across all curing ages, with the 50% PMA – 50% GGBS blend achieving the highest strength results for the blended pastes, thus making it the optimum replacement content.

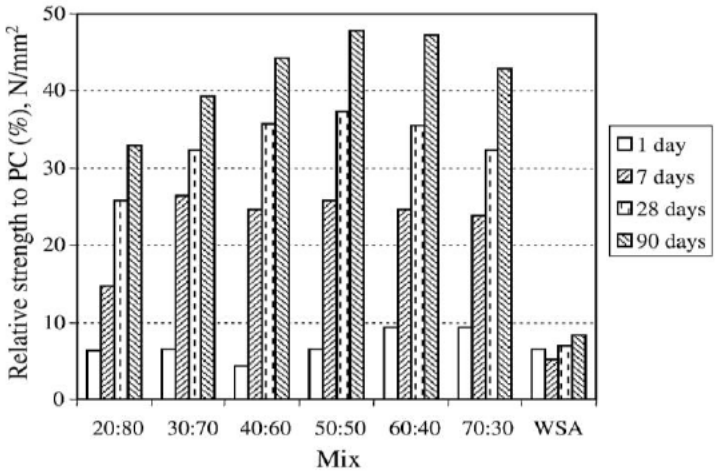

Figure 2-49: Relative compressive strength of blended pastes containing PMA-GGBS and PMA to PC (w/b = 0.5) (Source: Bai et al., 2003)

The effect of partial replacement of cement with 5, 10, 15 and 20% PMA on the compressive strength, and tensile splitting strength of concrete was also investigated by Ahmad et al. (2013).

As shown in Figure 2-50, the 5% PMA mix achieved the optimum compressive strength results for both the 7- and 28-day curing period, with the compressive strength decreasing after that. The strength increase displayed in the 5% PMA samples is approximately 15% at the 28-day mark. Similarly, the 5% PMA replacement level was also determined to be the optimum content for the tensile splitting strength, with the results reducing for the following PMA contents (Figure 2-51).

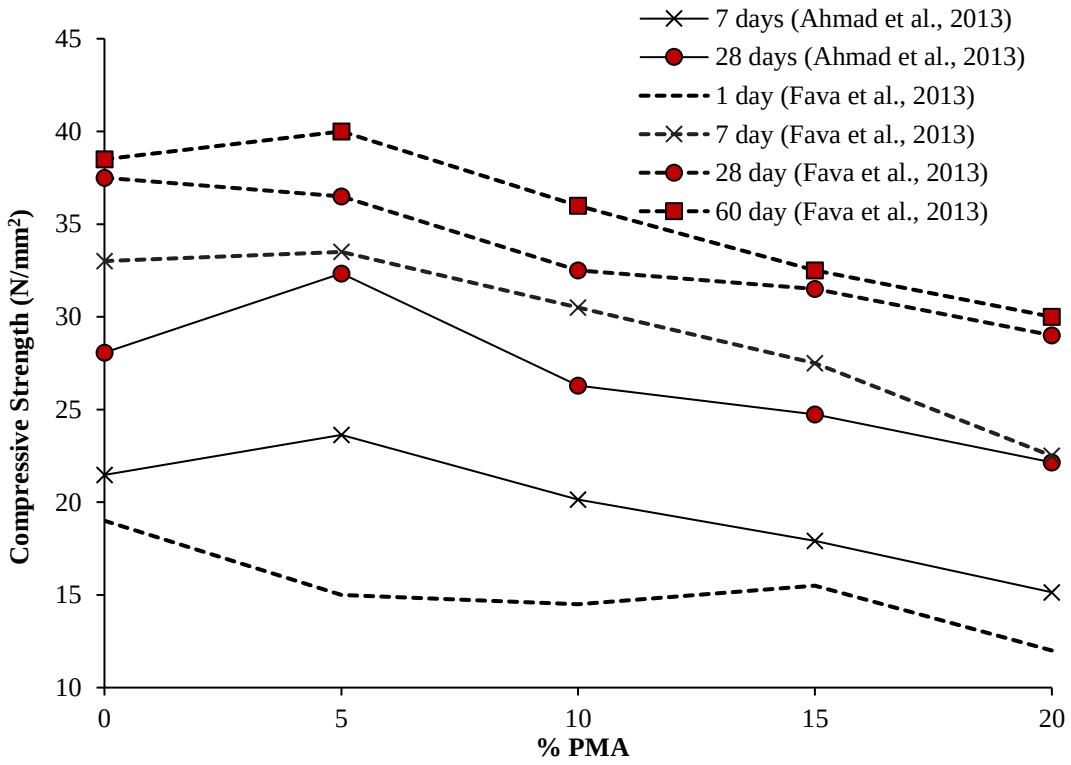

Figure 2-50: Compressive Strength Results for concrete samples containing various amounts of PMA (Source: Fava et al., 2011; Sudha et al., 2018; Ahmad et al., 2013)

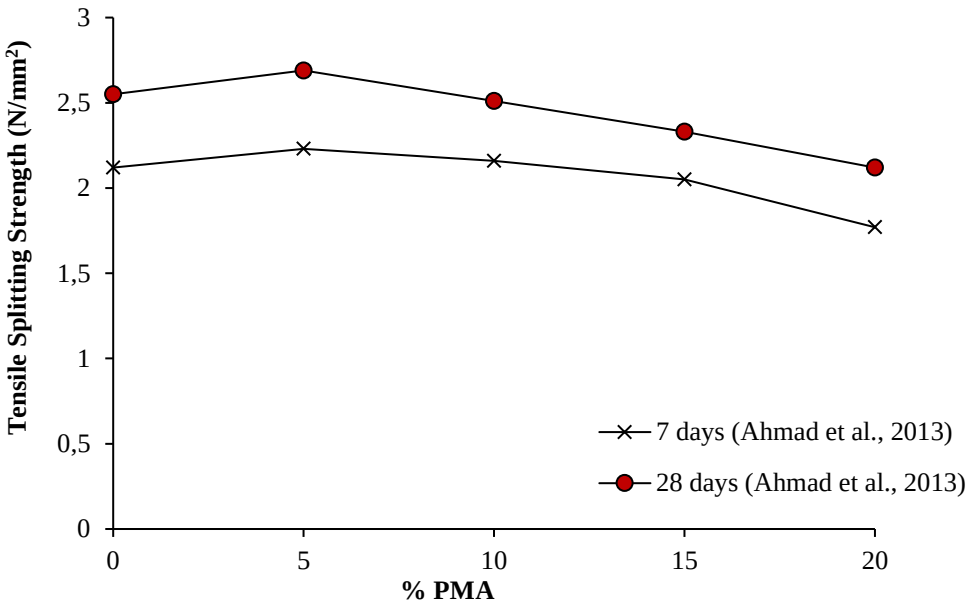

Figure 2-51: Tensile Splitting Strength Results (7 & 28 day) for concrete samples containing various amounts of PMA (Source: Ahmad et al., 2013)

Fava et al. (2011) examined the outcomes of replacing Portland-Limestone blended cement with 5, 10, 15 and 20% of PMA (replacement by weight of cement) in mortar mixtures designed to various w/b ratios (i.e. 0.4, 0.5 and 0.6). From the results presented in Figure 2-50, it is evident that the compressive strength of the 5% PMA mixture after 7-, 28- and 60-days of curing is relatively similar to that of the 0% PMA samples. The general trend present in the results obtained indicates that the compressive strength decreases as the PMA replacement level increases, with the 5% PMA mixture being the only exception. The results also show that the compressive strength of the mortar mixes decreases as the w/b ratio is inflated (Figure 2-52). The authors revealed that the proportion of PMA to OPC should be kept below 10% to maximise the contribution of PMA towards the hardening of the cement paste and development of the mechanical properties in concrete.

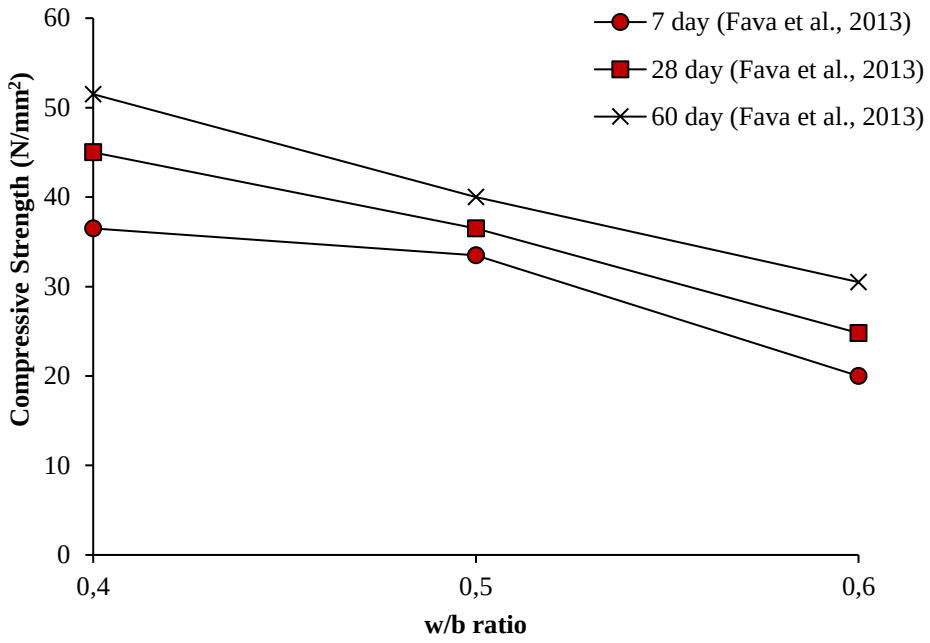

Figure 2-52: Compressive Strength Results for concrete samples with 5% PMA and varying containing w/b ratios (Source: Fava et al., 2011)

Sudha et al. (2018) further researched the mechanical properties of concrete containing various proportions of PMA to OPC. This included conducting the standard cube, cylinder splitting and beam tests to determine the respective compression, tensile splitting and flexural strength for concrete samples containing 5% (WPSA1), 10% (WPSA2), 15% (WPSA3) and 20% (WPSA4) PMA. The compressive strength results in Table 2-15 shows that 10% replacement of PMA is the optimum content for both 7- and 28-day tests.

The flexural and tensile splitting strength results presented in Table 2-15 indicates the optimum replacement level as being 10% for both the 7- and 28-day curing periods. The authors concluded that the feasibility of PMA as an alternative binder material could be improved by ensuring that the cement replacement with PMA does not exceed 10%, which is in agreement with the research study conducted by Fava et al. (2011). In a similar investigation, Poojitha and Bhanu Pravallika (2017) examined the compressive, tensile and flexural strengths of concrete specimens containing 5, 10 and 15% of PMA as a supplementary cementitious material. The concrete strength results attained indicates that PMA improves the compressive, tensile splitting and flexural strengths over a 28-day time period, with 10% being the optimum PMA content. Furthermore, the authors reported that PMA produced a 15.86% increase in concrete strength when compared to conventional concrete.

Table 2-15 shows that the compressive, flexural, and tensile splitting strength results attained for the 10% PMA samples in Poojitha and Bhanu Pravallika (2017) are higher than the respective

results achieved by Sudha et al. (2018). This could be associated with the higher percentages of Al_2O_3 and Fe_2O_3 (which are two of the main oxide constituents in pozzolanic materials) found in the PMA sample that was used. The increased oxide concentration of the PMA sample results in the development of additional C-S-H gel and improved concrete strength (Babalola et al., 2020).

Table 2-15: Effect of PMA on the compressive, tensile splitting and flexural strengths of concrete (Source: Sudha et al., 2018; Poojitha and Bhanu Pravallika, 2017)

%PMA	Compressive Strength		Tensile Splitting Strength		Flexural Strength	
	7 Days	28 Days	7 Days	28 Days	7 Days	28 Days
Sudha et al. (2018)						
0%	22.35	29.76	1.52	2.13	3.3	3.81
5%	23.59	30.54	1.63	2.25	3.39	3.86
10%	24.89	33.46	1.72	3.25	3.49	4.04
15%	21.54	26.48	1.65	2.3	3.24	3.6
Poojitha and Bhanu Pravallika (2017)						
0%	19.38	34.50	2.12	2.34	4.01	4.21
5%	23.84	35.11	2.21	2.45	4.05	4.38
10%	25.52	38.26	2.32	2.68	4.38	5.01
15%	24.54	36.89	2.24	2.54	4.12	4.62

Vegas et al. (2009) conducted experimental investigations to determine the compressive strength properties of cement mortar samples blended with 0, 10 and 20% of calcined paper sludge or PMA. From Figure 2-53, it can be seen that the early compressive strength (i.e. after 2 days of curing) of the 10 and 20% PMA samples is similar to that of the control samples. After a curing time of 7 days, the mortar specimens containing 10 and 20% of PMA achieved higher compressive strength results than the control. This can be attributed to the presence of metakaolin in the PMA sample used in the research study, which impacts on the hydration reaction thus creating additional C-S-H gel and improving the strength results attained (Vegas et al., 2009). In addition, the metakaolin also serves as a filler material, which subsequently reduces the porosity and produces a more densified microstructure. The results also show that 20% of PMA is the optimum replacement level achieved in this research study.

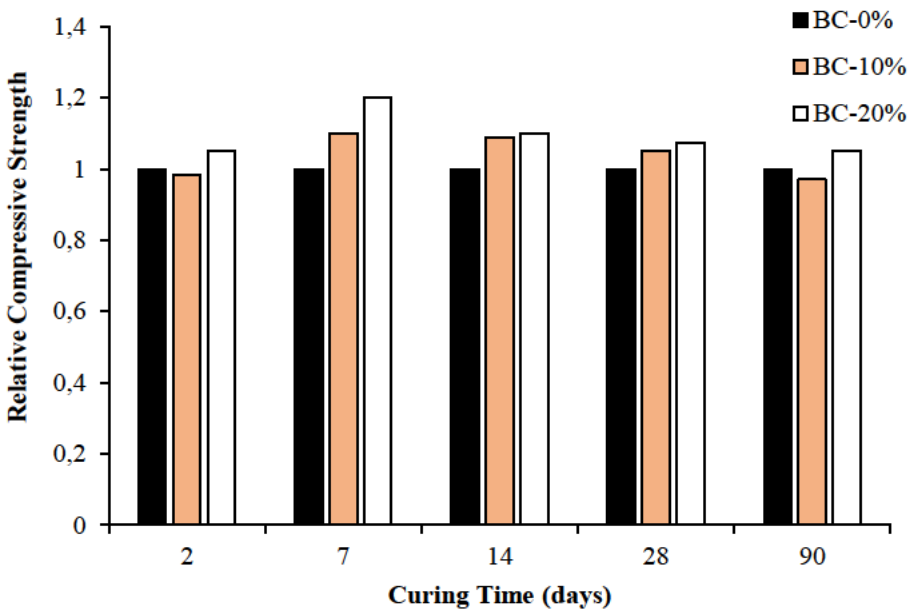

Figure 2-53: Compressive strength results of PMA blended cement mortar specimens (Source: Vegas et al., 2009)

Sharipudin and Ridzuan (2012) examined the concrete strength properties of foamed concrete containing 5, 10, 15, 20 and 30% of PMA as supplementary cementitious material. The results attained indicate that the incorporation of 5–20% PMA improved the strength of the foamed concrete samples, with 20% PMA achieving the optimum 28-day strength. The authors also noted that increasing the percentage PMA to 30% resulted in a decrease of the compressive strength. This can be attributed to the increased levels of PMA, resulting in reduced pozzolanic reactivity and decreased strength development in foamed concrete.

Mavroulidou et al. (2013) studied the compressive and tensile strength of concrete mixes containing various proportions of PMA, GGBS, PFA and MK as supplementary cementitious materials. Figure 2-54 shows that all mixes containing OPC and PMA only achieved a compressive strength either equivalent or superior to that of the control samples for both the 7- and 28-day curing period. The tensile strength of the specimens was evaluated using the tensile splitting test and the beam or modulus of rupture (MoR) test (Mavroulidou et al., 2013). Much like the compressive strength results obtained in (Sharipudin and Ridzuan, 2012), Mavroulidou et al. (2013) observed that the tensile strength of the specimens comprising of OPC and PMA only was either similar or higher than the control mix strength (Figure 2-55).

The 7 and 28-day compressive strength results obtained for the 5 and 10% PMA replacement level in Mavroulidou et al. (2013), are significantly higher than the results achieved by Poojitha and Bhanu Pravallika (2017). This can be attributed to higher concentrations of CaO and Al_2O_3 present in the PMA sample used in (Mavroulidou et al., 2013; Babalola et al., 2020), which

improves the pozzolanic properties of these concrete specimens and thereby enhances the strength performance of the PMA concrete.

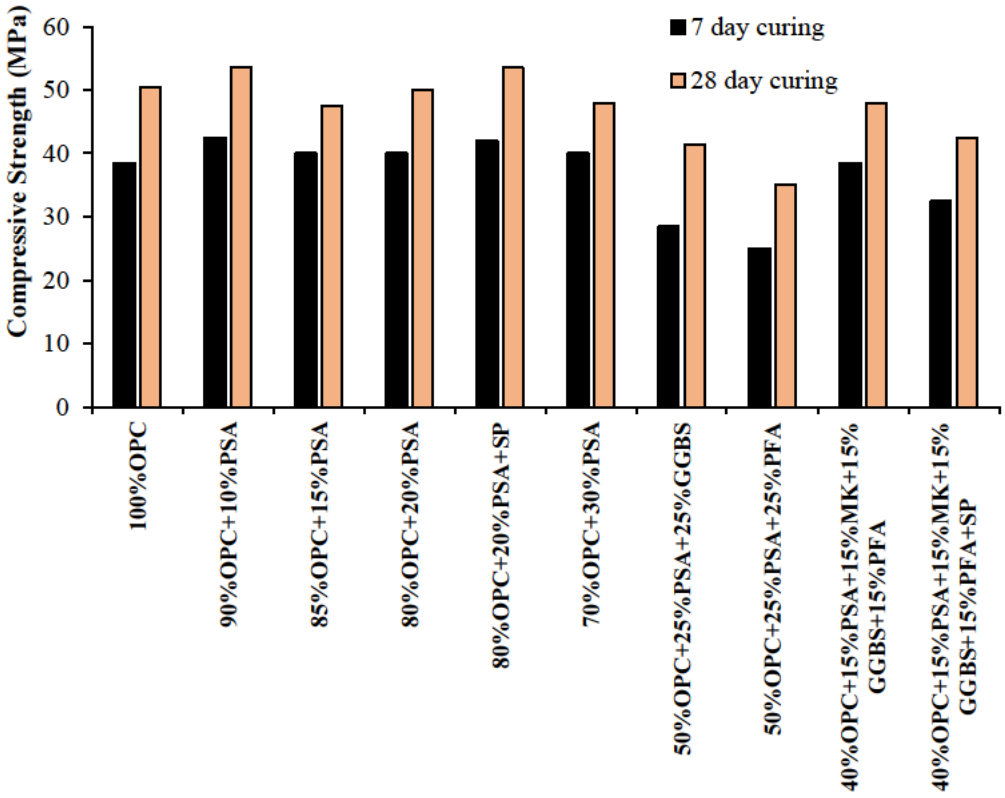

Figure 2-54: Compressive strength test results for concrete mixes containing various combinations of PMA, GGBS, MK and PFA (Source: Mavroulidou et al., 2013)

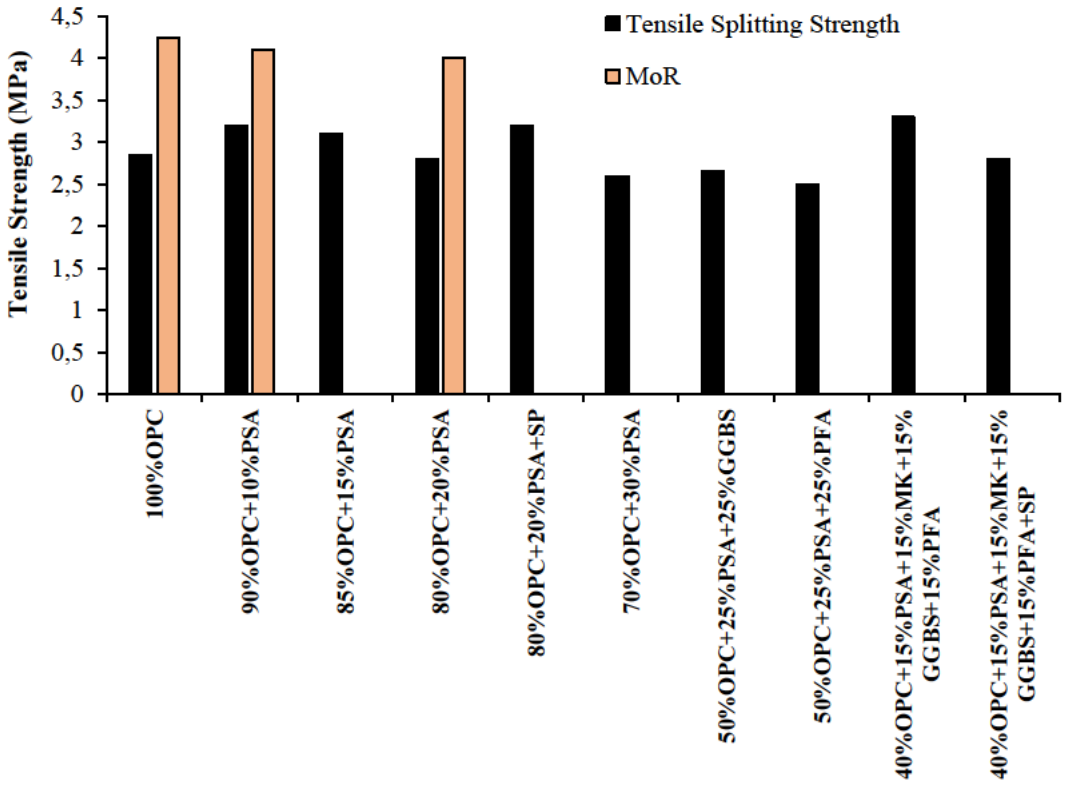

Figure 2-55: Tensile strength test results for concrete mixes containing various combinations of PMA, GGBS, MK and PFA (Source: Mavroulidou et al., 2013)

Kumar and Rani (2016) investigated the strength properties of concrete containing 5, 10 and 15% of paper sludge ash (or PMA) as a partial cement replacement (by mass). The compressive strength and tensile strength of the laboratory specimens were determined using the cube and tensile splitting tests, respectively. The strength results obtained in Table 2-16 indicate that PMA reduces the compressive strength across all curing periods. Kumar and Rani (2016) also found that there was an increase in the tensile strength of the mix containing 5% of PMA, with a gradual decrease existing for the subsequent increments of PMA.

Table 2-16: Compressive strength and tensile splitting strength test results obtained (Source: Kumar and Rani, 2016)

Designation of specimen	Avg. Compressive Strength of specimen in N/mm^2 at curing period in days of			Avg. Tensile Strength of specimen in N/mm^2 at curing period in days of		
	7 days	14 days	28 days	7 days	14 days	28 days
CC (0%)	28.04	30.48	33.19	2.12	2.98	3.67
PSA_1 (5%)	26.99	28.80	32.81	2.83	3.53	3.98
PSA_2 (10%)	23.40	26.54	29.03	2.24	2.62	3.01
PSA_3 (15%)	22.51	23.03	23.25	2.16	2.54	2.83

As discussed above, experimental investigations conducted by (Fava et al., 2011; Sudha et al., 2018; Ahmad et al., 2013; Poojitha and Bhanu Pravallika, 2017) showed that PMA enhanced the mechanical properties, with 5–10% PMA content level achieving the optimum concrete strength results. Likewise, Vegas et al. (2009) also documented a significant improvement in the strength properties of mortar samples containing PMA. However, the study found the optimum replacement content to be 20%. The improved mechanical properties noted in most of the previous experimental studies can be attributed to the presence of metakaolin in the PMA samples. Metakaolin has a direct correlation with the hydration process of PMA, which leads to the development of additional C-S-H gel and improved concrete strength properties. Besides, the characteristics of metakaolin are similar to that of filler material, which improves the concrete microstructure and reduces the porosity. Gailius and Laurikietytė (2003) and Bai et al. (2003) revealed that GGBS serves as a good blending agent with PMA to replace OPC. The studies reported that the replacement ratio of 50% PMA to 50% GGBS achieved favourable concrete strength properties. Bai et al. (2003) attributed the strength development to the following:

- Addition of GGBS to the system, which reduces the quantity of expansive product available per unit of internal pore space and reduces the amount of disruption experienced by the hardened cement paste
- Increased w/b ratio resulting in a higher amount of CaO hydration taking place before the commencement of setting
- Reduction of expansion with the subsequent provision of a surface upon which lime can be absorbed and used to activate the slag hydration process
- Minimal hydration of GGBS during the early stages combined with more advanced hydration of the PMA

The results obtained by (Bai et al., 2003; Gailius and Laurikietytė, 2003) indicated that the optimum PMA content level increases with the addition of GGBS. This can be attributed to the complementary relationship existing between the two blending agents. Thus, the strength performance of concrete containing PMA as a partial cement replacement can be further improved by incorporating GGBS as a supplementary blending material. However, additional experimental investigations are needed to determine the optimum replacement ratio of PMA to GGBS.

In contrast with the studies mentioned above, Kumar and Rani (2016) noted a decrease in the compressive strength of PMA concrete. This variation in test results can be attributed to the different chemical compositions and particle sizes of the various PMA samples used in the experimental studies. Therefore, additional research is required to determine the definitive optimum content level, chemical composition and particle size distribution of PMA for use as a supplementary cementitious material.

The South African Pavement Engineering Manual (SAPEM) (2013d) recommended a target flexural strength of not less than 4 MPa at 28 days for concrete pavement minor roads. Generally, this flexural strength requirement can be satisfied through a minimum 28-day characteristic compressive strength of 30 MPa (SAPEM, 2013d). The SAPEM target flexural and compressive strength for concrete pavement is achieved for the respective optimum PMA replacement levels in the research studies conducted by (Fava et al., 2011; Sudha et al., 2018; Ahmad et al., 2013; Poojitha and Bhanu Pravallika, 2017).

2.11.3.2) Drying shrinkage

Vegas et al. (2009) investigated the drying shrinkage properties of mortar samples manufactured with a blended cement containing 0, 10 and 20% of PMA. The results indicated that the incorporation of PMA into the mix design increased the drying shrinkage by up to 2.5 times more than the control samples. This trend of results can be attributed to the following (Vegas et al., 2009):

- The crystallisation of the calcite particles presents in the PMA, which increases the hydration process and accelerates shrinkage.
- Pozzolanic reaction of metakaolin from the PMA with the calcium hydroxide produced by the cement.
- Increased capillary tension resulting from the fine particle size distribution of the PMA sample.

2.11.4) Durability Properties of Concrete Containing Paper Mill Ash

The durability of a concrete element is the ability to withstand extreme environmental conditions over its design life, without disproportionate loss of serviceability or need for drastic repair and rehabilitation strategies (Owens, 2013). The durability properties of concrete considered for both structural and pavement design purposes is directly linked to the concrete performance properties, which suggests that it may be durable in a certain setting but not in another (Owens, 2013). Concrete durability is directly related to the porosity, permeation and microstructure properties of the specimen (Poongodi et al., 2020; Saleh, 2008). The durability performance of concrete can be enhanced with the addition of a supplementary cementitious material that has the holistic effect of strengthening the internal pore structure and improving the permeation properties (Saleh, 2008). According to Owens (2013), the transport (permeation, absorption, diffusion and migration), mechanical, physical and chemical properties have the most significant impact on the durability performance of both concrete structures and pavements. Each of the properties mentioned above should be linked to the prevalent environmental conditions during the concrete production and construction phase. The incorporation of paper mill ash, as a partial cement

replacement, has a meaningful effect on the durability properties of concrete. This section includes an overview of the experimental results obtained from the literature pertaining to the durability properties of concrete containing paper mill ash.

2.11.4.1) Resistance to acid attack

An acid attack usually takes place when concrete is exposed to liquids with a pH below 6.5, while the severity of the attack increases as the pH value decreases. The progression of acid attack in concrete results in the deterioration and leaching away of the cement compounds present in the hardened cement paste. Owens (2013) explains that it is impossible to produce acid-resistant concrete using PC; however, an acid-resistant coating may be applied as a protective layer to concrete that is exposed to severe acidic environments.

Poojitha and Bhanu Pravallika (2017) investigated the durability properties of concrete incorporating PMA as supplementary cementitious material. This was achieved by observing the acid resistance results obtained from the acid attack factor test and acid durability factor test. In the research study, concrete samples containing 10% of PMA and varying amounts of steel and glass fibres were exposed to hydrochloric acid (HCl) and sulphuric acid (H_2SO_4). In order to simulate a very severe acid attack, both acids had a concentration of 5% and pH values of 3.01 and 2.75, respectively.

From the durability results presented in Tables 2-17 and 2-18, it can be determined that the specimens exposed to H_2SO_4 displayed a higher percentage weight loss after 28 days and reduced compressive strengths, which can be attributed to increased deterioration and greater severity of acid attack experienced. The study also proved that glass fibres had a better effect on improving the durability properties of concrete containing PMA.

Table 2-17: Durability results for concrete samples exposed to HCl (Source: Poojitha and Bhanu Pravallika, 2017)

% Replacement	% weight loss after 28 days	Compressive Strength (N/mm^2)	
		7 days	28 days
0.1% Glass Fibres	2.3	16.12	28.88
0.2% Glass Fibres	2.46	17.22	29.76
0.3% Glass Fibres	2.66	18.44	30.23
0.4% Glass Fibres	2.69	16.81	28.11
0.5% Steel Fibres	2.33	16.67	28.41
1% Steel Fibres	2.41	18.81	30.41
1.5% Steel Fibres	2.58	17.16	28.12
2% Steel Fibres	2.63	16.81	27.41

Table 2-18: Durability results for concrete samples exposed to H_2SO_4 (Source: Poojitha and Bhanu Pravallika, 2017)

% Replacement	% weight loss after 28 days	Compressive Strength (N/mm^2)	
		7 days	28 days
0.1% Glass Fibres	4.16	12.66	22.35
0.2% Glass Fibres	5.59	13.58	23.44
0.3% Glass Fibres	6.34	14.99	24.68
0.4% Glass Fibres	6.35	13.24	23.33
0.5% Steel Fibres	4.46	14.44	23.04
1% Steel Fibres	5.66	15.85	24.81
1.5% Steel Fibres	6.41	15.50	24.54
2% Steel Fibres	7.11	14.21	24.11

2.11.4.2) Water absorption and porosity

Water absorption by submersion is a key variable for assessing concrete performance. It indicates the porosity properties of concrete by determining the percentage of water absorbed into the microstructure when the sample is immersed and is related to the square root of time (Babafemi et al., 2018). Ahmad et al. (2013) conducted a water absorption test on specimens containing 5, 10, 15 and 20% PMA, which served as an indirect measure of the concrete durability properties. This was determined by measuring the average weight of concrete cube samples after the samples are demoulded and again after 28 days of curing. The results graphically depicted in Figure 2-56 indicate that the percentage of water absorption rose as the PMA content increased. This can be attributed to the high-water demand required to form hydration products.

Mavroulidou et al. (2013) also used the percentage of water absorption to quantify the durability properties of concrete mixes containing various amounts of OPC, PMA, MK, GGBS and PFA. The water absorption test procedure involved oven-drying 100 × 100 × 100 mm cubes for 72 h, before leaving the samples to cool in an airtight container for 24 h. The percentage water absorption was calculated by measuring the mass increase of the cube after submerging it in water for 30 min and dividing it by the dry mass of the cube (Mavroulidou et al., 2013). The results attained show that the percentage of water absorption decreases as the PMA replacement level increased (Figure 2-56). This contradicts the results obtained by Ahmad et al. (2013) (Figure 2-56).

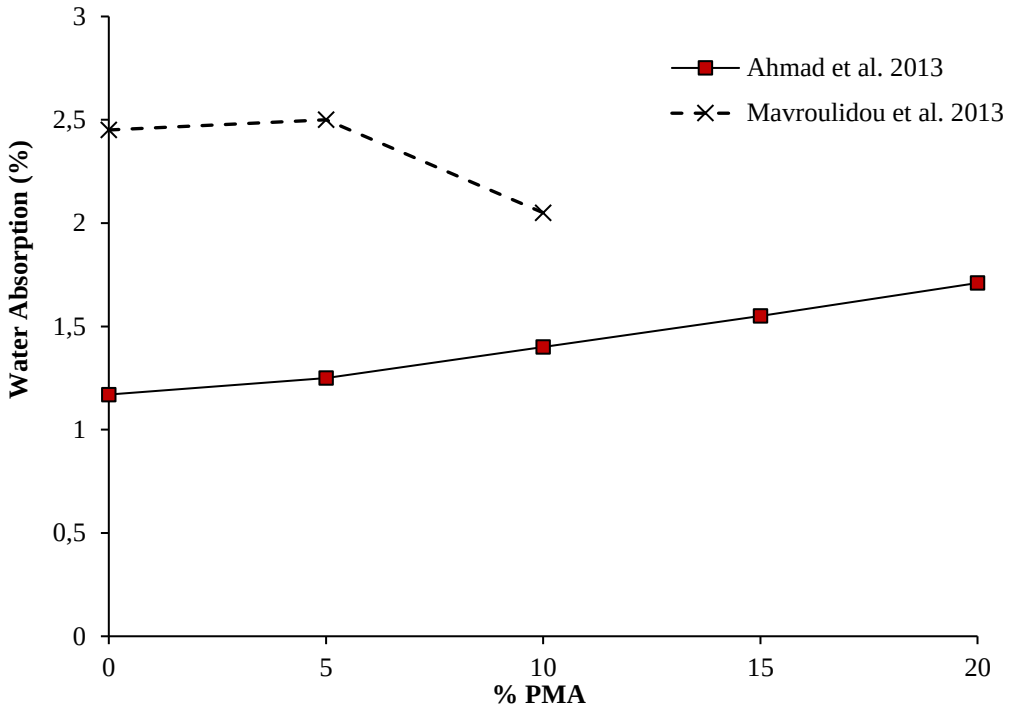

Figure 2-56: Durability results from the water absorption test (Monosi et al., 2012; Dunster, 2007)

Based on the review of the existing studies undertaken in this section, it can be seen that minimal research has been conducted on the durability properties of concrete incorporating PMA as supplementary cementitious material. It is also worth noting that there is no research pertaining to the microstructure properties of concrete containing PMA. Besides, the durability performance of PMA concrete has not been investigated in accordance with the South African durability index tests. Therefore, further experimental studies are required to examine the durability properties of concrete containing PMA as a partial cement replacement.

2.11.5) Summary

Table 2-19: Previous studies on the concrete properties of cement-based materials with varying amounts of paper mill ash (PMA)

Research Study	Concrete/ Mortar	PMA (%)	Water-Binder Ratio	Properties Researched	Findings
Fava et al. (2011)	Mortar	5 to 20	0.4 to 0.6	Mechanical	Compressive strength decreased as the w/b ratio increased
Bai et al. (2003)	Mortar	20 to 100*	-	Mechanical	Low development of initial strength up until 28 days; 50% PMA-GGBS blend achieved optimum results
Kumar and Rani (2016)	Concrete	5 to 15	-	Mechanical	PMA reduced the compressive strength; optimum tensile strength results for 5% PMA
Mavroulidou et al. (2013)	Concrete	10 to 30**	0.55	Fresh	Workability decreased as the PMA content increased
				Mechanical	Strength of PMA samples are equivalent or superior to the control samples
				Durability	Water absorption results decreased as the PMA content increased
Sharipudin and Ridzuan (2012)	Concrete	5 to 30	-	Mechanical	Compressive strength improved up until 20% PMA
Sudha et al. (2018)	Concrete	5 to 20	-	Mechanical	10% PMA attained the optimum strength results
Vegas et al. (2009)	Mortar	10 to 20	0.5	Fresh	Workability decreased as the PMA content increased
				Mechanical	20% PMA achieved the highest results
Ahmad et al. (2013)	Concrete	5 to 20	0.45	Fresh	Workability decreased as the PMA content increased
				Mechanical	5% PMA obtained the optimum results; strength decreased after 28 days
				Durability	Water absorption results increased as the PMA content increased
Gailius and Laurikietytė (2003)	Concrete	30 to 70*	0.4 & 0.5	Fresh	Workability decreased as the PMA content increased
				Mechanical	50% PMA and GGBS achieved the optimum compressive strength

*blended with various proportions of ground granulated blast furnace slag (GGBS)
**blended with various proportions of GGBS, pulverised fuel ash (PFA) and metakaolin (MK)

Incineration of paper mill sludge in combined heat and power plants to produce PMA serves as an alternative to disposing of the waste via land spreading or landfilling operations. This section of the dissertation included an extensive review of the performance properties of concrete incorporating PMA as a supplementary cementitious material. The concrete properties under consideration in this review comprised of the following: fresh state, mechanical and durability properties. The main findings noted in existing research studies on the concrete properties of cement-based materials with varying amounts of PMA are summarised in Table 2-19. From the presented review of previous literature, the following conclusions can be deduced:

- Workability, namely slump and setting time, declined as the PMA content increased.
- Mechanical properties, specifically compressive, flexural and tensile splitting strength, improved as the PMA replacement level increased. The optimum PMA content level was deemed to lie between 5 and 10%, with concrete strength decreasing beyond this level. However, it was also shown that the optimum PMA content level increases when GGBS is incorporated as a supplementary blending agent.
- Drying shrinkage properties increased, by up to 2.5 times, with the incorporation of PMA.
- A gradual increase in the percentage water absorption takes place with an increase in PMA content.

The reduced workability of PMA concrete mixes can be attributed to the finer PMA particle size distribution in comparison with PC. This, coupled with the presence of metakaolin in PMA, means that PMA has a higher water requirement for the hydration reactions to occur. The high-water demand for PMA is also responsible for the increase in percentage water absorption, which is directly related to the porosity and durability properties in concrete. There was a consensus that the incorporation of PMA results in reduced concrete workability properties. However, there was a notable disparity in the w/b ratios applied across the various research studies. Therefore, future experimental investigations are required to determine the impact of higher w/b ratio towards enhancing the fresh state performance of PMA concrete.

The favourable development of concrete strength that has been documented in the majority of past experimental investigations can also be associated with the fact that metakaolin is a chemical constituent of PMA. The metakaolin found in PMA has a direct impact on the hydration process, which results in the formation of additional C-S-H gel and the subsequent improvement of concrete strength. Furthermore, metakaolin also behaves like a filler material, which reduces the porosity and produces a more densified concrete microstructure.

This review also found that the PMA hydration process can be improved by incorporating GGBS as a blending agent, with the replacement ratio of 50% PMA to 50% GGBS achieving superior concrete strength results. However, the experimental investigations conducted by Kumar and

Rani (2016) documented a decrease in the compressive strength of concrete containing PMA as an alternative binder material. This, in combination with the minimal research pertaining to the durability and microstructure properties of PMA concrete, highlights the need for additional research to determine the definitive optimum content level, chemical composition and particle size distribution of PMA for use as supplementary cementitious material. It is also worth mentioning that no experimental research has been undertaken to assess the microstructure and skid resistance properties of concrete containing PMA. This could provide additional information to determine the feasibility of PMA as supplementary cementitious material for rigid pavement applications.

According to SAPEM (2013d), the 28-day target flexural strength of concrete roads should be greater than 4 MPa. This requirement is generally satisfied when a minimum characteristic 28-day compressive strength of 30 MPa is achieved (SAPEM, 2013d). The 28-day flexural strength requirement has been achieved for the respective optimum PMA replacement levels in the research studies conducted by Fava et al. (2011), Poojitha and Bhanu Pravallika (2017), Sudha et al. (2018) and Ahmad et al. (2013). Considering that tensile or flexural strength is the defining variable used for the design of rigid pavements, and the favourable flexural and tensile splitting strength results documented in this research study, it can be concluded that concrete incorporating PMA as a partial cement replacement is a viable option for use in rigid pavement applications. The advantageous development of long-term strength and durability of concrete containing PMA coupled with the negligible CO_{2e} emission value of PMA can have the beneficial effect of improving both the sustainability and serviceability states of rigid pavements.

2.12) Conclusion

Chapter 2 comprised of a systematic review of various works of literature related to the predetermined areas of interest for the research topic. The literature review introduced the South African road network and the main uses of concrete in the roads and transportation engineering sector. This chapter then discussed the functional properties, design requirements, variations and joint design techniques for rigid pavements. The construction processes that are typically followed were also outlined along with the most widely used repair and rehabilitation strategies. The engineering (fresh state, mechanical, durability and microstructure) properties of concrete used to construct rigid pavements was critically assessed. This led to the establishment of the main area of interest for this research topic – incorporating supplementary cementitious materials (namely paper mill ash) in rigid pavement designs. This point was expanded on with a detailed analysis of the engineering performance of paper mill ash based concrete. The analysis encompassed a review of the results obtained from the experimental investigations undertaken in

past year studies. From this analysis, it was determined that paper mill ash is viable as a partial cement replacement in concrete used for sustainable rigid pavement construction.

CHAPTER 3: METHODOLOGY

3.1) Introduction

This chapter outlines the research areas that were identified and the research approaches that were implemented, while also detailing the experimental procedures that have been used to meet the aims and objectives documented in Chapter 1. These techniques comprise of experimental investigations that primarily focused on assessing the engineering performance of PMA as an alternate binder material for concrete production. The following concrete properties were studied: workability, compressive strength, tensile splitting strength, flexural strength and durability. Skid resistance tests, an equivalent carbon dioxide (CO_{2e}) assessment and a construction cost analysis based on a real-world scenario were used to determine the feasibility of PMA concrete for sustainable rigid pavement construction.

3.2) Research approaches

An experimental and theoretical research approach are the two methods that have been adopted to assess the feasibility of paper mill ash as an alternate binder material for rigid pavement construction in South Africa. The theoretical research approach provides an overview of the investigation, while the experimental research approach further enhances the accuracy of the study by offering a detailed analysis of the engineering performance of concrete containing paper mill ash as a supplementary cementitious material.

3.2.1) Theoretical research approach

The theoretical approach entailed a literature review that outlined and evaluated the functional properties, design requirements, variations, joint design techniques, construction procedures, repair and rehabilitation strategies for concrete pavements. Chapter 2 also analysed the viability of paper mill ash as an alternate binder material with a critical assessment of the engineering performance documented in past year experimental investigations.

The theoretical approach played a key role in documenting the important information pertaining to the research study. However, this approach on its own proves to be insufficient in meeting the aims and objectives that were outlined in Chapter 1. Therefore, the theoretical research approach was combined with the experimental research approach in order to provide a thorough assessment of the feasibility of paper mill ash as an alternate binder material for concrete used in rigid pavement applications.

First, a rigorous search of published research articles on the use of PMA, as alternative binder material for concrete production, from different peer-reviewed sources, was carried out. Major

search engines (ScienceDirect and Google Scholar) were used. The focus was on literature published on PMA as an alternative binder material. The articles were selected based on their relevance to this research topic. The second step was the collection and categorisation of the relevant articles into those dealing with the fresh state, mechanical and durability properties of concrete (Figure 3-1). The various engineering properties discussed in the collected research articles were carefully extracted. After that, each engineering property was thoroughly reviewed from the numerous collected articles, including the findings and conclusions arrived at by the respective authors. The differences or similarities were identified and discussed extensively.

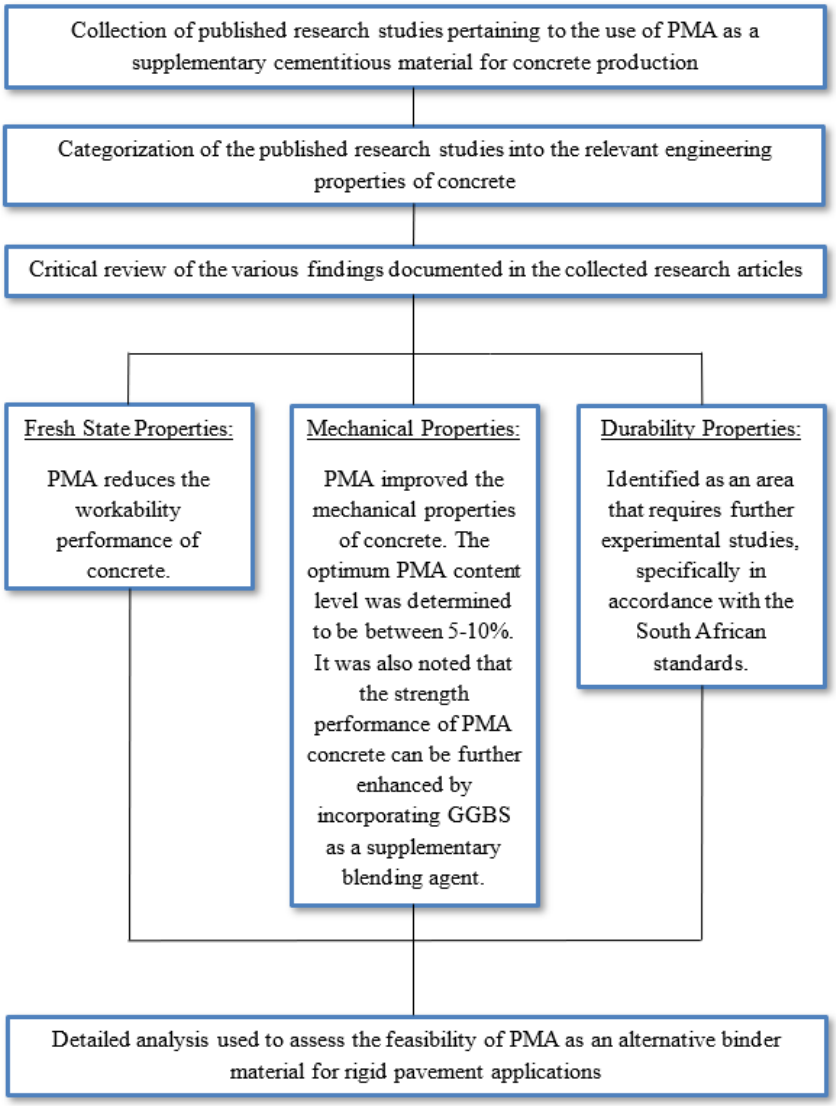

Figure 3-1: Schematic diagram outlining the theoretical research approach

3.2.2) Experimental research approach

The experimental research approach includes a critical analysis of the engineering performance of paper mill ash-based concrete, which is then used to assess its viability for rigid pavement applications. From Figure 3-2, it can be seen that this research approach consists of an

experimental investigation of the fresh state, mechanical (compressive, flexural and tensile splitting strengths), durability and frictional resistance properties of concrete incorporating paper mill ash as a supplementary cementitious material. A construction cost analysis and an assessment of the equivalent carbon dioxide (CO_{2e}) levels were also used to provide a definitive answer to the feasibility of concrete containing paper mill ash for real world applications.

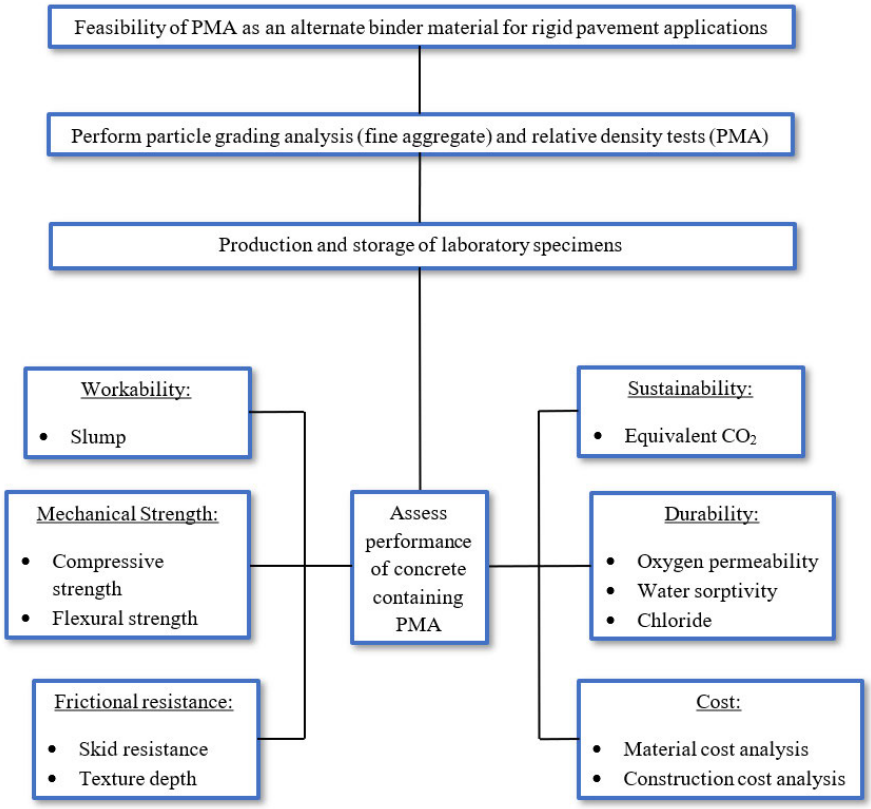

Figure 3-2: Schematic diagram outlining the experimental research approach

3.3) Project information for construction cost analysis

3.3.1) Project background

The economic feasibility of PMA as an alternate binder material for rigid pavements was assessed by performing a construction cost analysis for a typical rigid pavement scenario in South Africa. This cost analysis was based on the concrete platform or bullpen at the OneLogix Vehicle Distribution Facility situated in the Umlaas Road area (north west of Durban). OneLogix Group primarily functions as a logistics provider that caters to a wide range of specialised logistic services across local and global markets. These specialised logistic services include Primary Logistics, Abnormal Logistics and Logistics Services. Under OneLogix's Abnormal Logistics unit, the group provides Vehicle Delivery Service (OneLogix VDS).

The bullpen area at the OneLogix Umlaas Road Vehicle Distribution Facility comprises of a 170 mm thick unreinforced concrete surface bed with an average slope of 1:100. The area of the surface bed (including the entrance area) is estimated to be 13 500 m^2. The main traffic movement within this area is predominantly focused on a 9 m wide access loop used by car carriers. The 9 m wide section, which has an approximate length of 500 m, is showing signs of premature failure.

Figure 3-3: Locality map of OneLogix Umlaas Road Vehicle Distribution Facility

Figure 3-4: Damage documented during the visual inspection of the concrete panels in the bullpen

3.3.2) Overview of the works

In light of the extensive cracking evident in the bullpen area, the engineers requested geotechnical investigations from Drennan Maud (Pty) Ltd to determine the pavement layerworks and subgrade materials/depth/condition. Three inspection pits were manually excavated by hand at predetermined locations to evaluate the existing layerworks and subgrade materials. The in-situ

CBR density of the layerworks was determined by performing Dynamic Cone Penetrometer (DCP) and CBR DCP tests. Drennan Maud also classified the existing pavement materials by collecting samples from the inspection pits, which were taken to Thekwini Soils Laboratory for further testing.

From the abovementioned geotechnical investigations, Drennan Maud classified the existing soil profile for the bullpen as follows:

- 170 mm thick concrete
- Cement stabilized G7 of 200 – 110 mm thickness
- G9 of 490 – 400 mm thickness
- G10 of 170 mm thickness
- G10 Colluvium/Residuum of >1.4 m thickness

Figure 3-5: Soil profile of existing layerworks in bullpen

Drennan Maud concluded that the cause of the pavement failure in certain areas of the bullpen can be attributed to the combination of the following:

- Inadequate pavement design (material selection and layerworks thickness) in relation with the traffic loading
- Founding of existing layerworks on unsuitable subgrade and in-situ material
- Localised perched water table leading to deterioration of layerworks

With this in mind, the engineers recommended that the existing layerworks in the predetermined areas with severe damage would be excavated to a depth of 800 mm and replaced as follows:

- 200 mm Concrete (Class 40/19 – reinforced with Ref 617 mesh)
- 250 mm C3 (2.5% Lime stabilized)
- 200 mm G7
- 150 mm G7 Pioneer

All new construction joints were sealed with Sikaflex Pro 3 and a 12 mm backing rod. In order to enable load transfer, the new concrete panels were also keyed 50 mm into the existing concrete.

3.4) Materials

3.4.1) Cement

Portland Cement was the binding agent used for the experimental investigations in this research study. The cement produced by Natal Portland Cement (NPC) in South Africa, was classified as CEM II/B-S 42.5N Plus. This cement classification is indicative of Portland-Slag cement and satisfies the strength and quality requirements that have been outlined in SANS 50197-1. As discussed in Chapter 2, Gailius and Laurikietytė (2003) proved that GGBS serves as a good blending agent with PMA to replace PC. For this reason, CEM II/B-S 42.5N Plus was selected as the primary binder material for this experimental investigation.

3.4.2) Fine aggregate (sand)

The fine aggregate selected for this research study was Umgeni River Sand (in accordance with SANS 1083). Having performed a sieve analysis for the fine aggregate (refer to Appendix A), the fineness modulus was calculated to be 2.39. According to SAPEM (2013c), the fineness modulus of fine aggregate material used to produce concrete pavements should lie between 1.2 and 3.5. Therefore, the fine aggregate selected for this study satisfies the abovementioned requirement. Figure 3-6 represents the particle size distribution curve for the fine aggregate.

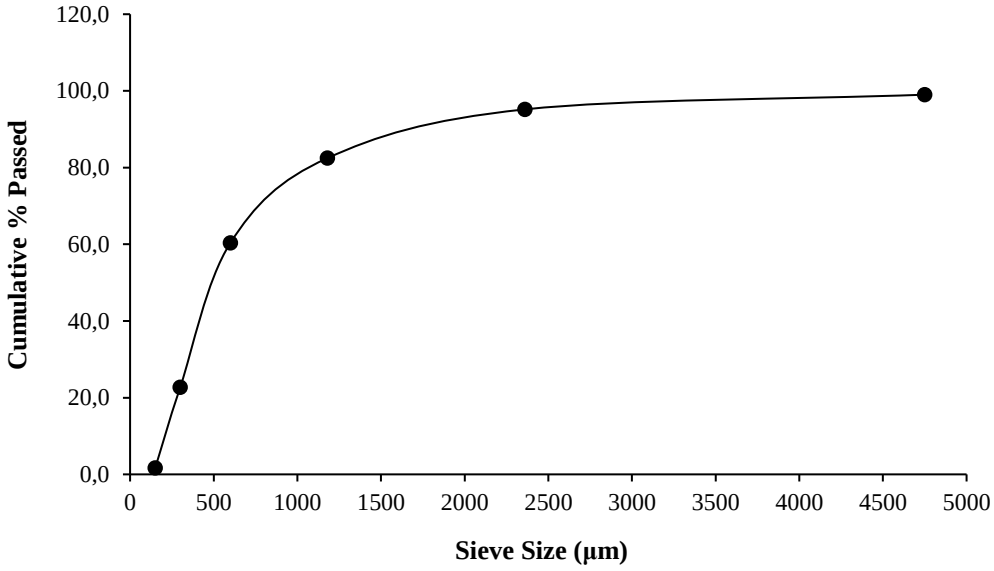

Figure 3-6: Particle size distribution of the Umgeni River Sand

3.4.3) Coarse aggregate (stone)

Coedmore Quartz Stone (nominal size = 19 mm) was used as the coarse aggregate in this study. The quartzite stone was pre-graded and conformed with the requirements in SANS 1083.

3.4.4) Water

Potable water was added to the dry ingredients during the mixing and curing phases of the experimental study. The quality of the water added to the concrete mixes complied with specifications outlined in SANS 51008.

3.4.5) Paper mill waste ash

The paper mill ash used in this research study was obtained from the Mondi Merebank Mill in Durban, South Africa. Mondi Merebank produces the waste ash by incinerating paper mill sludge (generated during the pulp and paper manufacturing process) with bituminous coal, coal ash, sawdust and bark in a Multi Fuel Boiler (MFB) (Miller, 2010). The calcination process, which occurs at a temperature of 750 °C, also produces steam and generates electricity used to power the paper mill (Miller, 2010). For the purposes of this research study, the ash produced by the MFB has been referred to as paper mill waste ash or paper mill ash in order to differentiate it from the coarse ash that is produced in the coal boiler.

The experimental investigations performed by Byiringiro (2014) also used an ash sample obtained from Mondi Merebank, and the following chemical composition was noted during the scanning electron microscope (SEM) analysis:

Table 3-1: Chemical composition of paper mill waste ash sample from Mondi Merebank (Source: Byiringiro, 2014)

Oxide Compound	Percentage (by weight)
CaO	32.58
SiO_2	35.83
Al_2O_3	22.41
Fe_2O_3	1.11
MgO	1.55
SO_2	4.93
K_2O	0.43
TiO_2	1.16

According to ASTM (2008), a material can be classified as pozzolanic if the summation of the percentage of the three main oxide constituents (SiO_2, Al_2O_3 and Fe_2O_3) is a minimum of 50%. Based on the chemical composition results documented in Table 3-1, it can be concluded that the waste ash from Mondi Merebank is pozzolanic. In accordance with SANS 5844, the relative density of the paper mill ash was determined to be 2.25, which is significantly lower than the relative density of the cement (3.1).

Figure 3-7: Sample of the paper mill waste ash used in this research study

3.5) Concrete mix design

The experimental investigations were performed by using concrete mix designs containing 0%, 5%, 10%, 15% and 20% of paper mill ash (PMA) as a partial replacement (by volume) for Portland Cement (PC). In accordance with Everitt (2016), the Cement & Concrete Institute (C&CI) concrete mix design method was followed, and the proportions of each mix have been summarized in Table 3-2.

Table 3-2: Proportions of the concrete mixes used for this research study

Designation	w/b	Water (l)	Sand (kg)	Stone (kg)	Binder	
					PC (kg)	PMA (kg)
0% PMA	0.64	40.6	137.7	212.7	63.4	0
5% PMA	0.64	40.6	137.7	212.7	60.3	2.3
10% PMA	0.64	40.6	137.7	212.7	57.1	4.6
15% PMA	0.64	29.3	99.3	153.4	38.9	5
20% PMA	0.64	29.3	99.3	153.4	36.6	6.6

3.6) Casting and curing of laboratory samples

The concrete samples used in the experimental study were cast and cured in accordance with SANS 5861-3. The dry materials, i.e. sand, stone, cement and PMA, were first mixed in a revolving drum tilting mixer for a duration of one minute. Water was then added, and the mixing process continued until the concrete achieved an even consistency, texture and colour. The fresh concrete was allowed to stand while the slump tests were conducted.

After the workability of the concrete mix was determined, the cube (100 x 100 x 100 mm & 150 x 150 x 150 mm), beam (100 x 100 x 500 mm), cylinder (Ø150 x 300 mm) and slab (600 x 300 x 50 mm) moulds were filled. A vibrating table was used to compact the concrete, while a trowel was used to finish the concrete surface. In order to determine the skid resistance properties of PMA concrete, a broom was used to add surface texturing (longitudinal and transverse) to the two slabs. The concrete samples were demoulded twenty-four hours later and cured under normal conditions until the 7-day strength tests. After the 7-day period had elapsed, the specimens were removed from the curing bath and air cured. Alternatively, the two concrete slabs were air cured after they were demoulded.

Due to the lockdown restrictions resulting from the Coronavirus (Covid-19) pandemic in South Africa, the 28-day strength tests for the 0%, 5% and 10% PMA samples could not be performed. In consultation with the research supervisors, it was agreed upon to conduct 180-day and 200-day tests in order to create an accurate data set that will be used to predict the 28-day strength for the abovementioned mixes.

3.7) Testing procedures

The experimental procedures used to determine the fineness modulus of the fine aggregate and the relative density of the paper mill waste ash have been detailed below. Table 3-3 provides a summary of the test variables, standards/specifications that were followed and the type of tests that were performed on the PMA concrete.

Table 3-3: Summary of the testing procedures performed on concrete containing paper mill waste ash

Test Variable	Standard/specification	Concrete State	Age	Type of test
Workability	SANS 5862-1	Fresh state	0 days	Non-destructive
Compressive strength	SANS 5860, 5861-2, 5861-3 & 5863	Hardened state	7, 28, 180 & 200 days	Destructive
Flexural strength	SANS 5864	Hardened state	7, 28, 180 & 200 days	Destructive
Tensile splitting strength	SANS 6253	Hardened state	7, 28, 180 & 200 days	Destructive
Durability	SANS 3001	Hardened state	≥ 28 days	Non-destructive
Skid resistance	TMH 6	Hardened state	≥ 28 days	Non-destructive
Texture depth	TMH 6	Hardened state	≥ 28 days	Non-destructive
Equivalent carbon dioxide (CO_{2e})*	–	–	–	–
Cost*	–	–	–	–

*Desktop study used to assess this test variable

3.7.1) Fineness modulus – fine aggregate

As specified in SANS 201, a particle grading analysis was used to determine the particle size distribution curve and the fineness modulus of the fine aggregate utilized during the concrete manufacturing process. A 600 g sample of Umgeni river sand was oven dried, at a temperature of 110°C, for 24 hours. A 500 g sample of dried sand was then weighed out and with the assistance of a vibrating machine the aggregate was passed through standard SABS sieves (4750, 2360, 1180, 600, 300, and 150 microns). The mass of the sand retained by each sieve was measured and used to determine the particle size distribution curve (Figure 3-3) and fineness modulus (Equation 3-1).

$$Fineness\ Modulus\ (FM) = \frac{\sum Cumulative\ \%\ Retained}{100} \ldots\ldots\ldots\ldots\ldots\ldots\ldots\ldots\ldots\ldots\ldots\ldots\ldots\ldots\ldots\ldots\ldots (3-1)$$

3.7.2) Relative density – PMA

The relative density of the coarse and fine aggregates was predetermined by the technicians at UKZN's Civil Engineering laboratory, while the relative density of the paper mill ash was quantified by using a pycnometer. The procedure followed was in line with the specifications documented in SANS 5844. A 400 g sample of the paper mill ash was oven dried, at a temperature of 110°C, for 24 hours. The mass of the empty pycnometer (M_1) was recorded before a 300 g

sample of the oven dried ash was added to it and the subsequent mass was measured (M_2). The pycnometer containing the dried ash sample was filled with distilled water and a stirrer was used to mix the contents before the mass (M_3) was recorded. The pycnometer was then emptied, cleaned and dried. The pycnometer is filled with distilled water only, and the mass was measured (M_4). This process was repeated two more times, and the average relative density was determined. Equation 3-2 was used to calculate the relative density for each of the three scenarios.

$$Relative\ Density\ (RD) = \frac{M_2 - M_1}{M_4 - M_1 - (M_3 - M_2)} \dots\dots\dots\dots\dots\dots\dots\dots\dots\dots\dots\dots\dots\dots\dots\dots\dots\dots\dots\dots (3-2)$$

where:

M_1 = Mass of the pycnometer (empty) in grams (g)

M_2 = Mass of the pycnometer and oven dried PMA sample in grams (g)

M_3 = Mass of the pycnometer, oven dried PMA sample and distilled water in grams (g)

M_4 = Mass of the pycnometer and distilled water in grams (g)

3.7.3) Workability

In accordance with SANS 5862-1, the slump test was used to quantify the workability properties of the fresh concrete. The apparatus utilized when performing the slump test includes the following:

- Conical mould
- Base plate
- Tamping rod
- Hand shovel
- Measuring ruler

Figure 3-8: Apparatus used to perform the slump test (Source: Owens, 2013)

The conical mould was clamped with the larger opening sitting on the base plate. The hand shovel was used to fill the mould with three layers of concrete with equal depth before each layer was tamped 25 times with a tamping rod. The mould was unclamped, inverted and placed alongside the slumped concrete. The slump was documented by placing the tamping rod on the rim of the mould and measuring the distance from the top of the slumped concrete to the tamping rod.

3.7.4) Compressive strength

As depicted in Figure 3-9, the compressive strength was determined by crushing three 150 x 150 x 150 mm concrete cube specimens with a hydraulic press equipped with two platens. As outlined in SANS 5860, 5861-2, 5861-3 and 5863, a uniform loading rate of 0.3 MPa/s ± 0.1 MPa/s was applied to the cubes (Afrisam, 2018). For each concrete age, the tests were performed while the samples were in a saturated condition.

Figure 3-9: Apparatus used to perform the compressive strength test

Equation 3-3 can then be used to calculate the average compressive strength from the three values.

$$f_c = \frac{F_c}{A_c} \ldots\ldots\ldots\ldots\ldots\ldots\ldots\ldots\ldots\ldots\ldots\ldots\ldots\ldots\ldots\ldots\ldots\ldots\ldots (3-3)$$

where:

f_c = Compressive strength (MPa)

F_c = Maximum failure load (N)

A_c = Cross-sectional area of the specimen (cube) (mm^2)

SANS 5863 states that the compressive strength test is only valid if the range between the lowest and highest compressive strengths within the set of three cubes is less than 15% of the average (Owens, 2013).

3.7.5) Flexural strength

The laboratory set up used to determine the flexural strength performance of concrete beam specimens can be seen in Figure 3-10. The experimental apparatus is made up of two plates with two rollers that apply vertical point loads along the entire length of 100 x 100 x 500 mm beams. The rollers on the top plate are spaced 100 mm apart, while the rollers on the bottom plate are 300 mm apart. For each concrete age, the tests were performed while the samples were in a saturated condition.

Figure 3-10: Apparatus used to perform the flexural strength test

The average flexural strength of the three replicate samples can be determined by applying the following equation:

$$f_F = \frac{F_f l}{bd^2} \quad \ldots \ldots \ldots (3-4)$$

where:

f_F = Flexural strength (MPa)

F_f = Maximum failure load (N)

l = length of beam specimen (mm)

b = breadth of beam specimen (mm)

d = depth of beam specimen (mm)

3.7.6) Tensile splitting strength

As described in SANS 6253, the laboratory test used to quantify the tensile strength properties consists of subjecting a concrete cylindrical specimen (Ø150 x 300 mm) to compressive forces acting along diametrically opposed lines (Owens, 2013). The apparatus used can be seen in Figure 3-11 below. For each concrete age, the tests were performed while the samples were in a saturated condition.

Figure 3-11: Apparatus used to perform the tensile splitting strength test

Equation 3-5 is then used to quantify the average tensile splitting strength of the three replicate samples.

$$f_T = \frac{2F_T}{\pi l d} \quad \ldots \ldots \ldots (3-5)$$

where:

f_T = Tensile splitting strength (MPa)

F_T = Maximum failure load (N)

l = length of concrete cylinder (mm)

d = diameter of concrete cylinder (mm)

3.7.7) Durability

The durability of concrete containing paper mill ash as a partial cement replacement was assessed with concrete durability index tests. Oxygen permeability, water sorptivity and chloride conductivity were the three durability index tests that were selected. The experimental procedure followed for the abovementioned tests, which were performed by Contest – Concrete Technology Services, has been detailed below.

Prior to performing three durability index tests, the specimens first needed to be prepared by using a coring drill to remove concrete cores (Ø70 ± 2 mm) from 100 x 100 x 100 mm cubes. The outer 5 mm layer of the cores were discarded, and a diamond blade saw was used to cut 30 ± 2 mm thick slices from each core. A total of four slices were required for each test. The slices were then marked, and the durability index tests commenced immediately after the coring process.

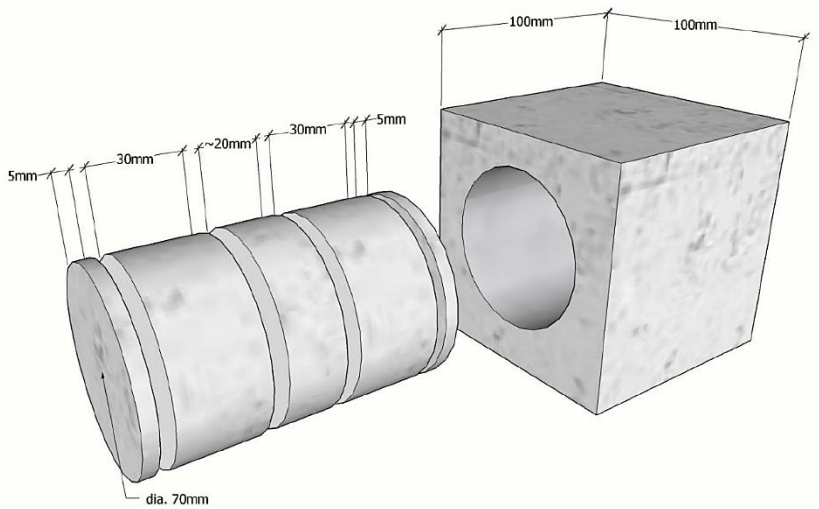

Figure 3-12: Details for cutting the concrete test specimens (Source: CoMSIRU, 2018)

3.7.7.1) Oxygen permeability

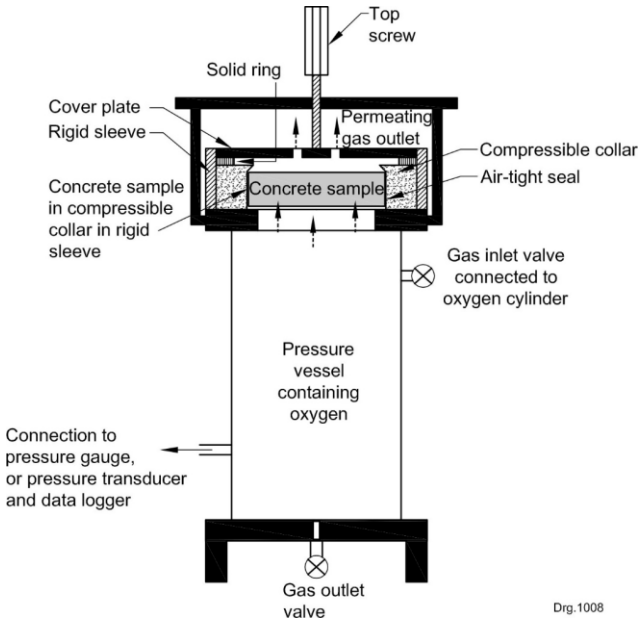

Figure 3-13: Experimental set up for the permeability cell (Source: CoMSIRU, 2018)

Directly after cutting the concrete slices are oven dried at a temperature of 50°C for 7 days. The specimens are then cooled to 23 ± 2°C in a desiccator, for a period of 2 – 4 hours. After the cooling period has concluded, the dimensions of the samples are measured with vernier callipers. The test sample, compressible collar, rigid sleeve, solid ring and cover plate are assembled and placed on the permeability cell (see Figure 3-13). The permeability cell was filled with oxygen until the pressure gauge registered a starting pressure above 100 kPa. The oxygen inlet valve was closed, and the test commenced. After 5 minutes had elapsed, the first pressure reading was recorded. Subsequent pressure and time readings were taken every time the cell pressure dropped by 5 kPa.

The oxygen permeability test was stopped when the recorded pressure dropped below 50 kPa or after 6 hours had passed, whichever came first.

Linear regression was used to determine the line of best fit (passing through the origin) for the $\ln(P_0/P_t)$ vs t graph, where:

P_0 = Initial pressure reading when the test commences

P_t = Subsequent pressure readings at time 't'

t = Time elapsed

The slope of the linear regression line is then calculated from Equation 3-6.

$$z = \frac{\sum[\ln P_0/P_t]^2}{\sum[\ln(P_0/P_t)t]} \ldots \ldots (3-6)$$

Having calculated the slope of the regression line, the D'arcy coefficient of permeability can now be determined as follows:

$$k = \frac{\omega V g d z}{R A \varphi} \ldots \ldots (3-7)$$

where,

k = D'arcy coefficient of permeability for the sample (m/s)

ω = Molecular mass of O_2 = 32 g/mol

V = Volume of pressurised oxygen in the permeability cell (m^3)

g = Gravitational acceleration = 9.81 m/s^2

R = Universal gas constant = 8.313 Nm/K mol

d = Thickness of test specimen (m)

φ = Temperature (K)

z = Slope of regression line

The permeability coefficient is calculated for each of the four test specimens and the following equation is used to determine the oxygen permeability index (OPI).

$$OPI = -\log\left[{}^{1}/_{4}\,(k_1 + k_2 + k_3 + k_4)\right] \ldots \ldots (3-8)$$

3.7.7.2) Water sorptivity

Much like the oxygen permeability test, the concrete slices are first oven dried at a temperature of 50°C for 7 days. According to CoMSIRU (2018), the test specimens used for the oxygen permeability test can also be used to perform the water sorptivity test, in which case the samples do not require any additional drying. Epoxy was used to seal the sides of the concrete slices and the dimensions and mass of the specimens were measured after the epoxy had dried. The samples were placed on rollers/supports in a tray, and the tray was filled with $Ca(OH)_2$ solution until the bottom 2 mm layer of each sample was submerged. The saturated mass of the test specimens was recorded for 3, 5, 7, 9, 12, 16, 20- and 25-minute time periods. This involved dabbing the submerged face of each slice with a damp paper towel, when it was removed from the $Ca(OH)_2$ solution. After the saturated mass had been measured, the samples were placed back in the solution. Once the water sorptivity test had concluded, the test specimens were placed in a vacuum saturation tank for 3 hours (vacuum pressure between -75 and -80 kPa). After the 3-hour period had elapsed, the tank was filled with $Ca(OH)_2$ solution until the solution level was 40 mm above the top of the samples. The vacuum saturation tank was exposed to a vacuum pressure between -75 and -80 kPa for 1 hour, before the vacuum pressure was released and the test samples were left to soak for an additional 18 hours. Once the 18-hour period had concluded, the specimens were removed from the solution, dried with a paper towel and their respective masses (M_{sv}) were recorded.

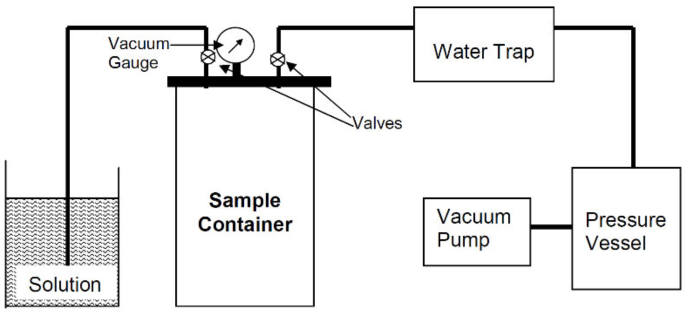

Figure 3-14: Experimental set up for the vacuum saturation facility (Source: CoMSIRU, 2018)

According to CoMSIRU (2018), the following calculation process was used to quantify the water sorptivity for the PMA concrete. The effective porosity (n) for each test specimen was calculated as follows:

$$n = \frac{M_{sv} - M_{s0}}{Ad\rho_w} \quad (3-9)$$

where,

M_{sv} = Vacuum saturated mass for the sample (g)

M_{s0} = Mass of the sample at time 't=0' (g)

A = Cross-sectional area of the sample (mm^2)

d = Average thickness of the sample (mm)

ρ_w = Density of water (10^{-3} g/mm^3)

Equation 3-10 is used to determine the mass gain (M_{wt}).

$$M_{wt} = M_{st} - M_{s0} \quad (3-10)$$

where,

Mst = mass of the sample at time 't'

The mass gain (M_{wt}) vs square root of time graph can then be plotted.

$$M_{wt} = F\sqrt{t} \quad (3-11)$$

where,

F = Slope of the line of best fit ($g/\sqrt{hr}$)

t = Time after the test commences (hr)

Equation 3-12, 3-13 and 3-14 are used to calculate the correlation coefficient (R^2). If R^2 is less than 0.98, then the last experimental reading (i.e. the value for t = 25 minutes) should be discarded and R^2 should be recalculated.

$$\bar{M}_{wt} = \frac{\sum M_{wti}}{n} \quad (3-12)$$

$$T = \frac{\sum \sqrt{t_i}}{n} \quad (3-13)$$

$$R^2 = \left[\frac{\sum\left(\sqrt{t_i} - T\right)(M_{wti} - \bar{M}_{wt})}{\sqrt{\sum\left(\sqrt{t_i} - T\right)^2 - \sum(M_{wti} - \bar{M}_{wt})^2}} \right] \quad (3-14)$$

where,

M_{wti} = Mass gain at each time interval (g)

t_i = Corresponding time for the mass gain (hr)

n = Number of experimental readings

The slope of the line of best fit (F) can be determined as follows:

$$F = \frac{\sum(\sqrt{t_i} - T)(M_{wti} - \bar{M}_{wt})}{\sqrt{\sum(\sqrt{t_i} - T)^2}} \ldots \ldots \ldots \ldots (3-15)$$

Likewise, the water sorptivity of the test specimen (S) is calculated by using Equation 3-16.

$$S = \frac{Fd}{M_{sv} - M_{s0}} \ldots \ldots \ldots \ldots (3-16)$$

3.7.7.3) Chloride conductivity

The test specimens were first conditioned by oven drying the concrete slices at a temperature of 50°C for 7 days. The dimensions and dry mass of the samples were then recorded before they were placed in a vacuum saturation tank (see Figure 3-14). A vacuum pressure between -75 and -80 kPa was applied to the saturation tank for a duration of 3 hours. After this time period elapsed, the tank was filled (without releasing the vacuum pressure) with a 5.0 M NaCl solution until the solution level was 40 mm above the top of the samples. The samples are exposed to the same vacuum pressure for an hour, before the pressure is released and the samples are soaked in the NaCl solution for a further 18 hours. After the 18-hour period had concluded, the test specimens were removed from the salt solution, dried with a paper towel and their respective masses (M_s) were recorded.

The chloride conductivity test was performed by first filling the connection points of the conduction cell with the NaCl solution. Each test specimen was then placed on their curved side in the conduction cell, before the voltmeter and ammeter were connected. A test voltage of 10V is applied to the specimens and the voltage and current readings are recorded. The chloride conductivity of each test specimen can be calculated by using the following equation:

$$\sigma = \frac{it}{VA} \ldots \ldots \ldots \ldots (3-17)$$

where,

σ = Chloride conductivity of the sample (mS/cm)

i = Electric current (mA)

V = Voltage

t = average sample thickness (cm)

A = Cross-sectional area of the sample (cm^2)

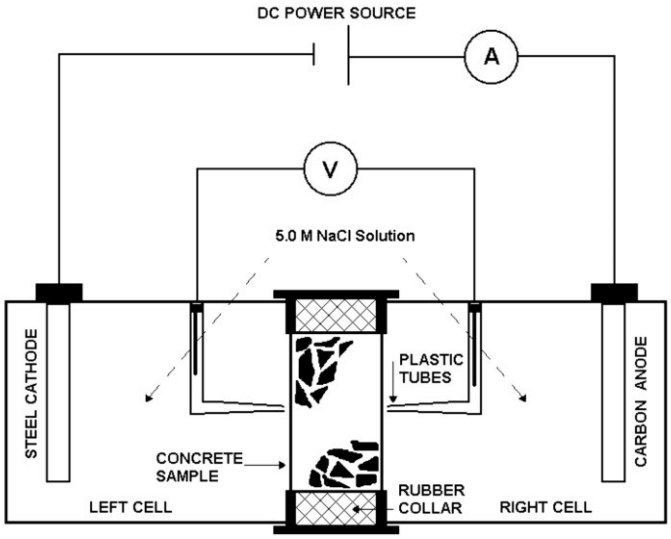

Figure 3-15: Experimental set up for the conduction cell (Source: CoMSIRU, 2018)

The calculated oxygen permeability, water sorptivity and chloride conductivity index values are then used to determine the durability class from the criterion specified in Table 3-4.

Table 3-4: Criterion used to determine the class of durability performance (Source: Alexander et al., 1999; Zulu, 2017)

Durability Class	**Oxygen Permeability (log value)**	**Water Sorptivity ($mmh^{-0.5}$)**	**Chloride Conductivity (mS/cm)**
Excellent	>10	<8	<0.75
Good	9.5 – 10	6 – 10	0.75 – 1.50
Poor	9.0 – 9.5	10 – 15	1.50 – 2.50
Very Poor	<9.0	>15	>2.50

3.7.8) Skid resistance

The skid resistance test was used to assess the resistance to skidding of concrete slabs containing PMA. In order to simulate the finishing and texturing methods that are typically applied to concrete pavements, a broom was used to add longitudinal and transverse surface texturing to each of the concrete slabs. A Portable Pendulum Skid Resistance Tester (see Figure 3-16) was used to quantify the frictional resistance of each concrete surface. The testing apparatus simulates the sliding effect experienced between the pavement surface and vehicle tyre at a speed of 50 km/h. Prior to commencing the skid resistance test, the portable tester first needs to be levelled by means of the three levelling screws and the spirit level. The head of the portable test is raised until the pendulum swings clear of the concrete surface. The zero setting is then checked by releasing the pendulum arm from the horizontal start point and catching the arm on its return swing. Adjustments are made to the friction rings and this process is repeated until the pointer reading is zero. The concrete surface is cleaned with a brush and water is used to wet the test area.

The pendulum arm is lowered until the rubber slider makes minimal contact with the concrete surface. The pendulum arm and pointer are then released from the horizontal start point and the arm is caught in its return swing. The pointer reading is documented, and the testing process is repeated four more times.

Figure 3-16: Portable Pendulum Skid Resistance Tester used to assess the frictional resistance of pavement surfaces

3.7.9) Texture depth

In accordance with TMH 6, the surface texture depth of each concrete slab was determined by conducting the sand patch test. The sand patch test was performed on the same concrete slabs that were used for the skid resistance tests. The surface of each slab was once again cleaned with a brush to remove any loose grit and dust that may be present. A cylinder (with known volume) is then filled with natural sand that passed through a 300 µm sieve and was retained on a 150 µm sieve. The sand is poured into a heap on the test area and spread in a circular pattern with a flat faced disc. Once the surface voids in the test area have been filled to the level of the high points, a ruler was used to measure five different diameters for the resulting circular sand patch. Equation 3-18 can then be used to calculate the texture depth.

$$Texture\ Depth\ (mm) = \frac{Volume\ of\ sand\ (mm^3)}{Area\ of\ patch\ (mm^2)} \ldots\ldots\ldots\ldots\ldots\ldots\ldots\ldots\ldots\ldots\ldots\ldots\ldots\ldots\ldots\ldots\ldots\ldots .. (3-18)$$

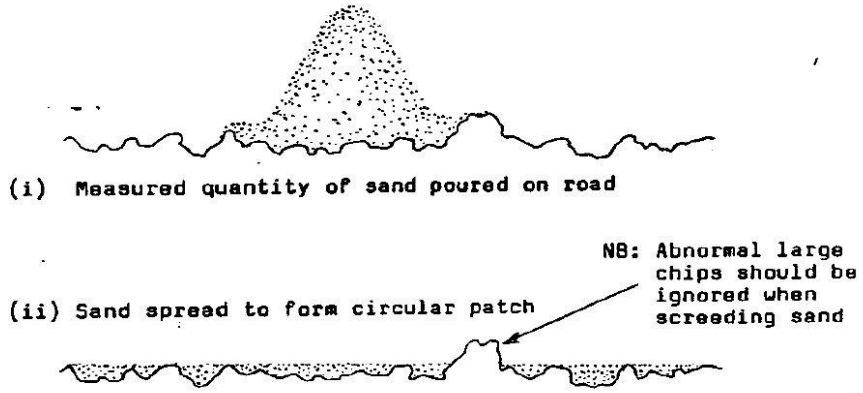

Figure 3-17: Sand patch test method used to measure the surface texture depth (Source: Transit New Zealand, 1981)

3.7.10) Equivalent carbon dioxide (CO_{2e})

A desktop study was the selected method for analysing the equivalent carbon dioxide (CO_{2e}) of concrete containing 0, 5, 10, 15 and 20% of PMA as a supplementary cementitious material. This assessment was carried out for a hypothetical 1 m^3 concrete mix. The average CO_{2e} emission value for each material has been summarized in Table 2-12. The same concrete mix design parameters were considered when calculating the material quantities for the 1 m^3 concrete mix used in this study. These quantities were then multiplied with their respective average CO_{2e} emission values to determine the equivalent carbon dioxide for each mix.

$$Equivalent\ Carbon\ Dioxide\ (CO_{2e}) = Material\ Quantity \times Average\ CO_{2e}\ emissions \ldots\ldots (3-19)$$

3.7.11) Cost

Along with favourable structural and durability performance, the PMA concrete also needed to be economically feasible for use in industry. Much like the equivalent carbon dioxide (CO_{2e}) analysis, a desktop study was again selected to assess the cost implications of incorporating PMA as an alternate binder material for concrete pavement applications. This test variable was investigated by performing a material cost analysis and construction cost analysis as described below.

3.7.11.1) Material cost analysis

A material cost analysis was used to evaluate the cost (per m^3) for each of the concrete mix designs used for the experimental investigations that were performed in this study. Due to the variation in the number of concrete specimens that were cast for each laboratory mix, it was decided that the material cost analysis would be conducted for the same hypothetical 1 m^3 concrete mix that was used for the equivalent carbon dioxide study. This resulted in a consistent and accurate comparison of the results obtained. Table 3-5 represents the market rates (to date) that were

provided by local suppliers for each of the constituent materials. This investigation exclusively focused on the cost of each material used to manufacture the concrete mixes. Therefore, transportation costs were not considered (i.e. all rates excluded delivery). The material cost of the PMA was R0 per kg, as it is a waste product produced by Mondi Merebank and was provided free of charge. The only cost variable associated with PMA is the transport costs, which will be considered later on in the construction cost analysis. Presently, Mondi Merebank does not sell any of the paper mill ash that is produced during the paper manufacturing process. If PMA was to be used for large scale concrete production, then a commercial agreement will need to be reached with Mondi Group. This will have ramifications on the material costs associated with the PMA. However, for the purposes of this research study, an undelivered rate of R0 per kg was used, as the PMA sample was donated to the student.

Table 3-5: Undelivered rates for the various constituent materials used to produce concrete containing PMA

Material	Rate	Supplier/Source
Portland-Slag Cement (CEM II/B-S)	R 92 per 50kg bag	Just Build
Umgeni River Sand	R 550 per m^3	Umlaas Road Cartage
Coedmore Quartz Stone (19mm)	R 650 per m^3	Umlaas Road Cartage
Water	R 36.52 per kl	eThekwini Municipality
Paper Mill Ash (PMA)	R 0 per kg	Mondi Merebank

3.7.11.2) Construction cost analysis

A construction cost analysis based on a typical rigid pavement scenario in South Africa was also used to evaluate the economic feasibility of PMA as a supplementary cementitious material for concrete pavement construction. This cost analysis was performed for the rehabilitative works undertaken on the concrete platform or bullpen at the OneLogix Umlaas Road Vehicle Distribution Facility. As discussed in Section 3.3, 29 of the existing concrete panels needed to be excavated and replaced with the new layerworks provided by the Engineer. In order to assess the economic impact of PMA concrete, this analysis only considered the costs incurred when constructing the final 200 mm concrete (Class 40/19 – reinforced with Ref 617 mesh) layer. This implies that the preliminary and general costs and the construction costs associated with excavating the existing layerworks and reinstating the new pavement structure below the concrete surface were not included. The construction cost analysis for each concrete mix consisted of the corresponding material, transport, plant and labour costs.

3.7.11.2.a) Material costs

As per the Engineer's specifications, the new pavement structure included a Class 40/19 concrete surfacing. Therefore, the C&CI concrete mix design method was used to determine new material

quantities, as the mix designs used in this study were for Class 30/19 concrete. Table 3-6 represents the new material quantities. The rates documented in Table 3-5 were once again used to determine the material costs. The transportation costs for the Portland-Slag cement and PMA were included in the next section, while Umlaas Road Cartage indicated that the undelivered and delivered rates for the river sand and 19 mm stone were the same as the construction site was only situated 1.4 km away from their location. Therefore, no transportation costs would be incurred for these materials. The curing compound (Sika Cemflex) and joint sealant (Sikaflex Pro3) had rates of R 90.40 (per litre) and R 120.70 (per meter) respectively. These rates were provided by the main contractor (Raubex KZN), who also indicated that the transportation costs were already included. The Ref 617 mesh had a rate of R 94.40 (per m^2) and would also be supplied by the contractor.

Table 3-6: Proportions of the concrete mixes used for the construction cost analysis

Designation	w/b	Water (kl)	Sand (m^3)	Stone (m^3)	Binder	
					PC (kg)	PMA (kg)
0% PMA	0.54	32.42	38.48	64.10	60030	0
5% PMA	0.54	32.42	38.48	64.10	57028.5	2178.7
10% PMA	0.54	32.42	38.48	64.10	54027	4357.4
15% PMA	0.54	32.42	38.48	64.10	51025.5	6536.1
20% PMA	0.54	32.42	38.48	64.10	48024	8714.8

3.7.11.2.b) Transportation costs

The transport costs for the Portland-Slag cement and PMA were included in this section. The time period for each cost item was based on the estimated construction time of 30 days to complete the concrete works. The contractor hired a 4-ton truck (wet rate of R 1500 per day) to collect the PMA. The number of days was based on the assumption that 3600 kg of PMA could be transported from Mondi Merebank to the construction site per day. The 7-ton gang truck (provided by Raubex) was used to collect the cement from the supplier and transport the labourers to and from site. The contractor estimated that the gang truck would consume 60 litres of diesel per day, with an additional 30 litres used to transport 100 bags of cement per day. The respective fuel costs were determined by applying the standard diesel cost per litre (R 11.89). The foreman's bakkie was also included in the transportation costs (R 964.68 per day).

3.7.11.2.c) Equipment/plant costs

The contractor estimated that two concrete mixers (revolving drum type) and two 10 kVA generators would be used to complete the concrete works. Each concrete mixer had a rate of R 1800 per day, whereas each generator had a dry rate of R 460 per day. A saw cutter was also used to cut the pavement joints (dry rate of R 850 per day). The fuel costs were based on the assumption

that each generator would use 5 litres per day, while the saw cutter consumed 10 litres per day. The vibrating poker, which was used to compact the concrete, had a rate of R 200 per day. The contractor also used a trailer to transport the concrete mixers, generators and saw cutter to and from site (R 250 per day).

3.7.11.2.d) Labour costs

The foreman, semi-skilled labourers (3) and unskilled labourers (12) were included when calculating the labour costs. The labour costs for the engineer and site agent were not considered as this cost analysis solely focused on the actual construction of the new concrete layer. All rates were provided by the contractor. The contractor also estimated a total construction time of 30 days, with a labour time of 9 working hours per day. The total labour time did not include the 28-day curing period and was not measured until handover.

3.8) Summary

Chapter 3 summarised the study areas that were recognized and the research approaches that were adopted, while the testing procedures that were used to satisfy the main aims and objectives have also been described. The abovementioned approaches and procedures were primarily used to critically analyse the viability of PMA as a supplementary cementitious material for rigid pavement applications. The key concrete properties that have been evaluated in this research study includes workability, durability and mechanical strength (namely compressive, flexural and tensile splitting strength). The feasibility of PMA concrete for sustainable concrete pavement construction was also assessed by carrying out skid resistance tests, performing a CO_{2e} assessment and conducting a construction cost analysis based on a typical rigid pavement scenario. This chapter concluded with a summary of the limitations that were experienced during the course of this research study.

CHAPTER 4: RESULTS AND DISCUSSION

4.1) Introduction

This chapter presents the experimental results obtained from the testing procedures that have been outlined in Chapter 3. The results, which were represented in tabular and graphical form, were then critically analysed in order to evaluate the effect paper mill ash has on the workability, mechanical strength, durability, frictional resistance, sustainability and economic properties of concrete. This assessment was then used to determine the viability of paper mill ash as an alternate binder material for rigid pavement applications in South Africa, which sets the background for the final concluding remarks and recommendations that will be documented in the next chapter.

4.2) Fresh state properties

4.2.1) Workability

Table 4-1: Slump test results of concrete containing varying quantities of paper mill waste ash

PMA Content (%)	Slump (mm)
0% PMA	84
5% PMA	70
10% PMA	65
15% PMA	60
20% PMA	35

The workability properties of the concrete mixes were assessed by performing the standard slump test. From the results documented in Table 4-1 and Figure 4-1, it was noted that the addition of paper mill ash (PMA) as a supplementary cementitious material resulted in a reduced slump and workability performance. As discussed in Chapter 2, this is in agreement with the results obtained in the research studies undertaken by Ahmad et al. (2013), Gailius and Laurikietytė (2003), Mavroulidou et al. (2013) and Vegas et al. (2009). The reduced workability of the fresh concrete can be attributed to the high-water demand needed by the PMA (which is finer than PC) for the formation of the hydration products (Mavroulidou et al., 2013).

In this research study it was also documented that the PMA produced by Mondi Merebank contains high percentages of CaO, SiO_2 and Al_2O_3. The high oxide content, in combination with the presence of metakaolin in PMA, will accelerate the hydration of C_3S, thus decreasing the setting time and reducing the workability performance of the fresh concrete (Vegas et al., 2009). The abovementioned effect also serves as an explanation for the significantly lower slump test result (35 mm) attained for the 20% PMA concrete mix.

According to SAPEM (2013c), the slump tolerance of conventional concrete designed to a target slump between 50 – 100 mm is ±25 mm. In this research study, the 0% PMA mix had a target slump of 75 mm, therefore the achieved slump (i.e. 84 mm) falls within the specified tolerance range. SAPEM (2013c) also states that paving concrete should have a slump between 20 and 70 mm when fixed form paving equipment is used, while the slump of the fresh concrete should range from 10 to 50 mm in scenarios where slipform paving machinery is used. Hence, from the slump test results attained, it was determined that all PMA concrete mixes were suitable for fixed form paving operations, while the 20% PMA replacement level was the optimum concrete mix for slipform paving.

In Chapter 2, it was observed that the w/b ratios adopted in the past year investigations ranged from 0.4 to 0.55. Therefore, for this experimental study a w/b ratio of 0.64 was selected in order to examine if a higher w/b ratio will improve the fresh state performance of concrete containing PMA. From the results obtained it was determined that increasing the w/b ratio had no effect on enhancing the concrete slump. However, it is also worth mentioning that concrete used for rigid pavement construction not only requires sufficient workability but should also retain sufficient rigidity to resist flow on roads with steep cross falls and gradients (SAPEM, 2013d). Therefore, it can be concluded that the fresh state performance of PMA concrete makes it suitable for utilization in rigid pavement applications.

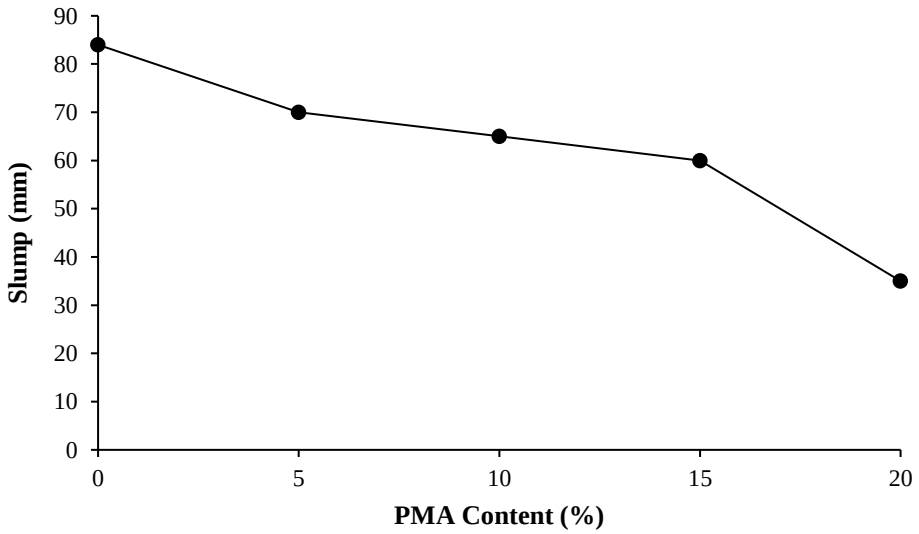

Figure 4-1: Results obtained from the slump test

4.3) Mechanical strength properties

4.3.1) Compressive strength

Table 4-2: Measured and predicted compressive strength results of concrete containing varying quantities of paper mill waste ash

PMA Content (%)	Type of Result	Mathematical Relationship	Concrete Age (days)	Average Compressive Strength (MPa)
0% PMA	Measured	–	7	18.0
	Predicted	$f_c = 5.2421\ln(t) + 7.954$	28	25.5
5% PMA	Measured	–	7	24.0
	Predicted	$f_c = 5.7904\ln(t) + 12.518$	28	32.0
10% PMA	Measured	–	7	22.5
	Predicted	$f_c = 6.9545\ln(t) + 8.9929$	28	32.0
15% PMA	Measured	–	7	21.0
	Measured	–	28	31.5
20% PMA	Measured	–	7	20.0
	Measured	–	28	31.0

As discussed previously, the 28-day tests could not be performed for the 0%, 5% and 10% PMA specimens due to the local lockdown restrictions resulting from the Coronavirus (Covid-19) pandemic. Alternatively, 180- and 200-day compression tests were conducted for the aforementioned concrete mixes. These results were then used to predict the 28-day compressive strengths. Due to the small sample size (i.e. 9 compressive strength readings per concrete mix), it was decided that it would be more favourable to quantify a mathematical relationship (in relation to the concrete age, 't') for each of the affected PMA replacement levels. In accordance with Abdul Ghani et al. (2015), Sharipudin and Ridzuan (2012), Fava et al. (2011) and Abd Elaty (2014), a logarithmic regression curve was adopted to determine each mathematical relationship and the corresponding correlation factor (R^2).

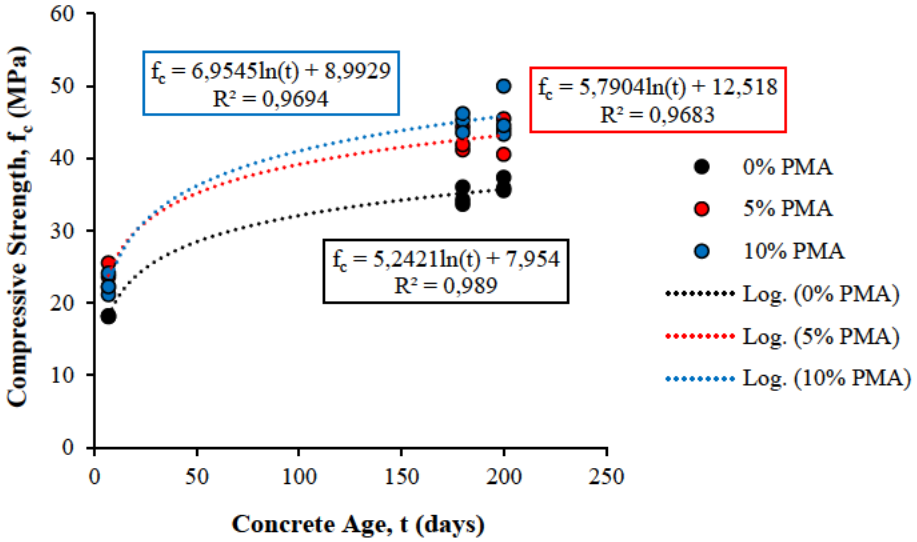

Figure 4-2: Mathematical relationship for predicting the compressive strength in relation to the concrete age

From Figure 4-2 above and the results documented in Appendix D, it was determined that R^2 ranged from 0.9683 to 0.989 for the three concrete mixes. This points to a good correlation and indicates a strong logarithmic relationship between the compressive strength and concrete age. Each derived mathematical relationship was then used to calculate the average compressive strength (at t = 28 days) for the 0% , 5% and 10% PMA concrete mixes. The measured and predicted compressive strengths for all the experimental samples can be viewed in Table 4-2 and Figure 4-3.

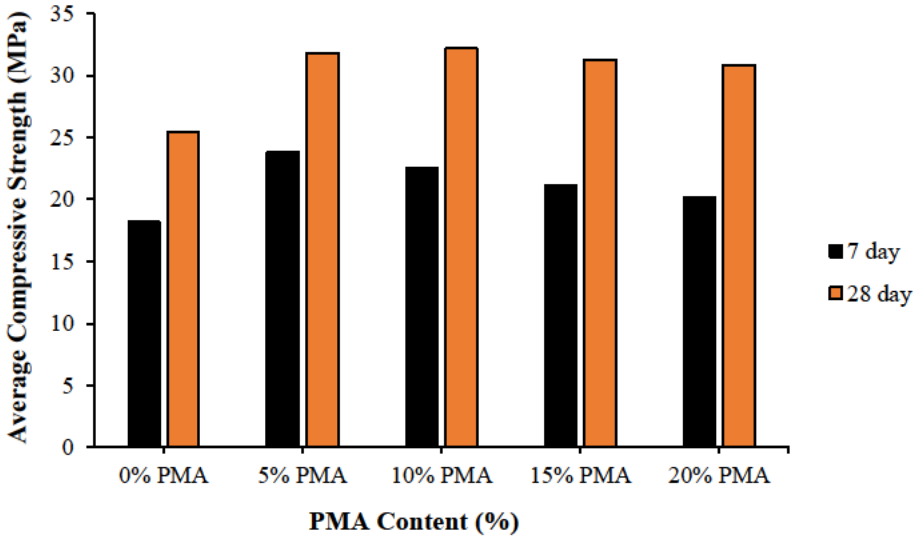

Figure 4-3: Results obtained from the compressive strength test

From the results obtained, it was noted that the compressive strength of all concrete specimens increased as time progressed. This was anticipated as sufficient temperature and curing conditions were provided across the entire testing period. The results indicate that incorporating PMA as an

alternate binder material led to improved compressive strengths compared to conventional concrete (0% PMA). This can be attributed to the higher concentrations of CaO, SiO_2 and Al_2O_3 found in the PMA sample used in this study. The increased oxide percentages coupled with the presence of metakaolin will have a direct correlation with the PC-PMA hydration process, which results in the formation of additional C-S-H gel and improved compressive strength properties (Babalola et al., 2020; Vegas et al., 2009).

The 5% PMA and 10% PMA concrete mixes achieved the highest 7- and 28-day compressive strength respectively, with reduced strength readings noted for subsequent PMA replacement levels. This trend is in agreement with the experimental results documented in the investigations undertaken by Fava et al. (2011), Sudha et al. (2018), Poojitha and Bhanu Pravallika (2017) and Ahmad et al. (2013), where a PMA content between 5 and 10% achieved the optimum compressive strength results. The variation in the optimum 7- and 28-day concrete mix can be due to the lack of blending equipment in the laboratory, which leads to an uneven distribution among the constituent materials and directly influences the results obtained. Other possible reasons include human error, unreliable testing apparatus and an uneven water level during curing which results in some specimens documenting a larger strength gain in comparison with other samples.

The reduced strength readings noted for the PMA replacement levels after the optimum content can be associated with the higher PMA concentrations in these samples, which results in reduced pozzolanic reactivity and strength development (Sharipudin and Ridzuan, 2012). The experimental results also showed limited compressive strength development after 7 days (25.21% – 34.77%), which is due to the curing procedure that was followed, whereby the concrete specimens were removed from the curing bath after 7 days, and air cured until the 28 day strength tests. The favourable compressive strength results that were achieved can also be attributed to the Portland-Slag cement (CEM II/B-S 42.5N Plus) that was used as the binding agent in this experimental study. In Chapter 2, Gailius and Laurikietytė (2003) and Bai et al. (2003) proved that GGBS serves as a good blending agent with PMA to replace OPC.

According to SAPEM (2013d), the minimum 28-day characteristic compressive strength of concrete pavements is 30 MPa. Therefore, the experimental results show that all concrete mixes containing PMA have satisfied this requirement. This, coupled with the high early strength development and enhanced compressive strength performance, proves that PMA is a viable alternate binder material for concrete pavement construction.

4.3.2) Flexural strength

Table 4-3: Measured and predicted flexural strength results of concrete containing varying quantities of paper mill waste ash

PMA Content (%)	Type of Result	Mathematical Relationship	Concrete Age (days)	Average Flexural Strength (MPa)
0% PMA	Measured	–	7	3.05
	Predicted	$f_F = 0.6628\ln(t) + 1.7527$	28	3.96
5% PMA	Measured	–	7	3.94
	Predicted	$f_F = 0.665\ln(t) + 2.6392$	28	4.86
10% PMA	Measured	–	7	4.48
	Predicted	$f_F = 0.8656\ln(t) + 2.7874$	28	5.67
15% PMA	Measured	–	7	4.06
	Measured	–	28	4.91
20% PMA	Measured	–	7	3.91
	Measured	–	28	4.24

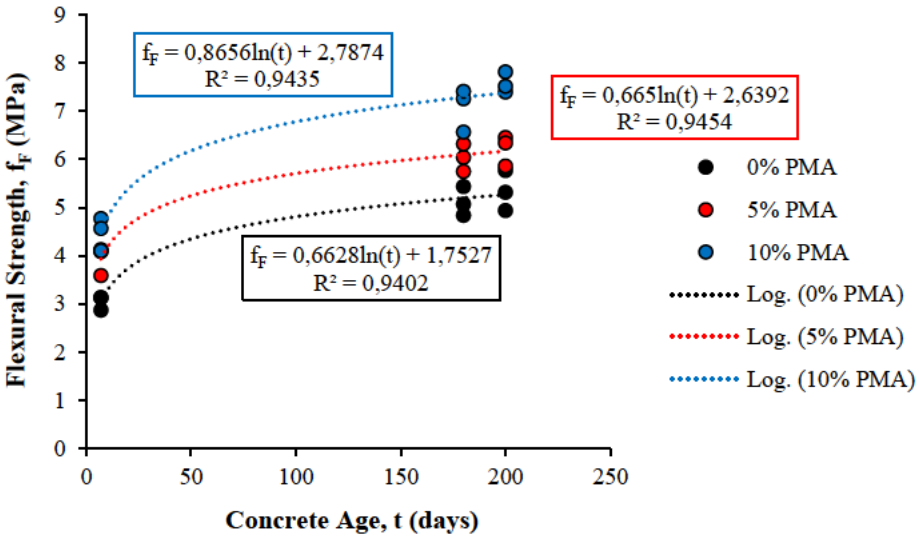

Figure 4-4: Mathematical relationship for predicting the flexural strength in relation to the concrete age

Due to the reasons outlined in Chapter 1, it was not possible to perform 28-day flexural strength tests on 0%, 5% and 10% PMA specimens. Instead, 180- and 200-day flexural strength tests were conducted for these concrete beam samples. The results obtained were then used to calculate the corresponding 28-day flexural strength for each of the affected concrete mixes (i.e. 0%, 5% and 10% PMA). As there was a limited number of test readings to work with (9 flexural strength results per concrete mix), it was decided that a mathematical relationship would be determined for each of the abovementioned concrete mixes. As researched by Abdul Ghani et al. (2015), Sharipudin and Ridzuan (2012), Fava et al. (2011) and Abd Elaty (2014), the mathematical

relationship was quantified in terms of concrete age (t) and consisted of a logarithmic regression curve.

As seen in Figure 4-4, R^2 was determined to lie between 0.9402 and 0.9454 for the 0%, 5% and 10% PMA concrete mixes. This indicates that the test results have a good correlation, and there is a strong logarithmic relationship between the flexural strength and age of the concrete specimens. The average 28-day flexural strength was then calculated by using the logarithmic expressions that were derived. Table 4-3 and Figure 4-5 presents the measured and predicted average flexural strength results for all the test specimens.

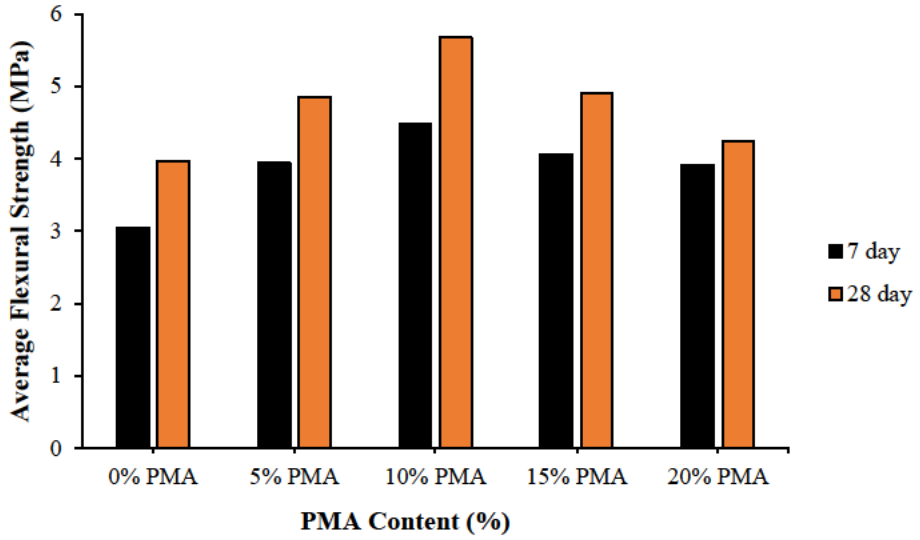

Figure 4-5: Results obtained from the flexural strength test

The results attained show that the flexural strength increased with time for all the concrete mixes. This trend was expected as satisfactory temperature and curing conditions were provided for the duration of the strength testing period. From the results achieved, it was determined that the addition of PMA as a supplementary cementitious material improved the flexural strength of the concrete in comparison with the results obtained for conventional concrete. Much like the compressive strength results in the previous section, this effect is due to the higher percentage of CaO, SiO_2 and Al_2O_3 present in the PMA sample from Mondi Merebank. According to ASTM (2008), SiO_2 and Al_2O_3 make up two of the three main oxide constituents in pozzolanic materials, therefore the increased oxide concentration will have a direct influence on the PC-PMA hydration process. Babalola et al. (2020) and Vegas et al. (2009) state that this correlation leads to the development of additional C-S-H gel and results in enhanced flexural strength performance.

From Figure 4-5 it was noted that the flexural strength improved as the PMA replacement level increased, with the 10% PMA concrete samples achieving the highest 7- and 28-day strength readings. It is also worth mentioning that the flexural strength decreased after the optimum PMA content. This correlation was also noted in the experimental results acquired by Poojitha and

Bhanu Pravallika (2017) and Sudha et al. (2018). According to Sharipudin and Ridzuan (2012), the decrease in the flexural strength results for the PMA contents after the optimum replacement level can be attributed to the higher amounts of PMA in these concrete specimens, which leads to reduced pozzolanic reactivity and a consequent decrease in strength development.

The results obtained from the flexural strength investigations also proved that the majority of the strength development occurred within the first 7 days, with limited flexural strength development noted after 7 days (7.67% – 23.13%). However, it was concluded that this trend can be associated with the curing procedure that was adopted (i.e. the test samples were removed from the curing bath after 7 days and air cured for the remaining time period). Gailius and Laurikietytė (2003) and Bai et al. (2003) discussed the favourable influence of GGBS when used as a blending agent with PMA and OPC. Therefore, the improved flexural strength performance documented in this study can also be attributed to the Portland-Slag cement which served as the main binding agent.

SAPEM (2013d) prescribed a target 28-day flexural strength greater than 4 MPa for rigid pavements in South Africa. Hence, the results attained prove that all PMA concrete mixes have achieved this strength requirement. Furthermore, flexural strength is the defining variable considered when designing concrete pavements. Therefore, the favourable flexural strength performance in combination with the high early strength development highlights the feasibility of concrete incorporating PMA as a supplementary cementitious material for use in rigid pavement applications.

4.3.3) Tensile splitting strength

Table 4-4: Measured and predicted tensile splitting strength results of concrete containing varying quantities of paper mill waste ash

PMA Content (%)	Type of Result	Mathematical Relationship	Concrete Age (days)	Average Splitting Strength (MPa)
0% PMA	Measured	–	7	1.53
	Predicted	$f_T = 0.3248\ln(t) + 0.9$	28	1.98
5% PMA	Measured	–	7	1.61
	Predicted	$f_T = 0.471\ln(t) + 0.6909$	28	2.26
10% PMA	Measured	–	7	1.89
	Predicted	$f_T = 0.5751\ln(t) + 0.768$	28	2.68
15% PMA	Measured	–	7	1.79
	Measured	–	28	2.56
20% PMA	Measured	–	7	1.76
	Measured	–	28	2.44

Much like the compressive and flexural strength experimental investigations, the 28-day tensile splitting strength tests for the 0%, 5% and 10% PMA concrete cylinders could not be conducted. As an alternative, 180- and 200-day tensile strength investigations were performed for the

aforementioned laboratory specimens. The results attained were then combined to form a data set that was used to quantify the respective 28-day tensile splitting strength for the affected concrete mixes. A mathematical relationship was derived in terms of concrete age (t) for the 0%, 5% and 10% PMA samples, as there were only 9 tensile splitting strength results making up the sample size for each of these mixes. The mathematical relationship consisted of a logarithmic regression curve, which is in agreement with the predictive models developed by Abdul Ghani et al. (2015), Sharipudin and Ridzuan (2012), Fava et al. (2011) and Abd Elaty (2014).

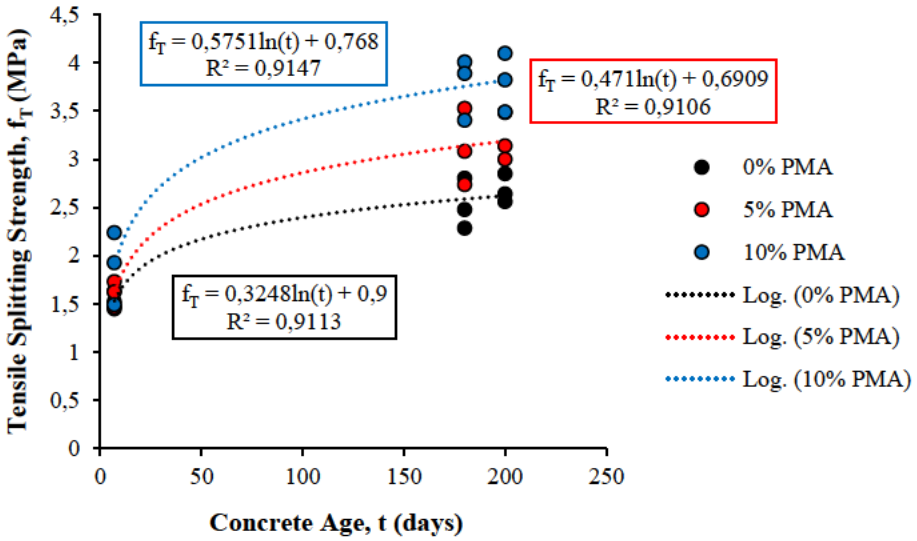

Figure 4-6: Mathematical relationship for predicting the tensile splitting strength in relation to the concrete age

As depicted in Figure 4-6, the correlation factor (R^2) was estimated to lie between 0.9106 and 0.9147 for the various concrete mixes. This indicates a strong correlation amongst the test results and signifies the favourable logarithmic relationship between the tensile splitting strength and the age of the concrete samples. However, it was also noted that the R^2 values for the tensile splitting strength investigations were lower than the corresponding values from the compressive and flexural strength tests. This points to a higher variation amongst the tensile splitting strength readings, which could be due to the lack of blending equipment that will lead to an uneven distribution of the constituent materials. The respective logarithmic relationships were then used to determine the average 28-day tensile splitting strength for the 0%, 5% and 10% PMA mixes. The measured and predicted tensile splitting strengths for all the concrete mixes have been presented in Table 4-4 and Figure 4-7 below.

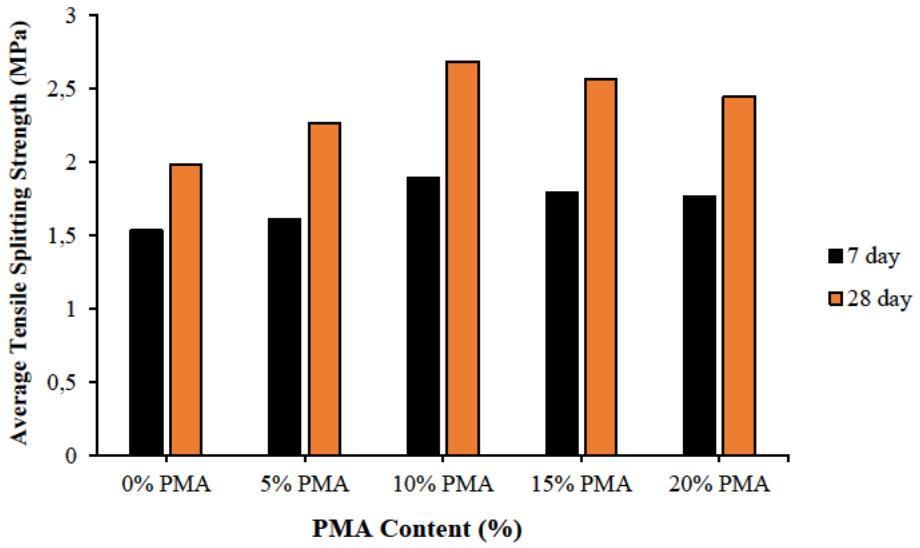

Figure 4-7: Results obtained from the tensile splitting strength test

From the results achieved, it was determined that the tensile splitting strength improved as the age of the concrete increased. This is in agreement with initial predictions as a suitable temperature and curing environment was provided for the entire strength testing period. The results attained also show that the inclusion of PMA as a partial cement replacement enhanced the tensile splitting strength performance of the concrete when compared to its conventional counterpart. Once again, this trend can be attributed to the high amounts of CaO, SiO_2 and Al_2O_3 found in the PMA sample, which will have a much greater influence on the hydration processes for the PMA and PC. This results in the production of additional C-S-H gel which consequently leads to improved tensile splitting strength performance (Babalola et al., 2020; Vegas et al., 2009).

The tensile splitting strength results followed a similar trend to the flexural strength results, whereby the tensile splitting strength improved until the optimum content of 10% PMA was achieved. Thereafter, the tensile splitting strength decreased for subsequent PMA replacement levels, which is in agreement with the conclusions drawn by Poojitha and Bhanu Pravallika (2017) and Sudha et al. (2018). Sharipudin and Ridzuan (2012) associate this correlation with the high amounts of PMA present in the concrete samples after the optimum PMA content had been exceeded, which results in decreased reactivity of the pozzolanic materials and leads to reduced strength development.

From the tensile splitting strength tests, it was also deduced that a large proportion of the strength development took place inside the first 7 days, with 22.61 to 30.09% of the tensile splitting strength gained after 7 days. However, this effect can be attributed to the curing process that was implemented, where the concrete specimens were removed from the curing bath after the 7-day tests were performed and air cured until the 28-day strength tests. It is also worth noting that the percentage strength development after 7 days for the tensile splitting strength results is higher

than the corresponding strength development for the compressive and flexural strength readings. In the experimental investigations undertaken by Gailius and Laurikietytė (2003) and Bai et al. (2003), it was documented that GGBS serves as a suitable blending agent in concrete containing OPC and PMA. Since Portland-Slag cement was selected as the primary binding agent in this research study, the favourable tensile splitting strength properties that were noted can also be attributed to the presence of GGBS.

Similarly, to flexural strength, tensile strength is also viewed as the defining design variable for rigid pavements. Hence, the favourable tensile splitting strength performance that was documented along with the high early strength development further validates the feasibility of PMA as an alternate binder material for rigid pavement construction.

4.4) Durability properties

4.4.1) Oxygen permeability

Table 4-5: Oxygen permeability test results of concrete containing varying quantities of paper mill waste ash

PMA Content (%)	Oxygen Permeability (log value)	Durability Class
0% PMA	9.84	Good
5% PMA	9.48	Poor
10% PMA	9.52	Good
15% PMA	9.20	Poor
20% PMA	10.09	Excellent

From the test results provided by Contest – Concrete Technology Services (Table 4-5 and Figure 4-8) and Table 3-4, it was determined that there was no discernible trend between the oxygen permeability value and PMA content. The variation in results contradicts the conclusions drawn from the literature review in Chapter 2. It was expected that there would be improved durability performance as the PMA content increased. An explanation for this disparity could be the lack of blending equipment in the UKZN laboratory, which leads to an uneven distribution of PC and PMA amongst the concrete cubes cast for durability testing purposes and results in inconsistent experimental readings. The laboratory specimens were removed from the curing bath after 7 days and air cured until the 28-day tests, which could also contribute to the unpredictable readings. The limited time spent in the curing bath will lead to an insufficient strengthening of the internal pore structure and reduced permeation properties in the test samples. There could have been foreign bodies, such as leaves and twigs, present in the aggregate materials which contaminate the concrete specimens and results in unreliable experimental results. Some of the concrete moulds were not fastened properly, which will lead to an inadequate degree of compaction being applied to these specimens and therefore impact on the permeability properties. Contest –

Concrete Technology Services also requested additional test samples for the 10% and 20% PMA mixes, as there was a glitch with the computer recording the results. Therefore, human error and unreliable laboratory equipment may have also impacted on the results obtained.

The test results also displayed that the 20% PMA concrete samples achieved the highest oxygen permeability value and was classified accordingly. This can be attributed to the presence of CaO, SiO_2 and Al_2O_3 in the PMA sample, which leads to the development of additional C-S-H gel. As outlined in Chapter 2, C-S-H has the largest influence on the HCP properties, which directly impacts on the durability performance of PMA concrete. PMA also consists of metakaolin which has characteristics similar to that of a filler material. Therefore, the addition of PMA as a supplementary cementitious material will reduce the concrete porosity and produce a microstructural matrix that is more densified. The GGBS found in the Portland-Slag cement also influences the durability performance of PMA concrete by reducing the amount of expansive product available per unit of internal pore space and thus improving the permeation and porosity properties.

The strengthening of the aggregate paste bond characteristics resulting from the incorporation PMA will decrease the occurrence of localised impact stresses and cavitation of concrete pavements. Furthermore, the densified concrete microstructure that was noted will also be an ideal design characteristic for combatting chloride attack and salt crystallization in concrete pavements located in coastal/marine environments. Therefore, it can be concluded that concrete containing PMA as an alternate binder material is viable for rigid pavement construction; however additional tests are needed to provide further clarification to the inconsistent experimental results that were noted.

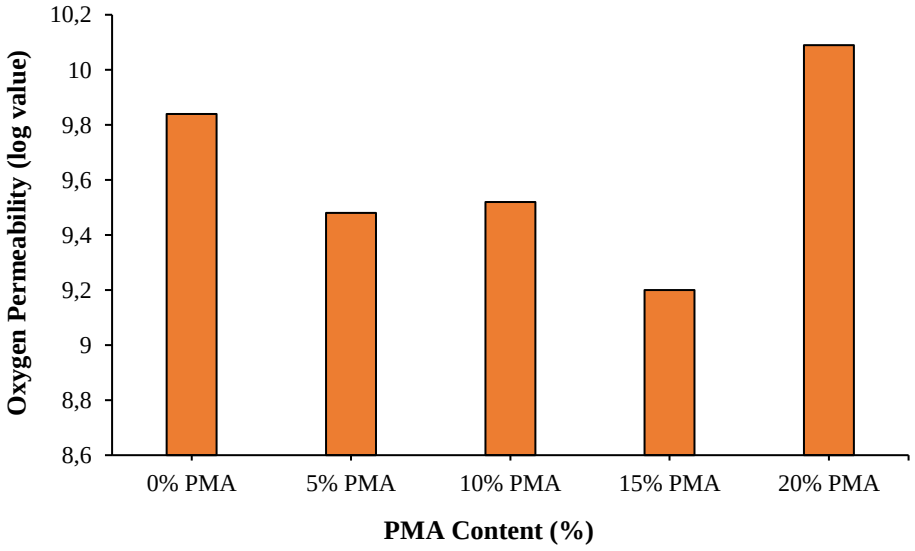

Figure 4-8: Results obtained from the oxygen permeability test

4.4.2) Water sorptivity

Table 4-6: Water sorptivity test results of concrete containing varying quantities of paper mill waste ash

PMA Content (%)	Water Sorptivity ($mmh^{-0.5}$)	Durability Class
0% PMA	4.66	Excellent
5% PMA	4.09	Excellent
10% PMA	3.95	Excellent
15% PMA	4.20	Excellent
20% PMA	4.29	Excellent

The water sorptivity results obtained shows that all the concrete mixes exhibited excellent durability performance, however there was no distinct relationship evident between the water sorptivity index value and the PMA replacement level. The inconsistent test results oppose the conclusions that were noted in Chapter 2, whereby the durability properties improved as the PMA replacement level increased. An uneven distribution of the constituent materials resulting from the lack of blending equipment could serve as a possible explanation for the variation in test readings. The curing procedure that was applied could have also impacted on results attained, as the concrete specimens only spent 7 days in the curing bath which results in inadequate pore structure development and leads to reduced permeation performance. As the coarse and fine aggregates were stockpiled outside, unwanted materials (i.e. twigs and leaves) could have contaminated the concrete, which leads to inaccurate experimental readings. The nuts and bolts on some of the concrete moulds were not tightened properly, thus affecting the degree of compaction applied to the samples and directly influencing the permeability performance. Contest – Concrete Technology Services experienced technical difficulties when performing the oxygen permeability tests; therefore, the same issues could have also influenced the test results.

However, even with the irregular water sorptivity values it is still worth mentioning that all concrete specimens displayed excellent durability performance, which can be associated with the high percentages of CaO, SiO_2 and Al_2O_3 present in the PMA sample. The high oxide concentrations result in the production of additional C-S-H, which directly influences the durability properties of concrete containing PMA as C-S-H has the biggest impact on HCP performance. The favourable durability performance can also be attributed to the presence of metakaolin in PMA. Metakaolin, which behaves like a filler material, will reduce the porosity of the concrete by filling the voids and consequently produce a densified microstructure. Portland-Slag cement was selected as the primary binding agent for this study, therefore the GGBS will also assist by reducing the quantity of expansive product available for each internal pore space, which leads to enhanced permeation and porosity performance.

The favourable characteristics of the aggregate paste bond in PMA concrete will reduce the amount of localised stresses and cavitation when used in rigid pavement applications. In addition, the densified microstructural matrix that was documented previously will be suitable for preventing chloride ingress and salt crystallization in concrete pavements situated in coastal/marine regions. Hence, from the aforementioned points, it was deduced that concrete incorporating PMA as a supplementary cementitious material will serve as a feasible construction material for rigid pavements. However, it was also noted that additional experimental investigations are required to provide clarity regarding the irregular water sorptivity readings that were documented.

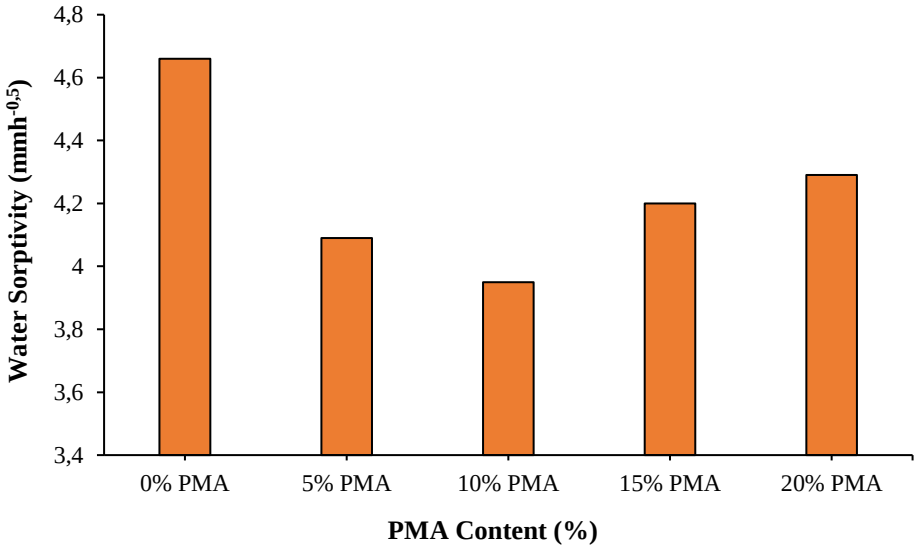

Figure 4-9: Results obtained from the water sorptivity test

4.4.3) Chloride conductivity

Table 4-7: Chloride conductivity test results of concrete containing varying quantities of paper mill waste ash

PMA Content (%)	Chloride conductivity (mS/cm)	Durability Class
0% PMA	0.23	Excellent
5% PMA	0.20	Excellent
10% PMA	0.25	Excellent
15% PMA	0.24	Excellent
20% PMA	0.25	Excellent

Much like the water sorptivity results in the previous section, the chloride conductivity results in Table 4-7 and Figure 4-10 indicated that all the concrete specimens achieved excellent durability performance. However, on closer inspection, there was once again no distinct trend between the chloride conductivity value and the PMA content. This contradicts with the initial observations made when conducting the literature review, where the durability performance was expected to

improve as the PMA content increased. The inconsistent test results obtained can be attributed to the uneven distribution of the PC and PMA resulting from the lack of blending of the pozzolanic materials. The concrete samples were only stored in the curing bath for 7 days which inhibits the strength development of the internal pore structure of the concrete and results in reduced permeability performance. The presence of unwanted objects, such as leaves and twigs, may have contaminated the concrete and resulted in imprecise experimental results. Some of the concrete moulds were not fastened correctly, which impacts on the level of compaction applied to the concrete specimens and affects the permeability properties of these samples. Human error and technical difficulties could also be contributing factors for the unpredictable test results, as Contest – Concrete Technology Services encountered unreliable laboratory equipment when conducting the oxygen permeability investigations.

Even though the chloride conductivity values were inconsistent, it is still worth noting that the durability performance of all concrete mixes was classified as excellent. This can be attributed to the high concentrations of CaO, SiO_2, and Al_2O_3 found the PMA sample that will lead to the development of additional C-S-H gel. This has a direct impact on the durability properties of PMA concrete as C-S-H has a major influence on HCP performance. PMA also contains metakaolin, which exhibits characteristics similar to a filler material, and will improve the durability performance of concrete. This is due to the fine particle size of metakaolin, which enables it to fill the pores and voids, therefore producing concrete that is more impermeable. The cement used for the investigations contained GGBS, which also contributed to improved permeability and porosity performance by decreasing the amount of expansive product available for each unit of internal pore space.

Rigid pavements constructed with PMA concrete will experience limited amounts of localised stresses and cavitation due to the strengthening of the aggregate paste bond that was documented above. Furthermore, the densely packed microstructure of PMA concrete makes it a suitable method for combatting salt crystallization and chloride ingress in rigid pavements located in coastal/marine environmental settings. Therefore, it was concluded that concrete containing PMA as a partial cement replacement will be a viable option for rigid pavement applications. Nevertheless, additional laboratory investigations are needed to provide a definitive answer regarding the unreliable chloride conductivity results.

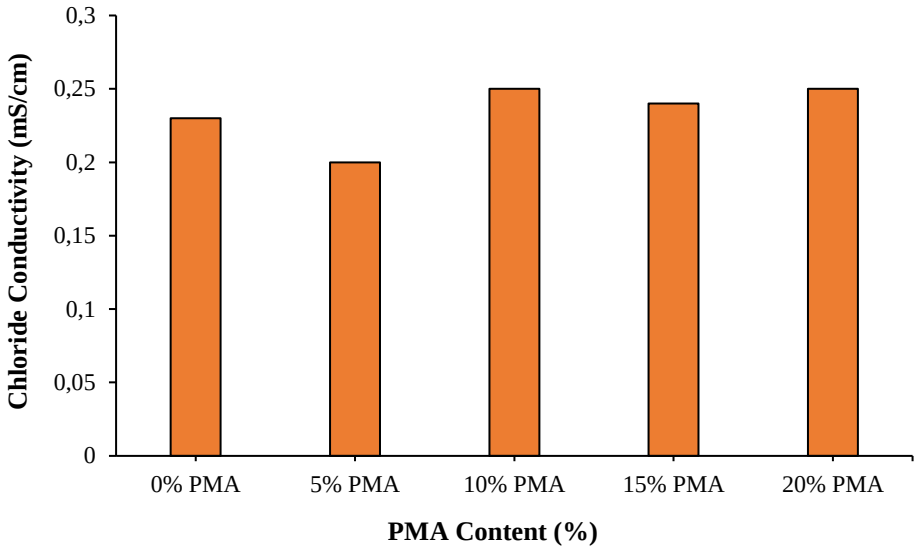

Figure 4-10: Results obtained from the chloride conductivity test

4.5) Frictional resistance

4.5.1) Skid resistance

Table 4-8: Skid resistance test results of concrete slabs containing varying quantities of paper mill waste ash

PMA Content (%)	Surface Texturing	Average Skid Resistance Value
0% PMA	Broom (longitudinal)	74
	Broom (transverse)	77
5% PMA	Broom (longitudinal)	73.2
	Broom (transverse)	77.4
10% PMA	Broom (longitudinal)	74.8
	Broom (transverse)	77.8
15% PMA	Broom (longitudinal)	73.8
	Broom (transverse)	76.6
20% PMA	Broom (longitudinal)	73.6
	Broom (transverse)	77.2

The skid resistance test was used to evaluate the frictional resistance properties of concrete slabs containing various proportions of PMA. A broom was used to manually apply longitudinal and transverse surface texturing to each of the concrete slabs. From the results documented in Table 4-8 and Figure 4-11, it was noted that there was no discernible trend between the average skid resistance value and PMA replacement level. According to the Federal Highway Administration (2019), aggregate texture, road gradation, pavement finishing technique, pavement age and wear has a major influence on the overall surface texture characteristics of rigid pavements. Therefore, the abovementioned trend was expected as PMA and PC have a fine material texture, while the type and quantity of aggregate material remained constant across all mix designs.

From the results attained it was also noted that the concrete slabs with surface texturing applied in the transverse direction had a higher average skid resistance value when compared to the slabs with longitudinal texturing. According to the Federal Highway Administration (2018), transverse surface texturing provides more frictional resistance than longitudinal surface texturing. However, it was also determined that transverse texturing leads to a pavement that is noisier when exposed to traffic; therefore, longitudinal texturing is the more widely used option. The variations in the average skid resistance values between each concrete mix can be attributed to the fact that the surface texturing was applied manually, which leads to inconsistent texture depths.

Hence, it was concluded that incorporating PMA as an alternate binder material in rigid pavements has a minimal effect on the skid resistance performance. Due to time constraints and limitations resulting from the Coronavirus (Covid-19) pandemic in South Africa, the optimum surface texturing technique could not be identified for concrete pavements containing PMA. Therefore, further investigations are needed to provide a definitive answer.

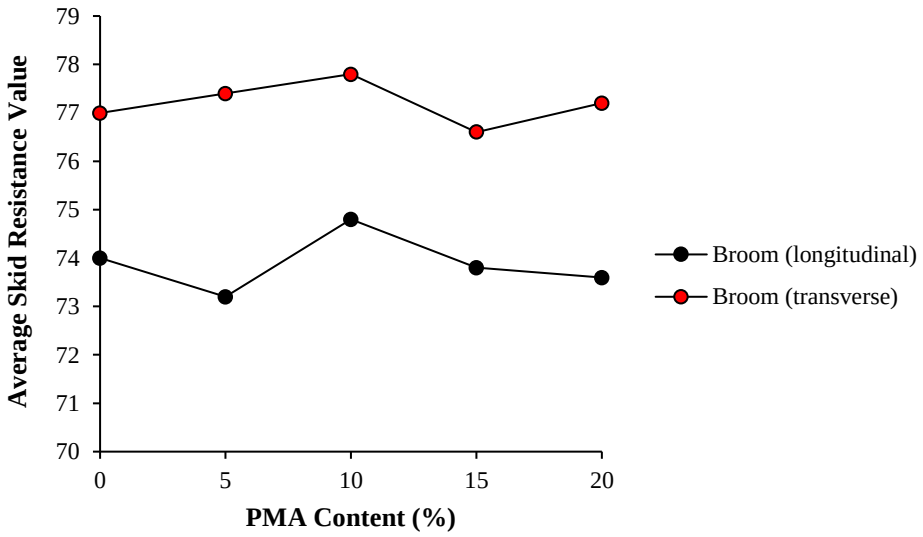

Figure 4-11: Results obtained from the skid resistance test

4.5.2) Texture depth

Table 4-9: Sand patch test results of concrete slabs containing varying quantities of paper mill waste ash

PMA Content (%)	Surface Texturing	Average Texture Depth (mm)
0% PMA	Broom (longitudinal)	1.03
	Broom (transverse)	1.05
5% PMA	Broom (longitudinal)	1.02
	Broom (transverse)	1.06
10% PMA	Broom (longitudinal)	1.04
	Broom (transverse)	1.07
15% PMA	Broom (longitudinal)	1.02
	Broom (transverse)	1.03
20% PMA	Broom (longitudinal)	1.02
	Broom (transverse)	1.06

In addition to the skid resistance test, the sand patch test was also used to assess the texture depth and frictional resistance performance of concrete slabs incorporating PMA as a partial cement replacement. The slabs used to perform the skid resistance tests were once again used for the sand patch tests. The corresponding test results have been provided in Table 4-9 and Figure 4-12 below, from which it was determined that there was no distinct trend visible between the average texture depth and PMA content. Federal Highway Administration (2019) states that the surface texture of the aggregate material has a major impact on the overall texture depth of concrete pavements. Hence, the aforementioned trend was anticipated as the type and quantity of aggregate material remained the same for all the concrete mixes. Furthermore, PMA and PC content were the only variables that were changing, and both materials had a fine material texture, thereby having minimal effect on the texture depth.

The experimental results also proved that the texture depth of the concrete slabs with transverse surface texturing was slightly higher than the corresponding slabs with longitudinal surface texturing. Likewise, the 0% PMA (longitudinal) slab and the 15% PMA (transverse) slab both had the same texture depth (1.03) but achieved different skid resistance values (74 and 76.6 respectively). This further supports the fact that surface texturing applied in the transverse direction provides more frictional resistance in comparison with surface texturing applied longitudinally. However, it is worth mentioning that longitudinal texturing is the preferred option amongst engineers as transverse texturing is noisier for road users. The disparities noted between the various texture depth results can be attributed to the surface texturing being applied manually.

Therefore, from the experimental results obtained, it was concluded that the addition of PMA as a supplementary cementitious material has minimal influence on the surface texture depth of concrete pavements. As a result of the limited time available and local restrictions resulting from

the Coronavirus (Covid-19) pandemic, the ideal surface texturing technique for rigid pavements constructed with PMA concrete could not be determined. Hence, additional experimental studies are required in order to reach a definitive conclusion.

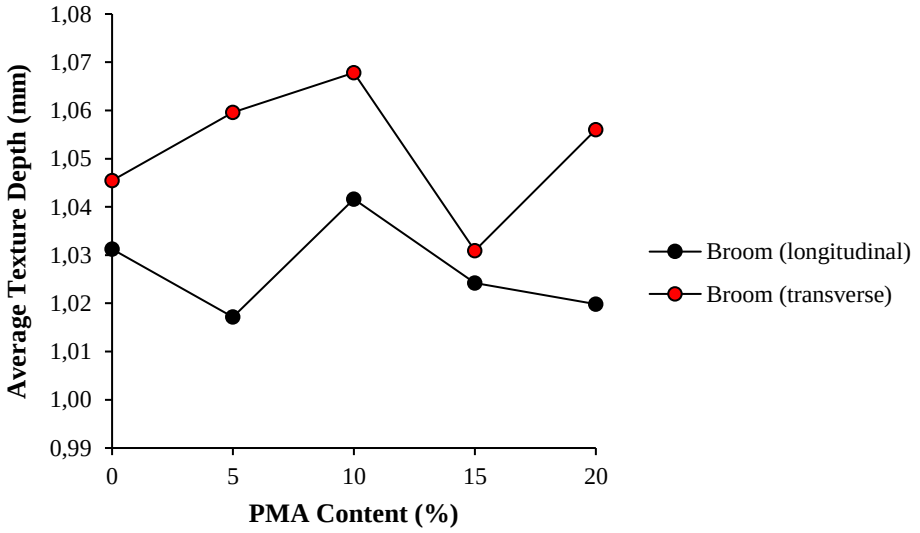

Figure 4-12: Results obtained from the sand patch test

4.6) Sustainability

4.6.1) Equivalent carbon dioxide (CO_{2e})

Table 4-10: Equivalent carbon dioxide (CO_{2e}) results of 1 m^3 concrete mix containing varying quantities of paper mill waste ash

PMA Content (%)	Equivalent Carbon Dioxide (CO_{2e}) (kg CO_{2e})
0% PMA	284.35
5% PMA	270.7
10% PMA	256.98
15% PMA	243.32
20% PMA	229.6

The sustainability effects of incorporating PMA as a supplementary cementitious material were assessed by performing an equivalent carbon dioxide (CO_{2e}) study for a hypothetical 1 m^3 concrete mix. From the favourable results documented in this section and Appendix I, it was determined that the CO_{2e} of the concrete mixes decreased as the PMA content increased. This trend was anticipated as the average CO_{2e} emission value for PMA was zero (Fava et al., 2011; Gavrilescu, 2008; Babalola et al., 2020; Jarnerud, 2019). It is also worth noting that Mondi Merebank produces PMA by incinerating paper mill sludge, which is classified as a waste product, for energy recovery purposes. Improper disposal of the PMA can have a detrimental environmental impact. Therefore, utilizing PMA as an alternate binder material for rigid

pavement applications will reduce the environmental impacts of the PMA disposal process and simultaneously decrease the carbon footprint related to the cement manufacturing industry.

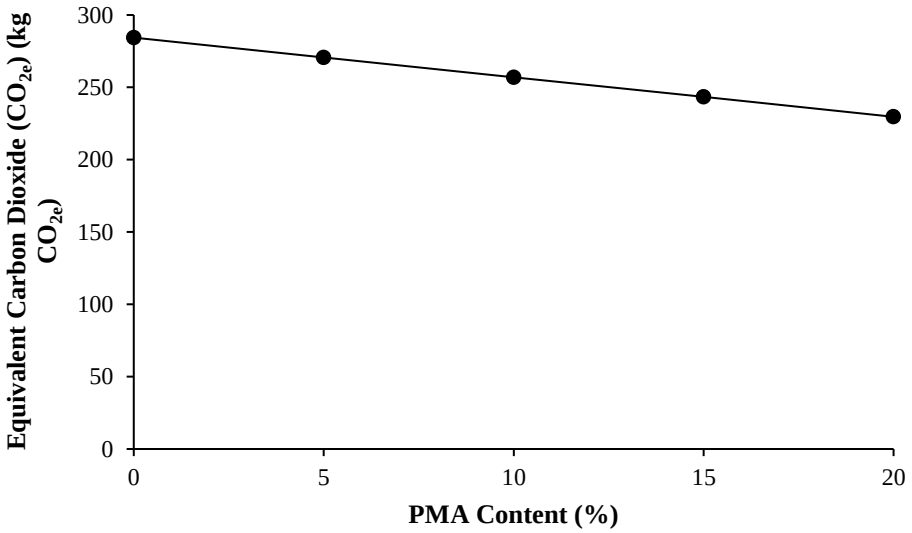

Figure 4-13: Results obtained from the equivalent carbon dioxide (CO_{2e}) study

4.7) Cost

4.7.1) Material cost analysis

Table 4-11: Material cost analysis results of 1 m^3 concrete mix containing varying quantities of paper mill waste ash

PMA Content (%)	Cost (R/m^3)
0% PMA	R 1222.27
5% PMA	R 1222.27
10% PMA	R 1130.27
15% PMA	R 1130.27
20% PMA	R 1038.27

A detailed breakdown of the cost for each concrete mix has been provided in Appendix J. From the results attained in Table 4-11 and Figure 4-14, it was noted that the cost per m^3 decreased as the PMA content increased. This relationship was expected as the PMA was provided free of charge by Mondi Merebank. It is also worth mentioning that the 0% and 5% PMA concrete mixes had the same material cost, which is due to the fact that the cement and PMA were the only quantities that were changing per mix design. The cement quantities were measured per 50 kg bag, therefore the variation in the amount of cement used for the 0% and 5% PMA concrete mixes (375 kg and 356.3 kg respectively) will not be detected in the material cost analysis. The same trend was also documented for the 10% and 15% PMA concrete mixes. Hence, from the material cost analysis results, it can be determined that concrete containing PMA as an alternate binder material is viable in an economic sense. However, a definitive conclusion can only be drawn after

considering the transportation costs associated with the PMA – this will be discussed in the next section.

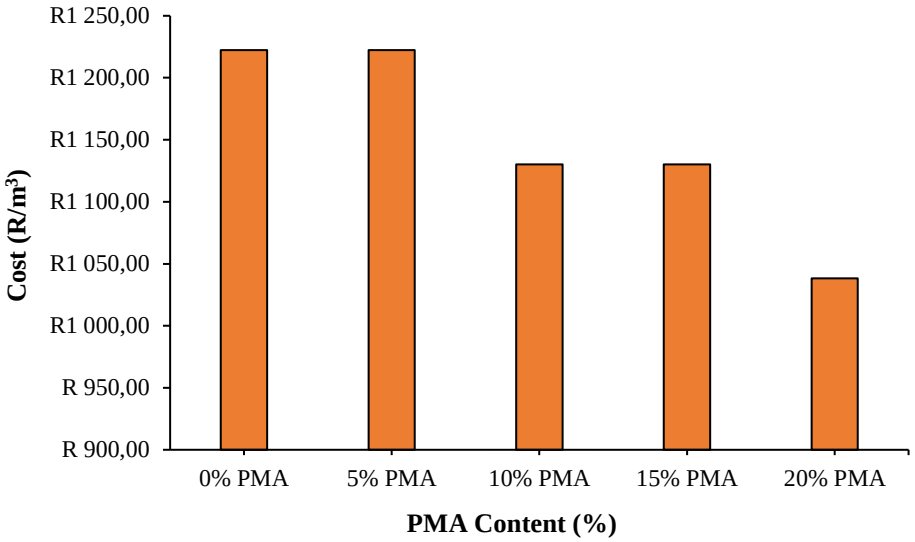

Figure 4-14: Results obtained from the material cost analysis

4.7.2) Construction cost analysis

Table 4-12: Construction cost analysis results for concrete containing varying quantities of paper mill waste ash when used in a typical rigid pavement scenario

PMA Content (%)	Material Costs	Transport Costs	Plant Costs	Labour Costs	TOTAL
0% PMA	R456 865,38	R99 738,90	R177 934,00	R276 006,00	**R1 010 544,28**
5% PMA	R451 345,38	R101 238,90	R177 934,00	R276 006,00	**R1 006 524,28**
10% PMA	R445 825,38	R102 382,20	R177 934,00	R276 006,00	**R1 002 147,58**
15% PMA	R440 305,38	R102 382,20	R177 934,00	R276 006,00	**R996 627,58**
20% PMA	R434 785,38	R103 525,50	R177 934,00	R276 006,00	**R992 250,88**

The economics associated with the incorporation of alternate binder materials plays a major role in determining the feasibility of the material for construction purposes, as industry professionals are unlikely to use concrete mixes with high costs unless there are favourable concrete performance benefits. With this in mind, a construction analysis based on a real-world scenario was conducted. This included evaluating the economic viability of concrete containing PMA for use in the rehabilitative works taking place on the concrete bullpen at the OneLogix Umlaas Road Vehicle Distribution Facility. A comprehensive breakdown of the construction costs for each concrete mix has been documented in Appendix J.

The results documented in Table 4-12 and Figure 4-15 indicate that the total cost of the construction work decreased as the PMA replacement level increased. The PMA had no material cost as it was obtained for free from Mondi Merebank, therefore the aforementioned relationship

was projected. The transportation cost was the only cost variable associated with the PMA however, it was also noted that in general the material costs were considerably higher than the transports costs. Therefore, the increased transport costs (i.e. R 1500 per day) for each PMA replacement level will have a minimal effect in counteracting the corresponding decrease in material cost, which led to the reduced overall cost that was documented.

Much like the results from the material cost analysis in the previous section, the material costs in the construction cost analysis once again decreased with increased PMA contents. However, the decrease is more pronounced in this scenario, as the material quantities are significantly higher than the quantities used for the material cost analysis. It was also noted that the plant and labour costs remained the same across all PMA replacement levels, as a variation in PMA content will not influence these cost variables. Therefore, from the favourable construction cost analysis results that were achieved in this study, it was concluded that concrete incorporating PMA as a supplementary cementitious material is an economically feasible construction material for use in rigid pavement applications.

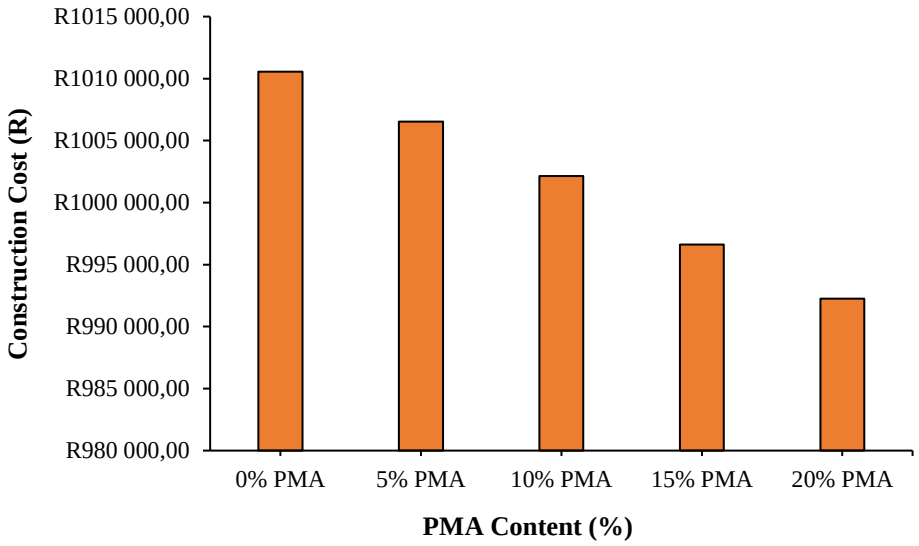

Figure 4-15: Results obtained from the construction cost analysis

The main findings documented in this research study, which analysed the feasibility of PMA as an alternate binder material for sustainable rigid pavement construction in South Africa, have been summarised in Table 4-13 below.

Table 4-13: Summary of the findings from the various testing procedures that were performed in this research study

Properties Research	Test Variable	Findings
Fresh	Workability	Workability decreased as the PMA content increased. All PMA concrete mixes were suitable for fixed form paving equipment, while 20% PMA concrete is optimum for slipform paving operations.
Mechanical	Compressive Strength	Compressive strength improved until the optimum replacement level (10% PMA). High early strength development was noted.
	Flexural Strength	Flexural strength improved until the optimum replacement level (10% PMA). High early strength development was noted.
	Tensile Splitting Strength	Tensile splitting strength improved until the optimum replacement level (10% PMA). High early strength development was noted.
Durability	Oxygen Permeability	Inconclusive test results were obtained. No discernible trend present between the oxygen permeability results and the PMA content. 20% PMA replacement level achieved the optimum oxygen permeability value.
	Water Sorptivity	All concrete specimens achieved excellent durability performance. No discernible trend present between the water sorptivity results and the PMA content. 0% PMA replacement level achieved the optimum water sorptivity value.
	Chloride Conductivity	All concrete specimens achieved excellent durability performance. No discernible trend present between the chloride conductivity results and the PMA content. 10 & 20% PMA replacement levels achieved the optimum chloride conductivity values.
Frictional Resistance	Skid Resistance	PMA had a minor influence on the skid resistance properties. No discernible trend present between the average skid resistance value and the PMA content.
	Texture Depth	PMA had a minor influence on the texture depth properties. No discernible trend present between the average texture depth and the PMA content.
Sustainability	CO_{2e}	The equivalent carbon dioxide (CO_{2e}) readings decreased as the PMA replacement level increased.
Cost	Material Costs	Material costs decreased as the PMA replacement level increased.
	Construction Costs	Material costs decreased as the PMA content increased, while transportation costs increased with higher PMA replacement levels. Reduced overall cost was noted.

4.8) Summary

This chapter provided a detailed assessment of the fresh state, strength, durability, frictional resistance, sustainability and economic performance of concrete containing PMA as a partial cement replacement. This was achieved by critically analysing the experimental results from the

various laboratory tests that were conducted. Desktop based investigations were also adopted for the sustainability and economic studies. The points discussed in this analysis were then used to evaluate the feasibility of PMA based concrete as an alternate construction material for rigid pavement applications. This sets the foundations for the final conclusions and future recommendations that will be discussed in Chapter 5.

CHAPTER 5: CONCLUSION AND RECOMMENDATIONS

5.1) Conclusion

The popularity of concrete within the transportation and roads engineering sector can be traced back to its versatility, superior strength and favourable durability performance. Along with rigid pavements, concrete also services various purposes in road structures and furniture for pavements. However, the advantageous material properties of concrete come at the expense of the environment. The harmful greenhouse gases that are emitted during the cement manufacturing process has a detrimental impact on the environment, while the production process also consumes significant quantities of raw materials and energy. As seen in Section 4.7.2, the construction of concrete pavements utilizes large quantities of cement and aggregate material. Therefore, a pavement design that incorporates sustainable construction materials and attains a consistent level of service is one of the main goals for enhancing the sustainability aspects of rigid pavements.

The amount of cement being manufactured for concrete production purposes can be reduced by incorporating alternate binder materials, such as paper mill ash (PMA). PMA is a waste material that is produced by incinerating paper mill sludge in combined heat and power plants. This method of disposal serves as a more environmentally friendly alternative to disposing of the waste sludge via land spreading or landfilling processes. This research study included a comprehensive analysis of the engineering performance of concrete incorporating PMA as a partial cement replacement, with a large emphasis placed on the fresh state, mechanical and durability properties. Frictional resistance investigations, an equivalent carbon dioxide (CO_{2e}) assessment, a material cost analysis and construction cost analysis were also performed to evaluate the feasibility of PMA as a supplementary cementitious material for sustainable rigid pavement applications. From the experimental results documented in Chapter 4, the following concluding remarks were made:

- Fresh state performance, namely concrete workability decreased as the PMA replacement level increased.
- Mechanical strength properties improved with the addition of PMA, with the 10% PMA content achieving the optimum strength results.
- Increased concrete durability (oxygen permeability, water sorptivity and chloride conductivity) with the incorporation of PMA, however, some irregularities were also noted.
- There was no discernible relationship between the frictional resistance (i.e. skid resistance and texture depth) and the corresponding PMA replacement level.
- Favourable sustainability characteristics were documented, with the CO_{2e} value decreasing for each subsequent PMA content.

- Both the material costs and construction costs associated with concrete containing PMA decreased for increased PMA replacement levels.

The reduced slump and workability properties documented in this study were in agreement with the results achieved in the experimental investigations performed by Ahmad et al. (2013), Gailius and Laurikietytė (2003), Mavroulidou et al. (2013) and Vegas et al. (2009). The trend was attributed to the finer PMA particle size characterisation compared to that of the cement. This results in the PMA having a high-water demand for the formation of the hydration products. The PMA sample used in this investigation contained metakaolin and high concentrations of CaO, SiO_2 and Al_2O_3, which will increase the hydration rate of the C_3S and consequently reduce the setting time and workability performance of the PMA concrete. The 0% PMA concrete mix was designed to a target slump of 75 mm; therefore, the achieved slump of 84 mm satisfied the slump tolerance (±25 mm) that was specified in SAPEM (2013c). This indicates that the conventional concrete mix was suitable for paving purposes. This point was further elaborated because all PMA concrete mixes achieved slump test results that were ideal for fixed form paving operations. Likewise, the 20% PMA concrete mix was deemed to be the most suitable mix for use in slipform paving techniques.

In the literature review, it was noted that there was a disparity in the w/b ratios that were adopted in the numerous past year studies (0.4 to 0.55). Therefore, a w/b ratio of 0.64 was selected for the concrete mix designs in this investigation in order to assess the effect a higher w/b ratio would have on the workability performance of PMA based concrete. From the reduced slump test results, it was concluded that increasing the w/b ratio does not lead to improved workability performance. Incorporating superplasticisers and water-reducing admixtures will be more viable options for improving the fresh state properties. SAPEM (2013d) also documented that fresh concrete used to construct rigid pavements should retain sufficient rigidity in order for the concrete to resist flow when paving roads with steep gradients and cross falls. Therefore, the reduced setting times and workability properties of concrete containing PMA makes it a feasible construction material for rigid pavement applications.

The mechanical properties were assessed by evaluating the compressive, flexural and tensile splitting strength performance of PMA based concrete specimens. Favourable mechanical strength development was documented across all concrete mixes containing PMA. The 10% PMA replacement level achieved the optimum 28-day compressive, flexural and tensile splitting strength results, which is in agreement with the strength results obtained in the investigations performed by Fava et al. (2011), Sudha et al. (2018), Poojitha and Bhanu Pravallika (2017) and Ahmad et al. (2013). The favourable strength results were also attributed to the high percentages of CaO, SiO_2 and Al_2O_3 present in the PMA sample that was used. The increased oxide

concentrations in combination with the metakaolin found in PMA has a direct correlation with the hydration process, which leads to the production of additional C-S-H gel and subsequently improves the concrete strength properties.

From the strength readings, it was also determined that the concrete strength decreased for PMA replacement levels after the optimum content. This trend was also noted in the research work undertaken by Sharipudin and Ridzuan (2012), who associated this relationship with the increased PMA concentrations in these concrete mixes, which led to reduced pozzolanic reactivity and development of strength. The literature review also proved that GGBS is a favourable blending agent with PMA to replace OPC. Therefore, the improved strength performance can also be attributed to the Portland-Slag cement that was selected as the main binding agent in this study.

High early strength development was documented for all strength classes. However, it was hypothesised that this effect could be due to the curing procedure that was followed. Nevertheless, the development of sufficient early strength is an important criterion for concrete used to construct rigid pavements as it enables early traffic use, while also reducing the delays and inconveniences resulting from road closures. Since tensile/flexural strength is the defining design variable for rigid pavements, the favourable flexural and tensile splitting strength readings indicate that pavements constructed with PMA concrete will have adequate strength to withstand tensile stresses resulting from warping, loading and shrinkage.

According to SAPEM (2013d), the minimum 28-day characteristic compressive strength for concrete pavements is 30 MPa, while a target 28-day flexural strength greater than 4 MPa was also specified. Therefore, from the results obtained it was determined that all concrete mixes containing PMA achieved the specified strength requirements, which when coupled with the favourable strength readings and high early strength development, highlights the feasibility of PMA concrete for use in rigid pavement applications.

The oxygen permeability, water sorptivity and chloride conductivity tests were used to analyse the durability properties of concrete containing PMA in accordance with the South African standards. Overall, favourable durability performance was documented across all the concrete mixes containing PMA. The water sorptivity and chloride conductivity test results were classified as excellent, whereas the oxygen permeability test readings were inconclusive. The enhanced durability properties were attributed to the high percentages of CaO, SiO_2 and Al_2O_3 found in the PMA sample, which results in the production of additional C-S-H gel. C-S-H has the highest impact on HCP performance, which directly influences the durability properties of concrete containing PMA. The strengthened aggregate paste bond found in PMA concrete will reduce the occurrence of localised stresses and cavitation when utilized in concrete pavements.

The GGBS present in the Portland-Slag cement will reduce the amount of expansive product available per internal pore space and therefore improves the concrete permeability and porosity properties. Likewise, metakaolin is also one of the mineral constituents of PMA and displays attributes similar to that of a filler material. Therefore, the incorporation of PMA as a partial cement replacement will produce more impermeable concrete with a densified microstructural matrix. The improved permeability properties will be a suitable design characteristic for preventing chloride attack and salt crystallization in rigid pavements located in a coastal/marine environmental setting. This effect will be visible in a SEM analysis; however, as outlined in Section 1.6, a concrete microstructural assessment could not be performed. Thus, additional experimental investigations are required to provide further clarification on this point.

Although favourable durability index test results were attained, on closer inspection, it was also noted that there was no discernible trend between the durability index values and PMA content. The inconsistent test results contradict with the conclusions that were drawn from the review of past year research studies performed in Chapter 2. Possible contributing factors for these disparities included the following: lack of blending equipment, curing procedure, contaminated aggregate material, unreliable laboratory equipment and human error. The literature review also revealed that minimal research has been performed to analyse the durability performance of PMA concrete in accordance with the South African durability index testing standards. This meant that the results obtained in this study could not be compared with the findings documented in past year studies. Therefore, further durability testing is needed to create a comparable data set and provide clarity regarding the irregular durability index test results that were noted.

The frictional resistance properties were assessed by performing skid resistance and texture depth tests on concrete slabs containing PMA. In order to simulate the design characteristics of rigid pavements, longitudinal and transverse surface texturing was manually applied to the concrete slabs with a broom. Both the skid resistance and sand patch tests returned inconsistent experimental results, i.e. there was no distinct correlation between the average skid resistance value, texture depth and PMA replacement level. These disparities were due to the surface texturing being applied manually which resulted in a lower degree of accuracy and inconsistent texture depths.

Nevertheless, PMA was not expected to have a major influence on the overall frictional resistance properties of concrete pavements, as both the PC and PMA had a fine material texture, while the material type and quantities of the coarse and fine aggregates remained the same for all concrete mix designs. This is in agreement with the specifications outlined in Federal Highway Administration (2019), where it was documented that only the aggregate texture, road inclination,

pavement finishing technique, pavement age and wear had the largest impact on the frictional resistance performance of concrete pavements.

From the results attained, it was found that the concrete slabs with transverse surface texturing exhibited higher frictional resistance properties when compared to the slabs with surface texturing in the longitudinal direction. This trend correlates with the findings documented in the Federal Highway Administration (2018). However, it is also worth noting that transverse texturing results in a more noisy pavement surface when exposed to traffic, which makes longitudinal surface texturing the more widely selected option. Due to the limitations outlined in Section 1.6, the optimum surface texturing procedure could not be determined for rigid pavements constructed with PMA concrete. Therefore, additional laboratory investigations are required to provide a definitive conclusion.

The sustainability effects of PMA concrete were analysed by conducting an equivalent carbon dioxide (CO_{2e}) study. The findings from this study proved that the CO_{2e} of the concrete mixes decreased as the PMA replacement level increased. This favourable relationship was expected as Fava et al. (2011), Gavrilescu (2008), Babalola et al. (2020) and Jarnerud (2019) all calculated the average CO_{2e} emission value for PMA to be zero. The PMA sample used in this research study was acquired from Mondi Merebank and was produced by incinerating paper mill sludge for energy recovery purposes. As discussed earlier in this chapter, the improper disposal of both paper mill sludge and PMA (which is classified as a waste material) can have an adverse environmental impact. Therefore, incorporating PMA as a supplementary cementitious material for concrete pavement construction works will reduce the probability of adverse environmental impacts related to the PMA disposal process and concurrently decrease the greenhouse gas emissions associated with the cement manufacturing industry.

The economics related to the addition of alternate binder materials is a key criterion when considering the viability of the material for construction purposes. This is largely due to the fact that industry professionals will only use expensive concrete mixes when there are advantageous concrete performance benefits. Therefore, the cost implications associated with incorporating PMA as an alternate binder material in concrete was evaluated with a material and construction cost analysis. The material cost analysis was carried out for a hypothetical 1 m^3 class 30/19 concrete mix containing various amounts of PMA, while the construction cost analysis was based on the concrete pavement rehabilitative works taking place at the OneLogix Umlaas Road Vehicle Distribution facility (Class 40/19 concrete). The results attained for both cost assessments proved that the costs incurred decreased as the PMA replacement level increased. This correlation was anticipated as the PMA was obtained from Mondi Merebank for free. The construction cost analysis showed that the transportation costs were significantly lower than the material costs.

Therefore, the increased transportation costs associated with each subsequent PMA content increase has no effect in counteracting the reduced material costs. This resulted in the overall decrease in costs incurred that was noted in both cost studies.

The aims and objectives of this research study primarily focused on identifying the benefits of utilizing PMA concrete as a construction material for rigid pavements. The reduced workability performance and the improved mechanical strength and durability performance proved that concrete containing PMA successfully meets the minimum strength requirements for rigid pavements in South Africa. The favourable strength and durability performance of PMA concrete also highlights the fact that it should not be restricted to concrete pavements only and can also be adopted for use in a wide variety of structural applications within the civil engineering industry. Furthermore, the positive findings that were documented from the frictional resistance investigations, equivalent carbon dioxide assessment, material cost analysis and construction cost analysis also indicate the benefits of utilizing PMA based concrete as a construction material for concrete pavements. Therefore, it can be concluded that the research work undertaken in this study proves that concrete incorporating PMA as an alternate binder material is a feasible option for improving the sustainability and serviceability states of rigid pavements in South Africa.

5.2) Recommendations

The following research gaps were identified when conducting this study, and recommendations for future investigations were made accordingly:

- Due to the national lockdown restrictions resulting from the Coronavirus (Covid-19) pandemic, the actual 28-day strength for the 0%, 5% and 10% PMA concrete samples could not be determined. Therefore, additional experimental investigations can be conducted to obtain the measured compressive, flexural and tensile splitting strength results.
- As per the previous point, 120- and 200-day strength tests were used to predict the mechanical strength performance of the aforementioned specimens. The mathematical relationships were derived in terms of concrete age for each of the affected PMA replacement levels. Hence, future research studies can be used to develop a universal predictive model for all PMA contents.
- Superplasticisers and water reducing admixtures can also be included in the concrete mix designs to enhance the workability of PMA concrete when used in structural applications.
- PMA is still a relatively new binder material to South Africa's concrete industry; therefore, additional experimental investigations can be undertaken to support the conclusions that were drawn in this research study.
- Blending the PMA and PC will improve the accuracy of the results obtained.

- The effect of various different curing procedures can be assessed to determine the optimum technique for concrete containing PMA.
- Additional durability index tests are required to provide further clarification for the inconsistent experimental results that were documented in this study.
- Electron microscopy studies can be performed to evaluate the concrete microstructure and durability performance of concrete incorporating PMA as a supplementary cementitious material.
- Further laboratory investigations related to frictional resistance can be undertaken to determine the optimum surface texturing procedure for rigid pavements constructed with concrete containing PMA.
- Future research studies can be adopted to analyse the cracking resistance, shrinkage, elastic modulus and creep performance of PMA based concrete.
- The environmental impact of concrete containing PMA can also be assessed by performing a life cycle analysis.
- In Chapter 2 it was determined that GGBS served as a suitable blending agent with PMA to replace PC. Therefore, future experimental investigations can focus on determining the optimum GGBS-PMA replacement level. Alternatively, the effect of blending PMA with other pozzolanic materials, such as FA, CSF, coal bottom ash, wood ash and sugarcane bagasse ash, can also be researched.
- Depending on the funds available, a trial section can be constructed to evaluate the interaction between the PMA concrete layer and the underlying pavement layers.
- A detailed analysis of the costs and indirect CO_2 emissions related to the production of PMA at Mondi Merebank can be performed to provide a more accurate representation of the cost and sustainability characteristics of concrete containing PMA that has been produced at Mondi Merebank.

REFERENCES

Abd Elaty, M.A.A. (2014). Compressive strength prediction of Portland cement concrete with age using a new model. *HBRC Journal, 10(2)*, pp.145-155.

Abdul Ghani, A.H., Fadzil Arshad, M., Salehuddin, N.A. and Ridzuan, A.R.M. (2015). Hydration Kinetics and Strength Development of Waste Paper Sludge Ash (WPSA) with Different Particle Size as Binary Blended Cement. *Applied Mechanics and Materials*, Vol. 754, pp.382-388.

Ahmad, S., Iqbal Malik, M., Bashir Wani, M. and Ahmad, R. (2013). Study of Concrete Involving Use of Waste Paper Sludge Ash as Partial Replacement of Cement. *IOSR Journal of Engineering*, 3(11), pp.06-15.

Aini, N.S., Haniff, M.A., Fadzil, M.A., Ridzuan, A.R.M. and Halim, A.A. (2013). Effect of WPSA particle size to the morphology and compressive strength properties of hydrated cement paste contain WPSA as SCM. In: *2013 IEEE Business Engineering and Industrial Applications Colloquium (BEIAC)*, pp.301-305.

Alexander, M. G., Mackechnie, J. R. and Ballim, Y. (1999). Research Monograph 2: Guide to the use of durability indexes for achieving durability in concrete structures.

Anderson, S.D., Ullman, G.L. and Blaschke, B.C. (2002). *A Process for Selecting Strategies for Rehabilitation of Rigid Pavements*. College Station, Texas: Texas Transportation Institute, Texas A&M University.

ASTM. (2008). Standard specification for coal fly ash and raw or calcined natural pozzolan for use in concrete. *C618*, West Conshohocken, PA.

Ayub, T., Khan, S.U. and Memon, F.A. (2014). Mechanical Characteristics of Hardened Concrete with Different Mineral Admixtures: A Review. *The Scientific World Journal*, 2014, pp.1-15.

Babafemi, A., Savija, B., Paul, S.C. and Anggraini, V. (2018). Engineering Properties of Concrete with Waste Recycled Plastic: A Review. *Sustainability*, 10(11), p.3875.

Babalola, O.E., Awoyera, P.O., Tran, M.T., Le, D.H., Olalusi, O.B., Viloria, A. and Ovallos-Gazabon, D. (2020). Mechanical and durability properties of recycled aggregate concrete with ternary binder system and optimised mix proportion. *Journal of Materials Research and Technology*, 9:6521–6532.

Bai, J., Chaipanich, A., Kinuthia, J.M., O'Farrell, M., Sabir, B.B., Wild, S. and Lewis, M.H. (2003). Compressive strength and hydration of wastepaper sludge ash-ground granulated blastfurnace slag blended pastes. *Cement and Concrete Research*, 33(8), pp.1189-1202.

Berrocal, C., Lundgren, K. and Löfgren, I. (2016). Corrosion of steel bars embedded in fibre reinforced concrete under chloride attack: State of the art. *Cement and Concrete Research*, 80, pp.69-85.

bin Mohd Sani, M.S.H., bt Muftah, F. and Ab Rahman, M. (2011). Properties of Waste Paper Sludge Ash (WPSA) as Cement Replacement in Mortar to Support Green Technology Material. In: *3rd International Symposium & Exhibition in Sustainable Energy & Environment*, pp.94-99.

Braam, C.R., Buitelaar, P. and Buitelaar, N. (2004). Reinforced High Performance Concrete Overlay System for Steel Bridges. *Proceedings of 5th International CROW Workshop on Fundamental Modelling of the Design and Performance of Concrete Pavements, Istanbul, Turkey.*

Bujulu, P.M.S., Sorta, A.R., Priol, G. and Emdal, A.J. (2007). Potential of wastepaper sludge ash to replace cement in deep stabilisation of quick clay. In: *2007 Annual Conference of the Transportation Association of Canada*, Saskatoon, Saskatchewan.

Byiringiro, A. (2014). *Effect of Paper Mill Ash on Properties of Expansive Soils*. Master of Engineering. Stellenbosch University.

Chaipanich, A., Bai, J., O'Farrell, M., Kinuthia, J.M., Sabir, B.B. and Wild, S. (2005). Setting time and heat of hydration of wastepaper sludge ash-ground granulated blastfurnace slag blended cements. In: *Cement Combinations for Durable Concrete: Proceedings of the International Conference held at the University of Dundee, Scotland, UK on 5-7 July 2005*, pp.825-834. Thomas Telford Publishing.

CoMSIRU (2018). *Durability Index Testing Procedure Manual*. University of Cape Town, University of Witwatersrand. ver.4.5.1, pp. 22-30.

Constro Facilitator (2020). *Different Types Of Concrete Slip Form Paver Machines*. [online] Constro Facilitator. Available at: <https://www.constrofacilitator.com/different-types-of-concrete-slip-form-paver-machines/> [Accessed 8 July 2020].

Courard, L., Darimont, A., Schouterden, M., Ferauche, F., Willem, X. and Degeimbre, R. (2003). Durability of mortars modified with metakaolin. *Cement and Concrete Research*, 33(9), pp.1473-1479.

Cunliffe, C., Mehta, Y.A., Cleary, D., Ali, A. and Redles, T. (2016). Impact of dynamic loading on backcalculated stiffness of rigid airfield pavements. *International Journal of Pavement Engineering*, *17*(6), pp.489-502.

Day, M. (2020). *Concrete Construction Joints - How To Minimize Cracking In Concrete Slabs*. [online] everything-about-concrete.com. Available at: <https://www.everything-about-concrete.com/concrete-construction-joints.html> [Accessed 19 May 2020].

Department of Transport (DOT). (2017). Draft Roads Policy For South Africa.

Di Mascio, P., Loprencipe, G., & Moretti, L. (2019). Technical and economic criteria to select pavement surfaces of port handling plants. *Coatings*, 9(2), 126.

Diamond, S. (2004). The microstructure of cement paste and concrete—a visual primer. *Cement and Concrete Composites*, 26(8), pp.919-933.

Doudart de la Grée, G.C.H., Yu, Q.L. and Brouwers, H.J.H. (2018). Upgrading and Evaluation of Waste Paper Sludge Ash in Eco-Lightweight Cement Composites. *Journal of Materials in Civil Engineering*, 30(3): 04018021.

du Plessis, L., Strauss, P. and Kilian, A. (2011). Monitoring the Behaviour of Thin Reinforced Concrete Pavements through Accelerated Pavement Testing. In: *Emerging Technologies for Material, Design, Rehabilitation and Inspection of Roadway Pavements*, pp.43-50.

Dunster, A.M. (2007). Paper sludge and paper sludge ash in Portland cement manufacture. *MinRes Case Study, Building Research Establishment, Garston*.

Ebels, L.J., Burger, A.F. and Fontini, D. (2007). Construction of an ultra-thin continuously reinforced concrete pavement.

Elliott, A. and Mahmood, T. (2006). Beneficial uses of pulp and paper power boiler ash residues. *Tappi Journal*, 5(10), pp.9-16.

Environmental Paper Network. (2018). *The State of the Global Paper Industry*.

Everitt, P.R. (2016). Practical Number 3: Concrete Mix Design. *ENCV2MTH1, Civil Engineering Materials*. Civil Engineering Programme, School of Civil Engineering, Surveying and Construction, University of KwaZulu-Natal.

Fava, G., Ruello, M. and Corinaldesi, V. (2011). Paper Mill Sludge Ash as Supplementary Cementitious Material. *Journal of Materials in Civil Engineering*, 23(6), pp.772-776.

Federal Highway Administration. (2019). *Concrete Pavement Texturing*.

Ferrándiz-Mas, V., Bond, T., García-Alcocel, E. and Cheeseman, C.R. (2014). Lightweight mortars containing expanded polystyrene and paper sludge ash. *Construction and Building Materials*, 61, pp.285-292.

FP&M SETA. (2014). *A profile of the paper and pulp sub-sector*. Paper and Pulp Sector.

Frías, M., García, R., Vigil, R. and Ferreiro, S. (2008a). Calcination of art paper sludge waste for the use as a supplementary cementing material. *Applied Clay Science*, 42(1-2), pp.189-193.

Frías, M., Sánchez de Rojas, M.I., Rodríguez, O., García Giménez, R. and Vigil de la Villa, R. (2008b). Characterisation of calcined paper sludge as an environmentally friendly source of metakaolin for manufacture of cementitious materials. *Advances in Cement Research*, 20(1), pp.23-30.

Furlani, E., Brückner, S., Minichelli, D. and Maschio, S. (2008). Synthesis and characterisation of ceramics from coal fly ash and incinerated paper mill sludge. *Ceramics International*, 34(8), pp.2137-2142.

Gailius, A. and Laurikietytė, Ž. (2003). Waste paper sludge ash and ground granulated blast furnace slag as binder in concrete. *Journal of Civil Engineering and Management*, 9(3), pp.198-202.

García Giménez, R., Vigil de la Villa, R., Goñi, S. and Frías, M. (2015). Fly ash and paper sludge on the evolution of ternary blended cements: Mineralogy and hydrated phases. *Journal of Materials in Civil Engineering*, 27(9): 04014249.

García. R., Vigil de la Villa, R., Vegas, I., Frías, M. and Sánchez de Rojas, M.I. (2008). The pozzolanic properties of paper sludge waste. *Construction and Building Materials*, 22(7), pp.1484-1490.

Gavrilescu, D. (2008). Energy from biomass in pulp and paper mills. *Environmental Engineering and Management Journal*, 7(5), pp.537-546.

Goel, A. and Das, A. (2004). Emerging road materials and innovative applications. In: *National Conference on Materials and their Application in Civil Engineering*.

Goñi, S., Frías, M., Vegas, I., García. R. and Vigil de la Villa, R. (2012). Effect of ternary cements containing thermally activated paper sludge and fly ash on the texture of C-S-H gel. *Construction and Building Materials*, 30, pp.381-388.

Jarnerud, T. (2019). Utilization of recovered lime-containing materials from pulp and paper industries as slag formers in stainless steel production (Doctoral dissertation, KTH Royal Institute of Technology).

Jiao, X. (2013). Comparison of Fuel Consumption on Rigid Versus Flexible Pavements along I-95 in Florida.

Kannemeyer, L., Perrie, B.D., Strauss, P.J. and Du Plessis, L. (2008). Ultra-Thin Continuously Reinforced Concrete Pavement Development in South Africa. *Proceedings of the 9th International Conference on Concrete Pavements,* San Francisco, USA, August 2008.

Kessy, J. (2013). *Durability Specifications for Structural Concrete – An International Comparison*. Ph.D. University of Cape Town.

Kinuthia, J.M., O'Farrell, M., Sabir, B.B. and Wild, S. (2001). A preliminary study of the cementitious properties of wastepaper sludge ash – ground granulated blastfurnace slag (WSA-GGBS) blends. In: *Recovery and Recycling of Paper: Proceedings of the International Symposium Organised by the Concrete Technology Unit and Held at the University of Dundee, Scotland, UK on 19 March 2001* (p. 93). Thomas Telford.

Koratich, D. (2020). Drying Shrinkage. [online] Engr.psu.edu. Available at: <https://www.engr.psu.edu/ce/courses/ce584/concrete/library/cracking/dryshrinkage/dryingshrinkage.html.[Accessed 23 March 2020].

Kumar, A. and Rani, D. (2016). Performance of Concrete Using Paper Sludge Ash and Foundry Sand. *International Journal of Innovative Research in Science, Engineering and Technology*, 5, pp.171-176.

Kumar, K. R., Shyamala, G., Awoyera, P. O., Vedhasakthi, K., & Olalusi, O. B. (2020). Cleaner production of self-compacting concrete with selected industrial rejects-an overview. *Silicon*, 1-12.

Likon, M. and Trebše, P. (2012). Recent advances in paper mill sludge management. *Industrial waste*, pp.73-90.

Mabee, W. and Roy, D.N. (2003). Modeling the role of papermill sludge in the organic carbon cycle of paper products. *Environmental Reviews*, 11(1), pp.1-16.

Mavroulidou, M., Boulouki, G. and Unsworth, C. (2013). Incorporating waste paper sludge ash as partial cement replacement in concrete. In: *13th International Conference of Environmental Science and Technology*.

Mehta, P.K. and Monteiro, P.J.M. (2001). Concrete: Microstructure, Properties and Materials.

Miller, M. (2010). *The Mondi Merebank Multi Fuel Boiler* [PowerPoint presentation]. Available at: https://www.esi-africa.com/wp-content/uploads/Mark_Miller.pdf. [Accessed 23 March 2020].

Mitchell, M.F., Marais, L.R. and Freeme, C.R. (1988). *Experience with Concrete Highways in the Republic of South Africa* (No. 1182).

Mohod, M.V. and Kadam, K.N. (2016). A comparative study on rigid and flexible pavement: a review. *IOSR Journal of Mechanical and Civil Engineering (IOSR-JMCE)*, *13*(3), pp.84-88.

Monosi, S., Sani, D. and Ruello, M.L. (2012). Reuse of Paper Mill Ash in Plaster Blends. *The Open Waste Management Journal*, 5(1), pp.5-10.

Mozaffari, E., Kinuthia, J.M., Bai, J. and Wild, S. (2009). An investigation into the strength development of Wastepaper Sludge Ash blended with Ground Granulated Blastfurnace Slag. *Cement and Concrete Research*, 39(10), pp.942-949.

Mozaffari, E., O'Farrell, M., Kinuthia, J.M. and Wild, S. (2006). Improving strength development of wastepaper sludge ash by wet-milling. *Cement and Concrete Composites*, 28(2), pp.144-152.

Murthi P., Poongodi K., Awoyera P.O., Gobinath R., Raja K.T., Olalusi O.B. (2020) Fresh properties of self-compacting concrete incorporating electric arc furnace oxidising slag (EAFOS) as coarse aggregate. SN Applied Sciences 2(4):1–8.

Owens, G. (2013). *Fundamentals of concrete*. 3rd ed. Midrand, South Africa: The Concrete Institute.

Pachamuthu, S. and Thangaraju, P. (2017). Effect of incinerated paper sludge ash on fly ash-based geopolymer concrete. *Journal of the Croatian Association of Civil Engineers*, 69(9), pp.851-859.

PAMSA. (2018). *South African Pulp and Paper Industry – Summary of 2018 production, import and export statistics*. Paper Manufacturers Association of South Africa (PAMSA).

Pandey, A., & Kumar, B. (2020). A comprehensive investigation on application of microsilica and rice straw ash in rigid pavement. *Construction and Building Materials*, 252: 119053.

Pera, J. and Amrouz, A. (1998). Development of Highly Reactive Metakaolin from Paper Sludge. *Advanced Cement Based Materials*, 7(2), pp.49-56.

Perrie, B.D. (2003). Low-volume Concrete Roads. *Concrete Beton*, 105, pp.8-13.

Plati, C. (2019). Sustainability factors in pavement materials, design, and preservation strategies: A literature review. *Construction and Building Materials*, 211, pp.539-555.

Poojitha, B. and Bhanu Pravallika, S. (2017). Study on Partial Replacement of Cement with Waste Paper Sludge Ash in Fibre Reinforced Concrete. *International Journal of Engineering Science and Computing (IJESC)*, 7(5), pp.11329-11335.

Poongodi, K., Murthi, P., Awoyera, P. O., Gobinath, R., & Olalusi, O. B. (2020). Durability properties of self-compacting concrete made with recycled aggregate. *Silicon*, 1-9.

Saleh, A. (2008). Chloride Induced Corrosion and Sulphate Attack – A Literature Review on Concrete Durability.

Schneider, M. (2019). The cement industry on the way to a low-carbon future. *Cement and Concrete Research*, 124: 105792.

Scrivener, K.L. (1998). *The microstructure of concrete*. Imperial College London.

Segui, P., Aubert, J.E. and Husson, B. (2011). Characterisation of wastepaper sludge ash for its use as component for hydraulic binders. In: *Innovation & Valorisation in Civil Engineering & Construction Materials (INVACO2)*, Rabat, Morroco.

Segui, P., Aubert, J.E., Husson, B. and Measson, M. (2012a). Characterisation of wastepaper sludge as for its valorisation as a component of hydraulic binders. *Applied Clay Science*, 57, pp.79-85.

Segui, P., Aubert, J.E., Husson, B. and Measson, M. (2012b). Valorisation of Wastepaper Sludge Ash as Main Component of Hydraulic Road Binder. *Waste and Biomass Valorisation*, 4(2), pp.297-307.

Sharipudin, S. and Ridzuan, A.R.M. (2012). Influence of Waste Paper Sludge Ash (WPSA) and Fine Recycled Concrete Aggregate (FRCA) on the Compressive Strength Characteristic of Foamed Concrete. *Advanced Materials Research*, 626, pp.376-380.

Singh, N. B., & Middendorf, B. (2020). Geopolymers as an alternative to Portland cement: An overview. *Construction and Building Materials*, 237: 117455.

South African National Department of Transport (DOT). (2017). *Draft Roads Policy for South Africa*.

South African National Roads Agency Ltd (SANRAL) (2020). [online] Nra.co.za. Available at: https://www.nra.co.za/live/content.php?Item_ID=279 [Accessed 15 Jan. 2020].

South African Pavement Engineering Manual (SAPEM). (2013a). Chapter 2: Pavement Composition and Behaviour. South African National Roads Agency Ltd (SANRAL).

South African Pavement Engineering Manual (SAPEM). (2013b). Chapter 3: Materials Testing. South African National Roads Agency Ltd (SANRAL).

South African Pavement Engineering Manual (SAPEM). (2013c). Chapter 4: Standards. South African National Roads Agency Ltd (SANRAL).

South African Pavement Engineering Manual (SAPEM). (2013d). Chapter 9: Materials Utilisation and Design. South African National Roads Agency Ltd (SANRAL).

South African Pavement Engineering Manual (SAPEM). (2013e). Chapter 10: Pavement Design. South African National Roads Agency Ltd (SANRAL).

South African Pavement Engineering Manual (SAPEM). (2013f). Chapter 12: Construction Equipment and Method Guidelines. South African National Roads Agency Ltd (SANRAL).

Stacks, D.L. (2019). Chapter 10: Rigid Pavement Rehabilitation. In: Pavement Manual. Available at: http://onlinemanuals.txdot.gov/txdotmanuals/pdm/rigid_pave_rehab.htm [Accessed 29 June 2020].

Steyn, W.J., du Plessis, L. and Strauss, P.J. (2005). Roodekrans trial sections: The role of structural support under very thin jointed CRC pavements subjected to heavy traffic.

Sudha, J.L., Sagar, D.S.V.S.R. and Ram, R.J. (2018). Experimental studies on strength characteristics of concrete with waste paper sludge ash as partial replacement for cement. *International Journal of Research and Analytical Reviews (IJRAR)*, 5(4), pp.342-347.

Tamanna, K., Raman, S. N., Jamil, M., & Hamid, R. (2020). Utilisation of wood waste ash in construction technology: A review. *Construction and Building Materials*, 237: 117654.

Thangapandi K., Anuradha R., Awoyera P.O., Gobinath R., Archana N., Berlin M., Oladimeji O.B. (2020) Durability phenomenon in manufactured sand concrete: effects of zinc oxide and Alcofine on behaviour. Silicon.

Transit New Zealand. (1981). *Standard Test Procedure for Measurement of Texture by the Sand Circle Method,* Transit New Zealand (TNZ), New Zealand.

Veerappan, G., Kinuthia, J.M., O'Farrell, M., Sabir, B.B. and Wild, S. (2003). Compressive strength of concrete blocks manufactured using wastepaper sludge ash. *Recycling and Reuse of Waste Materials*, pp.563-575.

Vegas, I., Frías, M., Urreta, J. and San José, J.T. (2006). Obtaining a pozzolanic addition from the controlled calcination of paper mill sludge. Performance in cement matrices. *Materiales de Construcción*, 56(283), pp.49-60.

Vegas, I., Urreta, J., Frías, M., Rodríguez, O., Ferreiro, S., Nebreda, B., García, R. and Vigil, R. (2009). Engineering Properties of Cement Mortars Containing Thermally Activated Paper Sludge. In: *7th International Conference on Sustainable Management of Waste and Recycled Materials in Construction*, pp.225-232.

Vigil de la Villa, R., Frías, M., Sánchez de Rojas, M., Vegas, I. and García, R. (2007). Mineralogical and morphological changes of calcined paper sludge at different temperatures and retention in furnace. *Applied Clay Science*, 36(4), pp.279-286.

Wong, H.S., Barakat, R., Alhilali, A., Saleh, M. and Cheeseman, C.R. (2015). Hydrophobic concrete using waste paper sludge ash. *Cement and Concrete Research*, 70, pp.9-20.

Wu, H., Huang, B., Shu, X. and Yin, J. (2016). Utilisation of solid wastes/byproducts from paper mills in Controlled Low Strength Material (CLSM). *Construction and Building Materials*, 118, pp.155-163.

Zhang, Z., Scherer, G.W. and Bauer, A. (2018). Morphology of cementitious material during early hydration. *Cement and Concrete Research*, 107, pp.85-100.

Zollinger, D.G. and Tayabji, S.D. (2007). *Best Practices of Concrete Pavement Transition Design and Construction* (No. FHWA/TX-07/0-5320-1).

Zulu, S.N. (2017). *Optimizing the usage of fly ash in concrete mixes* (Doctoral dissertation).

APPENDICES

Appendix A: Particle Grading Analysis – Fine Aggregate

The results acquired from the sieve analysis (in accordance with SANS 201) for the fine aggregate has been documented in Table A-1.

Table A-1: Particle grading analysis results for the fine aggregate (Umgeni River Sand)

Sieve size (µm)	Mass Retained (g)	Mass Retained (%)	Cumulative % Retained	Cumulative % Passed
4750	4.9	1.0	1.0	99.0
2360	19.2	3.8	4.8	95.2
1180	63.6	12.7	17.5	82.5
600	110.5	22.1	39.6	60.4
300	188.3	37.6	77.3	22.7
150	105.6	21.1	98.4	1.6
Passing 150	8.2	1.6	–	–
TOTAL	**500.3**	**100**	**238.6**	–

By applying Equation 3-1, the fineness modulus was calculated as follows:

$$Fineness\ Modulus\ (FM) = \frac{\sum Cumulative\ \%\ Retained}{100} = \frac{238.6}{100} = 2.39$$

Appendix B: Relative density – PMA

As per SANS 5844, the relative density of the paper mill ash was calculated as follows:

Table B-1: Recorded masses from Test 1

Symbol	Parameter	Value
M_1	Mass of pycnometer (empty) (g)	570
M_2	Mass of pycnometer and oven dried PMA sample (g)	870
M_3	Mass of pycnometer, oven dried PMA sample and distilled water (g)	1824
M_4	Mass of pycnometer and distilled water (g)	1656

$$RD_1 = \frac{M_2 - M_1}{M_4 - M_1 - (M_3 - M_2)} = \frac{870 - 570}{1656 - 570 - (1824 - 870)} = 2.273$$

Table B-2: Recorded masses from Test 2

Symbol	Parameter	Value
M_1	Mass of pycnometer (empty) (g)	570
M_2	Mass of pycnometer and oven dried PMA sample (g)	870
M_3	Mass of pycnometer, oven dried PMA sample and distilled water (g)	1821
M_4	Mass of pycnometer and distilled water (g)	1656

$$RD_2 = \frac{M_2 - M_1}{M_4 - M_1 - (M_3 - M_2)} = \frac{870 - 570}{1656 - 570 - (1821 - 870)} = 2.222$$

Table B-3: Recorded masses from Test 3

Symbol	Parameter	Value
M_1	Mass of pycnometer (empty) (g)	570
M_2	Mass of pycnometer and oven dried PMA sample (g)	870
M_3	Mass of pycnometer, oven dried PMA sample and distilled water (g)	1823
M_4	Mass of pycnometer and distilled water (g)	1656

$$RD_3 = \frac{M_2 - M_1}{M_4 - M_1 - (M_3 - M_2)} = \frac{870 - 570}{1656 - 570 - (1823 - 870)} = 2.256$$

$$Average\ RD = \frac{RD_1 + RD_2 + RD_3}{3} = \frac{2.273 + 2.222 + 2.256}{3} = 2.25$$

Appendix C: Concrete Mix Designs

C.1) Calculations for C&CI design method

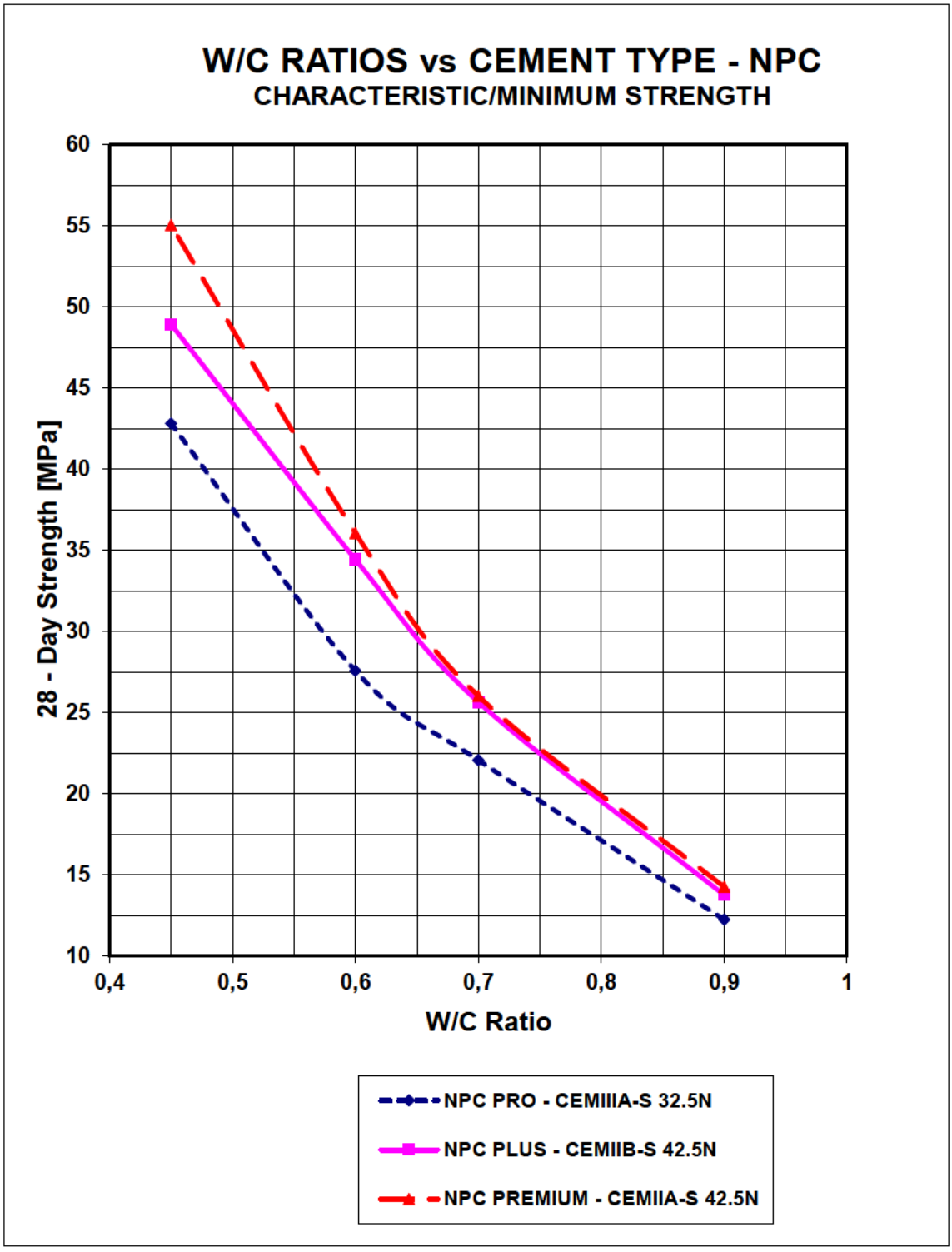

Figure C-1: Graphical representation of the w/c ratios for the different types of cement (Source: Everitt, 2016)

Table C-1: Water requirement for concrete mixes containing average quality sand and CEM 1 type cement (75 mm slump) (Source: Everitt, 2016)

Nominal size of stone (mm)	Water requirement (l/m^3)
9.5	235
13.2	225
19.0	210
26.5	200
37.5	190

Table C-2: K values based on the level of compaction, slump range and nominal size of stone (Source: Everitt, 2016)

Slump (mm)	Level of compaction	K value			
		Nominal size of stone (mm)			
		9.5	13.2	19.0	26.5
75 – 150	Hand Compaction	0.75	0.84	0.94	1
25 – 100	Moderate Vibration	0.8	0.9	1	1.06
0 – 25	Heavy Vibration	1	1.05	1.05	1.1

Table C-3: Total volume of concrete required for 0%, 5% and 10% PMA concrete mixes

Sample	Mould dimensions (mm)	Number of samples	Volume (m^3)
Cube	100 x 100 x 100	6	0.0060
	150 x 150 x 150	9	0.0304
Beam	500 x 100 x 100	9	0.0450
Cylinder	Ø150 x 300	9	0.0477
Slab	600 x 300 x 50	2	0.0180
	Subtotal		0.1471
	15% Wastage		0.0221
	TOTAL		**0.1691**

Table C-4: Total volume of concrete required for 15% and 20% PMA concrete mixes

Sample	Mould dimensions (mm)	Number of samples	Volume (m^3)
Cube	100 x 100 x 100	6	0.0203
	150 x 150 x 150	6	0.0060
Beam	500 x 100 x 100	6	0.0300
Cylinder	Ø150 x 300	6	0.0318
Slab	600 x 300 x 50	2	0.0180
	Subtotal		0.1060
	15% Wastage		0.0159
	TOTAL		**0.1219**

In accordance with the C&CI design method documented in Everitt (2016), the following calculation process was followed to determine the concrete mix designs:

1. <u>Select water content:</u>

Water content = 210 l/m^3 → Nominal size of stone = 19 mm (Table C-1)

2. <u>Select strength and water-binder ratio (w/b):</u>

From Figure C-1, 28-day strength = 30 MPa → w/b = 0.64

3. <u>Calculate total binder content:</u>

$$Total\ Binder\ Content = \frac{Water\ Content}{w/b} \quad (C-1)$$

4. <u>Calculate PMA content:</u>

$$V_{PMA} = \frac{Total\ Binder\ Content}{RD_{CEM}} \times \frac{x}{100} \quad (C-2)$$

where,

V_{PMA} = Volume of PMA (l)

RD_{CEM} = Relative density of cement = 3.1

x = PMA content level

$$M_{PMA} = V_{PMA} \times RD_{PMA} \quad (C-3)$$

where,

M_{PMA} = Mass of PMA (kg)

RD_{PMA} = Relative density of PMA = 2.25

5. <u>Calculate cement content:</u>

$$V_{CEM} = \frac{Total\ Binder\ Content}{RD_{CEM}} - V_{PMA} \quad (C-4)$$

where,

V_{CEM} = Volume of cement (l)

$$M_{CEM} = V_{CEM} \times RD_{CEM} \quad (C-5)$$

where,

M_{CEM} = Mass of cement (kg)

6. <u>Calculate stone content:</u>

CBD_{stone} = 1446 kg/m^3 → Pre-graded by UKZN Civil Engineering Laboratory Staff

FM_{sand} = 2.39 → Appendix A

K = 1 → Table C-2 (19 mm stone, moderate vibration)

$$M_{stone} = CBD_{stone}(K - 0.1FM_{sand}) \ldots\ldots (C - 6)$$

7. Calculate sand content:

$$V_{stone} = \frac{M_{stone}}{RD_{stone}} \ldots\ldots (C - 7)$$

where,

V_{stome} = Volume of stone (l)

M_{stone} = Mass of stone (kg)

RD_{stone} = Relative density of stone = 2.65 (Everitt, 2016)

$$V_{sand} = 1000 - V_{PMA} - V_{CEM} - V_{stone} \ldots\ldots (C - 8)$$

where,

V_{sand} = Volume of sand (l)

$$M_{sand} = V_{sand} \times RD_{sand} \ldots\ldots (C - 9)$$

where,

M_{sand} = Mass of sand (kg)

RD_{sand} = Relative density of sand = 2.65 (Everitt, 2016)

8. Calculate laboratory mix:

$$Adjustment\ Factor\ for\ Mix\ \text{"x"} = V_{TOTAL} \times \frac{V_{Water\ (mix\ 1)}}{V_{water\ (mix\ \text{"x"})}} \ldots\ldots (C - 10)$$

where,

V_{TOTAL} = Total volume of concrete (m^3) (Table C-3 and C-4)

$V_{water\ (mix\ 1)}$ = Volume of water for mix 1 (l)

$V_{water\ (mix\ x)}$ = Volume of water for mix “x” (l)

C.2) Final concrete mix designs for experimental investigations

Laboratory mix for 0% PMA:

CONCRETE MIX DESIGN (0% PMA)

CLIENT: STUDENT No: 214510044 PROJECT: ENCV8FY - MASTERS THESIS
REQUIREMENTS: STRENGTH: 30 MPa SLUMP: 75 mm W/C: 0,64

MATERIAL	TYPE AND SOURCE	SIZE [mm]	RD:	LBD [kg/m^3]	CBD [kg/m^3]	FM	K VALUES STONE	HAND COMP	MOD VIBR	HEAVY VIBR
CEMENT	NPC PRO CEM IIB-S 42.5N		3,1				9,5	0,75	0,8	1
PMA	MFB WASTE ASH		2,25				13,2	0,84	0,9	1,05
STONE 1	COEDMORE QRTZ	19	2,65	1360	1446		19,0	0,94	1	1,05
STONE 2							26,5	1	1,06	1,1
SAND 1	UMGENI RIVER SAND		2,65	1320	1400	2,39		FOR CBD [kg/m^3]		1446
SAND 2								STONE		19
PERCENTAGE			Dosage:	0	% volume			SELECTED K		1
1 m^3 (1000 l)			NOTE: kg/RD = litres					STONE REQD [kg]		1100,41

STONE REQUIRED [from formula using stone size and FM of sand] 1100,41 kg

	MIX 1		MIX 2		MIX 3		MIX 4	
MATERIAL	kg	litre	kg	litre	kg	litre	kg	litre
WATER	240	240	230	230	220	220	210	210
CEMENT	375	121	359	116	344	111	328	106
PMA	0	0	0	0	0	0	0	0
STONE 1	1100	415	1100	415	1100	415	1100	415
STONE 2								
SAND 1	593	224	633	239	673	254	713	269
SAND 2								
ADMIXTURE		ml		ml		ml		ml
TOTAL	2308	1000	2323	1000	2337	1000	2351	1000
FACTOR	mix size/1000 x (water mix 1)/(water mix X)							
0,1691	0,1691		0,1765		0,1845		0,1933	

LAB MIX

	MIX 1		Add kg	MIX 2		Add kg	MIX 3		Add kg	MIX 4	
MATERIAL	kg	litre		kg	litre		kg	litre		kg	litre
WATER	40,6	40,6	0	40,6	40,6	0	40,6	40,6	0	40,6	40,6
CEMENT	63,4	20,5	0	63,4	20,5	0	63,4	20,5	0	63,4	20,5
PMA	0,0	0,0	0	0,0	0,0	0	0,0	0,0	0	0,0	0,0
STONE 1	186,1	70,2	8,1	194,2	73,3	8,8	203,0	76,6	9,7	212,7	80,3
STONE 2	0,0		0	0,0		0	0,0		0	0,0	
SAND 1	100,3	37,8	11,4	111,7	42,1	12,4	124,1	46,8	13,6	137,7	52,0
SAND 2	0,0			0,0			0,0			0,0	
ADMIXTURE		ml			ml			ml			ml
Total	390,4	169,1		409,9	176,5		431,2	184,5		454,4	193,3

SLUMP		mm		mm		mm	84	mm

Comments: Mix 4 achieved a desirable slump, therefore it was the final mix design
Mix done by: Deveshan Pillay Date: 04/03/2020
Cubes marked: C

Laboratory mix for 5% PMA:

CONCRETE MIX DESIGN (5% PMA)

CLIENT: STUDENT No: 214510044 PROJECT: ENCV8FY - MASTERS THESIS
REQUIREMENTS: STRENGTH: 30 MPa SLUMP: mm W/C: 0,64

MATERIAL	TYPE AND SOURCE	SIZE [mm]	RD:	LBD [kg/m^3]	CBD [kg/m^3]	FM	K VALUES STONE	HAND COMP	MOD VIBR	HEAVY VIBR
CEMENT	NPC PRO CEMIIB-S 42.5N		3,1				9,5	0,75	0,8	1
PMA	MFB WASTE ASH		2,25				13,2	0,84	0,9	1,05
STONE 1	COEDMORE QRTZ	19	2,65	1360	1446		19,0	0,94	1	1,05
STONE 2							26,5	1	1,06	1,1
SAND 1	UMGENI RIVER SAND		2,65	1320	1400	2,39				
SAND 2										
PERCENTAGE			Dosage:	5	% volume					

FOR CBD [kg/m^3]	1446
STONE	19
SELECTED K	1
STONE REQD [kg]	1100,41

1 m^3 (1000 l) NOTE: kg/RD = litres

STONE REQUIRED [from formula using stone size and FM of sand] 1100,41 kg

	MIX 1		MIX 2		MIX 3		MIX 4	
MATERIAL	kg	litre	kg	litre	kg	litre	kg	litre
WATER	240	240	230	230	220	220	210	210
CEMENT	356	115	341	110	327	105	312	101
PMA	14	6	13	6	12	6	12	5
STONE 1	1100	415	1100	415	1100	415	1100	415
STONE 2								
SAND 1	593	224	633	239	673	254	713	269
SAND 2								
ADMIXTURE		ml		ml		ml		ml
TOTAL	2303	1000	2318	1000	2332	1000	2347	1000
FACTOR	mix size/1000 x (water mix 1)/(water mix X)							
0,1691	0,1691		0,1765		0,1845		0,1933	

LAB MIX

	MIX 1		Add kg	MIX 2		Add kg	MIX 3		Add kg	MIX 4	
MATERIAL	kg	litre		kg	litre		kg	litre		kg	litre
WATER	40,6	40,6	0	40,6	40,6	0	40,6	40,6	0	40,6	40,6
CEMENT	60,3	19,4	0	60,3	19,4	0	60,3	19,4	0	60,3	19,4
PMA	2,3	0,0	0	2,3	0,0	0	2,3	0,0	0	2,3	0,0
STONE 1	186,1	70,2	8,1	194,2	73,3	8,8	203,0	76,6	9,7	212,7	80,3
STONE 2	0,0		0	0,0		0	0,0		0	0,0	
SAND 1	100,3	37,8	11,4	111,7	42,1	12,4	124,1	46,8	13,6	137,7	52,0
SAND 2	0,0			0,0			0,0			0,0	
ADMIXTURE		ml			ml			ml			ml
Total	389,5	169,1		409,0	176,5		430,3	184,5		453,6	193,3

SLUMP		mm		mm		mm	70	mm

Comments: Mix 4 achieved a desirable slump, therefore it was the final mix design
Mix done by: Deveshan Pillay Date: 09/03/2020
Cubes marked: PMA 5

Laboratory mix for 10% PMA:

CONCRETE MIX DESIGN (10% PMA)

CLIENT: STUDENT No: 214510044 PROJECT: ENCV8FY - MASTERS THESIS
REQUIREMENTS: STRENGTH: 30 MPa SLUMP: mm W/C: 0,64

MATERIAL	TYPE AND SOURCE	SIZE [mm]	RD:	LBD [kg/m^3]	CBD [kg/m^3]	FM	K VALUES STONE	HAND COMP	MOD VIBR	HEAVY VIBR
CEMENT	NPC PRO CEMIIB-S 42.5N		3,1				9,5	0,75	0,8	1
PMA	MFB WASTE ASH		2,25				13,2	0,84	0,9	1,05
STONE 1	COEDMORE QRTZ	19	2,65	1360	1446		19,0	0,94	1	1,05
STONE 2							26,5	1	1,06	1,1
SAND 1	UMGENI RIVER SAND		2,65	1320	1400	2,39				
SAND 2										
PERCENTAGE			Dosage:	10	% volume					

FOR CBD [kg/m^3]	1446
STONE	19
SELECTED K	1
STONE REQD [kg]	1100,41

1 m^3 (1000 l) NOTE: kg/RD = litres

STONE REQUIRED [from formula using stone size and FM of sand] 1100,41 kg

	MIX 1		MIX 2		MIX 3		MIX 4	
MATERIAL	kg	litre	kg	litre	kg	litre	kg	litre
WATER	240	240	230	230	220	220	210	210
CEMENT	356	115	341	110	327	105	295	95
PMA	14	6	13	6	12	6	24	11
STONE 1	1100	415	1100	415	1100	415	1100	415
STONE 2								
SAND 1	593	224	633	239	673	254	713	269
SAND 2								
ADMIXTURE		ml		ml		ml		ml
TOTAL	2303	1000	2318	1000	2332	1000	2342	1000
FACTOR	mix size/1000 x (water mix 1)/(water mix X)							
0,1691	0,1691		0,1765		0,1845		0,1933	

LAB MIX

	MIX 1		Add kg	MIX 2		Add kg	MIX 3		Add kg	MIX 4	
MATERIAL	kg	litre		kg	litre		kg	litre		kg	litre
WATER	40,6	40,6	0	40,6	40,6	0	40,6	40,6	0	40,6	40,6
CEMENT	60,3	19,4	0	60,3	19,4	0	60,3	19,4	0	57,1	18,4
PMA	2,3	0,0	0	2,3	0,0	0	2,3	0,0	0	4,6	0,0
STONE 1	186,1	70,2	8,1	194,2	73,3	8,8	203,0	76,6	9,7	212,7	80,3
STONE 2	0,0		0	0,0		0	0,0		0	0,0	
SAND 1	100,3	37,8	11,4	111,7	42,1	12,4	124,1	46,8	13,6	137,7	52,0
SAND 2	0,0			0,0			0,0			0,0	
ADMIXTURE		ml			ml			ml			ml
Total	389,5	169,1		409,0	176,5		430,3	184,5		452,7	193,3

SLUMP mm mm mm 65 mm

Comments: Mix 4 achieved a desirable slump, therefore it was the final mix design
Mix done by: Deveshan Pillay Date: 11/03/2020
Cubes marked: PMA 10

Laboratory mix for 15% PMA:

CONCRETE MIX DESIGN (15% PMA)

CLIENT: STUDENT No: 214510044 PROJECT: ENCV8FY - MASTERS THESIS
REQUIREMENTS: STRENGTH: 30 MPa SLUMP: mm W/C: 0,64

MATERIAL	TYPE AND SOURCE	SIZE [mm]	RD:	LBD [kg/m^3]	CBD [kg/m^3]	FM
CEMENT	NPC PRO CEMIIB-S 42.5N		3,1			
PMA	MFB WASTE ASH		2,25			
STONE 1	COEDMORE QRTZ	19	2,65	1360	1446	
STONE 2						
SAND 1	UMGENI RIVER SAND		2,65	1320	1400	2,39
SAND 2						
PERCENTAGE			Dosage:	15	% volume	

K VALUES	HAND	MOD	HEAVY
STONE	COMP	VIBR	VIBR
9,5	0,75	0,8	1
13,2	0,84	0,9	1,05
19,0	0,94	1	1,05
26,5	1	1,06	1,1

FOR CBD [kg/m^3]	1446
STONE	19
SELECTED K	1
STONE REQD [kg]	1100,41

1 m^3 (1000 l) NOTE: kg/RD = litres

STONE REQUIRED [from formula using stone size and FM of sand] 1100,41 kg

	MIX 1		MIX 2		MIX 3		MIX 4	
MATERIAL	kg	litre	kg	litre	kg	litre	kg	litre
WATER	240	240	230	230	220	220	210	210
CEMENT	356	115	341	110	327	105	279	90
PMA	14	6	13	6	12	6	36	16
STONE 1	1100	415	1100	415	1100	415	1100	415
STONE 2								
SAND 1	593	224	633	239	673	254	713	269
SAND 2								
ADMIXTURE		ml		ml		ml		ml
TOTAL	2303	1000	2318	1000	2332	1000	2338	1000
FACTOR	mix size/1000 x (water mix 1)/(water mix X)							
0,1219	0,1219		0,1273		0,1330		0,1394	

LAB MIX

	MIX 1		Add kg	MIX 2		Add kg	MIX 3		Add kg	MIX 4	
MATERIAL	kg	litre		kg	litre		kg	litre		kg	litre
WATER	29,3	29,3	0	29,3	29,3	0	29,3	29,3	0	29,3	29,3
CEMENT	43,4	14,0	0	43,4	14,0	0	43,4	14,0	0	38,9	12,5
PMA	1,7	0,0	0	1,7	0,0	0	1,7	0,0	0	5,0	0,0
STONE 1	134,2	50,6	5,8	140,0	52,8	6,4	146,4	55,2	7,0	153,4	57,9
STONE 2	0,0		0	0,0		0	0,0		0	0,0	
SAND 1	72,3	27,3	8,2	80,5	30,4	9,0	89,5	33,8	9,8	99,3	37,5
SAND 2	0,0			0,0			0,0			0,0	
ADMIXTURE		ml			ml			ml			ml
Total	280,9	121,9		294,9	127,3		310,3	133,0		325,8	139,4

SLUMP mm mm mm 60 mm

Comments: Mix 4 achieved a desirable slump, therefore it was the final mix design
Mix done by: Deveshan Pillay Date: 15/09/2020
Cubes marked: PMA 15

Laboratory mix for 20% PMA:

CONCRETE MIX DESIGN (20% PMA)

CLIENT: STUDENT No: 214510044 PROJECT: ENCV8FY - MASTERS THESIS
REQUIREMENTS: STRENGTH: 30 MPa SLUMP: mm W/C: 0,64

MATERIAL	TYPE AND SOURCE	SIZE [mm]	RD:	LBD [kg/m^3]	CBD [kg/m^3]	FM
CEMENT	NPC PRO CEMIIB-S 42.5N		3,1			
PMA	MFB WASTE ASH		2,25			
STONE 1	COEDMORE QRTZ	19	2,65	1360	1446	
STONE 2						
SAND 1	UMGENI RIVER SAND		2,65	1320	1400	2,39
SAND 2						
PERCENTAGE			Dosage:	20	% volume	

K VALUES	HAND	MOD	HEAVY
STONE	COMP	VIBR	VIBR
9,5	0,75	0,8	1
13,2	0,84	0,9	1,05
19,0	0,94	1	1,05
26,5	1	1,06	1,1

FOR CBD [kg/m^3]	1446
STONE	19
SELECTED K	1
STONE REQD [kg]	1100,41

1 m^3 (1000 l) NOTE: kg/RD = litres

STONE REQUIRED [from formula using stone size and FM of sand] 1100,41 kg

	MIX 1		MIX 2		MIX 3		MIX 4	
MATERIAL	kg	litre	kg	litre	kg	litre	kg	litre
WATER	240	240	230	230	220	220	210	210
CEMENT	356	115	341	110	327	105	263	85
PMA	14	6	13	6	12	6	48	21
STONE 1	1100	415	1100	415	1100	415	1100	415
STONE 2								
SAND 1	593	224	633	239	673	254	713	269
SAND 2								
ADMIXTURE		ml		ml		ml		ml
TOTAL	2303	1000	2318	1000	2332	1000	2333	1000
FACTOR	mix size/1000 x (water mix 1)/(water mix X)							
0,1219	0,1219		0,1273		0,1330		0,1394	

LAB MIX

	MIX 1		Add kg	MIX 2		Add kg	MIX 3		Add kg	MIX 4	
MATERIAL	kg	litre		kg	litre		kg	litre		kg	litre
WATER	29,3	29,3	0	29,3	29,3	0	29,3	29,3	0	29,3	29,3
CEMENT	43,4	14,0	0	43,4	14,0	0	43,4	14,0	0	36,6	11,8
PMA	1,7	0,0	0	1,7	0,0	0	1,7	0,0	0	6,6	0,0
STONE 1	134,2	50,6	5,8	140,0	52,8	6,4	146,4	55,2	7,0	153,4	57,9
STONE 2	0,0		0	0,0		0	0,0		0	0,0	
SAND 1	72,3	27,3	8,2	80,5	30,4	9,0	89,5	33,8	9,8	99,3	37,5
SAND 2	0,0			0,0			0,0			0,0	
ADMIXTURE		ml			ml			ml			ml
Total	280,9	121,9		294,9	127,3		310,3	133,0		325,2	139,4

SLUMP		mm		mm		mm	35	mm

Comments: Mix 4 achieved a desirable slump, therefore it was the final mix design
Mix done by: Deveshan Pillay Date: 22/09/2020
Cubes marked: PMA 20

Appendix D: Compressive strength test results

D.1) 7-day test results

Table D-1: Compressive strength test results (7 day)

PMA Content (%)	Specimen	Fracture Load (kN)	Average Fracture Load (kN)
0% PMA	Cube 1	407.7	408.87
	Cube 2	408.1	
	Cube 3	410.8	
5% PMA	Cube 1	531.4	535.27
	Cube 2	574.6	
	Cube 3	499.8	
10% PMA	Cube 1	476.2	506.90
	Cube 2	501.3	
	Cube 3	543.2	
15% PMA	Cube 1	465.2	475.50
	Cube 2	514.9	
	Cube 3	446.3	
20% PMA	Cube 1	432.1	452.60
	Cube 2	496.3	
	Cube 3	429.4	

Sample calculation for 0% PMA:

$A_c = 150 \times 150 = 22500\ mm^2$

$f_c = \frac{F_c}{A_c} = \frac{408.87 \times 1000}{22500} = 18.17\ MPa$

Check validity of compressive strength test (0% PMA):

$Cube\ 1\text{:}\ \ f_c = \frac{F_c}{A_c} = \frac{407.7 \times 1000}{22500} = 18.12\ MPa$

$Cube\ 3\text{:}\ \ f_c = \frac{F_c}{A_c} = \frac{410.8 \times 1000}{22500} = 18.26\ MPa$

$18.17 \times \frac{15}{100} = 2.7255 > 18.26 - 18.12 = 0.14 \therefore Test\ is\ valid$

D.2) 28-day test results

Table D-2: Compressive strength test results (28 day)

PMA Content (%)	Specimen	Fracture Load (kN)	Average Fracture Load (kN)
15% PMA	Cube 1	704.1	704.10
	Cube 2	662.3	
	Cube 3	745.8	
20% PMA	Cube 1	652.7	693.80
	Cube 2	738.1	
	Cube 3	690.6	

Sample calculation for 15% PMA:

$A_c = 150 \times 150 = 22500\ mm^2$

$f_c = \frac{F_c}{A_c} = \frac{704.1 \times 1000}{22500} = 31.29\ MPa$

Check validity of compressive strength test (15% PMA):

$Cube\ 2\text{:}\ \ f_c = \frac{F_c}{A_c} = \frac{662.3 \times 1000}{22500} = 29.44\ MPa$

$Cube\ 3\text{:}\ \ f_c = \frac{F_c}{A_c} = \frac{745.8 \times 1000}{22500} = 33.15\ MPa$

$31.29 \times \frac{15}{100} = 4.6935 > 33.15 - 29.44 = 3.71 \therefore Test\ is\ valid$

D.3) 180-day test results

Table D-3: Compressive strength test results (180 day)

PMA Content (%)	Specimen	Fracture Load (kN)	Average Fracture Load (kN)
0% PMA	Cube 1	810.2	779.20
	Cube 2	756.8	
	Cube 3	770.6	
5% PMA	Cube 1	926.5	955.33
	Cube 2	997.6	
	Cube 3	941.9	
10% PMA	Cube 1	1019.1	1012.60
	Cube 2	1038.5	
	Cube 3	980.2	

Sample calculation for 0% PMA:

$A_c = 150 \times 150 = 22500\ mm^2$

$f_c = \frac{F_c}{A_c} = \frac{779.2 \times 1000}{22500} = 34.63\ MPa$

Check validity of compressive strength test (0% PMA):

$Cube\ 1\text{:}\ \ f_c = \frac{F_c}{A_c} = \frac{810.2 \times 1000}{22500} = 36.01\ MPa$

$Cube\ 2\text{:}\ \ f_c = \frac{F_c}{A_c} = \frac{756.8 \times 1000}{22500} = 33.67\ MPa$

$34.63 \times \frac{15}{100} = 5.1945 > 36.01 - 33.67 = 2.34 \therefore Test\ is\ valid$

D.4) 200-day test results

Table D-4: Compressive strength test results (200 day)

PMA Content (%)	Specimen	Fracture Load (kN)	Average Fracture Load (kN)
0% PMA	Cube 1	799.3	815.77
	Cube 2	840.4	
	Cube 3	807.6	
5% PMA	Cube 1	1022.8	974.73
	Cube 2	912.1	
	Cube 3	989.3	
10% PMA	Cube 1	1124.6	1033.60
	Cube 2	974.8	
	Cube 3	1001.5	

Sample calculation for 0% PMA:

$A_c = 150 \times 150 = 22500\ mm^2$

$f_c = \frac{F_c}{A_c} = \frac{815.77 \times 1000}{22500} = 36.26\ MPa$

Check validity of compressive strength test (0% PMA):

$Cube\ 1\text{:}\ \ f_c = \frac{F_c}{A_c} = \frac{799.3 \times 1000}{22500} = 35.52\ MPa$

$Cube\ 2\text{:}\ \ f_c = \frac{F_c}{A_c} = \frac{840.4 \times 1000}{22500} = 37.35\ MPa$

$36.26 \times \frac{15}{100} = 5.439 > 37.35 - 35.52 = 1.83 \therefore Test\ is\ valid$

Appendix E: Flexural strength test results

E.1) 7-day test results

Table E-1: Flexural strength test results (7 day)

PMA Content (%)	Specimen	Fracture Load (kN)	Average Fracture Load (kN)
0% PMA	Beam 1	6.26	6.09
	Beam 2	5.74	
	Beam 3	6.27	
5% PMA	Beam 1	8.26	7.87
	Beam 2	7.18	
	Beam 3	8.17	
10% PMA	Beam 1	8.20	8.96
	Beam 2	9.54	
	Beam 3	9.13	
15% PMA	Beam 1	8.41	8.12
	Beam 2	7.25	
	Beam 3	8.69	
20% PMA	Beam 1	7.63	7.83
	Beam 2	8.34	
	Beam 3	7.51	

Sample calculation for 0% PMA:

$$f_F = \frac{F_f l}{bd^2} = \frac{6.09 \times 1000 \times 500}{100(100)^2} = 3.05\ MPa$$

E.2) 28-day test results

Table E-2: Flexural strength test results (28 day)

PMA Content (%)	Specimen	Fracture Load (kN)	Average Fracture Load (kN)
15% PMA	Beam 1	10.45	9.82
	Beam 2	9.28	
	Beam 3	9.73	
20% PMA	Beam 1	8.95	8.48
	Beam 2	8.41	
	Beam 3	8.07	

Sample calculation for 15% PMA:

$$f_F = \frac{F_f l}{bd^2} = \frac{9.82 \times 1000 \times 500}{100(100)^2} = 4.91\ MPa$$

E.3) 180-day test results

Table E-3: Flexural strength test results (180 day)

PMA Content (%)	Specimen	Fracture Load (kN)	Average Fracture Load (kN)
0% PMA	Beam 1	10.87	10.23
	Beam 2	9.68	
	Beam 3	10.14	
5% PMA	Beam 1	12.08	12.07
	Beam 2	12.64	
	Beam 3	11.50	
10% PMA	Beam 1	13.13	14.15
	Beam 2	14.51	
	Beam 3	14.82	

Sample calculation for 0% PMA:

$$f_F = \frac{F_f l}{bd^2} = \frac{10.23 \times 1000 \times 500}{100(100)^2} = 5.12\ MPa$$

E.4) 200-day test results

Table E-4: Flexural strength test results (200 day)

PMA Content (%)	Specimen	Fracture Load (kN)	Average Fracture Load (kN)
0% PMA	Beam 1	9.88	10.68
	Beam 2	10.63	
	Beam 3	11.54	
5% PMA	Beam 1	12.90	12.43
	Beam 2	11.72	
	Beam 3	12.68	
10% PMA	Beam 1	14.79	15.15
	Beam 2	15.03	
	Beam 3	15.62	

Sample calculation for 0% PMA:

$$f_F = \frac{F_f l}{bd^2} = \frac{10.68 \times 1000 \times 500}{100(100)^2} = 5.34\ MPa$$

Appendix F: Tensile splitting strength test results

F.1) 7-day test results

Table F-1: Tensile splitting strength test results (7 day)

PMA Content (%)	Specimen	Fracture Load (kN)	Avg. Fracture Load (kN)
0% PMA	Cylinder 1	107.6	108.43
	Cylinder 2	115.3	
	Cylinder 3	102.4	
5% PMA	Cylinder 1	122.3	113.67
	Cylinder 2	103.9	
	Cylinder 3	114.8	
10% PMA	Cylinder 1	105.5	133.37
	Cylinder 2	136.3	
	Cylinder 3	158.3	
15% PMA	Cylinder 1	119.6	126.63
	Cylinder 2	121.6	
	Cylinder 3	138.7	
20% PMA	Cylinder 1	113.2	124.40
	Cylinder 2	132.6	
	Cylinder 3	127.4	

Sample calculation for 0% PMA:

$$f_T = \frac{2F_T}{\pi ld} = \frac{2 \times 108.43 \times 1000}{\pi \times 300 \times 150} = 1.53\ MPa$$

F.2) 28-day test results

Table F-2: Tensile splitting strength test results (28 day)

PMA Content (%)	Specimen	Fracture Load (kN)	Avg. Fracture Load (kN)
15% PMA	Cylinder 1	168.6	181.13
	Cylinder 2	196.1	
	Cylinder 3	178.7	
20% PMA	Cylinder 1	198.2	172.67
	Cylinder 2	162.5	
	Cylinder 3	157.3	

Sample calculation for 15% PMA:

$$f_T = \frac{2F_T}{\pi ld} = \frac{2 \times 181.13 \times 1000}{\pi \times 300 \times 150} = 2.56\ MPa$$

F.3) 180-day test results

Table F-3: Tensile splitting strength test results (180 day)

PMA Content (%)	Specimen	Fracture Load (kN)	Avg. Fracture Load (kN)
0% PMA	Cylinder 1	175.1	178.27
	Cylinder 2	198.2	
	Cylinder 3	161.5	
5% PMA	Cylinder 1	217.8	220.17
	Cylinder 2	193.4	
	Cylinder 3	249.3	
10% PMA	Cylinder 1	283.2	266.27
	Cylinder 2	240.7	
	Cylinder 3	274.9	

Sample calculation for 0% PMA:

$$f_T = \frac{2F_T}{\pi ld} = \frac{2 \times 178.27 \times 1000}{\pi \times 300 \times 150} = 2.52\ MPa$$

F.4) 200-day test results

Table F-4: Tensile splitting strength test results (200 day)

PMA Content (%)	Specimen	Fracture Load (kN)	Avg. Fracture Load (kN)
0% PMA	Cylinder 1	186.7	189.67
	Cylinder 2	180.9	
	Cylinder 3	201.4	
5% PMA	Cylinder 1	246.2	226.73
	Cylinder 2	221.9	
	Cylinder 3	212.1	
10% PMA	Cylinder 1	270.2	268.83
	Cylinder 2	246.6	
	Cylinder 3	289.7	

Sample calculation for 0% PMA:

$$f_T = \frac{2F_T}{\pi ld} = \frac{2 \times 189.67 \times 1000}{\pi \times 300 \times 150} = 2.68\ MPa$$

Appendix G: Durability index test results provided by Contest

G.1) Oxygen permeability test results

Table G-1: Oxygen permeability (OPI) test results for concrete containing varying amounts of PMA

PMA Content (%)	Sample	OPI (log value)	Average OPI (log value)
0% PMA	Sample A	10.24	9.84
	Sample B	10.14	
	Sample C	9.45	
	Sample D	10.07	
5% PMA	Sample A	9.22	9.48
	Sample B	9.42	
	Sample C	9.71	
	Sample D	9.84	
10% PMA	Sample A	9.61	9.52
	Sample B	9.49	
	Sample C	10.82	
	Sample D	9.21	
15% PMA	Sample A	10.01	9.20
	Sample B	10.10	
	Sample C	8.71	
	Sample D	9.40	
20% PMA	Sample A	9.88	10.09
	Sample B	10.38	
	Sample C	10.23	
	Sample D	10.05	

G.2) Water sorptivity test results

Table G-2: Water sorptivity (WS) test results for concrete containing varying amounts of PMA

PMA Content (%)	Sample	WS ($mmh^{-0.5}$)	Average WS ($mmh^{-0.5}$)
0% PMA	Sample A	5.23	4.66
	Sample B	4.42	
	Sample C	4.43	
	Sample D	4.56	
5% PMA	Sample A	4.27	4.09
	Sample B	4.39	
	Sample C	3.93	
	Sample D	3.78	
10% PMA	Sample A	3.89	3.95
	Sample B	3.93	
	Sample C	4.03	
	Sample D	3.94	
15% PMA	Sample A	3.96	4.20
	Sample B	4.46	
	Sample C	4.29	
	Sample D	4.10	
20% PMA	Sample A	4.29	4.29
	Sample B	4.35	
	Sample C	4.25	
	Sample D	4.28	

G.3) Chloride conductivity test results

Table G-3: Chloride conductivity (CC) test results for concrete containing varying amounts of PMA

PMA Content (%)	Sample	CC (mS/cm)	Average CC (mS/cm)
0% PMA	Sample A	0.22	0.23
	Sample B	0.24	
	Sample C	0.23	
	Sample D	0.24	
5% PMA	Sample A	0.19	0.20
	Sample B	0.22	
	Sample C	0.20	
	Sample D	0.19	
10% PMA	Sample A	0.25	0.25
	Sample B	0.27	
	Sample C	0.24	
	Sample D	0.25	
15% PMA	Sample A	0.23	0.24
	Sample B	0.22	
	Sample C	0.25	
	Sample D	0.23	
20% PMA	Sample A	0.27	0.25
	Sample B	0.25	
	Sample C	0.25	
	Sample D	0.25	

Appendix H: Frictional resistance

H.1) Skid resistance

Table H-1: Skid resistance values (SRV) obtained from the skid resistance test

PMA Content (%)	Surface Texturing	SRV 1	SRV 2	SRV 3	SRV 4	SRV 5	AVG SRV
0% PMA	Broom (longitudinal)	75	76	74	71	74	**74**
	Broom (transverse)	81	79	76	74	75	**77**
5% PMA	Broom (longitudinal)	73	72	70	75	76	**73.2**
	Broom (transverse)	77	79	78	76	77	**77.4**
10% PMA	Broom (longitudinal)	72	75	76	75	76	**74.8**
	Broom (transverse)	78	80	79	77	75	**77.8**
15% PMA	Broom (longitudinal)	73	76	74	75	71	**73.8**
	Broom (transverse)	76	79	76	77	75	**76.6**
20% PMA	Broom (longitudinal)	76	72	71	76	73	**73.6**
	Broom (transverse)	79	77	76	78	76	**77.2**

Sample calculation for 0% PMA (Broom – Longitudinal):

$$Average\ Skid\ Resistance\ Value = \frac{\sum SRV}{5} = \frac{75 + 76 + 74 + 71 + 74}{5} = 74$$

H.2) Texture depth

Table H-2: Texture depth results from the sand patch test

PMA Content (%)	Surface Texturing	Test 1			Test 2			Test 3			Test 4			Test 5			Avg TD (mm)
		D (mm)	A (mm^2)	TD (mm)	D (mm)	A (mm^2)	TD (mm)	D (mm)	A (mm^2)	TD (mm)	D (mm)	A (mm^2)	TD (mm)	D (mm)	A (mm^2)	TD (mm)	
0% PMA	Longitudinal	180	25446,9	**0,99**	173	23506,2	**1,07**	177	24605,7	**1,02**	176	24328,5	**1,03**	175	24052,8	**1,04**	**1,03**
	Transverse	171	22965,8	**1,09**	175	24052,8	**1,04**	178	24884,6	**1,01**	175	24052,8	**1,04**	176	24328,5	**1,03**	**1,05**
5% PMA	Longitudinal	179	25164,9	**1,00**	176	24328,5	**1,03**	180	25446,9	**0,99**	177	24605,7	**1,02**	175	24052,8	**1,04**	**1,02**
	Transverse	176	24328,5	**1,03**	173	23506,2	**1,07**	172	23235,2	**1,08**	175	24052,8	**1,04**	173	23506,2	**1,07**	**1,06**
10% PMA	Longitudinal	170	22698,0	**1,11**	178	24884,6	**1,01**	173	23506,2	**1,07**	175	24052,8	**1,04**	181	25730,4	**0,98**	**1,04**
	Transverse	169	22431,8	**1,12**	177	24605,7	**1,02**	170	22698,0	**1,11**	174	23778,7	**1,06**	176	24328,5	**1,03**	**1,07**
15% PMA	Longitudinal	175	24052,8	**1,04**	181	25730,4	**0,98**	177	24605,7	**1,02**	176	24328,5	**1,03**	175	24052,8	**1,04**	**1,02**
	Transverse	177	24605,7	**1,02**	174	23778,7	**1,06**	175	24052,8	**1,04**	178	24884,6	**1,01**	177	24605,7	**1,02**	**1,03**
20% PMA	Longitudinal	175	24052,8	**1,04**	177	24605,7	**1,02**	182	26015,5	**0,97**	178	24884,6	**1,01**	174	23778,7	**1,06**	**1,02**
	Transverse	173	23506,2	**1,07**	179	25164,9	**1,00**	174	23778,7	**1,06**	177	24605,7	**1,02**	168	22167,1	**1,13**	**1,06**

Sample calculation for 0% PMA (Longitudinal) Test 1:

$$Volume\ of\ sand = \frac{1}{4}\pi D^2 H = \frac{1}{4}\pi(80)(20)^2 = 25132.74\ mm^3$$

$$Area\ of\ patch\ (A) = \frac{1}{4}\pi D^2 = \frac{1}{4}\pi(180)^2 = 25446.9\ mm^2$$

$$Texture\ Depth\ (TD) = \frac{Volume\ of\ sand}{Area\ of\ patch} = \frac{25132.74}{25446.9} = 0.9\ mm$$

Appendix I: Equivalent Carbon Dioxide (CO_{2e})

Table I-1: Proportions of the hypothetical 1 m^3 concrete mixes used for the CO_{2e} analysis

Designation	w/b	Water (kg)	Sand (kg)	Stone (kg)	Binder	
					PC (kg)	PMA (kg)
0% PMA	0.64	240	814.4	1257.6	375	0
5% PMA	0.64	240	814.4	1257.6	356.3	13.6
10% PMA	0.64	240	814.4	1257.6	337.5	27.2
15% PMA	0.64	240	814.4	1257.6	318.8	40.8
20% PMA	0.64	240	814.4	1257.6	300	54.4

Table I-2: Equivalent Carbon Dioxide (CO_{2e}) for 0% PMA mix

Material	Material Quantity (kg)	Average CO_{2e} emissions (kg CO_2/ton)	Equivalent Carbon Dioxide (CO_{2e}) (kg CO_{2e})
Portland-Slag Cement (CEM II/B-S)	375	730	273,75
Umgeni River Sand	814,4	5	4,07
Coedmore Quartz Stone (19 mm)	1257,6	5	6,29
Water	240	1	0,24
Paper Mill Waste Ash	0	0	0
TOTAL			**284.35**

Table I-3: Equivalent Carbon Dioxide (CO_{2e}) for 5% PMA mix

Material	Material Quantity (kg)	Average CO_{2e} emissions (kg CO_2/ton)	Equivalent Carbon Dioxide (CO_{2e}) (kg CO_{2e})
Portland-Slag Cement (CEM II/B-S)	356,3	730	260,1
Umgeni River Sand	814,4	5	4,07
Coedmore Quartz Stone (19 mm)	1257,6	5	6,29
Water	240	1	0,24
Paper Mill Waste Ash	13,6	0	0
TOTAL			**270.7**

Table I-4: Equivalent Carbon Dioxide (CO_{2e}) for 10% PMA mix

Material	Material Quantity (kg)	Average CO_{2e} emissions (kg CO_2/ton)	Equivalent Carbon Dioxide (CO_{2e}) (kg CO_{2e})
Portland-Slag Cement (CEM II/B-S)	337,5	730	246,38
Umgeni River Sand	814,4	5	4,07
Coedmore Quartz Stone (19 mm)	1257,6	5	6,29
Water	240	1	0,24
Paper Mill Waste Ash	27,2	0	0
TOTAL			**256.98**

Table I-5: Equivalent Carbon Dioxide (CO_{2e}) for 15% PMA mix

Material	Material Quantity (kg)	Average CO_{2e} emissions (kg CO_2/ton)	Equivalent Carbon Dioxide (CO_{2e}) (kg CO_{2e})
Portland-Slag Cement (CEM II/B-S)	318,8	730	232,72
Umgeni River Sand	814,4	5	4,07
Coedmore Quartz Stone (19 mm)	1257,6	5	6,29
Water	240	1	0,24
Paper Mill Waste Ash	40,8	0	0
TOTAL			**243.32**

Table I-6: Equivalent Carbon Dioxide (CO_{2e}) for 20% PMA mix

Material	Material Quantity (kg)	Average CO_{2e} emissions (kg CO_2/ton)	Equivalent Carbon Dioxide (CO_{2e}) (kg CO_{2e})
Portland-Slag Cement (CEM II/B-S)	300	730	219
Umgeni River Sand	814,4	5	4,07
Coedmore Quartz Stone (19 mm)	1257,6	5	6,29
Water	240	1	0,24
Paper Mill Waste Ash	54,4	0	0
TOTAL			**229.6**

Appendix J: Cost

J.1) Material cost analysis

Table J-1: Proportions of the hypothetical 1 m^3 concrete mixes used for the material cost analysis

Designation	w/b	Water (kl)	Sand (m^3)	Stone (m^3)	Binder	
					PC (kg)	PMA (kg)
0% PMA	0.64	0.24	0.3073	0.4746	375	0
5% PMA	0.64	0.24	0.3073	0.4746	356.3	13.6
10% PMA	0.64	0.24	0.3073	0.4746	337.5	27.2
15% PMA	0.64	0.24	0.3073	0.4746	318.8	40.8
20% PMA	0.64	0.24	0.3073	0.4746	300	54.4

Table J-2: Material cost analysis for 0% PMA concrete mix

Material	Unit	Qty	Rate	Cost (R)
Portland-Slag Cement (CEM II/B-S)	50 kg bag	8	R92.00	R736.00
Umgeni River Sand	m^3	0.3073	R550.00	R169.02
Coedmore Quartz Stone (19 mm)	m^3	0.4746	R650.00	R308.49
Water	kl	0.24	R36.52	R8.76
Paper Mill Ash	kg	0	R0.00	R0.00
TOTAL				**R1222.27**

Table J-3: Material cost analysis for 5% PMA concrete mix

Material	Unit	Qty	Rate	Cost (R)
Portland-Slag Cement (CEM II/B-S)	50 kg bag	8	R92.00	R736.00
Umgeni River Sand	m^3	0.3073	R550.00	R169.02
Coedmore Quartz Stone (19 mm)	m^3	0.4746	R650.00	R308.49
Water	kl	0.24	R36.52	R8.76
Paper Mill Ash	kg	13.6	R0.00	R0.00
TOTAL				**R1222.27**

Table J-4: Material cost analysis for 10% PMA concrete mix

Material	Unit	Qty	Rate	Cost (R)
Portland-Slag Cement (CEM II/B-S)	50 kg bag	7	R92.00	R644.00
Umgeni River Sand	m^3	0.3073	R550.00	R169.02
Coedmore Quartz Stone (19 mm)	m^3	0.4746	R650.00	R308.49
Water	kl	0.24	R36.52	R8.76
Paper Mill Ash	kg	27.2	R0.00	R0.00
TOTAL				**R1130.27**

Table J-5: Material cost analysis for 15% PMA concrete mix

Material	Unit	Qty	Rate	Cost (R)
Portland-Slag Cement (CEM II/B-S)	50 kg bag	7	R92.00	R644.00
Umgeni River Sand	m^3	0.3073	R550.00	R169.02
Coedmore Quartz Stone (19 mm)	m^3	0.4746	R650.00	R308.49
Water	kl	0.24	R36.52	R8.76
Paper Mill Ash	kg	40.8	R0.00	R0.00
TOTAL				**R1130.27**

Table J- 6: Material cost analysis for 20% PMA concrete mix

Material	Unit	Qty	Rate	Cost (R)
Portland-Slag Cement (CEM II/B-S)	50 kg bag	6	R92.00	R552.00
Umgeni River Sand	m^3	0.3073	R550.00	R169.02
Coedmore Quartz Stone (19 mm)	m^3	0.4746	R650.00	R308.49
Water	kl	0.24	R36.52	R8.76
Paper Mill Ash	kg	54.4	R0.00	R0.00
TOTAL				**R1038.27**

J.2) Construction cost analysis

Table J-7: Construction cost analysis for 0% PMA concrete mix

Item	Unit	Qty	Rate	Cost
Material Costs:				
Portland-Slag Cement (CEM II/B-S)	50 kg bag	1201	R92,00	R110 492,00
Umgeni River Sand	m^3	38,48	R550,00	R21 164,00
Coedmore Quartz Stone (19 mm)	m^3	64,1	R650,00	R41 665,00
Water	kl	32,42	R36,52	R1 183,98
Paper Mill Waste Ash	kg	0	R0,00	R0,00
Ref 617 mesh	m^2	587,25	R94,40	R55 436,40
Sika Cemflex Curing Compound	l	2350	R90,40	R212 440,00
Sikaflex Pro 3	m	120	R120,70	R14 484,00
Sub Total				**R456 865,38**
Transport Costs:				
Foreman LDV (Bakkie)	day	30	R964,68	R28 940,40
7-ton Gang Truck (Dry rate)	day	30	R1 503,87	R45 116,10
Fuel Gang Truck (60 litres per day)	day	30	R713,40	R21 402,00
Fuel Gang Truck - cement (30 litres/day)	day	12	R356,70	R4 280,40
4-ton Truck (wet rate)	day	0	R1 500,00	R0,00
Sub Total				**R99 738,90**
Plant Costs:				
Revolving drum type concrete mixer (x2)	day	29	R3 600,00	R104 400,00
10 kVA Generator (Dry rate) x2	day	30	R920,00	R27 600,00
Fuel Generator (5 litres per day)	day	30	R118,90	R3 567,00
Trailer	day	30	R250,00	R7 500,00
Saw Cutter	day	30	R850,00	R25 500,00
Fuel Saw Cutter (10 litres per day)	day	30	R118,90	R3 567,00
Vibrating Poker	day	29	R200,00	R5 800,00
Sub Total				**R177 934,00**
Labour Costs:				
Foreman	day	30	R2 209,70	R66 291,00
Semi-skilled labour x 3	day	30	R1 950,50	R58 515,00
Unskilled labour x 12	day	30	R5 040,00	R151 200,00
Sub Total				**R276 006,00**

Table J-8: Construction cost analysis for 5% PMA concrete mix

Item	Unit	Qty	Rate	Cost
Material Costs:				
Portland-Slag Cement (CEM II/B-S)	50 kg bag	1141	R92,00	R104 972,00
Umgeni River Sand	m^3	38,48	R550,00	R21 164,00
Coedmore Quartz Stone (19 mm)	m^3	64,1	R650,00	R41 665,00
Water	kl	32,42	R36,52	R1 183,98
Paper Mill Waste Ash	kg	2178,7	R0,00	R0,00
Ref 617 mesh	m^2	587,25	R94,40	R55 436,40
Sika Cemflex Curing Compound	l	2350	R90,40	R212 440,00
Sikaflex Pro 3	m	120	R120,70	R14 484,00
Sub Total				**R451 345,38**
Transport Costs:				
Foreman LDV (Bakkie)	day	30	R964,68	R28 940,40
7-ton Gang Truck (Dry rate)	day	30	R1 503,87	R45 116,10
Fuel Gang Truck (60 litres per day)	day	30	R713,40	R21 402,00
Fuel Gang Truck - cement (30 litres/day)	day	12	R356,70	R4 280,40
4-ton Truck (wet rate)	day	1	R1 500,00	R1 500,00
Sub Total				**R101 238,90**
Plant Costs:				
Revolving drum type concrete mixer (x2)	day	29	R3 600,00	R104 400,00
10 kVA Generator (Dry rate) x2	day	30	R920,00	R27 600,00
Fuel Generator (5 litres per day)	day	30	R118,90	R3 567,00
Trailer	day	30	R250,00	R7 500,00
Saw Cutter	day	30	R850,00	R25 500,00
Fuel Saw Cutter (10 litres per day)	day	30	R118,90	R3 567,00
Vibrating Poker	day	29	R200,00	R5 800,00
Sub Total				**R177 934,00**
Labour Costs:				
Foreman	day	30	R2 209,70	R66 291,00
Semi-skilled labour x 3	day	30	R1 950,50	R58 515,00
Unskilled labour x 12	day	30	R5 040,00	R151 200,00
Sub Total				**R276 006,00**

Table J-9: Construction cost analysis for 10% PMA concrete mix

Item	Unit	Qty	Rate	Cost
Material Costs:				
Portland-Slag Cement (CEM II/B-S)	50 kg bag	1081	R92,00	R99 452,00
Umgeni River Sand	m^3	38,48	R550,00	R21 164,00
Coedmore Quartz Stone (19 mm)	m^3	64,1	R650,00	R41 665,00
Water	kl	32,42	R36,52	R1 183,98
Paper Mill Waste Ash	kg	4357,4	R0,00	R0,00
Ref 617 mesh	m^2	587,25	R94,40	R55 436,40
Sika Cemflex Curing Compound	l	2350	R90,40	R212 440,00
Sikaflex Pro 3	m	120	R120,70	R14 484,00
Sub Total				**R445 825,38**
Transport Costs:				
Foreman LDV (Bakkie)	day	30	R964,68	R28 940,40
7-ton Gang Truck (Dry rate)	day	30	R1 503,87	R45 116,10
Fuel Gang Truck (60 litres per day)	day	30	R713,40	R21 402,00
Fuel Gang Truck - cement (30 litres/day)	day	11	R356,70	R3 923,70
4-ton Truck (wet rate)	day	2	R1 500,00	R3 000,00
Sub Total				**R102 382,20**
Plant Costs:				
Revolving drum type concrete mixer (x2)	day	29	R3 600,00	R104 400,00
10 kVA Generator (Dry rate) x2	day	30	R920,00	R27 600,00
Fuel Generator (5 litres per day)	day	30	R118,90	R3 567,00
Trailer	day	30	R250,00	R7 500,00
Saw Cutter	day	30	R850,00	R25 500,00
Fuel Saw Cutter (10 litres per day)	day	30	R118,90	R3 567,00
Vibrating Poker	day	29	R200,00	R5 800,00
Sub Total				**R177 934,00**
Labour Costs:				
Foreman	day	30	R2 209,70	R66 291,00
Semi-skilled labour x 3	day	30	R1 950,50	R58 515,00
Unskilled labour x 12	day	30	R5 040,00	R151 200,00
Sub Total				**R276 006,00**

Table J-10: Construction cost analysis for 15% PMA concrete mix

Item	Unit	Qty	Rate	Cost
Material Costs:				
Portland-Slag Cement (CEM II/B-S)	50 kg bag	1021	R92,00	R93 932,00
Umgeni River Sand	m^3	38,48	R550,00	R21 164,00
Coedmore Quartz Stone (19 mm)	m^3	64,1	R650,00	R41 665,00
Water	kl	32,42	R36,52	R1 183,98
Paper Mill Waste Ash	kg	6536,1	R0,00	R0,00
Ref 617 mesh	m^2	587,25	R94,40	R55 436,40
Sika Cemflex Curing Compound	l	2350	R90,40	R212 440,00
Sikaflex Pro 3	m	120	R120,70	R14 484,00
Sub Total				**R440 305,38**
Transport Costs:				
Foreman LDV (Bakkie)	day	30	R964,68	R28 940,40
7-ton Gang Truck (Dry rate)	day	30	R1 503,87	R45 116,10
Fuel Gang Truck (60 litres per day)	day	30	R713,40	R21 402,00
Fuel Gang Truck - cement (30 litres/day)	day	11	R356,70	R3 923,70
4-ton Truck (wet rate)	day	2	R1 500,00	R3 000,00
Sub Total				**R102 382,20**
Plant Costs:				
Revolving drum type concrete mixer (x2)	day	29	R3 600,00	R104 400,00
10 kVA Generator (Dry rate) x2	day	30	R920,00	R27 600,00
Fuel Generator (5 litres per day)	day	30	R118,90	R3 567,00
Trailer	day	30	R250,00	R7 500,00
Saw Cutter	day	30	R850,00	R25 500,00
Fuel Saw Cutter (10 litres per day)	day	30	R118,90	R3 567,00
Vibrating Poker	day	29	R200,00	R5 800,00
Sub Total				**R177 934,00**
Labour Costs:				
Foreman	day	30	R2 209,70	R66 291,00
Semi-skilled labour x 3	day	30	R1 950,50	R58 515,00
Unskilled labour x 12	day	30	R5 040,00	R151 200,00
Sub Total				**R276 006,00**

Table J-11: Construction cost analysis for 20% PMA concrete mix

Item	Unit	Qty	Rate	Cost
Material Costs:				
Portland-Slag Cement (CEM II/B-S)	50 kg bag	961	R92,00	R88 412,00
Umgeni River Sand	m^3	38,48	R550,00	R21 164,00
Coedmore Quartz Stone (19 mm)	m^3	64,1	R650,00	R41 665,00
Water	kl	32,42	R36,52	R1 183,98
Paper Mill Waste Ash	kg	8714,8	R0,00	R0,00
Ref 617 mesh	m^2	587,25	R94,40	R55 436,40
Sika Cemflex Curing Compound	l	2350	R90,40	R212 440,00
Sikaflex Pro 3	m	120	R120,70	R14 484,00
Sub Total				**R434 785,38**
Transport Costs:				
Foreman LDV (Bakkie)	day	30	R964,68	R28 940,40
7-ton Gang Truck (Dry rate)	day	30	R1 503,87	R45 116,10
Fuel Gang Truck (60 litres per day)	day	30	R713,40	R21 402,00
Fuel Gang Truck - cement (30 litres/day)	day	10	R356,70	R3 567,00
4-ton Truck (wet rate)	day	3	R1 500,00	R4 500,00
Sub Total				**R103 525,50**
Plant Costs:				
Revolving drum type concrete mixer (x2)	day	29	R3 600,00	R104 400,00
10 kVA Generator (Dry rate) x2	day	30	R920,00	R27 600,00
Fuel Generator (5 litres per day)	day	30	R118,90	R3 567,00
Trailer	day	30	R250,00	R7 500,00
Saw Cutter	day	30	R850,00	R25 500,00
Fuel Saw Cutter (10 litres per day)	day	30	R118,90	R3 567,00
Vibrating Poker	day	29	R200,00	R5 800,00
Sub Total				**R177 934,00**
Labour Costs:				
Foreman	day	30	R2 209,70	R66 291,00
Semi-skilled labour x 3	day	30	R1 950,50	R58 515,00
Unskilled labour x 12	day	30	R5 040,00	R151 200,00
Sub Total				**R276 006,00**